Coactivator Associated Arginine Methyltransferase 1 (CARM1) as a Contributor to Motoneuron Biology

Julie Bourassa

Thesis submitted to the University of Ottawa

in partial Fulfillment of the requirements for the Doctorate in Philosophy degree

in Cellular and Molecular Medicine

Department of Cellular and Molecular Medicine

Faculty of Medicine

University of Ottawa

Contributions

In all chapters, Dr. Jocelyn Côté contributed to the experimental design, result interpretation and manuscript review. The contributions of others to each chapter goes as follows. Dr. Laura Trinkle-Mulcahy and Genevieve Paris contributed to the experimental design, data interpretation and review of the manuscript in Chapter 3. In Chapter 4, Gareth Palidwor from The Ottawa Hospital Research Institute's Bioinformatics Core Facility guided the RIP-seq analysis process and contributed to data interpretation. The motif analysis shown in Figure 11 was done by Dr. Martin Pelchat and I adapted the figure. In Chapter 5, Dr. Laura Trinkle-Mulcahy contributed to the experimental design and Zhibin Ning from the Proteomics Resource guided the MS analysis process. In all experiments I contributed to the experimental design. I conducted all experiments in this work and am the author of all its content.

Abstract

Coactivator Associated Arginine Methyltransferase 1 **(**CARM1) is a ubiquitously expressed protein arginine methyltransferase with essential roles in normal cell function. As such, CARM1 is often a part of the investigative rationale, where its quantification through Western Blot (WB) is commonly assessed. Here, CARM1 is shown to form aggregates that prevent its migration in SDS-PAGE and introduces error in its quantification by WB. Heat denaturation, DTT and CARM1's own concentration in samples are found to contribute to its aggregation. An adapted sample buffer with higher SDS concentrations and without DTT prevents aggregation and permits accurate quantification. These findings reframe CARM1's biochemical properties as an essential component of its study in an experimental and potentially biological setting.

In motoneurons (MNs), CARM1 was previously found to methylate HuD, a major neuronal RNA binding protein, thereby altering its affinity with the p21 mRNA. Here, the notion that other mRNAs are similarly impacted was explored, and Schip1/Iqschfp, Smarca2, Stc2, Ptger4 and Phox2B mRNAs were found to be dependent on CARM1 levels for their interaction with HuD. These interactions were not previously characterized, making them novel elements in both HuD's and CARM1's biology. Moreover, the protein levels of Ptger4 and Smarca2 were regulated by CARM1's enzymatic activity expanding and attesting to its functional relevance in MNs. Akin to other work, CARM1's interactome identifies Alix as being by far its most prominent interactor. Also, ribosomal proteins are overrepresented in CARM1's interactome suggesting that translation remains a major facet of its function in MNs. In line with this assessment, this work identifies RPS7 as a novel substrate of CARM1.

This study solidifies CARM1 as a contributor to neuronal biology through its regulation of HuD mRNA interactions, its regulation of Ptger4 and Smarca2 protein levels and contribution to the MN methylome.

Table of contents

List of Figures

Supplementary Figures

List of Tables

Supplementary Tables

Acknowledgements

I am grateful to Dr. Gibbings for giving me the opportunity to join his research lab as an honours student and his continued support as a TAC member throughout my graduate studies. This extends to Dr. Lagacé, and Dr. Blais who have been of great help throughout this project. I am also very grateful for Dr. Jocelyn Côté for giving me the opportunity to join his lab and his supervision during this research. I would like to thank Dr. Trinkle-Mulcahy for the many helpful discussions we had. Her insight and suggestions were of immense help in this work. I would like to thank Gareth Palidwor from The Ottawa Hospital Research Institute's Bioinformatics Core Facility for his valuable input on the HuD RIP-seq analysis.

This experience was not without its challenges (such as a global pandemic), but it would not have been the same without the great company of many brilliant lab members and friends. I would like to thank Genevieve Paris for being a great mentor that helped focus my scattered brain. I would also like to thank Andréanne Didillon, Grace Liu, and Janelle Nordin for being unbeatable pumpkin carvers, escape room geniuses and constant support throughout this adventure. Janelle, our book club meetings were a highlight.

Last but not least, it would have been impossible for me to achieve this without the support of friends and family. To Lyzanne, thank you for being such a great friend. You steadied me in what felt like a storm and your constant support means the world to me. To my sister, Valérie, thank you for being a role model. By pursuing your own PhD you taught me to follow my own ambitions and be true to myself. Pour ma mère et mon père, Carole et Yvan, merci de m'avoir soutenue inconditionnellement à chaque étapes et d'avoir toujours eu confiance en ma capacité d'atteindre mes buts. Vous m'inspirez chaque jour, et votre amour a toujours été - et

sera toujours - ma plus grande motivation. Eric, you were my anchor through it all. You were there to comfort me on bad days and celebrate on good ones. Your kindness and ability to see the best in me kept me going. Thank you for for taking on this journey with me.

Abbreviations

Ab-Antibody

AChE- Acetylcholinesterase

Actb- Actin Beta

aDMA- Asymmetrical Dimethylarginine

Adra2B- Adrenoceptor Alpha 2B

AIS- Axon Initial Segment

ALG-2- Apoptosis Linked Gene-2

Alix- Apoptosis Linked gene-2 Interacting Protein

ALS- Amyotrophic Lateral Sclerosis

AMV-RT- Avian Myeloblastosis Reverse Transcriptase

AnkB- Ankyrin B

AnkG- Ankyrin G

AP- Affinity Purification

APP- Amyloid Precursor Protein

ARE- AU-rich Element

Arg- Arginine

ATP- Adenosine Triphosphate

Aven- Apoptosis And Caspase Activation Inhibitor

BAF- BRG1/BRM Associated Factor

BAH- Bromo-Adjacent homology domain

BDNF- Brain-Derived Neurotrophic Factor

BRD4- Bromodomain-Containing Protein 4

BRG1- Brahma-Related Gene 1

BRM- Brahma Homolog

cAMP- Cyclic Adenosine Monophosphate

CARM1- Coactivator Associated Arginine Methyltransferase 1

CARM1FL- Coactivator Associated Arginine Methyltransferase 1 Full Length

CBP- CREB-Binding Protein

CDK1-Cyclin-dependent Kinase 1

CHAT- Choline Acetyltransferase

ChIP-seq- Chromatin Immunoprecipitation Sequencing

Clip-seq- Cross-Linking Immunoprecipitation Sequencing

CPM- Counts Per Minute

CREB- cAMP Response Element Binding Protein

Cys- Cysteine

DA- Dimerization Arm

DAPI- 4',6-diamidino-2-phenylindole

DMEM- Dulbecco's Modified Eagle Medium

DNA- Deoxyribonucleic Acid

DRG- Dorsal Root Ganglion

DTT- Dithiothreitol

EGFP- Enhanced Green Fluorescent Protein

eIF4A- Eukaryotic Initiation Factor-4A

Elavl- Embryonic Lethal Abnormal Vision-Like

ER- Endoplasmic Reticulum

ERα- Estrogen receptor alpha

ESCRT- Endosomal Sorting Complexes Required for Transport

EtBr- Ethidium Bromide

FBS- Fetal Bovine Serum

FUS- Fuse in Sarcoma

GAP-43- Growth Associated Protein 43

GAPDH- Glyceraldehyde-3-Phosphate Dehydrogenase

GDNF- Glial Cell Line Derived Neurotrophic Factor

GFP- Green Fluorescent Protein

GO- Gene Ontology

GPCR- G Protein-Coupled Receptor

GRIP1- Glutamate Receptor Interacting Protein 1

GSK-3β- Glycogen Synthase Kinase

GST- Glutathione S-Transferase

HAT- Histone Acetyltransferase

HDAC- Histone Deacetylase

hESC- Human Embryonic Stem Cells

HRP- Horseradish Peroxidase

HSP70- Heat Schock Protein 70

IB- Immunoblot

IgG- Immunoglobulin G

IP- Immunoprecipitation

iPSC- Induced Pluripotent Stem Cell

IPTG-Isopropyl β-d-1-thiogalactopyranoside

Iqschfp- IQ Motif Containing J-Schwannomin Interacting Protein

IRES- Internal Ribosome Entry Site

JmjC- Jumonji domain-containing protein

JMJD6- Jumonji domain–containing 6 protein

kDa- Kilodalton

KDM- Lysine Demethylase

KMT- Lysine Methyltransferase

KO- Knockout

KSRP- KH-Type Splicing Regulatory Protein

LB- Luria-Bertani

LFQ- Label-Free Quantification

LLPS- Liquid-Liquid Phase Separation

LSDs- Lysine-Specific Demethylases

Lys- Lysine

Marcks- Myristoylated Alanine-Rich C Kinase Substrate

MBT- Malignant Brain Tumor domain

MDM2- Mouse Double Minute 2

MED12- Mediator Complex Subunit 12

MEF- Mouse Embryonic Fibroblasts

MeK- Methylated Lysine

MEM- Minimum Essential Medium

MeR- Methylated Arginine

Met- Methionine

MLO- Membraneless Organelle

MMA- Monomethyl Arginine

MN- Motoneuron

mRNA- Messenger Ribonucleic Acid

MS- Mass Spectrometry

MW- Molecular Weight

MWCO- Molecualr Weight Cut Off

Myf5- Myogenic Factor 5

NaDOC- Sodium Deoxycholate

nBAF- Neuronal BRG1/BRM associated factor

NCBRS- Nicolaides-Baraitser Syndrome

NES- Nuclear Export Signal

NF-κB- Nuclear Factor Kappa-Light-Chain-Enhancer of Activated B cells

NF2- Neurofibromin 2

NFIB- Nuclear Factor 1 B-type

NGF- Nerve Growth Factor

Ngn2- Neurogenin 2

NLS- Nuclear Localization Sequence

NMDA- N-Methyl-D-Aspartate

NMJ- Neuromuscular Junction

Nova1- Neuro-Oncological Ventral Antigen 1

npBAF- Neural progenitor BRG1/BRM Associated Factor

NR- Nuclear Receptor

NT-3- Neurotrophin 3

NuRD- Nucleosome-Remodeling and Deacetylase complex

NXF1- Nuclear Export Factor 1

OGT- O-Linked N-Acetylglucosamine Transferase

Olig2- Oligodendrocyte Transcription Factor 2

PARP1- Poly (ADP-Ribose) Polymerase 1

PBS- Phosphate-Buffered Saline

PBS-T- Phosphate-Buffered Saline with Tween

PCR- Polymerase Chain Reaction

Pdcd6ip- Programmed Cell Death 6 Interacting Protein

PEI- Polyethylenimine

PGE2- Prostaglandin E2

PH- Plekstrin Homolohy

PHD- Plant Homeodomain

Phox2B- Paired-Like Homeobox 2B

PKA- Protein Kinase A

PKC- Protein Kinase C

PKMT- Protein Lysine Methyltransferase

PMSF- Phenylmethanesulfonyl Fluoride

PMT- Protein Methyltransferase

PRD- Proline Rich Domain

PRMT- Protein Arginine Methyltransferase

PSD95- Postsynaptic Density Protein 95

PSMD14- Proteasome 26S Subunit, Non-ATPase14

Ptger4- Prostaglandin E Receptor 4

PTM- Post Translational Modification

QC- Quality Control

RBP- RNA Binding Protein

RDM- Arginine Demethylase

RIP- RNA Immunoprecipitation

RIP-Seq- RNA Immunoprecipitation Sequencing

RIPA- Radioimmuniprecipitation Assay Buffer

RNA- Ribonucleic Acid

RNAPII- RNA Polymerase II

RNPs- Ribonucleoproteins

RPKM- Reads Per Kilobase per Million Mapped Reads

RPS7- Ribosomal Protein S7

RRM- RNA Recognition Motif

rRNA- Ribosomal Ribonucleic Acid

RT-PCR- Reverse Transcription Polymerase Chain Reaction

RUNX1- Runt-Related Transcription Factor 1

SAH- S-Adenosyl-L-Homocysteine

SAM- S-Adenosylmethionine

SAP49- Spliceosome-Associated Protein 49

SART3- Spliceosome-Associated Factor 3

SCG10- Superior Cervical Ganglia 10

Schip1- Schwannomin Interacting Protein 1

SD- Standard Deviation

sDMA- Symmetrical Dimethylarginine

SDS- Sodium Dodecyl Sulfate

SDS-PAGE- Sodium Dodecyl Sulfate Polyacrylamide Gel Electrophoresis

SEM- Standard Error of the Mean

SKP2- S-Phase Kinase-Associated Protein 2

SMA- Spinal Muscular Atrophy

Smarca2- SWI/SNF related BAF chromatin remodelling complex subunit ATPase 2

Smarca4- SWI/SNF related BAF chromatin remodelling complex subunit ATPase 4

SMN- Survival of Motoneuron

SOC- Super Optimal broth with Catabolite repression

Stc2- Stanniocalcin 2

SWI/SNF- Switch/Sucrose nonfermenting

TAD- Transactivation Domain

TAP- Transporter Associated with Antigen Processing

Tau- Tubulin Associated Unit

TDP-43- TAR DNA-Binding Protein 43

TDRD3- Tudor Domain Containing 3

TSG101- Tumor Susceptibility Gene 101

UHRF1- Ubiquitin-Like Containing PHD and RING Finger Domains 1

UTR- Untranslated Region

WB- Western Blot

Wnt- Wingless-Related Integration Site

WT- Wild Type

α2-AR- Alpha-2 Adrenergic Receptors

βME- β-mercaptoethanol

Chapter 1 Introduction

1.1 Protein Interaction

Protein interactions are the basis of cellular function, and their dynamicity is dictated by their timed and regulated expression. While DNA contains the genetic code to sustain cellular life, proteins are its main effectors. Through protein interactions, a cell divides, specializes, adapts to stress, answers to external signals, coordinates as part of a larger structure, recognizes imbalances and corrects them. The estimated 20,000 protein coding genes present in the human genome (Amaral et al., 2023) each play a part in these roles, and their interactions are therefore tightly regulated.

Protein interactions are first and foremost dependent on a protein's three-dimensional structure, which is itself dependent on its primary structure. The R group, or side chain of amino acids, confers localized charge, polarity, steric bulk, and aromaticity that further acts as a guide for protein folding (Anfinsen, 1973; Soleymani et al., 2022). Depending on sequence, any given peptide can further organize itself and be classified into secondary structures such as α-helices or β-sheets; the most observed secondary structures. The peptide can then bend and fold into a compact conformation termed as the tertiary structure. While this conformation may be sufficient for the intended protein's function, some will associate with one or more other protein peptides acting as subunits of a larger protein, accomplishing their roles as a quaternary structure (Soleymani et al., 2022).

The intermolecular forces grouping subunits of proteins together as macromolecular complexes are for the most part electrostatic in nature (Zhou & Pang, 2018). Through mirrored localized hydrogen bonding capacity, complementary steric bulk and ionic charge, binding sites

act as unique, recognizable fingerprints at which two proteins find affinity and interact. This most basic form of protein-protein interaction offers a mode of action for the cell to accomplish any given task. Nevertheless, the availability of each affinity site is not solely regulated at the level of protein expression, but also with modifications that proteins undergo thereafter.

1.2 Post Translational Modifications (PTMs)

Post translational modifications add another layer of complexity to cell signalling through the covalent modification of amino acid side chains. PTMs can be temporary or permanent in nature and alter the protein's chemical properties towards a different functional role (Ramazi & Zahiri, 2021). Their prevalent use in cell biology warrants entire molecular pathways dedicated to their distribution with PTMs integrated in all facets of normal cellular function. These modifications are categorized by the identity of the group covalently integrated into peptide chains as well as their target amino acid. There are more than 400 types of PTMs identified (Ramazi & Zahiri, 2021), each of varying prevalence through diverse and dynamic mechanisms. Of all reported PTMs, 90% fit under the umbrella terms of phosphorylation, acetylation, and ubiquitylation (Ramazi & Zahiri, 2021). However, less reportedly prevalent PTMs have also warranted their recognition as key regulators of cell function. To this effect, protein methylation is now the subject of research within a broad range of topics.

1.3 Protein Methylation

Protein methylation is one of the earliest PTM identified alongside phosphorylation, but despite its early identification, methylation research has been latent (Biggar & Li, 2015). Only in the mid-1990s did the research push forward with the arrival of modern molecular biology techniques (Murn & Shi, 2017; Paik et al., 2007). Currently, in humans, 26.7% of all proteins were found to be methylated, amongst which 67.9% were Arginine methylations, 32.0% were

Lysine methylations and 0.1% were methylations on other residues (Małecki et al., 2022). So, while Cysteine, Histidine, Glutamine, Asparagine, Glutamic acid, and Aspartic acid can be methylated (Murn & Shi, 2017; Sprung et al., 2008), by far the most commonly methylated residues are Arg and Lys (Dilworth & Barsyte-Lovejoy, 2019; Murn & Shi, 2017; Paik et al., 2007; Sprung et al., 2008). As such, protein methylation is often considered to be specific to these two residues.

The proteins involved in the protein methylation process are categorized as methyl writers, readers or erasers and are based on their ability to, respectively, catalyze, recognize, or remove the methyl mark on the amino acid side chains. While they vary in function, their structural commonalities are often used as markers for their classification (Liu et al., 2023).

1.4 Protein Methyl Writers

Protein methyl writers, or PMTs, consist of the family of protein Lys methyltransferase (PKMT) and protein Arg methyltransferase (PRMT), both using S-Adenosylmethionine (SAM or AdoMet) as a methyl donor to catalyse the methylation reaction yielding a methylated substrate and a S-Adenosyl-L-Homocysteine (SAH or AdoHcy) molecule by-product (Biggar & Li, 2015). SAM is deemed the cell's universal methyl donor (Mentch & Locasale, 2016), used for protein methylation, as well as DNA, RNA, and lipid methylation (Liu et al., 2023; Papsdorf & Brunet, 2019). It is generated through the folate and Met cycle, also known as the One-carbon metabolism pathway, which contributes one ATP molecule per Met to form the SAM co-factor. After the methylation reaction by methyltransferases, the SAH by-product is then returned to the One-carbon cycle and converted to Met once more. (Blasi et al., 2021; Mentch & Locasale, 2016; Ouyang et al., 2020; Teperino et al., 2010). In addition, methylation reactions are not

limited to the addition of a single methyl group to each residue. Lys can be methylated up to three times, while Arg can be methylated up to two times.

For both PKMTs and PRMTs, methylation reactions occur on two groups of substrates appropriately named histone, or non-histone substrates. While both are significant, histone methylation is a well-established function of PMTs, as this epigenetic process is reliant on the modifications they impart. Non-histone substrates, although less described, are emerging as a field of interest in post transcriptional modification research.

1.4.1 Histone Methylation

Epigenetics is a complex process defined by local nucleosomal conformation changes that alter gene accessibility to the transcriptional machinery. These changes are orchestrated responses adapted to the need of a cell, aimed at altering the cell's proteome towards functional changes. The changes are conveyed through PTM of the histone tails; a concept known as the histone code (Miller & Grant, 2013). The hypothesis of the histone code assumes that epigenetic changes are mainly accomplished through specific and recognizable PTM patterns of histone tail, as opposed to other potential drivers of nucleosome conformational changes (Prakash & Fournier, 2017). Histone tails can be modified in a variety of ways, most commonly through acetylation, phosphorylation, and methylation (Bannister & Kouzarides, 2011). These modifications are subject to crosstalk; an interdependent and context dependent alteration that enables or prevents further modifications (Lee et al., 2010). Since these modifications are dependent on the cellular context, they are a reliable snapshot of the epigenetic inclinations at play. The modularity and interdependence of methyl marks make their influence just as changeable, and Lys and Arg histone methylation can either transcriptionally activate or repress gene expression (Litt et al., 2009; Stark et al., 2011).

1.4.2 Non Histone Methylation

In addition to the epigenetic impact of methylation, PRMTs and PKMTs also count an array of non-histone proteins as their substrates. Their scope involves nearly all, if not all, cellular facets. Non-histone methylated substrates are involved in protein stability (Chuikov et al., 2004; Hwang et al., 2021; H. Liu et al., 2013), cell cycle (Chuikov et al., 2004; Hwang et al., 2021), translation (Jakobsson et al., 2018; Miao et al., 2024; Wei et al., 2021), splicing (Liu et al., 2013; Wei et al., 2021), metabolism (Wang & Liu, 2024; Yan et al., 2018; Zhu et al., 2022), protein localization (Cornett et al., 2019; Tradewell et al., 2012) and signalling (Biggar & Li, 2015), to name a few.

Over 60% of protein methylations in non-histone substrates are in proximity to a phosphorylation mark (Blasi et al., 2021). It goes without saying that phosphorylation is an indispensable mechanistic component of cellular function (Ardito et al., 2017), therefore the tight association of protein methylation to this PTM suggests its functional significance to be equally vital. It also hints towards unknown involvement of PMTs into well-established molecular pathways.

The ubiquitous involvement of protein methylation makes it a broad subject. Therefore, the protein methylations relevant to this body of work will further be explored in the following pages.

1.5 Protein Methyl Readers

There are a variety of protein domains that can recognize and bind methylated proteins, but the Tudor domain is the most prominent (Gayatri & Bedford, 2014). Its aromatic cage allows for a strong interaction with methylated positively charged residues (Vorreiter et al., 2024). For this reason, the Tudor domain structure is well adapted as a Lys and Arg methyl reader. It

contains a ~60 amino acid β-barrel-like core and is often found repeated in tandem (Jin et al., 2009). For this reason, Tudor domains display affinities to both MeK and MeR, however, Tudor domain containing protein themselves interact with either, but not both, methylated residues (Gayatri & Bedford, 2014; Wang & Bedford, 2023).

The distinctions of Lys and Arg protein methyl readers is further emphasized with other protein methyl sensing domains. MeK can additionally be recognized by the Chromo, WD40, PHD, Ank, PWWP, PHD, BAH and MBT domains, while MeR are limited to the Tudor domain (Wang & Bedford, 2023). A recent finding defined the HAT repeat domain within SART3 as a novel MeR reader (Wang et al., 2024), making it the first to join the Tudor domain in this category. This selective interaction towards either MeK or MeR, in terms of both domain affinity and type, suggest independent downstream applications of the two PTMs.

Tudor domain containing proteins can act on both histone and non-histone substrates. For instance, TDRD3 interacts with methylated H3R3, H3R17 (Yang et al., 2010) as well as MeR of RNAPII (Sikorsky et al., 2012). UHRF1, interacts with methylated H3K9 and methylated K126 of RNAPII (Vaughan et al., 2020). Similarly, SMN interacts with methylated H3K79 (Sabra et al., 2013), as well as MeR in SmD1, SmD3 in the context of snRNP biogenesis (Friesen et al., 2001). While the examples given here in no way encompass the entire breadth of TDRD3, UHRF1 or SMN interactions, it displays how the involvement of a protein methyl reader is not limited to either histone or non-histone subgroups.

Since SMN is well described, it is often used as an exemplar of Tudor domain containing protein methyl readers. As mentioned, Tudor domain containing proteins interact with either MeR or MeK (Wang et al., 2024; Wang & Bedford, 2023). Also mentioned is SMN's ability to recognize both MeR and MeK residues (Friesen et al., 2001; Sabra et al., 2013). The apparent

discrepancy in these statements makes SMN a notable exception to the MeK or MeR exclusivity rule. It is worth noting that, aside from the initial identification of SMN as an interactor of MeK in H3K79 (Sabra et al., 2013), there has been no convincing evidence for another site of MeK recognized by SMN, or of another Tudor domain containing protein methyl reader of equal bivalent ability. Therefore, based on the extensive evidence of SMN's affinity to MeR (Friesen et al., 2001; Tripsianes et al., 2011), SMN is widely considered a MeR reader.

The biological roles of protein methyl readers reflect the diversity of protein methyl marks themselves; they are broad ranging and complex. Since SMN is the protein methyl reader most relevant to this work, a comprehensive overview of its involvement in conjunction with other noteworthy contributors, will be presented in the following pages.

1.6 Protein Methyl Erasers

Methyl erasers are termed KDMs and RDMs, based on their ability to remove the methyl marks on Lys and Arg, respectively. KDMs are numerous and divided in families; the two main families being LSDs and JmjC, as determined by the catalytic core responsible for the reaction (Qu et al., 2023).

Arg methylation, while technically reversible, is a stable modification (Kouzarides, 2007). Its depletion is generally attributed to protein turnover, rather than demethylation (Wang & Bedford, 2023). Given the high energetic costs for each methylation event (Gayatri & Bedford, 2014), it reasons that their addition be made towards an enduring change.

The ample evidence of KDMs contrast strongly against the limited evidence of RDMs. So much so that the term RDM long stood as a placeholder for the presumed existence of a protein demethylase equivalent to KDMs. Still, there is an ongoing debate on the possibility of their biological relevance. As of now, JMJD6 is the only RDM candidate of histone and non-

histone PRMT substrates *in vivo* (Walport et al., 2016). It was first demonstrated that JMJD6 could demethylate H3 at Arg 2 (H3R2) and H4 at Arg 3 (H4R3) (Chang et al., 2007), followed by similar report of JMJD6 RDM activity at R469 of HSP70 (Gao et al., 2015). Other reports have also suggested RDM activity by JMJD6 (Lawrence et al., 2014; Poulard et al., 2014). However, this has been a highly contested subject and JMJD6 has yet to be confirmed as a RDM (Böttger et al., 2015; Liu et al., 2023). Recent work suggests that all KDM5s, a sub-family of the JmjC KDM family, can act as an RDM as demonstrated *in vitro* (Bonnici et al., 2023). This finding further suggests uncovered biological relevance to this catalytic reaction but leaves the current standing of RDMs as unconfirmed.

With the lack of certainty in *bona fide* RDMs, the only defined means of removal of the methyl group *in vivo* is through Arg demethylimination (Cuthbert et al., 2004; Wang et al., 2004). However, demethylimination is not a true demethylation reaction, as it does not reverse Arg to its unmodified state. Instead, it converts unmodified arginine or methylarginine residues to a citrulline in the process, therefore drastically altering its chemical properties (Walport et al., 2016). Accordingly, demethylimination antagonizes, rather than reverses the Arg methylation effect (Cuthbert et al., 2004).

The latent investigation of Arg and Lys protein methylation warrants both of their understanding in cell biology. Nevertheless, Arg methylation stands out from that of Lys, in its high prevalence (Małecki et al., 2022), distinct specificity in methyl sensing domain affinity, and apparent stability (Wang & Bedford, 2023) leaving much to be understood. As the first step of Arg methylation, PRMTs are still a new field of interest despite current research pointing towards their incredible potential as therapeutic tools in modern medicine (Wu et al., 2021).

Therefore, defining the knowledge gaps and unexplored interactions, is the first step in their push as therapeutic tools.

1.7 Protein Arginine Methyltransferases (PRMTs) in cell biology

PRMTs are an evolutionary conserved protein family with orthologues found in nearly all eukaryotic groups (Krause et al., 2007). PRMTs have been identified in fungi, nematodes, arthropods, amphibians, birds, mammals among others, with each group expressing varying numbers and iterations of PRMTs (Wang & Li, 2012). The methylations they impart have been reported to have a functional impact adapted to the diverse needs of each species with roles as evident as flowering timing in plants (Niu et al., 2007) and survival (Wei et al., 2021). Despite their uniquely adapted roles, their widespread presence and the remarkably conserved structure across species attests to the importance of this protein family in normal cell function.

In humans, nine PRMTs are expressed, which are further divided into three types depending on their methylation abilities (Figure 1). Type 1 encompass PRMT1, PRMT2, PRMT3, PRMT4 (or CARM1), PRMT6 and PRMT8, and can catalyse the formation of ω-NG-monomethylarginine (MMA) intermediate prior to catalysis ω-NG ,NG-asymmetric dimethylarginine (aDMA). Type II PRMTs consist of PRMT5 and PRMT9 which similarly catalyse the formation MMA followed by ω-NG ,N'G-symmetric dimethylarginine (sDMA). Lastly, PRMT7 is the only type III PRMT reported to only catalyse MMA reactions (Blanc & Richard, 2017). PRMT1-8 are considered the canonical members of the family (Herrmann et al., 2009) since PRMT9, to date, has only been reported to methylate a single substrate (Yang et al., 2015).

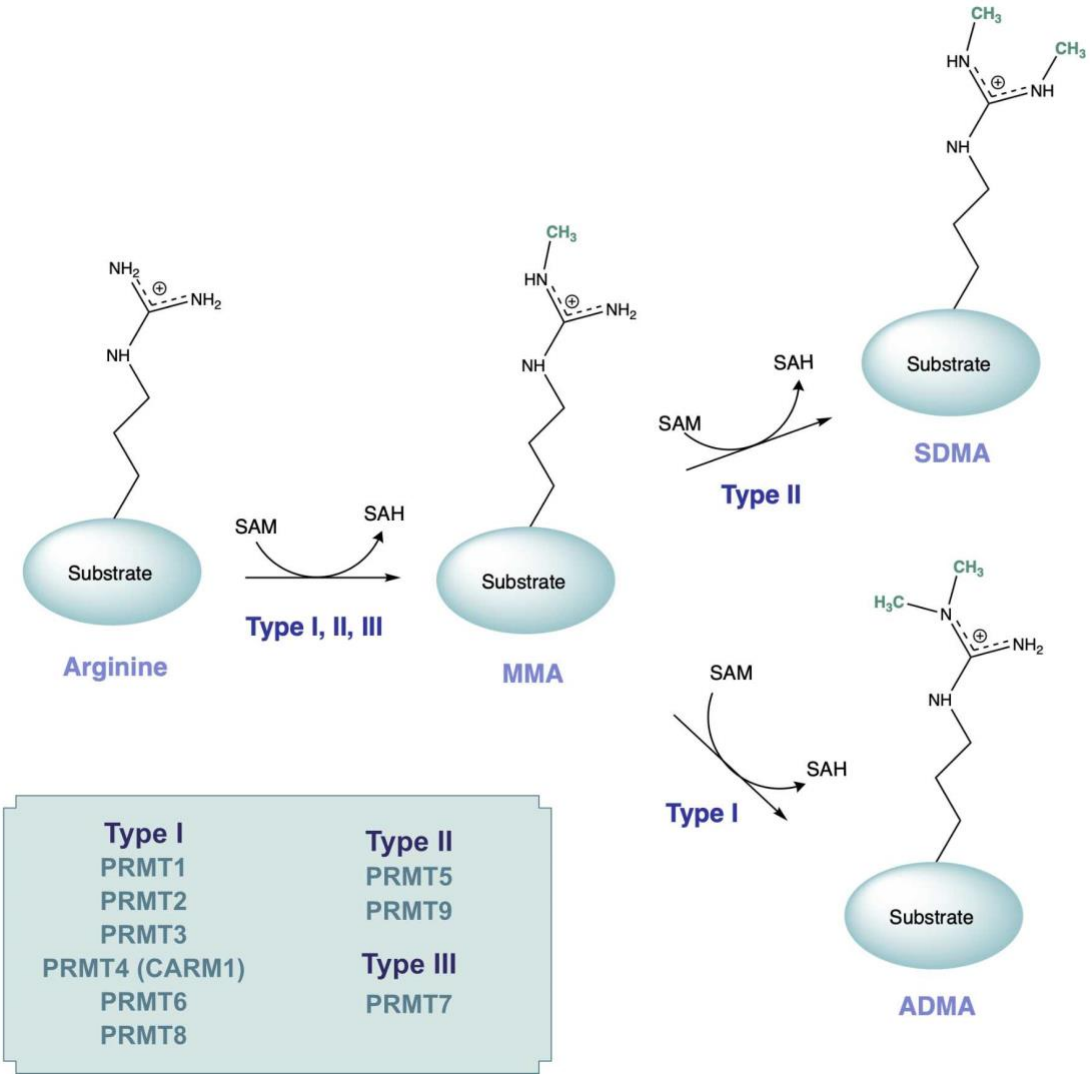

Figure 1: Overview of the arginine methylation reactions catalyzed by each PRMT type.

The PRMT family catalyzes the methylation of monomethylarginine (MMA), asymmetric dimethylarginine (aDMA) and symmetric dimethylarginine (sDMA), and are divided by type accordingly.

Initial work on PRMT methylation sites pointed towards a general preference of Gly and Arg rich motifs, denoted as the GAR motif (Najbauers et al., 1993) or RGG motifs (Chowdhury & Jin, 2023; Thandapani et al., 2013). While for the most part this remains true, this has since been further refined and expanded, more recently, with the SR-rich, DR-rich and ER-rich motifs (Wei et al., 2021).

Arg methylations are highly energetic reactions requiring 12 ATPs per methylation event (Gayatri & Bedford, 2014). The high energetic cost of this PTM heavily implies that their use be advantageous in cell survival. As such, the roles of PRMTs and the distinctions each family member carries is essential in defining how PRMT type and function come together.

It was estimated that aDMA marks surpass the combined MMA and sDMA prevalence at a ratio of about 9:1 (Maron et al., 2021; Quoc et al., 2023). Interestingly, PRMT1 alone is responsible for 85% of total aDMA (Tang et al., 2000; Thiebaut et al., 2021) and is considered the predominant PRMT. Even so, most PRMTs are consistently widespread in their expression. Aside from PRMT8's brain specific expression (Lee et al., 2005), PRMTs are ubiquitously expressed (Bedford & Clarke, 2009; Herrmann et al., 2009). Their roles, however, are not necessarily conserved between tissue and cell type, and their substrates are not necessarily mutually exclusive from each other (Herrmann et al., 2009; Hong et al., 2012). It is known that loss of a PRMT, such as PRMT1, will lead to substrate scavenging by other PRMTs, even by those of a different type. For instance, PRMT1 inhibition will lead to broad substrate scavenging by PRMT5. In the same work, it was found that the resulting global decrease in aDMA and accumulation of MMA and sDMA marks altered the stoichiometry of each type of Arg methylation (Dhar et al., 2013). Nonetheless, other work suggests that PRMT1 knockdown could

also lead to scavenging of its substrates by other Type I PRMTs (Hartel et al., 2019) thereby also imparting aDMA marks. Hence, substrate methylation could be regulated by more than one PRMT, depending on the cellular context at play. This premise of modularity expands in Tudor containing effector proteins, as they are well known to have differential affinities between MMA, aDMA or sDMA (Bedford & Clarke, 2009). For that reason, the type of methyl mark left by PRMTs can easily define the type of downstream impact carried through.

As discussed, PRMT interplay is dynamic and adaptable, but not without limits. Substrate scavenging is generally accepted as a part of PRMT biology, however, PRMTs themselves are not considered redundant. PRMT1, PRMT5 and CARM1 were found necessary to sustain life in mice (Pawlak et al., 2000; Tee et al., 2010; Yadav et al., 2003). The specific requirement of these three PRMTs indicates unique functions that cannot be carried through by other PRMT family members, placing limits on PRMT scavenging abilities. The specifics of those essential functions are not elucidated, but these findings have put emphasis on the biological relevance carried through by PRMT1, PRMT5 and CARM1, as well as the elements that make them stand apart.

1.8 PRMT Structure

Structurally, PRMTs share a common conserved catalytic core made of two domains; the AdoMet-binding domain (or Rossmann fold) situated at the N-terminal and β-barrel at the C-terminal (Tewary et al., 2019). The Rossmann fold contains most key motifs characteristic to the PRMT family; named motif I, post-I, II, III and double-E loop, while the β-barrel domain contains the THW motif (Figure 2) (Bedford & Clarke, 2009; Herrmann et al., 2009; Tewary et al., 2019). These motifs have been identified in all canonical PRMTs (PRMT1-8) and therefore have been structures of interest in the study of PRMTs.

Enzymatically, the double E loop is essential for the catalysis of the methylation reaction. The consensus motif (SEMxMGxxLxxExM) places two glutamic acid residues deep inside the substrate binding pocket, providing the negative charge needed to orient the arginine of the target substrate through the stabilization of its guanidium group (Tewary et al., 2019). This placement provides the environment needed to stabilize transfer of the methyl group from the methyl donor (SAM) to the substrate, leaving a methylated substrate and a SAH molecule by-product.

Dimerization is required for catalytic activity of PRMT1 (Zhang & Cheng, 2003), PRMT3 (Siarheyeva et al., 2012), and CARM1 (Troffer-Charlier et al., 2007), and highly suggested for the rest of PRMTs based on their conserved structural core (Tewary et al., 2019). Heterodimerization and heterooligomerization between PRMTs was also found to have functional relevance that differ from homooligomers, although their biological implications are still unknown (Hobble & Schaner Tooley, 2024).

1.9 Liquid Liquid Phase Separation (LLPS) and Membraneless Organelles (MLOs)

Beyond the local affinities of protein-protein interactions regulated by protein methylation, MeR, and therefore PRMTs, are meshed into the biology of biomolecular condensate (Hofweber & Dormann, 2019). Through LLPS, one homogenous solution can form condensates that are distinct in role and composition. P-granules, neuronal transport granule, Cajal bodies, stress granules, paraspeckles and the nucleolus are some of the condensates known to date (Hirose et al., 2022; Takakuwa et al., 2023) and due to their crucial involvement in cell biology are aptly denoted as MLOs. They typically are high in protein density and are dynamic (Wang et al., 2021), with the ability to adopt unique features for each cell type and/or conditions (Hirose et al., 2022).

Macromolecular forces contributing to MLOs include hydrophobicity, charge distribution, temperature, pH and ionic strength (Hirose et al., 2022). Since they were found in many instances to be a requirement for the formation of biocondensates, intrinsically disordered regions are heavily associated with phase separation (Elbaum-Garfinkle et al., 2015; Martin & Holehouse, 2020; Molliex et al., 2015; Nott et al., 2015). It is worth noting that globally, intrinsically disordered regions are neither necessary nor sufficient to drive phase separation. Instead, disordered regions are often rich in PTMs, contributing to their modularity in their ability to phase separate and acts as an additional level of regulation beyond protein sequence. Therefore, the disordered regions and their PTMs, particularly phosphorylation and Arg methylation, are considered the primary driving force of MLOs formation (Bah & Forman-Kay, 2016; Ibrahim et al., 2022; Orti et al., 2021; Wang & Li, 2024).

For instance, hypomethylated Arg in FUS promotes its localization to biocondensates, while the addition of an aDMA mark promoted the opposite (Qamar et al., 2018). Meanwhile, aDMAs enabled binding of FUS by SMN and is required for its recruitment to RNA granules (Wang & Li, 2024). MeRs in disordered regions are therefore not necessarily an indicator to a protein's propensity to recruit to condensates, as additional interactors are also at play. Nevertheless, a global investigation of MeRs found that aDMA of a common target site of PRMTs, the RGG motif, is heavily implicated in stress granule dynamics (Wang et al., 2022). The elements needed and events leading to MLO formation are currently a topic of interest due to the increasing evidence that they take part of disease pathophysiology, particularly in the context of neurodegeneration (Elbaum-Garfinkle, 2019; Wang et al., 2021). As such, the implications of Arg methylation in LLPS cannot be ignored as the investigation of PRMTs continues.

1.10 CARM1 (or PRMT4)

MeRs are an undeniably intrinsic part of cell biology. The type of methyl mark left by PRMTs as well as the signals causing their placement are evidently complex. While there is some redundancy to PRMT roles, their distinctions make individual PRMTs stand out across different cellular pathways. Consistent with its distinct nomenclature, one of the PRMTs with an abundance of outstanding roles is CARM1. As will be explored at length in this work, these roles range across a plethora of key cellular functions in a range of cell types. Beyond the extensive literature on the wide reach of CARM1 in normal cell function, CARM1 deregulation stands out as a contributor to disease and its promising capacity as a therapeutic target. Consequently, the exploration of CARM1's roles beyond our current knowledge is a promising step towards the discovery of therapeutic avenues. As the protein of interest in this work, the relevant literature surrounding its function will be reviewed in the following sections.

1.10.1 CARM1's Histone Substrate

As mentioned, PRMTs are known to contribute to histone methylation. H3R17 is understood to be CARM1's predominant histone methylation site, but it is also capable of methylating H3R2, H3R26 (Bauer et al., 2002; Bedford & Clarke, 2009; Ma et al., 2001; Shishkova et al., 2017). Mechanistically, the H3R17me2a mark is generally associated with transcriptional activation as the modifications act towards the recruitment of transcription factors (Wu & Xu, 2012). Interestingly, the methylation of H3R17 can also be catalyzed via PRMT6, making CARM1's most notable histone substrate under the control of more than one PRMT (Cheng et al., 2020). Still, CARM1 has undeniably strong ties to transcriptional biology since its influence is not limited to histone methylation.

1.10.2 CARM1 as a Coactivator and Transcriptional Regulator

CARM1 stands for Coactivator Associated Arginine Methyltransferase 1, and was named, at the time, on its unique ability among other PRMTs to act transcriptionally through association to nuclear receptors (NRs). In its first reported publication in 2000, CARM1's direct association to GRIP1, a member of the p160 steroid receptor coactivator family, contributed to enhanced gene transcription, thereby implicating CARM1 in co-activation biology (Chen et al., 2000). Since then, it was found that PRMT1 could also act as a coactivator (Teyssier et al., 2005; Zhao et al., 2008) and that both PRMTs could act synergistically towards p53 transcriptional activation (An et al., 2004). Nevertheless, CARM1's coactivator functions are not fully tied to PRMT1's as they both have distinctive influences.

For instance, CARM1 counts CBP and p300 as substrates (Chevillard-Briet et al., 2002; Feng et al., 2009). Both are acetyltransferases and interactors of GRIP1 via one of its activation domains. Mutations of CBP's methylated Arg led to the loss of GRIP1 transcriptional activation (Chevillard-Briet et al., 2002). On the other hand, CARM1 methylation of p300 inhibits its interaction with GRIP1 and altered its downstream transcriptional abilities (Lee et al., 2005). As such, CARM1's transcriptional regulation of GRIP1 can occur through CBP and p300 methylation.

Taken together, CARM1's influence on GRIP1 occurs in two ways, first through CBP/p300 methylation (Chevillard-Briet et al., 2002; Lee et al., 2005) and second through CARM1's direct interaction (Chen et al., 2000). As a steroid receptor coactivator, GRIP1 acts on a variety of nuclear receptors. In conjunction with CARM1, GRIP1 transcriptionally activated androgen, estrogen and thyroid hormone receptors (Chen et al., 1999). Accordingly, CARM1 carries extensive transcriptional influence via GRIP1. Still, this interaction does not fully encompass CARM1's coactivator functions.

Pax7 is a transcription factor also under the influence of CARM1. The interaction is heavily studied in skeletal muscle due to its particular relevance in myogenic biology. In satellite cells, Pax7 methylation by CARM1 recruits the necessary complexes to promote the transcriptional activation of Myf5, leading to the initiation of the myogenic program (Kawabe et al., 2012). CARM1's coactivator activity has also been identified in disease settings. In colorectal cancer, CARM1interacts with β-Catenin to activate the transcription of Wnt related genes (Ou et al., 2011). In a breast cancer model, CARM1 methylated BAF155, a member of the SWI/SNF complex, to promote oncogene activation (Kim et al., 2021; Wang et al., 2014). Also in breast cancer, CARM1 directly associated to ERα and promoted its activity (Carascossa et al., 2010). As a whole, the involvement of CARM1's co-activator or transcriptional interactions appears to be tied to the cell type, disease or biological context.

As a whole, this is not an extensive list of CARM1's co-activator or transcriptional activity. Other related interactions include SOX9, RUNX, MED12, BRD4, PARP1 and NFIB (Santos et al., 2023). Nonetheless, what is described above displays how its transcriptional influence is no small part of its function.

1.10.3 CARM1 in Splicing and RNA Biology

As discussed, CARM1 takes part of transcriptional regulation through its interaction and methylation of transcription factors. Splicing occurs co-transcriptionally and is also under the influence of transcription factors (Boumpas et al., 2023). As such the interaction and methylation of these factors with and by CARM1 extends its influence to splicing biology. For instance, CARM1 methylation of CA150; a transcription elongation regulator, was found to promote exon skipping in of the CD44 pre-mRNA transcript (Cheng et al., 2007). Other transcription elongation factors (SmB, SAP49 and U1C) were also found to be methylated by CARM1

suggesting a splicing influence beyond CA150 (Cheng et al., 2007; Saber & Rudnicki, 2022). Corroborating this, a comprehensive RNA-seq exploration found that each PRMT, including CARM1, significantly influenced alternative splicing events for hundreds of genes (Wei et al., 2021).

CARM1 continues to influence RNA biology after pre-mRNA processing. RBPs are a well-known subgroup of PRMT substrates and also known to have altered RNA interactions dependent on their MMA and aDMA modifications (Maniaci et al., 2021). In the case of CARM1, its best known RBP substrates are KSRP, HuR and HuD. For each of these, the methylation of CARM1 allowed their association with SMN and influenced their localization and/or affinity with mRNA targets (Fujiwara et al., 2006; Hubers et al., 2011; Ravel-Chapuis et al., 2022; Tadesse et al., 2008). As a primary topic in this work, the link between CARM1 and HuD will be expanded within the following pages.

1.10.4 CARM1 within Translation Biology

The role of CARM1, as well as other PRMTs, is gaining interest in translation biology for their emergence as major contributors to the process. In a global analysis of PRMT interactomes, it was found that ribosomal proteins were overrepresented within the list of putative substrates. PRMT1 and CARM1 particularly were found to be required for normal ribosomal function. The inhibition of each of these PRMTs decreased global translation as well as polysome abundance. Since the ribosomal footprint remained unaltered, the authors suggest that aDMAs are required for ribosomal complex biogenesis (Wei et al., 2021). As mentioned, the identity of ribosomal proteins part of CARM1's methylome is extensive but mostly putative since few were validated experimentally. In the same line of thought, the mechanisms involved

are for the most part unelucidated. As an emerging topic, CARM1's translation biology stands to be a hallmark as its study progresses.

1.10.5 CARM1 as a Distinct Member of the PRMT Family

In addition to CARM1's notable coactivator functions, other features make it a distinct member of the PRMT family. As mentioned, PRMTs share a catalytic core in addition to generally overlapping motif affinity; the GAR and RGG motifs (Chowdhury & Jin, 2023; Najbauers et al., 1993; Thandapani et al., 2013). Interestingly, CARM1 uniquely presents little affinity to the GAR motif (Santos et al., 2023; Shishkova et al., 2017). Instead, it diverges in capacity through a strong preference towards the PGM motif (Cheng et al., 2007), which was further narrowed to proline rich motifs (Shishkova et al., 2017). The distinctions in substrate recognition motifs and imparted methylation supports the notion that CARM1 is a mainly non-redundant member of the PRMT family, standing apart in its biological contributions.

1.10.6 CARM1 and Survival

CARM1 is among the three PRMTs required to sustain life (Yang & Bedford, 2013). While PRMT1 and PRMT5 knockouts mice models were found to be embryonically lethal (Nicholson et al., 2009; Pawlak et al., 2000; Tee et al., 2010), CARM1 knockout mice models die perinatally (Yadav et al., 2003).

The necessity of CARM1 is further associated with its enzymatic activity, as a catalytically inactivated knock-in led to the same phenotypical outcome observed of the knock-out model. While some residual coactivator activity remained in the absence of catalytic activity, it was not sufficient to rescue any phenotype (Kim et al., 2010). Another report corroborates its enzyme independent transcriptional activation functions, as CARM1, but not its enzymatic activity, was sufficient to activate NF-κB dependent gene transcription in a MEF cell model

(Jayne et al., 2009). Additionally, our group found that CARM1 interacted with nonsense-mediated decay factor UFP1 in an enzymatically independent manner to promote the decay of premature terminating codon containing transcripts (Sanchez et al., 2015).

As such, CARM1's influence is not entirely tied to enzymatic ability, but its requirement for survival does make it heavily integrated into CARM1's function.

1.10.7 Structural Features of CARM1

In addition to the common structural features of PRMTs described above, CARM1's N-terminal and C-terminal domains contains a plekstrin homology (PH) domain (Troffer-Charlier et al., 2007) and transactivation domain (TAD) (Ma et al., 2023; Teyssier et al., 2002), respectively (Figure 2). The N-terminal domain is a requirement for substrate recognition, without which there is a global reduction in CARM1 interactions (Shishkova et al., 2017). Additionally, without this domain, the methylation of CARM1 substrates was greatly diminished, strongly correlating with what was observed of a CARM1 KO model (Shishkova et al., 2017). As such, the N-terminal domain is undeniably required for CARM1 function. Meanwhile, the C-terminal domain is required for CARM1's role as a coactivator to nuclear receptors (Teyssier et al., 2002). It contains essential motifs for the interaction of transcriptional proteins (Xie et al., 2024). Other notable features include the dimerization arm (DA) and nuclear localization sequence (NLS) (Liu et al., 2018). As the name of these structures imply, the dimerization arm is mediating the dimer formation (Itonaga et al., 2024), and the NLS required for its nuclear import (Liu et al., 2018). In addition to these structures, CARM1 receives PTMs that further impact its function.

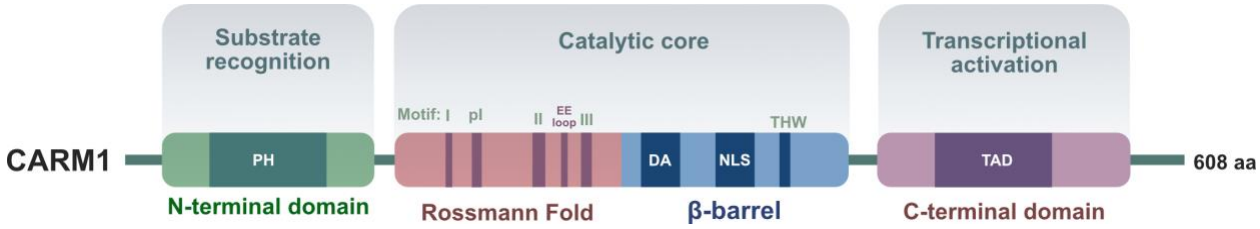

Figure 2: Schematic of the structural features of CARM1 .

In addition to the catalytic core which is conserved among PRMTs, CARM1 contains unique N-terminal and C-terminal domains which act towards substrate recognition and transcriptional activation. PH; Pleckstrin Homology domain, DA; Dimerization Arm, NLS; Nuclear Localization Sequence, TAD: Transactivation Domain. Schematic is representative of the full length protein. Not to scale.

1.10.8 CARM1 Post Translational Modifications

CARM1 is known to receive a plethora of PTMs, several of which are established as being major regulatory elements integrated into its biology. Those with a known functional impact will be discussed below.

A notable PTM of CARM1 is its own automethylation (R551). CARM1's automethylation site is located within its 15th exon, which also is excluded from one of its major isoforms. The most common isoform, CARM1FL, contains all 16 exons, whereas CARM1Δ15, is named as such for its alternatively spliced exon 15, and therefore exclusion of the automethylation site. While both have a similar composition of substrates, some exceptions applied and CARM1Δ15 had decreased overall methylation activity (Wang et al., 2013). The CARM1Δ15 isoform and automethylation deficient mutant (R551K) had reduced ERα transcriptional activity implying its automethylation take part of its transcriptional activity. When considering that nearly 100% of CARM1FL is suggested to be endogenously automethylated, this regulatory feature appears to be directly dependent on the levels at which each isoform is expressed (Charoensuksai et al., 2015;Wang et al., 2013).

Several CARM1 phosphorylation sites are known. First, its phosphorylation at site T132 by GSK-3β protects CARM1 from ubiquitination (Li et al., 2017). CARM1 phosphorylation at S217, located in its catalytic core, abrogates its methyltransferase ability, likely through the disruption of the SAM-binding pocket. It also disrupted its ERα transcriptional activation but not its coactivator related interactions, or its dimerization (Feng et al., 2009). Another group found this modification to be mediated by CDK1 (Cho et al., 2025). A phosphorylation at S228 by PKC, led to similar disruptions, but also disrupted CARM1's dimerization capabilities (Higashimoto et al., 2007). Additionally, CARM1 is phosphorylated by PKA at S448, which in a

breast cancer model allowed CARM1's direct interaction and activation of ERα (Carascossa et al., 2010). The last phosphorylation that will be outlined is S595 (or S572 in CARM1Δ15). For both isoforms, the reaction is catalyzed by p38γ. In the case of CARM1Δ15, its phosphorylation inhibited its nuclear import, but not its methyltransferase activity (Chang et al., 2018).

CARM1 is also O-GlcNAcylated at sites S595 (or S572 in CARM1Δ15), S598, T601 and T603 by OGT. In the mitotic process, these modifications altered the levels of H3R17me2, a well-known CARM1 substrate, suggesting they take part of CARM1's regulation of chromatin dynamics (Sakabe & Hart, 2010). Furthermore, the S595 O-GlcNAc modification prevented CARM1 phosphorylation, placing OGT as an upstream regulator of CARM1 function. In the mitotic process, OGT expression also altered CARM1's localization (Sakabe & Hart, 2010). Outside of the mitotic process, the modification did not impact CARM1's stability, localization, dimerization or H3R17me2 levels (Charoensuksai et al., 2015). OGT's influence on CARM1's activity, histone methylation, phosphorylation, and localization are seemingly narrowed to the mitotic process.

Lastly, CARM1 is ubiquitinated at T132 by SKP2, sending CARM1 for proteasomal degradation (Li et al., 2017; Lu et al., 2025). This modification coincides with the aforementioned GSK-3β phosphorylation site, which protects CARM1 against proteasomal degradation (Li et al., 2017). CARM1's ubiquitin mark can be removed by PSMD14, an event which stabilized CARM1 and mediated cancer progression (Lu et al., 2025).

This is not a comprehensive list of CARM1 modifications. Some modifications were found to be specific to disease models, and not necessarily representative of its typical role (Itonaga et al., 2024). Still, the investigations focusing on CARM1 modifications have found

them to be an intrinsic part of its function and regulation. As such, each modification adds an additional layer of complexity to CARM1's biology .

1.10.9 CARM1 Expression and Localization

CARM1 is ubiquitously expressed (Santos et al., 2023), but is notably highly expressed in skeletal muscle (Qiu et al., 2022). CARM1's expression patterns are further defined by the relative expression of its two isoforms. As outlined, both isoforms display different properties. Notably, the CARM1Δ15 had overall decreased methylation abilities when compared to CARM1FL and failed to act as a transcriptional coactivator (Wang et al., 2013). This factor is particularly relevant when considering that CARM1 isoforms have tissue specific expression patterns that are conserved across species. At the mRNA and protein level, CARM1FL was found to be predominant in brain, heart and muscle tissues. Meanwhile, CARM1Δ15 mRNA was expressed in conjunction with the full length protein in the lungs, ovaries, and liver (Wang et al., 2013).

As mentioned, CARM1 contains a NLS necessary for its nuclear import. As implied by its coactivator functions, CARM1 has the ability to localize to the nucleus, and can have a predominant localization to the compartment (Chang et al., 2018). However, CARM1 can also be expressed and active in the cytoplasm (Feng et al., 2009; Saber & Rudnicki, 2022). The expression levels of CARM1 in the nuclear and cytoplasmic compartments are variable, as it was found to be dependent on cell type (Herrmann et al., 2009). Its localization was also found to change according to the cellular state (Bao et al., 2018), or its PTMs (Chang et al., 2018; Cho et al., 2025). As such, while its subcellular localization is variable, CARM1's localization is recognized as being either nuclear and/or cytoplasmic.

1.10.10 CARM1 and Pluripotency

CARM1 takes part of many facets of cellular regulation. Among these roles, CARM1 has a strong association with proliferation due to its influence on pluripotency, cell cycle and its reoccurring deregulation across multiple cancers.

In embryonic stem cells, CARM1 was found to be required to maintain the pluripotent state. Its downregulation induced transcriptomic changes that promoted the expression of developmental genes and repressed those associated with self-renewal. Moreover, CARM1's overexpression in these stem cells conferred resistance to differentiation signals (Wu et al., 2009). Its expression is distinctively associated with pluripotency maintenance.

Throughout the cell cycle, CARM1's regulation via phosphorylation serves to regulate the transition between phases. CDK1 phosphorylation inhibits its activity and allows the transition from G2 to M phase and promotes mitotic entry (Cho et al., 2025). Expanding on this, it was found that CARM1's developmental contributions are carried through Yap1 and cell cycle related genes (Wnt signalling). CARM1's methylation of H3R17 was found to enhance their transcription, without which embryonic development is disrupted (Yang et al., 2019). CARM1 was found to hypermethylate the NuRD complex and to modulate the transcription of cell cycle related genes. In this context, CARM1 was found to promote cell cycle progression and proliferation in a manner dependent on its enzymatic activity (Chen et al., 2024). Therefore, CARM1's interaction with cell cycle genes and association with proliferation have been reported in many works of literature. Other studies expand on this by highlighting its involvement with aberrant cell cycle progression.

A pan-cancer systematic analysis of CARM1 expression in human tumors identifies it as being extensively deregulated in its protein levels. Across a plethora of cancer types, CARM1 was found to be overexpressed, correlating to increased proliferation and a poorer prognosis (Qiu

et al., 2022). The same correlation between CARM1 biology and cancer severity has also been extensively reported in other studies, and as such its ties to cancer biology is CARM1's main field of research interest (Bacabac et al., 2024; Cheng et al., 2013; Liu et al., 2021; O'Brien et al., 2010; Santos et al., 2023; Wang et al., 2021; Xie et al., 2024). The contributions of CARM1 towards cancer progression hints at the importance of its proper regulation in order to prevent aberrant proliferation.

Taken together, it is clear that CARM1 is a determining factor in pluripotency and proliferation. Nevertheless, CARM1 has the ability to act independently from these processes since additional roles outside the scope of proliferation have been reported. These will be explored below.

1.10.11 CARM1 in Muscle Biology

In skeletal muscle biology, CARM1 is known to be key in the maintenance and determination of satellite cell division. In this process, CARM1 acts towards the epigenetic changes required for cell fate determination. Its phosphorylation and association with p38γ prevents the CARM1 dependent transcriptional activation of Pax7 and maintains the cell in a stem state. On the other hand, without the involvement of p38γ, CARM1's activation of Pax7 initiates the myogenesis process (Saber & Rudnicki, 2022).

In C2C12 cell cultures, the methylation of HuR, a RBP and CARM1 substrate, was found to be influential in myotube formation (Ravel-Chapuis et al., 2022). Beyond myogenesis, CARM1 also contributed to the myofiber response to denervation or disuse. In the resulting muscle wasting, CARM1's expression correlated with an increase in muscle atrophy while its downregulation or inhibition was protective against the process (Liu et al., 2019; Stouth et al., 2020; Webb et al., 2023). Additionally, a muscle specific knockout of CARM1 led to

neuromuscular junction (NMJ) defects, including post-synaptic fragmentation, axonal swelling, and abnormal sprouting, along with impaired motor function (vanLieshout et al., 2022). Overall, CARM1 is involved in muscle cell maintenance, differentiation, response to muscle wasting and NMJ health.

1.10.12 CARM1 in Neuronal Biology

There is growing evidence that additional cell specific roles originate from CARM1 function. Neuronal cells have become a topic of interest in its research and frames CARM1 as a potentially important contributor to the cell type.

In PC12 cells, CARM1's methylation of HuD, a neuronal RBP in the same family as HuR, acted as a molecular switch between proliferation and differentiation. In this context, a CARM1 knockdown led to a HuD mediated increase of the p21 mRNA half-life and promoted neurogenesis when induced with NGFs (Fujiwara et al., 2006). In hippocampal cells, PKC phosphorylation and inhibition of CARM1 decreased HuD's methylation and promoted the expression of neurotrophic factors (BDNF, NGF, NT-3). The concurrent activation of PKC and inhibition of CARM1 led to an increase in branching and dendritic length (Lim & Alkon, 2012). During the differentiation of hippocampal neurons, CARM1 was found to colocalize with PSD-95, a post-synaptic marker. CARM1's knockdown led to aberrant dendritic spine morphology, including increased spine width and density, implying the involvement of CARM1 in dendritic maturation (Lim & Alkon, 2017). These findings argue that CARM1 contributes to neuronal function in the events that lead and contribute to the differentiation process.

While little else is known of CARM1 in a neuronal setting, these findings make a compelling argument for broader CARM1 contributions in neurobiology. As of yet, HuD is its best described neuronal substrate. Still, the breadth of impact surrounding its methylation is

unelucidated. It is clear that the role of CARM1 in neuronal cells is at its early stages of investigation in comparison to its other fields.

1.11 HuD

HuD is predominantly expressed in neuronal tissues and a well established regulator of neuronal functions (Akamatsu et al., 1999; Deschênes-Furry et al., 2006; Okano & Darnell, 1997). It is associated with neuronal differentiation, synaptic plasticity, regeneration, learning and memory (Dell'Orco et al., 2020; Deschênes-Furry et al., 2006). Its diverse contributions throughout these processes are attributed to its dynamic spatiotemporal regulation (Bronicki & Jasmin, 2013; Dell'Orco et al., 2020; Jung & Lee, 2021). HuD can be found in the nucleus and cytoplasm, but has a predominantly cytoplasmic localization (Burry & Smith, 2006). It also localizes to RNA granules; dynamic, biomolecular condensates (or MLOs), dense in RNA and RNPs (Antic & Keene, 1998; K. E. Bauer et al., 2023; Hubers et al., 2011; Smith et al., 2004). As an RBP, it is known to interact with several types of RNAs, including mRNAs, long non-coding RNAs, circular RNAs, micro RNAs and Y RNAs (Bronicki & Jasmin, 2013; Ryu et al., 2022; Valkov & Das, 2020). Accordingly, HuD is involved in a plethora of molecular pathways that reflect its various functions. These include alternative splicing, mRNA stability, translation and localization (Bronicki & Jasmin, 2013).

While HuD's RBP functions impact several types of RNAs, mRNAs are the most relevant type in the context of this work and also the most studied. As such, mRNAs will be the focus of this overview.

1.11.1 Splicing

The nervous system has been reported to be particularly prevalent in alternative splicing events (Lee & Irizarry, 2003). For this reason, proteins involved in the process, such as HuD, are

of particular interest in this cell type. HuD can directly interact with pre-mRNAs, RNAPII and HDAC2. Through these interactions, HuD is suggested to block the removal of acetyl marks and alter the speed of RNAPII leading to faster elongation and decreased alternative exon inclusion (Zhou et al., 2011; Zhu et al., 2007). In the neocortex of HuD knockout mice, over 300 genes were found to be affected in their splicing, most of which are related to neuronal functions (Sena et al., 2021). HuD's influence on its mRNA targets therefore starts at transcription, at the pre-mRNA stage.

1.11.2 Nucleocytoplasmic Shuttling

HuD contains a NLS and NES motif implying the ability to cross the nuclear envelope. These are contained in a linker region located between the second and third of its three RRMs which also contains the target methylation site of CARM1 (Bronicki & Jasmin, 2013; Hubers et al., 2011).

HuD's localization is particularly relevant to neuronal differentiation since its nuclear export is suggested to be required for the onset of neurite growth (Hayashi et al., 2015; Kasashima et al., 1999). In PC12 cells, RNA bound HuD interacts with TAP/NXF1 which is an export factor in the process of bulk mRNA export (Saito et al., 2004). While this interaction is not fully characterized, this suggests that HuD's export centers on the poly(A) tail of its mRNA targets as opposed to a more specific export motif (Bronicki & Jasmin, 2013; Culjkovic-Kraljacic & Borden, 2013; Saito et al., 2004). The full mechanism of its nuclear export is not fully elucidated (Bronicki & Jasmin, 2013). The same stands for its NLS. It is well known that HuD contains this motif, however it is suggested to be very weak (or non functional) since its effect was not observable (Burry & Smith, 2006; Kasashima et al., 1999). Still, a small amount

of HuD is found in the nucleus (Burry & Smith, 2006), meaning its shuttling capabilities are still unelucidated.

1.11.3 HuD Binding and mRNA Stability

HuD's binding to its mRNA targets is mediated by three RRMs. The first and second recognize AREs in the 3'UTR and the third interacts with the mRNA's poly(A) tails (Bolognani et al., 2010; Bolognani et al., 2008; Perrone-Bizzozero & Bird, 2013). For 92% of HuD's mRNA targets, its binding sites are localized within the 3'UTR with no apparent preference for poly(A) tail proximity (Tebaldi et al., 2018; Zhu et al., 2006; Zuccotti et al., 2017). As such, the whole of 3'UTRs can be subject to HuD binding. It was found that RRM1 and RRM2 were required for HuD to bind the GAP-43 mRNA, but all three RRMs were needed to mediate its stabilization (Bolognani et al., 2010). For these reasons, all three RRMs are suggested to be required for HuD to carry its function.

HuD's binding preferences have been of interest in many works. Its affinity to AREs is well reported (Akamatsu et al., 1999; Dell'orco et al., 2021; Sahoo et al., 2018; Wang & Tanaka Hall, 2001) although other work argues that U-rich sequences are a more representative motif (Table 1). In the investigation of HuD's interaction with β-actin mRNA, HuD was shown to bind a U-rich sequence that followed the 5'-ACACCC-3' motif. The 5'-ACACCC-3' sequence itself was however not required for its binding (Kim et al., 2015). Mechanistically, HuD displayed a preference towards poly(U) sequences when compared to AREs, suggesting adenosines serve to destabilise the interaction (Park-Lee et al., 2003). However, HuD does have affinity to poly(A) tails. HuD's affinity to the GAP-43 mRNA was found to be dependent on the length of the poly(A) tail. Experimentally, tails of 150 adenines had a 10 fold increase in affinity with HuD

when compared to a tail of 30 adenines (Beckel-Mitchener et al., 2002). For the most part, AREs, poly(U) motifs and poly(A) tails are associated with HuD's binding.

Table 1: HuD mRNA binding motifs

HuD Binding Motifs	Reference
5'-AUUUA-3' 5'-AUUUUA-3' 5'-AUUUUUA-3'	(Chung et al., 1996)
5'-UU(AUUU)$_n$AUU-3' (Where n≥3)	(Park et al., 2000)
5'-CCCUCCCUCUCUC-3' 5'-UUUUGUUUUGUUU-3' 5'-UUUUUUUUUUAAA-3'	(Bolognani et al., 2010)

Genes such as *p21* (or Cdkn1a) (Fujiwara et al., 2006; Hubers et al., 2011; Joseph et al., 1998), *Marcks* (Wein et al., 2003), *HuD* (Borgeson & Samson, 2005), *HuR* (Dai et al., 2012; Mansfield & Keene, 2011), *App* (Kang et al., 2014), *Bdnf* (Allen et al., 2013; Vanevski & Xu, 2015), *Nova1* (Ratti et al., 2008), *Ache* (Deschênes-Furry et al., 2007), *GAP-43* (Mobarak et al., 2000) and *Tau* (Aranda-Abreu et al., 1999) are recognized as *bona fide* HuD mRNA targets. Among these, *GAP-43* is HuD's best characterized mRNA target. As such, the mechanisms surrounfing its regulation are often used as an example of HuD function.

It was found that altering HuD's expression levels correlated with GAP-43's mRNA stability and levels. This further carried on at the protein level, since HuD's overexpression correlated to an increase in GAP-43 expression (Mobarak et al., 2000). Mechanistically, deadenylation is at least partially at cause for the correlation. *In vitro* work found HuD increased the stability of the GAP-43 mRNA by decreasing the rate of deadenylation; an early event of mRNA degradation (Beckel-Mitchener et al., 2002). Evidently, as discussed, the p21 mRNA is also subject to changes in stability in accordance to its HuD binding (Fujiwara et al., 2006;

Hubers et al., 2011). Similar observations on stability and expression were observed of other mRNA targets, making this a key functional role of HuD's (Lim & Alkon, 2012; Ryu et al., 2022). Collectively, the binding motifs of each mRNA and the capacity of HuD to bind the mRNA can have a determining impact on the stability of its mRNA targets.

1.11.4 Translation

HuD's influence on its mRNAs extends into the translation process. Through HuD's interaction with eIF4a and the mRNA's poly(A) tail, HuD can enhance their translation. Without both of these interactions, HuD is unable to induce the neurite outgrowth of PC12 cells associated with its overexpression. Interestingly, the RRM3 and linker region alone were able to cause the outgrowth. In other words, the RRM3 binding at the poly(A) tail and its interaction with eIF4a is sufficient to cause the increase in translation (Fukao et al., 2009). This suggests a general translational control as opposed to a more selective motif.

In a MN cell line (NSC-34), HuD enhances the translation of genes associated with differentiation and axonogenesis. In this setting, Y3 RNA was found to compete with mRNAs for HuD binding and prevent its recruitment to polysome (Tebaldi et al., 2018). Therefore, the mRNA's affinity with HuD and ability to compete with Y3 is a determining influence on the pool of mRNAs translated.

Notably, there is an exception to HuD's translation enhancing functions, as it could translationally repress p27. This occurred via an IRES element in the 5'UTR as opposed to its most prevalent 3'UTR affinities discussed so far (Kullmann et al., 2002; Tebaldi et al., 2018). Consequently, translation inhibition by HuD is possible, but what is known of the process suggests that this process might not be representative of its most abundant affinities.

Taken together, HuD has the ability to regulate its mRNA targets beyond its ability to stabilize transcripts through its interactions with translational proteins.

1.12 CARM1 in Motoneurons

CARM1's influence over HuR and HuD, two members of the Hu RBP family, suggest that the interactions have broader significance in muscle and neuronal cells. Accordingly, our group followed through the neuromuscular implications of these interactions and have identified CARM1 to have a particular relevance to the MN cell type. In fact, in MN-1 cells (a MN derived cell line) the downregulation of CARM1 was found to be sufficient to induce differentiation suggesting it is a major contributor to the process (Hubers et al., 2011).

As previously mentioned, CARM1 was found to methylate HuD in PC12 cells, acting as a molecular switch between proliferation and differentiation (Fujiwara et al., 2006). Our group determined that this interaction was replicated in the MN-1 cell model. Mechanistically, the methylation of HuD at R248 by CARM1 decreased its affinity to the 3'UTR of the p21 mRNA and maintained the cells in a proliferative state. This identified a novel mean of influence on HuD's affinities and solidified CARM1 as a regulator of its function in MNs (Hubers et al., 2011). As such, it is clear that CARM1 takes part of MN biology through the regulation of cell cycle, and that its influence is at least in part carried through by HuD.

CARM1 also contributes to HuD's regulation in MNs outside of its mRNA affinities. Our group found that CARM1's methylation of HuD at R248 was required for its interaction with the SMN protein. Functionally, SMN recruited HuD and its associated mRNA targets (*Tau* and *GAP-43*) to RNA granules and colocalized with HuD in the neurites of differentiated MNs. (Hubers et al., 2011). Moreover, without SMN HuD failed to localize to axons coinciding with a decrease in axonal poly(A) containing mRNAs (Fallini et al., 2011). As such, CARM1

methylation of HuD is crucial for its interaction with SMN which branches into broader implications for the axonal localization of its mRNA targets.

As mentioned, SMN is a protein methyl reader and effector protein of methylarginines. SMN stands for *survival motor neuron* for its apparent requirement for MN health. Its loss is characteristic of SMA, a neurodegenerative disease known for the specific vulnerability of its MNs (Burghes & Beattie, 2009). The cause of this vulnerability is an ongoing point of interest. Despite SMA having a clear etiology, the events connecting SMN loss to MN vulnerability have proved to be complex and numerous (Boyer et al., 2010; Hunter et al., 2014; Lauria et al., 2020; Murray et al., 2013; Shafey et al., 2008; Sharma et al., 2024). However, our group found that HuD's overexpression rescued the defects associated with SMN's loss in MN-1 cells. Specifically, HuD overexpression in shSMN MN-1 cells rescued the recruitment of RNA granule markers (KSRP and Staufen) and one of its mRNA targets (*GAP-43*) to dense RNA granules. It also increased the number of cells that displayed longer neurites (Hubers et al., 2011). As such, HuD can contribute to processes associated to SMN function and MN function. This strongly implies that HuD carries roles essential for MN health.

As a whole, there has been little work focused on HuD's contributions to the MN cell type, and even less in conjunction with CARM1. What we know of the proteins so far hint at an additional contribution to the MN phenotype that warrant more investigation.

1.13 Project Rationale

The multi-functionality attributed to CARM1, places it as a necessary part of basic cellular function, as well as that of specialized tasks. Accordingly, the functional impact of CARM1 in neuronal cells is well accepted but has yet to be broadened and solidified within the landscape of neurobiology. As CARM1's best described neuronal substrate, HuD brings forward the notion that CARM1 has so far undescribed roles both outside and within this interaction. To date, both CARM1 and HuD have scarcely been investigated in the context of MNs.

In the case of CARM1, the lack of neuron specific exploration suggests that the full scope of CARM1 interactions has yet to be determined. It cannot be ruled out that the methylation of other substrates are part of neuronal pathways so far not considered to be within CARM1's scope of influence. With so little known about its neuronal substrates, the investigation of its proteome is needed to fully contextualize its function in this cell type.

As for HuD, while the exploration of its mRNA targets has been of interest in many studies done to date, the MN cell type has been mostly omitted. This leaves a gap in our understanding of HuD's role in MNs. Additionally, the functional relevance of CARM1's methylation of HuD on cell cycle in MNs through a change in its affinity to the p21 mRNA implies that other mRNAs could be impacted in a similar way. As such, expanding the identities of HuD mRNA targets in MNs subject to CARM1's influence could consolidate the CARM1 and HuD interaction as a notable mechanism in MN health.

Taken together, what is known of CARM1's role in MN is shaping it to be a contributor to cellular mechanisms not yet attributed to its function. Through HuD methylation, CARM1 has the potential to influence the landscape of its mRNA targets and sway its many neuronal functions. In addition, the evident impact of CARM1 in MN through HuD is suggestive that its

role is not limited to a single substrate, but likely to have a broader reach. Accordingly, the exploration of CARM1 in MN through its impact on HuD and other potential substrates is a promising first step into defining the full scope of its impact.

Hypothesis

CARM1 can alter HuD's landscape of mRNA targets and contribute to MN proteome methylation.

Objective 1

i. Identify the full spectrum of HuD mRNA targets influenced by CARM1 in MNs

ii. Determine which mRNA motifs within HuD's mRNA targets are influenced by CARM1

iii. Determine which roles within HuD's mRNA targets are influenced by CARM1

Objective 2

iv. Identify CARM1 substrates in MNs

Chapter 2 Materials and Methods

The methodology described here encompasses the work of Chapter 3, 4 and 5, as well as the Supplementary data.

2.1 Cell culture

Motoneuron derived cell line (MN-1) cells (Salazar-Grueso et al., 1991) were grown in L-Glutamine free DMEM (Dulbecco's modified Eagle's medium) (09354; GIBCO) supplemented with 10% heat inactivated FBS (fetal bovine serum) (080150; Wisent), 100 U/ml penicillin streptomycin (SV30010; Cytiva), and 2 mM of L-Glutamine (25030081; GIBCO). C2C12, 293T, Hela, MCF7 and MDA-MB-231 cells were obtained from ATCC and grown in DMEM (319-015-CL; Wisent) supplemented with 10% FBS (080150; Multicell) and 100 U/ml penicillin streptomycin (SV30010; Cytiva). NIH3T3 were obtained from Dr. Livio Pellizzoni from Columbia University and cultivated as described for MN-1 cells. Patient fibroblasts from the Coriell Institute (GM00232F, GM08333C, GM03813F, GM03815B, GM03814F) were grown in MEM (10370021; Gibco) supplemented with 20% non heat inactivated FBS (080150; Wisent), 100 U/ml penicillin streptomycin (SV30010; Cytiva), and 2 mM of L-Glutamine (25030081; GIBCO). All cells were kept in a humidified incubator at 37°C and 5% CO2 and tested for mycoplasma routinely through a PCR detection kit (G238; Abm). All experiments were conducted before the cells reached 25 passages.

2.2 Mice tissues

Animal procedures were approved by the University of Ottawa Animal Care Committee and comply to the Canadian Council on Animal care guidelines and the Animals for Research Act (protocol #: CMMb-3995).

The brains and livers of healthy carriers of the spinal muscular atrophy SMNΔ7 transgene (Le et al., 2005) or gastrocnemius muscles of $SMN^{2B/-}$ SMA (Bowerman et al., 2012) mice models were excised and snap frozen in liquid nitrogen before being crushed into a powder prior to sample preparation.

2.3 Plasmids and stable cell lines

The human CARM1 open reading frame sequence was subcloned into the pEGFP-N1 empty vector using the Gibson method. The GFP tag (EGFP) is located at the C-terminal end. A site directed mutagenesis was used to create the CARM1 E266Q catalytically inactive mutant. The plasmids were amplified through transformation of DH5α E. Coli competent cells for amplification (see below). The correct insertion, sequence and mutation of each plasmid was validated through sequencing (Génome Québec services).

The stable MN-1 cells expression pGIP-Z or pGIP-Z shCARM1 used throughout this work were previously described (Hubers et al., 2011), and maintained in 2 μg/mL puromycin (Wisent Bioproducts, 400-160-EM).

To generate stable MN-1 cells, the pEGFP-N1, pEGFP-N1 CARM1 and pEGFP-N1 CARM1-E266Q were transfected as described below into WT MN-1 cells and selected with G418 at a concentration of 2000 μg/mL and maintained at a concentration of 200 μg/mL. The cells were sorted by flow cytometry to select for a cell population expressing GFP in comparable intensity between the three stable cell lines.

2.4 Transfections

A total of 8 μg of DNA (pEGFP-N1, pEGFP-N1 CARM1 and pEGFP-N1 CARM1-E266Q constructs) and 16 μg of PEI was incubated with pre-warmed Opti-MEM (Gibco, 31985070) for 5 min. After combining the DNA and PEI (Millipore Sigma, 764965), the samples were further incubated for 15 min before adding to 10 cm plates of 80% confluent MN-1 cells in Opti-MEM. After 3h30 incubation at 37°C, the transfection media was removed and replaced with their standard culture media. The cells were incubated for a duration of 48h prior subsequent use.

2.5 Bacterial transformation

DH5α and BL21 competent cells were mixed with a 200 ng of plasmid DNA and incubated on ice for 30 min. The samples were heat shocked at 42°C for 30 sec prior to a 5 min incubation on ice. 500 μL of pre-warmed LB at 37°C was added to the bacterial mix and incubated in a shaker for 1h. The bacterial culture was serial diluted in LB and spread on LB agar plates containing either 100 μg/ml ampicillin or 50 μg/mL kanamycin. The plates were incubated upside down in a 37°C incubator overnight. Each colony was picked and grown in LB containing ampicillin (Sigma, A9518) or kanamycin (100 μg/ml or 50 μg/mL respectively) for subsequent use.

2.6 GST recombinant fusion protein purification

Recombinant human HuD was inserted in the pGEX-4T2 backbone and transformed as described in BL21 competent E. Coli cells. A colony formed from the transformed cells was introduced to 1L of LB broth containing ampicillin and placed in a 37°C shaker until the exponential phase, i.e. when optical density at A_{600} reached about 0.6. An aliquot was conserved at this step as a control towards the confirmation of induction. IPTG was added to a final concentration of 0.2 mM and incubated on a shaker at 37°C for 4 hours, at which point an aliquot was conserved to

confirm the induction was successful. The bacterial culture was pelleted and resuspended in PBS supplemented with protease inhibitors (04693159001, Roche) and sonicated on ice. The cell debris was pelleted out of the sample and the supernatant mixed with 1% (v/v) Triton X-100 and 500 µl of 50% GST bead slurry for overnight tumbling at 4°C. The beads were pelleted, and an aliquot of the supernatant was conserved to confirm the affinity purification. The beads were washed in PBS with 1% Triton X-100 twice followed by a 5 min tumbling in PBS. The beads were pelleted, at which point an aliquot was set aside and mixed with Laemmli as a control for bead elution of the product. The remainder of the beads were mixed with a 32.5 mM Glutathione (G6529, Sigma) in PBS (pH 7.5) for tumbling at 4°C for 5 min, and heated at 37°C for 30 sec. This step was repeated four times, and the elution product set aside, and combined each time. An aliquot of the beads after the elution was set aside towards elution confirmation. 5 mL of PBS was added to the elution product, which was dialysed in a semi-permeable dialysis membrane (Spectrumlabs, 132 650) in 4L of PBS overnight at 4°C. The dialysis product was concentrated in a 10 kDa MWCO centrifugal filter tube (UFC9010, Millipore) until a final volume of about 500 µL was reached. The concentration of the final purified product was quantified through a Bradford Assay (DC protein assay, Biorad) for subsequent use.

2.7 Sample buffers

The standard 5X sample buffer consists of 250 mM Tris-HCl pH 6.8 (Multicell; 600-125-IK), 10% (w/v) SDS, 0.5M DTT (Fisher; BP166-500), 50% (w/v) Glycerol (Fisher; G31-1), 25% βME (MP Biochemicals; 190242) and 0.1% (w/v) bromophenol blue (Bio-Rad 161-0404) in water. The adapted 4X sample buffer consists of 200 mM Tris HCl pH 6.8, 24 % (w/v) SDS, 40% (w/v) Glycerol, 25% βME and 0.1% (w/v) bromophenol blue in water.

2.8 Sample preparation

Cells pelleted in PBS and mice tissue powder were resuspended in RIPA lysis buffer (100 mM Tris pH7.4, 100 mM NaCl, 1 mM EDTA, 1% NP-40, 0.5% (w/v) NaDOC and 0.1% (w/v) SDS in water) completed with complete protease inhibitors (04693159001, Roche) and 10 μg/mL PMSF before use. Cells were incubated on ice and vortexed intermittently for 15 min. Mice tissue powder samples were snap frozen in liquid nitrogen and vortexed repetitively, for 1h. Samples were centrifuged 15 min at 4°C at 13 000 rpm and supernatant collected. The protein concentration was determined through a Bradford Assay (DC protein assay, Biorad). These concentrations were considered for the preparation of samples, mixing with the specified sample buffer and heat denatured at 95°C for 8 min unless otherwise specified.

2.9 SDS-PAGE

The samples were resolved by SDS-PAGE with gels made of a 4% acrylamide stacking gel layer followed by a 10% acrylamide resolving gel and transferred on a nitrocellulose membrane (Biorad, 1620112), making sure to preserve the stacking gel. The membranes were blotted in 5% non-fat milk in PBS-T (with 0.05% Tween-20) prior to immunoblotting.

2.10 Antibodies and Immunoblotting

For western blotting, the antibodies used were; CARM1 from Cell Signalling Technologies (3379S) 1 :1000, GFP from ChromoTek (3H9-100) 1 :1000, PRMT2 from Proteintech (66885-1-Ig) 1 :1000, PRMT6 from Bethyl (A300-929A) 1 :3000, PRMT7 form Cell Signalling Technologies (14762s) 1 :1000, GAPDH from BioLegend (MMS-580S) 1: 3000, α-Tubulin from Millipore Sigma (T6199) 1: 10 000, Ptger4 from Proteintech (24895-1-AP) 1:1000, Smarca2 from Invitrogen (HL1115) 1:1000 and Adra2B from Abcam (ab151727) 1:1000. The

PRMT5 and PRMT1 antibodies were made in house. The HuD antibody used for WB purposes was from Santa Cruz (sc28299) 1:500. The H3R17 dimethyl antibody from Sigma (07-214) was used at a dilution of 1:2500. All antibodies were diluted into a gelatin blocking buffer for immunoblotting. Li-Cor IRDye 680LT Goat anti-Mouse IgG (926-68020) and IRDye 800CW Donkey anti-Rabbit IgG Secondary Antibody (926-32213) fluorescent secondary antibodies, or Horseradish Peroxidase (HRP) conjugate secondary antibodies (Jackson ImmunoResearch Laboratories Inc., 211-032-171, 112-035-175 and 115-035-174) and HRP substrate (Millipore, WBLUF0500) were used to visualize immunoblotting.

2.11 Statistical analysis

Statistical analyses were performed using paired or unpaired two tailed Student's t-test or One Way or Two way ANOVA with Tukey's or Dunnett's multiple comparisons test. All analysis and bar graphs were made with GraphPad Prism software (Version 10.2.2 (397)). $P<0.05$ was used as a threshold for significance. Error bars represent ± SEM (Standard Error of the Mean) or SD (Standard Deviation), as specified in figure captions.

2.12 HuD RNA Immunoprecipitation

A total of six to eight 10cm plates containing ~80% confluent MN-1 cells stably expressing pGIP-Z or pGIP-Z shCARM1 vectors were washed and scraped into PBS. The cells were pelleted, PBS aspirated and lysed in RIPA buffer as described under "Sample Preparation", but with the addition of 0.2 mM DTT (V3155; Promega) and 0.42U/mL RNAse out (10777019; ThermoFisher). The lysis was done on ice over the course of 40 min, pipetting up and down intermittently. The samples were pelleted three times, moving the supernatant to a new tube each time. The lysate concentration was then quantified using a Bradford Assay (DC protein assay,

Biorad). Each IP reaction was done within a final volume of 1ml containing 1.5 mg of protein and completed with RIPA buffer. An additional set of samples containing a 5% or 10% aliquot of input lysate was set aside as a loading control. The HuD IP set (Input, IgG, IP) were prepared in triplicates; one used towards the confirmation of efficient IP, and two for RNA extraction. The IP samples were pre-cleared with 20 µL of 50% slurry of Protein A/G agarose (sc-2003; Santa Cruz) for 20 min prior to sample centrifugation, removal of beads and addition of 3.75 µg of primary Ab α-HuD (Ab96474; Abcam) or 3.75 µg of rabbit IgG (homemade) for overnight tumbling at 4°C. After tumbling, 20 µl of a 50% slurry of Protein A/G agarose (sc-2003; Santa Cruz) was added, and samples tumbled for an additional hour. After pelleting the beads, the flow through was set aside, and beads washed 5 times with 1 mL of RIPA buffer. Laemmli was added to samples intended to be used for IP confirmation, or 1 mL of Trizol (15596026; Invitrogen) for samples intended for RNA extraction. The RNA extraction was performed as recommended by the manufacturer. The duplicate RNA pellets were resuspended together in 20 µL of RNAase free ddH2O for subsequent use.

2.13 HuD RIP Sequencing and Analysis

The RNA product from the HuD RIP triplicates was pooled prior to sequencing. For the HuD IP samples, the volume of RNA product used was normalized to the IP efficiency. The 10% input lysate samples, and IgG samples were pooled in equal volumes. The pooled RNA product was sent for library preparation and sequencing to Génome Québec. The RNA was analyzed through Bioanalyser, underwent NEB rRNA-depleted (HMR) stranded library preparation, and Illumina Library QC. Both the 10% inputs and IP products were found to pass the quality control and were used for sequencing. The Rb IgG samples did not contain enough RNA for sequencing and

were excluded from further analysis. The samples were sequenced using Illumina NovaSeq 6000 S2 PE100 - 50M reads.

On the Galaxy server (Abueg et al., 2024), the FASTQ sequencing data was mapped to the GRCmm38.p6 (mm10) mouse genome using STAR (Version 2.7.5b) (Dobin et al., 2012), read counts compiled using htseq-seq count (Version 0.9.1) (Anders et al., 2014), and the differential expression analysis done using GFOLD (V1.1.4) (J. Feng et al., 2012). The data was plotted in Perseus (Version 2.1.2.0) (Tyanova et al., 2016). Motif analysis was performed using MEME (Version 5.4.1) (Bailey & Elkan, 1994). The length of the motif discovery parameters was specified to range from 6 to 15 bases. STAR, ht-seq count, and MEME was used through the Galaxy server (Abueg et al., 2024). Gene ontology analysis was performed using g:Profiler (Raudvere et al., 2019).

2.14 RT-PCR

After the HuD-RIP, a total of 5 μL of RNA product was used for RT-PCR purposes. The RNA was primed with oligo-dT and at 65°C for 10 min and reverse transcribed in a solution of RNasin (Promega, N251), dNTP (Promega, U1515), and AMV-RT (Promega M510) at 42°C for 1h. The reverse transcription product was diluted for each product and amplified by PCR using GoTaq (Promega, M7123). The primer sequence used for each RNA target is further described in Supplementary Table 3. The PCR product was then run on a 1% agarose gel containing 1 μg/mL EtBr (Bio Basic, D0197) and imaged by using a transilluminator.

2.15 Densitometry Analysis

Quantification of signal was performed using Fiji (ImageJ2 Version 2.14.0/1.54f) (Schindelin et al., 2012) or ImageStudio (Version 5.5.4).

2.16 GFP-AP/MS

Stable MN-1 cells expressing pEGFP-N1, pEGFP-N1 CARM1 and pEGFP-N1 CARM1 E266Q constructs were used for GFP AP/MS, adapted from Trinkle-Mulcahy et al., 2008. A total of 15 mg of protein lysate of each cell line was used for each GFP-AP reaction using commercial GFP beads (Chromotek, gta-100). The GFP-AP bead product was used in an acidic elution step according to the GFP-Trap beads manufacturer's protocol and analyzed by MS. The MS data was analyzed using Perseus, using a Student's T test (Version 2.1.2.0) (Tyanova et al., 2016).

2.17 Histone methylation confirmation

The methylation of histones was adapted from Lee et al., 2002, using MN-1 cells transfected with pEGFP-N1, pEGFP-N1 CARM1 and pEGFP-N1 CARM1 E266Q constructs as described above. Histones were used as a substrate for CARM1 (Sigma, H9250).

2.18 Radiolabelled methylation assay

Recombinant CARM1 was purchased from Active Motif (Cat# 81807) and used as an enzyme source for the radiolabelled methylation reactions. A total of 4μg of CARM1 was incubated with 5μg of the substrate of interest; GST (purified as above), GST-HuD (purified as above), Histones (Sigma, H9250), GST-OGT (1-400aa) (Proteintech, Ag2160), OGT (606-1022aa) (MyBioSource, MBS1123899), RPS7 (MyBioSource, MBS204398), Alix (Pdcd6ip) (Origene, TP303735) at 37°C with 50 mM of Tris-HCl pH 7.4 and 0.55 μCi of SAM[^{3}H] (Perkin Elmer, NET155V250UC) for 2h, mixing the samples intermittently. The totality of the samples was passed through a nitrocellulose membrane using a Dot-Blot System (Schleicher & Schuell Minifold I system) and washed with PBS. The membranes of the wells of interest were cut and places in 2 mL of Cytoscint (MPbio, 882453). The ^{3}H ionizing radiation signal of each sample

was recorded as CPM using a radioisotope counter (Tri-Carb 4910TR Beta Liquid Scintillation Analyzer) throughout a 10 min read period.

Chapter 3 Biochemical Properties of CARM1: Impact on Western Blotting and Proteomic Studies

The rationale of the project outlined in this thesis is heavily dependent on the assessment of CARM1 protein level in MNs through WB. While this is not an outstanding methodology, the results observed with CARM1 were misleading. Under standard conditions, CARM1 was difficult to detect, even becoming undetectable by WB. If detectable, the observable signal was inconsistent with the predicted outcome. With persistent inconsistencies and without the ability to reliably assess CARM1 protein levels, it became clear that its study would be hindered. Therefore, to undergo the investigation of CARM1 premised by this work, I set out to understand the basis of these difficulties and define reliable means of its detection by WB.

The findings described in this chapter were published and adapted from;

Biochemical Properties of CARM1: Impact on Western Blotting and Proteomic Studies

Julie Bourassa, Genevieve Paris, Laura Trinkle-Mulcahy, and Jocelyn Côté

ACS Omega 2024 9 (38), 40204-40213

DOI: 10.1021/acsomega.4c06360

3.1 Defining CARM1 behavior in WB

WB is most often coupled with SDS-PAGE as a universal analytical tool for protein assessment warranted by its applicability to most proteins allowing for direct size comparison and quantification without confounding factors such as bulk or intrinsic charge. In the first step of the technique, standard practices of sample preparation call for protein denaturation by heating samples at 95°C for 5-10 min in the presence of Laemmli buffer composed of dithiothreitol (DTT), 2-mercaptoethanol (βME), Tris-HCl and sodium dodecyl sulfate (SDS). In this sample buffer, DTT or βME serve to break disulfide bonds preventing the formation of covalent bonds through cysteine residues. All the while SDS, a surfactant and strong denaturant, gathers around the peptides and promotes denaturation through its hydrophobic and hydrophilic moieties (Krainer et al., 2020). During the denaturation process, SDS binds denatured protein along their backbone and provides a uniform negative charge acting as a driving force for protein migration during SDS-PAGE. After size separation, the proteins are bound to a membrane which can further be used for immunoblotting (IB), visualization, and quantification.

The process of sample preparation for SDS-PAGE, is often inferred in the methodology of published work, leaving ambiguity in the conditions used in such a crucial step of western blotting. After its original definition (Laemmli, 1970), sample preparation is understood to have variability in its practice (Kurien & Scofield, 2012; Litovchick, 2018), as defined by user preference. As such, there is no true specification of a standard. Importantly, although there is a range of conditions belonging to the standard of procedure, these conditions have successfully been used and remain compatible with most proteins. Using the conditions successfully used by our group in the past, it was repeatedly found that the observed CARM1 IB signal often went against the predicted outcome.

For instance, MN-1 cells stably expressing GFP tagged CARM1 or CARM1 E266Q (catalytically inactive mutant) (Cheng et al., 2007) fusion proteins, displayed an apparent decrease of endogenous and exogenous CARM1 signal at their predicted molecular weight (63 kDa and 90 kDa, respectively) (Figure 3A, top panels) across sample of increasing protein amounts. The loss of the anticipated band correlated with the increased signal of a band at a larger size (>180 kDa), or at the junction between the resolving and running gel. The same pattern in signal was observed using GFP IB as secondary validation (Figure 3A, bottom panels). This concurrent shift suggests that CARM1 can assemble into large protein aggregates surpassing the maximum threshold for gel migration. Given that this trend is observed for both endogenous and exogenous CARM1, it is unlikely that the aggregates are an artifact of the constructs and additionally argues against the requirement of CARM1 catalytic activity for aggregation. It can be concluded that the size shift of the protein signal consists of CARM1 aggregation which prevents its migration through the gel. Given this property, only considering the predicted signal would erroneously imply an inverse correlation between detectable CARM1 protein levels and total protein amount for the same sample. Overall, under these standard conditions CARM1 protein signal should not be interpreted at face value.

3.2 Heat denaturation as a contributor of CARM1 aggregation

To resolve the events leading to CARM1 aggregation, the effect of temperature was investigated. Standard procedure of sample preparation (as shown in Figure 3A) relies on the heating of samples at 95°C for 5-10 min in the presence of sample buffer for protein denaturation (Kurien & Scofield, 2012; Litovchick, 2018). Heat is a known factor in protein aggregation (Ng et al., 2021). To test if high denaturing temperatures are a driving factor for CARM1 aggregation, the samples were exposed to lower temperatures for increased amounts of time with the aim of

achieving protein denaturation while avoiding aggregation (Figure S1). The resulting blots reveal that CARM1's signal remained visible at its expected molecular weight, but streaked from the top of the gel, acting as an intermediate between proper migration and complete aggregation. This was confirmed with GFP IB which matched CARM1's streaked signal pattern. In addition, the proportion of CARM1 migrating at its expected size was inversely proportional to the amount of total protein loaded (as shown in Figure 3A) and temperature, indicating a dependence on both temperature and protein concentration for aggregation.

With evidence that heat denaturation contributed to CARM1 aggregation, CARM1's ability to migrate through the gel without heat denaturation was tested. Here (Figure 3B), the samples are incubated at room temperature in standard sample buffer before running on a gel. CARM1 was able to migrate properly into the gel without detectable aggregations. As expected, CARM1 runs lower than its expected size due to its partially denatured state, most likely adopting a more compact conformation. The doublet is indicative that a subset of CARM1 protein was able to fully denature without the need for heat denaturation. Interestingly, CARM1 aggregates are so large that they can barely migrate into the stacking buffer (4% acrylamide), reflecting the widespread interlinking of the CARM1 proteins. Hence, to avoid CARM1 aggregation and allow complete protein migration heat denaturation must be avoided.

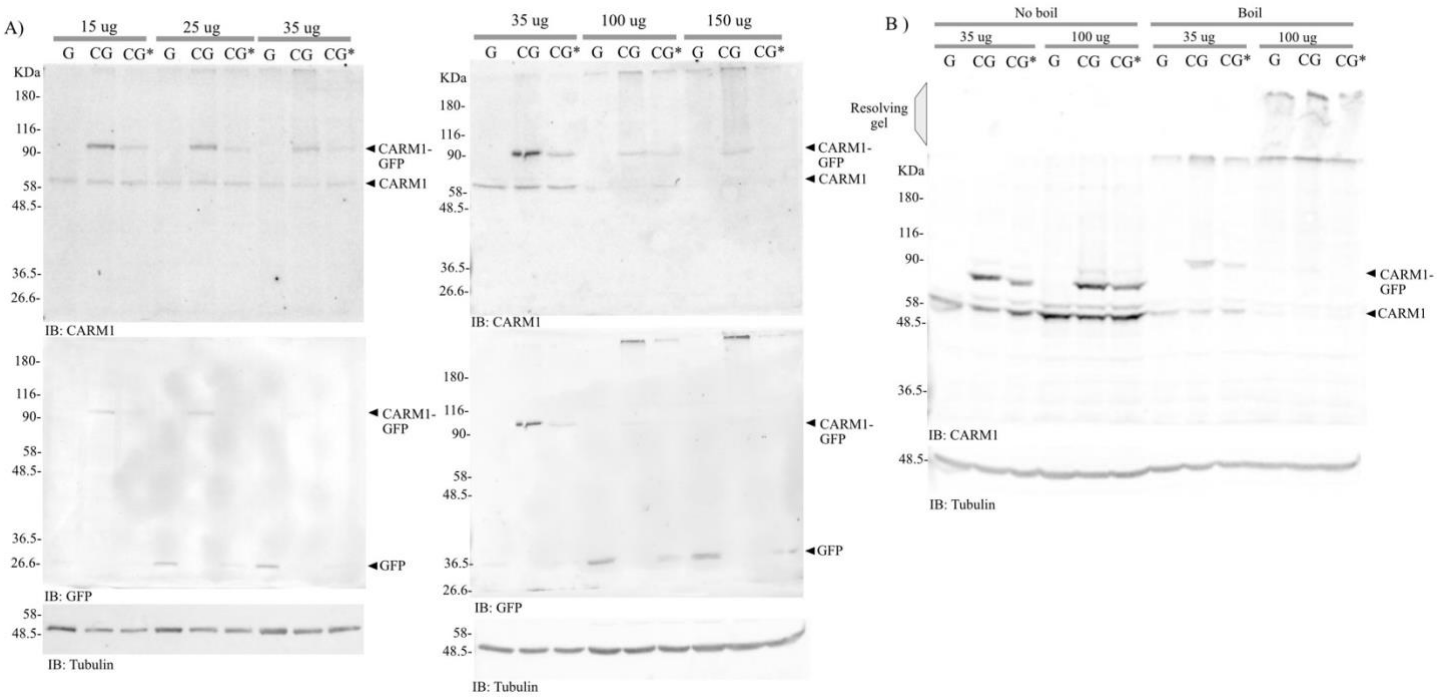

Figure 3: CARM1 aggregation is dependent on the amount of protein sampled.

Aggregation of CARM1 with loading samples of increasing protein amount (A,B), with or without heat denaturation (B). Protein lysates were prepared from MN-1 cells stably expressing GFP (G), CARM1-GFP (CG) and CARM1-GFP E266Q (CG*), mixed with standard sample buffer and either heated for 8 min at 95˚C (boil) or incubated at room temperature (no boil) before resolving by SDS-PAGE and immunoblotted. IB; immunoblot.

3.3 Protein Concentration and CARM1 Aggregation

To test if CARM1 aggregation is dependent on protein concentration rather than total protein amount loaded in a single well, samples containing equal amounts of protein in different final volumes were prepared (Figure 4A). Decreasing total protein concentration led to a decrease in aggregation.

To test the requirements needed for CARM1 aggregation, purified recombinant CARM1 was used in WB analysis with both heat denaturing and non-heat denaturing methods of sample preparation (Figure 4B). The ability of the purified recombinant purified CARM1 protein to form aggregates shows that the presence of other proteins is not required for CARM1 aggregation. This points towards an intrinsic ability to form aggregates.

Noticeably, aggregates also formed in the non-heat denatured sample which differs from what was seen in cell culture and mice tissues. These results imply a critical concentration threshold beyond which CARM1 will aggregate regardless of temperature and suggests that CARM1's own concentration within the sample - rather than total protein concentration - is a predominant factor contributing to aggregation. This is put in evidence in Figure 4B where CARM1 recombinant protein was able to form aggregates at much lower total protein concentrations than shown in total cell lysate Figure 4A.

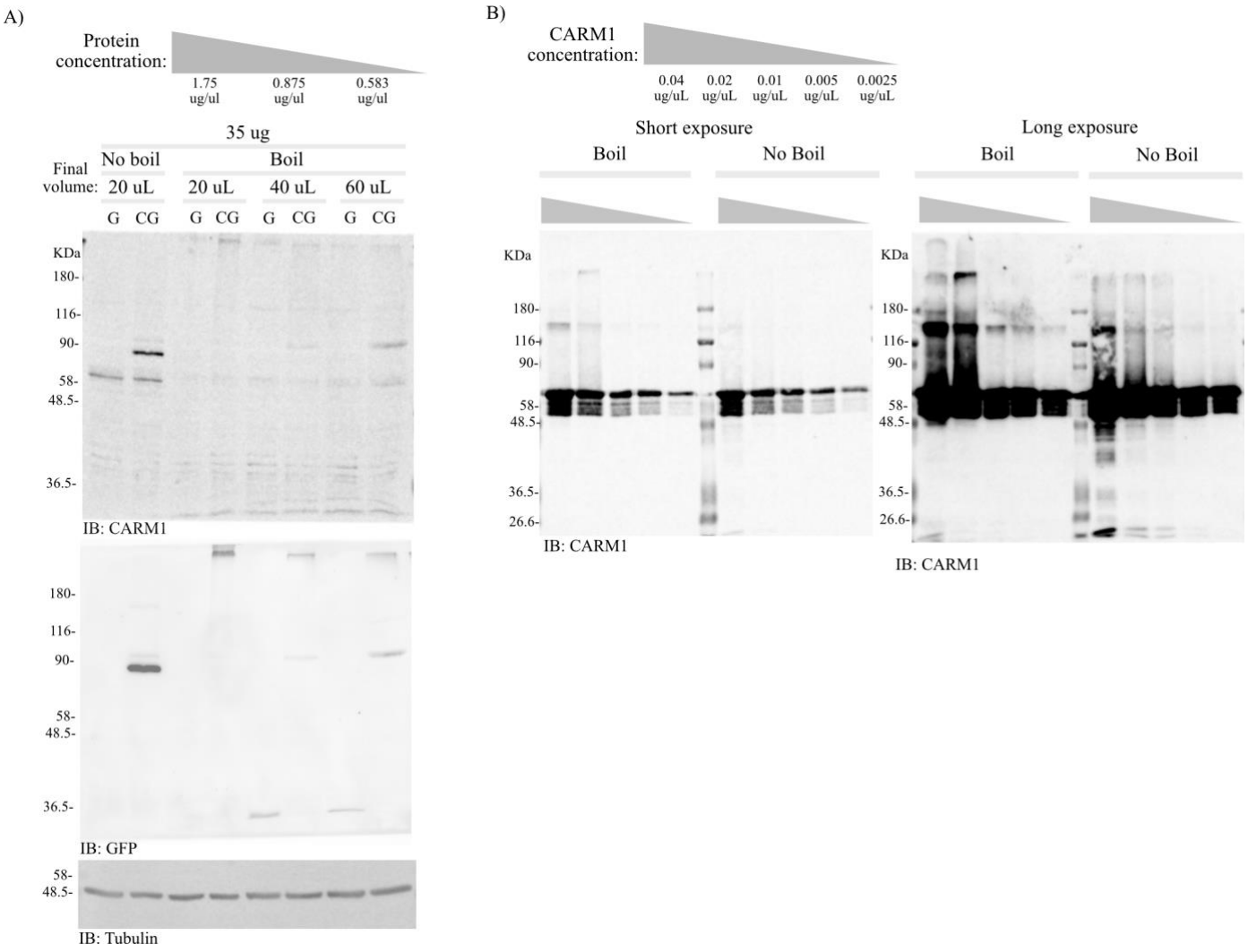

Figure 4: CARM1 aggregation is dependent on its concentration.

Protein lysate of MN-1 cells stably expressing GFP (G) and CARM1-GFP (CG) prepared in samples of equal protein amounts in differing volumes (A). CARM1 full length recombinant purified protein prepared in samples of equal volume (B). The samples were mixed with standard sample buffer and heated 8 min at 95˚C (boil) or incubated at room temperature (no boil) before running by SDS-PAGE and immunoblotted. IB; immunoblot.

3.4 CARM1 Aggregations in a Range of Models

To test if heat dependent CARM1 aggregation is relevant in other models, the ability of CARM1 to form aggregation was evaluated in various cell lines and mice tissues. In all cell lines and tissue types tested so far, which include NIH3T3, NSC-34, C2C12, HEK293T, Hela, MCF7, MDA-MB-231 (Figure 5A), MN-1 cell lines (Figure 3) as well as mouse brain and liver tissues (Figure 5B, Figure S2), CARM1 aggregates were detected. In addition, consistent with what was shown previously, CARM1 aggregation in mice brain and liver tissues (Figure 5B) formed aggregation in a protein concentration and temperature dependent fashion. This supports the idea that CARM1 aggregation is not limited to a specific cell type and suggests a widespread occurrence through a conserved mechanism.

The data shown so far suggest that CARM1 aggregation is an artifact of sample preparation that has potential to alter biological interpretation of results and invalidate their reliability for protein quantification. As shown, avoiding heat denaturation in cell lines or mice tissues allowed proper migration of CARM1 by SDS-PAGE. We therefore aimed to compare the intensity of CARM1 signal between the two methods of sample preparation in a range of protein concentrations.

In both mice brain and liver tissues and across all protein concentrations, the normalized non-heat denatured samples had a significantly stronger CARM1 signal when compared to their heat denatured equivalent (Figure 5B, Figure S2). As reflected in Figure 3A, the difference in signal was further accentuated with increasing protein concentration. This is consistent with our proposed model where aggregation sequesters CARM1 and prevents its migration in a protein concentration dependent manner. That being said, even CARM1 signal in the least concentrated samples (15 μg, or 0.43 μg/μL) was statistically different compared to their non heat denatured

equivalent, indicating that limiting protein concentration in samples is not enough to completely prevent a shift in quantification.

Contrastingly, GAPDH and PRMT7 quantifications remained proportional in either method of sample preparation, tissue type and protein range (Figure 5B). Here, GAPDH is used because of its extensive use as a loading control in WB without reports of aggregations impeding its migration. PRMT7, a protein in the same family as CARM1 with no detectable aggregation (Figure 6F), is used to contrast CARM1's own ability to do so. Overall, the data suggest that CARM1 is disproportionately impacted by sample preparation and demonstrates that the standard procedure of sample preparation in WB techniques inserts error in CARM1 protein quantifications, making standard sample preparation unsuited for its study.

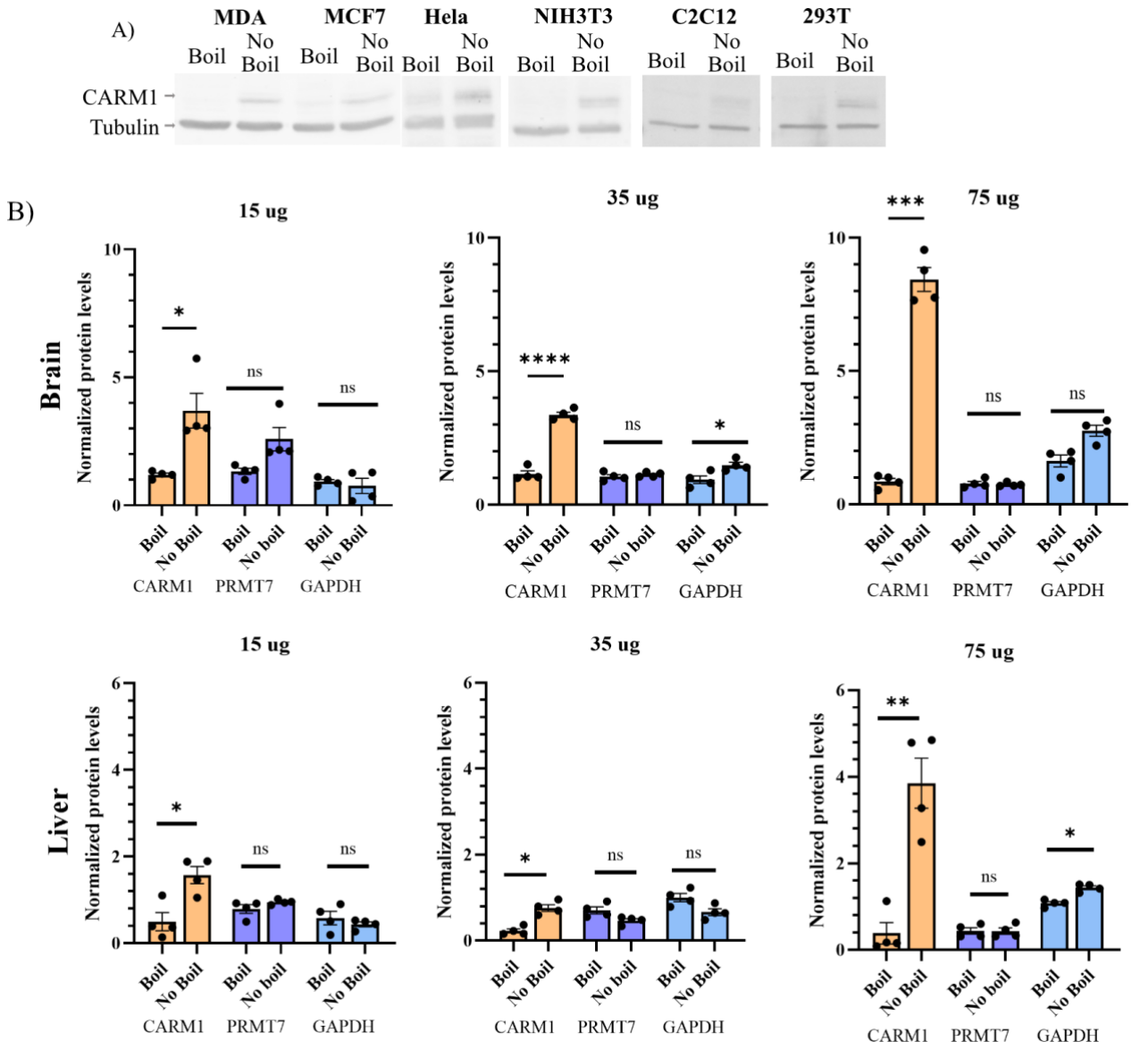

Figure 5: CARM1 aggregation occurs in multiple models

(A) Protein lysate of MDA-MB-231 (MDA), MCF7, Hela, NIH3T3, C2C12 and 293T cell lines prepared in samples containing 35 µg in a final volume of 30 uL. (B) Protein lysate of mice brain and liver tissue prepared in samples containing the indicated protein amount in a final volume of 40 uL. Values were normalized to total protein (Ponceau staining). The samples were heat denatured at 95˚C for 8 min (boil) or incubated at room temperature (no boil) prior to SDS-PAGE. Statistics; paired T-test, $P < 0.05$, Error bars show SEM, N=4

3.5 CARM1 VS other PRMTs

The data shown so far suggests that CARM1's ability to form aggregates is a consequence of its own structural features. That being said, all members of the PRMT family are known to have a largely conserved catalytic core. We set to determine if heat denaturation dependent aggregation also prevented gel migration of other canonical PRMTs. PRMT8 was excluded from this study because of its transmembrane nature which differentiates it to the other cytosolic or nuclear PRMTs. PRMT3 was also excluded due to its low expression in the same cell model. GAPDH was used to normalize PRMT2 instead of α-Tubulin because they are of equal size and have overlapping signals. Interestingly, the impact of heat denaturation did not significantly impact PRMTs (Figure 6), for the exception of PRMT1, PRMT5 and of course CARM1 (Figure 6A, C, D). While statistically significant, the protein signal of PRMT5 remains comparable in its quantification, while PRMT1's doubles when avoiding heat denaturation. PRMT1 aggregates at high molecular weights were also observed after heat denaturation of samples in a manner resembling what was seen with CARM1. It is worth noting that no aggregates were detected for the other PRMTs (Figure 6 B, D-F). The fact that other PRMTs remain largely unaffected by the method of sample preparation attests to the uniqueness of CARM1 and PRMT1 even among their paralogous and largely structurally conserved counterparts.

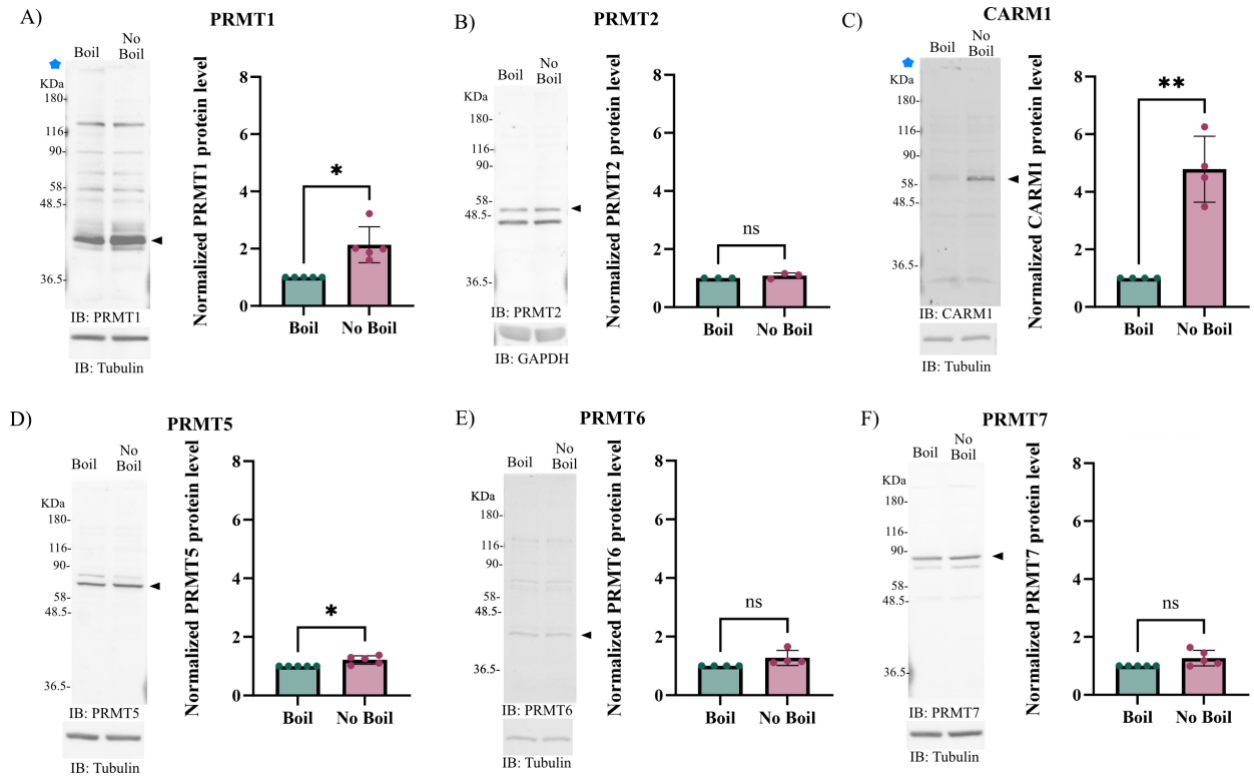

Figure 6: Aggregation of canonical PRMT proteins

(A-F) Immunoblots of canonical PRMTs in protein lysate of MN-1 cells prepared in samples of 35 µg in 30 µL in heat denaturing conditions (8 min at 95˚C, termed boil) or incubated at room temperature (termed no boil) followed by SDS-PAGE and western blotting. Arrowhead indicates the predicted band of each PRMT. Blue start indicates detectable aggregates. Statistics; paired t-test, $P< 0.05$, Error bars show SD, N=3-5.

3.6 CARM1 Aggregate Prevention

The data indicates that the minimum stringency required to prevent CARM1 aggregation is above what is provided by standard loading buffers. SDS is universally used in loading buffers for its ability to drive forward protein unfolding and mediate hydrophobic interactions. To this effect, standard SDS concentration in Laemmli buffer is typically kept at 2%. Since these conditions do not extend to CARM1, it reasons that increasing SDS availability might offer the stringency required to mediate the interactions at their cause. As described previously, the expression of a GFP tagged CARM1 is used as a secondary means of IB validation. It is worth noting that different migration heights of CARM1-GFP suggests incomplete or partial denaturation dependent on sample preparation method. Interestingly, SDS concentration had to be tripled before CARM1 aggregation was noticeably reduced. Even so, at a final concentration of 6% SDS, CARM1 aggregates were still present, albeit to a much lesser extent (Figure 7A). Further increasing SDS concentrations to 10% provided no extra benefit as compared to the 6% SDS (Figure 7A). These results suggest that aggregations are driven by hydrophobic interactions.

To test the stability of CARM1 aggregates, samples were heat denatured in 2% SDS to promote the formation of aggregates after which the SDS concentration was adjusted to a final concentration of 6% and either incubated at room temperature or heat denatured once more (Figure 7A). In both cases, increasing SDS concentration to 6% after aggregate formation was not able to resolve aggregation, displaying their strong resistance to SDS, and pointing toward a different mechanism also contributing to CARM1 aggregation.

While the driving force of aggregates seem to be of hydrophobic nature, their surprising stability to high SDS concentrations once formed suggests a potential covalent interaction between CARM1 proteins. To test if disulfide bonds are involved in the aggregations, samples were treated in a range of DTT concentrations prior to SDS-PAGE. We reasoned that

increasing DTT concentrations would resolve the aggregations should they be disulfide bond dependent. Surprisingly, the increase of DTT concentration further prevented normal migration of CARM1 when heat denatured (Figure 7B). While suggesting that disulfide bonds are involved in aggregation, it also concludes that it is not through a contributive manner. Since higher SDS concentrations are better at mediating aggregations, its ability to rescue aggregation in a high DTT concentration context was tested (Figure 7C). A concentration of 6% SDS was able to resolve the aggregations, meaning that the root cause leading to aggregation following DTT treatment in heat denaturing conditions was mediated by SDS, and therefore of a non-covalent nature.

The data shown so far point towards the use of higher concentrations of SDS in the absence of DTT for a more accurate representation of CARM1 protein level. A sample buffer suited to CARM1's properties was prepared and compared to standard sample buffer (Figure 7D). The use of the adapted buffer (6% SDS, no DTT) significantly increased the proportion of CARM1 properly migrating to the gel in heat denaturing conditions, leading to a complete recovery of CARM1 protein levels as compared to its non-heat denatured condition. This makes the use of an adapted sample buffer required for accurate assessment of CARM1 protein levels.

Importantly, the impact of DTT and high SDS concentrations observed for CARM1 extended to PRMT1 (Figure 7B,C), further pointing towards a common mechanism of aggregation. The use of an adapted sample buffer (Figure 7D) was beneficial for PRMT1 detection, albeit to a lesser significance due to a lower prevalence of aggregates. The use of an adapted sample buffer is therefore recommended for PRMT1 to ensure more accurate results.

Here, it was demonstrated that standardly used sample preparation conditions do not extend to CARM1 due to distinct biochemical properties. Standard WB conditions cause CARM1 to accumulate into SDS-resistant aggregates which sequester and prevent CARM1 migration in SDS-

PAGE. This disproportionally impacts its detection by WB, inserting error through inaccurate representation of its expression. We identify heat denaturation, CARM1 concentration and DTT as major driving factors for aggregation formation. Further investigation into the PRMT family shows that CARM1 is not the only PRMT impacted by these biochemical properties; they also extend to PRMT1 which can aggregate albeit to a lesser extent. In both instances, increasing SDS concentrations and avoiding DTT in loading samples have mediated the interactions at cause of aggregate formation and improved WB detection. These results argue that these modifications are required for sample preparations of CARM1 and PRMT1 to preserve their quantitative reliance in WB and SDS-PAGE and avoid misleading results.

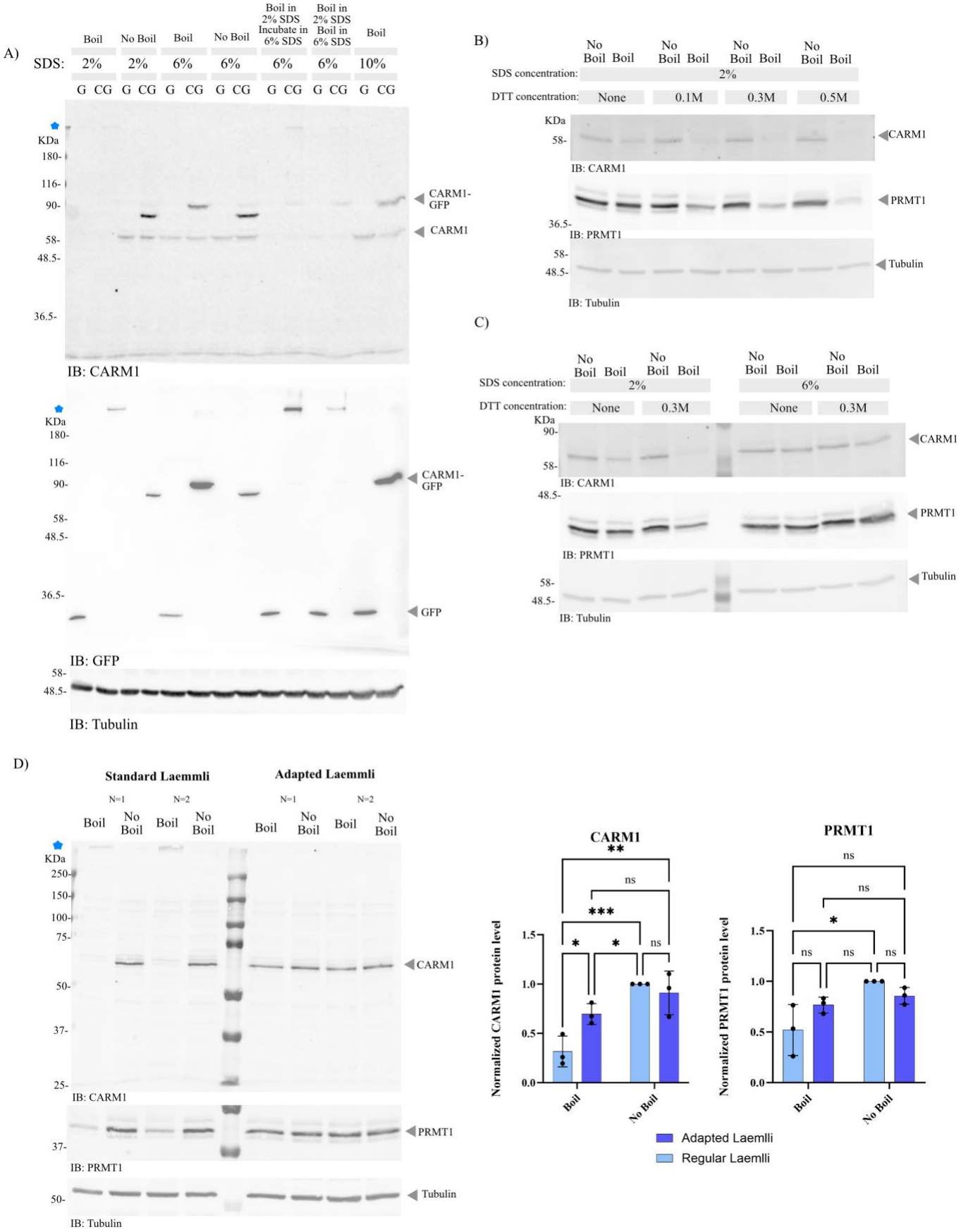
A)
Boil
No Boil
Boil
No Boil
Boil in 2% SDS Incubate in 6% SDS
Boil in 2% SDS Boil in 6% SDS
Boil
SDS:
2%
2%
6%
6%
6%
6%
10%
G CG G CG G CG G CG G CG G CG G CG
KDa
180-
116-
90-
58-
48.5-
36.5-
CARM1-GFP
CARM1
IB: CARM1
KDa
180-
116-
90-
58-
48.5-
36.5-
CARM1-GFP
GFP
IB: GFP
58-
48.5-
IB: Tubulin
B)
No Boil Boil
No Boil Boil
No Boil Boil
No Boil Boil
SDS concentration:
2%
DTT concentration:
None
0.1M
0.3M
0.5M
KDa
58-
CARM1
IB: CARM1
36.5-
PRMT1
IB: PRMT1
58-
48.5-
Tubulin
IB: Tubulin
C)
No Boil Boil
No Boil Boil
No Boil Boil
No Boil Boil
SDS concentration:
2%
6%
DTT concentration:
None
0.3M
None
0.3M
KDa
90-
58-
CARM1
IB: CARM1
48.5-
PRMT1
IB: PRMT1
58-
48.5-
Tubulin
IB: Tubulin
D)
Standard Laemmli
Adapted Laemmli
N=1
N=2
N=1
N=2
Boil
No Boil
Boil
No Boil
Boil
No Boil
Boil
No Boil
KDa
250-
150-
100-
75-
50-
37-
25-
CARM1
IB: CARM1
37-
PRMT1
IB: PRMT1
50-
Tubulin
IB: Tubulin
CARM1
PRMT1
Normalized CARM1 protein level
Normalized PRMT1 protein level
**
ns
***
*
*
ns
ns
*
ns
ns
ns
1.5
1.0
0.5
0.0
Boil
No Boil
Adapted Laemmli
Regular Laemmli

Figure 7: PRMT1 and CARM1 aggregates are inhibited by SDS at formation and promoted by DTT.

(A) Protein lysate samples of stable MN-1 cells expressing GFP (G) or CARM1-GFP (CG) containing 35 μg in 30 μL prepared and either heat denatured or incubated at room temperature with an increasing range of SDS. For samples with two SDS treatments, the concentration of SDS was increased from an initial 2% to 6% after the first heat denaturation step, prior to another heat denaturation or incubation at room temperature step. Samples of MN-1 WT protein lysate containing 35μg in 30μl prepared and either heat denatured or incubated at room temperature with increasing range of DTT (B) or DTT and SDS (C). (D) Using an adapted sample buffer (purple) with 6% SDS and no DTT, samples were prepared, and heat denatured or incubated at room temperature prior to SDS-PAGE, WB and quantification. N=4. Statistics; 2-way ANOVA, error bars show SD. All heat denaturation steps were done for 8 min at 95˚C. IB; immunoblot. Blue start indicates detectable aggregates

3.7 Discussion

3.7.1 CARM1 Aggregations in an Experimental Setting

WB is a standard procedure and indisputably a necessary tool in proteomics and molecular biology with the advantage of applicability to most proteins. Here, the data shows that CARM1 does not fall within this category, with prominent aggregation preventing its detection by conventional methods. The aggregates are shown to be dependent on temperature at the protein denaturation step as well as CARM1's own protein concentration (Figure 8). Aggregates are also widespread to a range of cell lines and mice tissue models suggesting their ubiquitous occurrence. Therefore it is plausible that these factors are unknowingly introducing inaccuracies in CARM1's study.

There is a lot of interest in the evaluation of CARM1 protein levels in cancer as its overexpression was found in many tumours when compared to healthy tissue, suggesting a role in cancer pathogenesis (Qiu et al., 2022). Consequently, modulating CARM1 expression as models of overexpression or knockdown in either cell or mice model is a strategy often used in investigative research (Bao et al., 2019; Dhang et al., 2025). It is therefore a requirement that it be assessed accurately, without confounding factors.

Considering this, we have set out to investigate the cause of the aggregates as well as defining conditions that allow accurate CARM1 quantification in SDS-PAGE with heat denaturation. Increasing SDS concentrations to 6%; or three times the conventional availability of SDS, was successful in preventing most of the aggregations. The successful use of SDS points towards hydrophobic interactions as being the primary driving force to aggregate formation. Surprisingly, DTT treatment led to stronger aggregation, demonstrating that disulfide bonds present in the protein are protective from aggregation and beneficial for CARM1 gel migration (Figure 8). Combining both findings by increasing SDS and removing DTT from standard

loading buffer provides a complete rescue of CARM1 protein migration and an alternative preparation method suited for CARM1's study.

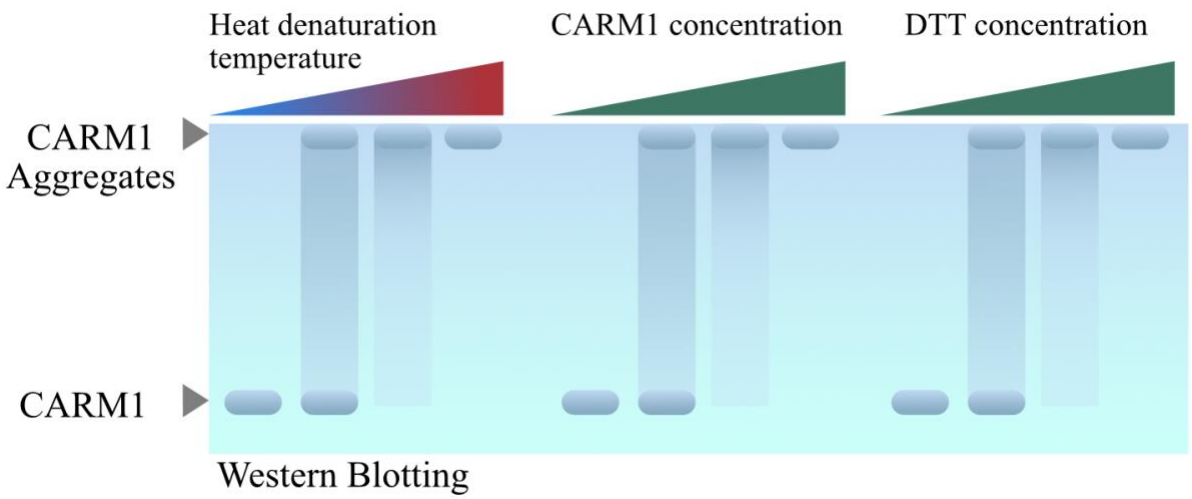

Figure 8: Graphical overview of the factors contributing to CARM1 aggregation in SDS-PAGE.

These findings are consistent with a model where a hidden hydrophobic core of CARM1 is at the cause of the aggregates but is shielded in the presence of disulfide bonds in its native state. When broken, the hydrophobic core is revealed and acts as a nucleation site to irreversibly sequester CARM1 protein into aggregates. When left intact, the bonds shield the hydrophobic core and allow for denaturation and CARM1 migration without exposure of the nucleation site. In either scenario, high concentrations of SDS seems to have the ability to mediate other hydrophobic moieties other than those shielded by disulfide bonds.

Even if the capabilities of SDS to denature proteins are well documented, the kinetics outlining its mechanism remain unelucidated (Bhuyan, 2010). Transmembrane proteins are well established as having the ability to form aggregates through their hydrophobic core that can unfold and initiate misfolding (Sagne et al., 1996). They also encompass most reports for aggregation, implying that only transmembrane protein has this ability. This study argues against this general standpoint and expands this premise to yet unidentified proteins in the process of sample preparation. This highlights the need of more biochemical studies focusing on the structural basis that leads to proteins to be excluded from the traditional method of sample preparation for SDS-PAGE and WB analysis.

CARM1 is not unique in its ability to form aggregates as demonstrated with PRMT1, but it stands out in terms of the degree of bias aggregates introduce. Given that PRMTs share a conserved catalytic core, this argues that the property of aggregation be allotted to CARM1 through its unique structural components. In the same line of thought, the C-terminal domain of CARM1 is unique among PRMTs and well known for its unstructured conformation and potential hindrance in CARM1 proteomic studies. The particularity of the domain has been suggested to be causing difficulties with X-ray crystallography methods (Troffer-Charlier et al.,

2007). Most successful X-ray crystallography structures reported so far have either found the C-terminal domain to have low electron density suggesting a disordered state or excluded it due to difficulties at its resolution (Troffer-Charlier et al., 2007). Additionally, full length recombinant CARM1 purification is difficult due to its propensity to accumulate into inclusion bodies as insoluble aggregates (Figure S3) (Chumanov et al., 2011). It is plausible that the unstructured C-terminal domain of the protein is at cause for all these challenges, however, more needs to be done before reaching this conclusion.

In any case, bypassing the effects of aggregation is in the best interest of proteomic studies used for CARM1's understanding. As mentioned, aggregations are dependent on CARM1's own concentration. This is of relevance when working with a model of CARM1 overexpression, as is often the case in exploratory research. It is also unknown if all isoforms of CARM1 are impacted equally, which may introduce another layer of variability when not considered.

The use and effect of other reducing agents such as βME has yet to be evaluated, but they may provide additional options for the prevention of CARM1 aggregate formation. While our adapted sample buffer does contain a reducing agent, it should also be noted that the complete absence of reducing agents could lead to the formation of non-CARM1 aggregates.

As demonstrated, CARM1 aggregation is dependent on a variety of factors which may vary with an experiment's specific conditions. Consequently, the presence of aggregates should be empirically evaluated, with comparison of heat denatured and non-heat denatured CARM1 signals as an additional control. Proteolytic activity, normally negated during heat denaturation (Pringle, 1975), is not addressed without heat denaturation, so use of parallel protease inhibition as an additional measure is advised.

The use of the adapted sample buffer described here is strongly recommended for CARM1 SDS-PAGE in heat denaturing conditions without which the introduction of aggregates is bound to mislead result interpretation. These findings should be considered in any study involving CARM1 and kept in mind in the interpretation of results published so far.

3.7.2 Implications of CARM1 Aggregations in Cell Biology

Until this publication, the particularities of CARM1 and their challenges in proteomics were not directly reported. This is remarkable given the rising interest it gathers in cancer biology and increasing number of publications. While the data presented here addresses these properties in the experimental setting of CARM1's investigation, it also opens the door to broader biological implications. As demonstrated, CARM1 stands out from most other PRMTs in its ability to form aggregates. This distinctive capacity brings forward the idea that the structural components at cause could be biologically relevant to CARM1's function.

This data does give insight to the nature of the structural component responsible for the change. One of the most surprising findings in this publication was the positive correlation between DTT concentration and CARM1 aggregation, suggesting that disulfide bonds are present in CARM1's native form. There are no reports of CARM1 having disulfide bonds in its structure, making this a conflicting assessment. Disulfide bonds are typically present in proteins exposed to the oxidizing conditions associated with extracellular space and the endoplasmic reticulum (Feige & Hendershot, 2010). Cytoplasmic or nuclear proteins for the most part do not contain disulfide bonds (Stewart et al., 1998). Based on this, CARM1 and other PRMTs do not fall under the umbrella of proteins typically associated with the modification. Still, two other PRMTs are known to contradict this general assumption.

First, disulfide bonds were found to connect PRMT1 homodimers in a crystallography experiment. This caused PRMT1 homodimers to create an extended polymer in the crystal lattice. Mutation of the disulfide site showed PRMT1 to maintain its ability to form oligomers *in vitro* without altering its enzymatic activity (Zhang & Cheng, 2003). Moreover, purified human PRMT1 and PRMT5 in 293T cells were found to contain disulfide bonds, which contributed along with other non-covalent interactions to their oligomerization (Rho et al., 2001). The functionality of this modification is unknown, but it is clear that they contribute at least in part to their oligomerization.

Interestingly, PRMT1 and PRMT5 are the only PRMTs aside from CARM1 that were significantly impacted by heat denaturation in sample preparation (Figure 6A, C, D), which as discussed suggests a common mechanism of aggregation. Also described in this chapter, the data suggests that CARM1 does in fact contain a disulfide bond. Taken together, this suggests that PRMT1, PRMT5 and CARM1 contain at least one disulfide bond as a conserved structural component. This points to a significant knowledge gap that needs to be addressed through more structural and biochemical studies. More work needs to be done in order to fully understand the implications of its properties.

There are no reports of a physiological relevance for CARM1 aggregates. Nevertheless, it cannot be ruled out that CARM1's ability to drastically alter its hydrophobicity might be connected to protein function. Hydrophobicity and electrostatic interactions are key elements for LLPS of MLOs. These include paraspeckles, to which a pool of CARM1 has been shown to localize (Hu et al., 2015; Hupalowska et al., 2018). Paraspeckles have been found to act as "sponges", with the ability to selectively sequester RNAs and proteins (Hirose et al., 2022). It is possible that CARM1's structure is modified to control its sub-cellular localization to such

organelles towards a functional goal. For these reasons, the premise of a broader biological meaning should be considered in future studies.

3.8 Conclusions and Future Directions

The unique properties of CARM1 have the potential to hinder its study. Here, the consequences of its aggregation and adaptations required for its study by WB were defined. Since the CARM1's aggregations described here occur outside of a biological context, the incentive to further characterize its properties may not be of urgent concern. However, as described, CARM1 crystallography and protein purification experiments have reportedly been difficult (Chumanov et al., 2011; Troffer-Charlier et al., 2007). Its biochemical properties may also be hindering other methodologies that hold back its study in biological contexts. As such, there is reason for more exploration of the properties described here.

Experimentally, since cysteine residues are the only amino acids capable of forming disulfide bonds (Wiedemann et al., 2020), the ten cysteine residues found in CARM1 are of particular interest. It would be relevant to determine if cysteine mutations alter its ability to aggregate, and if so, which cysteine residue(s) is or are responsible. It was also brought up that the properties responsible for CARM1's aggregations could have a biological function, potentially in LLPS. In the same line of thought, determining if cysteine mutations alters CARM1's ability to be recruited to paraspeckles would be an ideal starting point in characterizing the possible biological function of these properties.

Chapter 4 CARM1 Modulates HuD's mRNA interactions in Motoneurons

HuD is a major neuronal regulator under the influence of its methylation by CARM1. As mentioned, the p21 mRNA half-life was found to decrease upon methylation of HuD by CARM1 (Fujiwara et al., 2006). Among the best known HuD mRNA targets, *p21* is the only target investigated found to be under this influence (Hubers et al., 2011). This highlights a regulatory mechanism through which a subset of HuD's mRNA targets may be influenced. In this chapter, the identity of HuD's mRNA targets in MNs with dependencies on CARM1 will be explored.

4.2 Experimental Overview

A HuD RIP-Seq was performed in MN-1 pGIP-Z and pGIP-Z shCARM1 cells (referred as shCARM1 cells). The differential abundance of mRNAs between the HuD RIPs was analyzed using GFOLD. Motif analysis was performed to identify consensus motifs within the genes with the largest absolute fold change, as well as motifs directionally influenced by CARM1. In addition, GO analysis was performed to identify the molecular and biological functions influenced by CARM1. Finally, genes of interest were validated by RT-PCR, and their protein levels assessed by WB for CARM1 dependent changes in expression.

4.3 Results

Aim i. Identify the full spectrum of HuD mRNA targets influenced by CARM1 in MNs

4.3.1 Cell Lines

To replicate the MN cell type, the MN-1 cell model (Salazar-Grueso et al., 1991) was used. These cells were used in previous published work by our group as a model for the study of

CARM1 in MN biology (Hubers et al., 2011; Sanchez et al., 2013, 2015). Within these works, two MN-1 stable cell lines were generated to stably express a pGIP-Z shCARM1 (or empty) vector (Hubers et al., 2011). Most importantly, these cell lines replicated the initial finding that CARM1 methylation of HuD altered its affinity with the p21 mRNA target (Fujiwara et al., 2006; Hubers et al., 2011), making it an ideal model for the objective premised by this work.

CARM1 protein levels were evaluated in these cell lines prior to downstream application and were confirmed to have a CARM1 knockdown (Figure 9A). Additionally, HuD protein levels were found to be consistent between the two cell lines, ruling out its abundance as a potential variable in the comparison of its mRNA interactions (Figure 9A). With the baseline protein levels established, the cells were used for HuD's RIP.

4.3.2 RIP of HuD

In order to confirm the IP of HuD, the protein product was evaluated by WB. The HuD IP showed a clean pull down of the protein with no unspecificity in the IgG negative control (Figure 9B). This shows HuD to be enriched in the IP product.

To validate that the same conditions would translate to a HuD mRNA target enrichment, the concurrent pull down of some of its known mRNA targets; *p21* and *GAP-43*, was used to define the conditions leading to their specific and robust amplification (Figure 9C). Furthermore, the 18s rRNA was used as a marker of unspecific RNA pull down. As such, using these same conditions that yielded a HuD enrichment, the RT-PCR amplification showed an enrichment in p21 mRNA when compared to the input. *GAP-43* was not similarly enriched when compared to the input, but still showed a specific pull down within the HuD IP lanes. Lastly, 18s rRNA was still present at low levels across IgG and IP samples, suggesting the rRNA be binding to the protein A agarose beads or antibodies outside of the antigen binding sites. Taken together, these

experimental controls attest to the successful IP of HuD and its known mRNA targets, suggesting these conditions can be used towards HuD's RIP-seq.

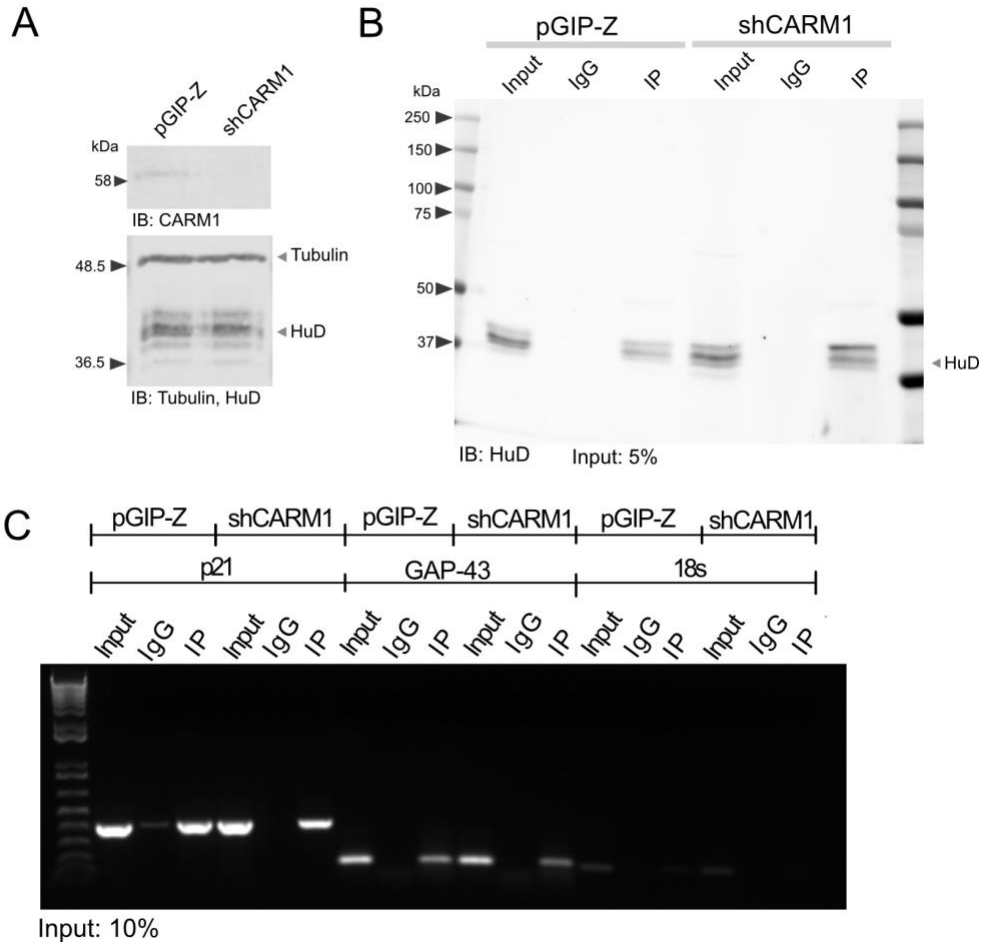

Figure 9: HuD immunoprecipitation and amplification of its known mRNA targets.
(A) Immunoblot of stable pGIP-Z and shCARM1 MN-1 cell lysate. (B) Representative immunoblot of a HuD IP performed in stable MN-1 pGIP-Z and shCARM1 cell lines. (C) Representative RT-PCR amplification of HuD mRNA targets (*p21* and *GAP-43*) using a HuD RIP as a template source. 18s serves as a control for unspecific binding.

4.3.3 RIP-seq Analysis

Having established the conditions that led to the isolation of HuD mRNA targets, the RNA product of biological triplicates was pooled and sent for RNA-seq. For each replicate, the RNA volume used for analysis was normalized to the HuD IP efficiency of pGIP-Z and shCARM1 MN-1 cells. This was done to avoid the addition of IP efficiency as a variable in data interpretation. Importantly, the samples were depleted of rRNA at library preparation, since the conditions used did not exclude all rRNAs as demonstrated by 18s. The 10% input and HuD RIP samples were found to pass the quality control, while the IgG did not contain enough RNA to sequence. For this reason, the IgG samples were excluded from sequencing. The sequencing data was mapped to the mouse genome and feature counts compiled and quantified. In order to compare the two conditions, the data was analyzed through GFOLD, a tool for differential expression RNA seq analysis (Figure 10) (Feng et al., 2012). GFOLD values can be interpreted similarly as fold-change and the largest absolute values reflect a more meaningful difference between samples.

To this end, an arbitrary threshold of GFOLD values of above 2, and below -2 was set (Figure 10, red dotted lines). Using this threshold, 123 genes are highlighted.

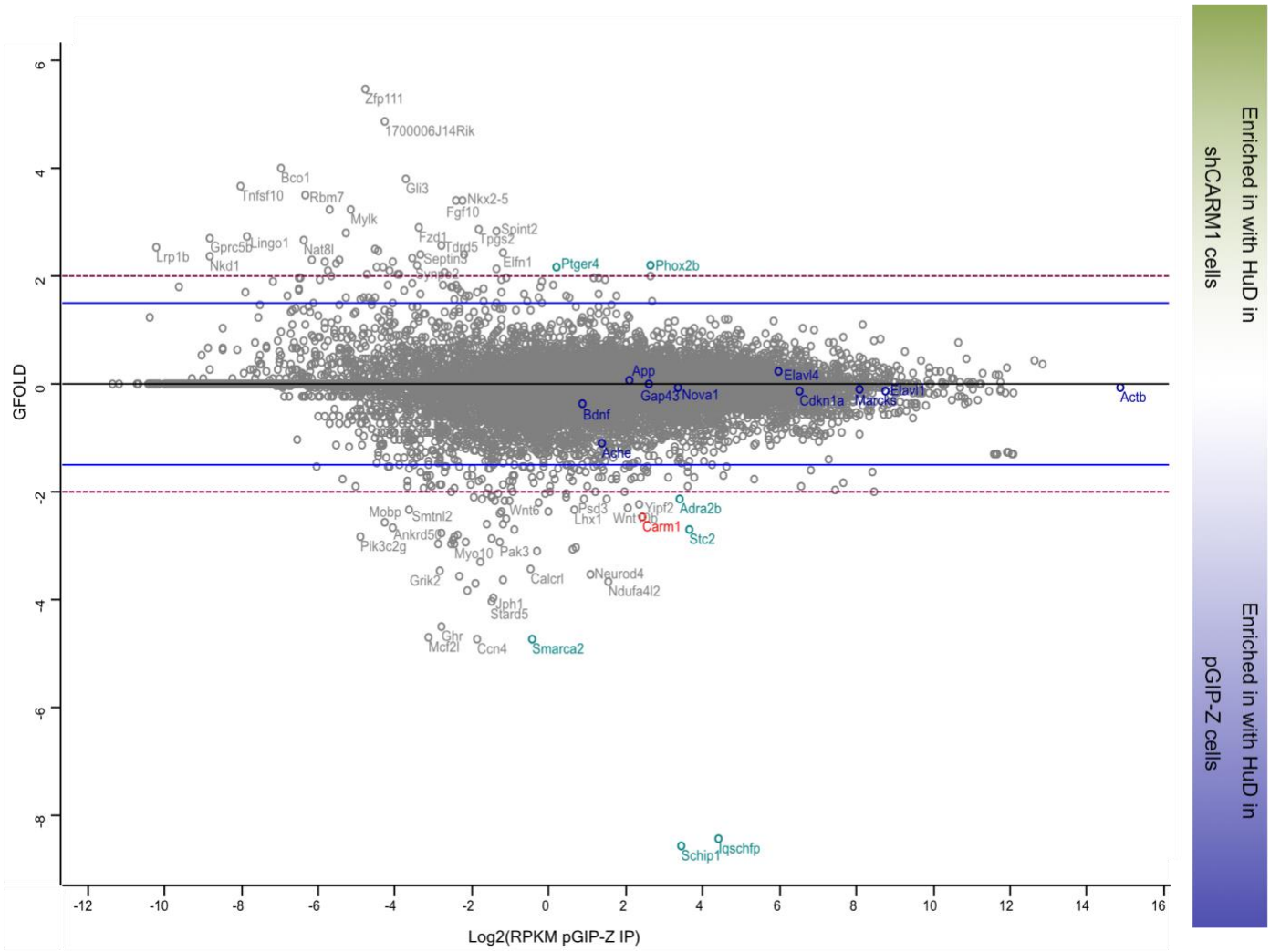

Figure 10: mRNA targets with CARM1 dependent levels of interaction with HuD.

GFOLD RNA-seq analysis of pooled biological triplicates of HuD RIPs performed in stable pGIP-Z or shCARM1 MM-1 cells. GFOLD values can be interpreted similarly to Fold Change. Green labels represent the selected genes of interest. Blue labels represent known HuD mRNA targets. CARM1 is highlighted in red. Dotted red line and solid blue line delineate the inclusion criteria for motif and GO analysis.

In addition, certain criteria were established to highlight the genes most relevant to the premise of this work. While HuD is involved in the regulation of many types of RNA, what is known of the CARM1 and HuD interaction is so far limited to protein coding genes. Since the objective of this work is to expand on genes impacted similarly, only protein coding proteins were considered for downstream analysis.

4.3.4 Motifs Analysis

Aim ii. Determine which mRNA motifs within HuD mRNA targets are influenced by CARM1

HuD's function is tied to its ability to bind mRNA. As such, it is expected that it's ARE, or U rich preference be reflected among the RNA yielded from its RIP. To test this, a motif enrichment analysis was performed. Only the 3'UTR sequences were considered as they are typically known to contain HuD binding sites (Zuccotti et al., 2017). Among the 91 protein coding genes of this group, a motif analysis revealed the AGAGAG motif as the most enriched (1.8 fold) within the 3'UTR, along with other AREs (Figure 11). This agrees with what is known of HuD, supporting the notion that HuD mRNA targets were the predominant component within the samples, as opposed to co-immunoprecipitated products.

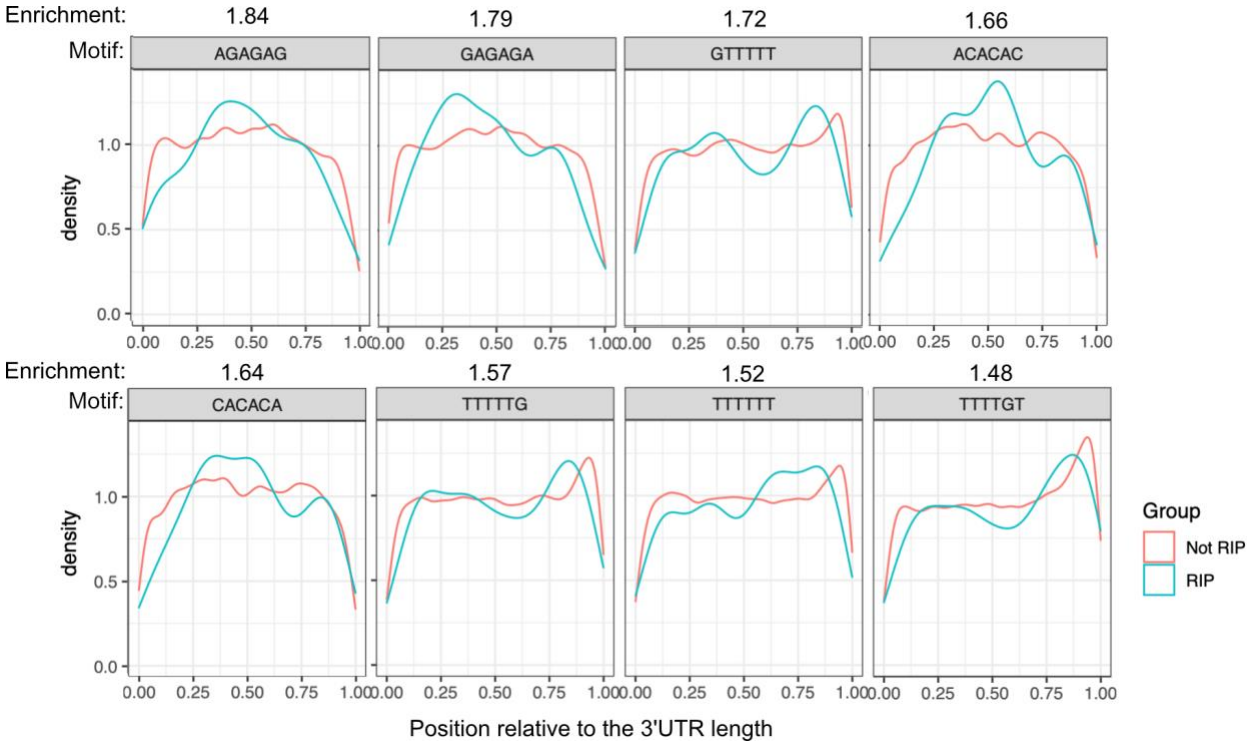

Figure 11: Motifs enriched in the 3'UTRs of genes coprecipitating with HuD in pGIP-Z and shCARM1 MN-1 cells.

The 3'UTR sequences of protein coding genes with GFOLD values of above 2 and below -2 were considered (91 genes) and compared to those of other protein coding genes in the mouse genome. The motif densities are presented in relation to their position in the 3'UTRs.

Beyond the general motif affinity of HuD, the ability of CARM1 to selectively alter HuD's affinity motifs within its mRNA targets was evaluated. Once again, only the 3'UTR sequences of protein coding genes were considered. In addition, the threshold was adjusted to include genes with a GFOLD value falling below -1.5 or above 1.5 (Figure 10, solid blue line). This was done in order to increase the sample size of protein coding genes included in the analysis. With these criteria, 90 genes fell above a GFOLD value of 1.5, and 101 genes fell below a GFOLD value of -1.5. For interpretation, positive GFOLD values are indicative of an enrichment within the experimental group (shCARM1), whereas a negative GFOLD value is indicative of an enrichment within the control group (pGIP-Z) (Figure 10).

Comparison between the experimental and control group reveals commonalities as well as a potential HuD motif preference dependent on CARM1 protein levels (Figure 12). As mentioned, AREs are expected of HuD mRNA targets. Such sequences are found within both groups, with an A-rich sequence falling at the second most enriched motif in the shCARM1 group. Additionally, U-rich sequences fell as third and first most enriched motif for the genes in the shCARM1 group and control group, respectively. These U-rich sequences found within both groups are consistent with what was found to be enriched within the combined 91 protein coding genes with the largest absolute GFOLD values (Figure 11). Uniquely, a CAG motif sequence was found to be enriched in the control group (Figure 12). This is also reminiscent of the most prevalent motifs found among the 91 genes with the largest absolute GFOLD values (Figure 11). Interestingly, the primary enriched motif within the experimental group was a G-rich sequence. A similar sequence was also enriched within the control group, albeit with a less meaningful e-value. HuD is not known to bind directly G-rich sequences, however G-rich sequences are often found near the polyadenylated 3'UTRs of mRNAs (Kostadinov et al., 2005), and polyadenylated

3'UTRs are known to be bound by HuD (Beckel-Mitchener et al., 2002; Bronicki & Jasmin, 2013). The presence of G-rich sequences is likely indicative of its prevalence in the mRNAs outside of HuD's binding site. However, these motifs were found to have vastly different e-values between the two groups. More specifically, they were found to have an e-value of $1.4e^{-16}$ and $2.8e^{-3}$ for the experimental and control group respectively (Figure 12). Altogether, a motif analysis finds enriched sequences to be consistent with what is known of HuD, with U-rich elements representing a large portion of identified motifs. A comparison between the experimental group and control highlights similarities, most notably the presence of AREs and G-rich motifs, but with a notable distinction. G-rich motifs are vastly more prominent within the MN-1 shCARM1 samples when compared to the control group. The e-values of the G-rich sequences suggest that HuD's ability to interact with transcripts containing this motif within their 3'UTRs is influenced by CARM1. While this cannot be ascertained from this data alone, this points towards a mechanism through which CARM1 can selectively diminish HuD's interaction through this motif.

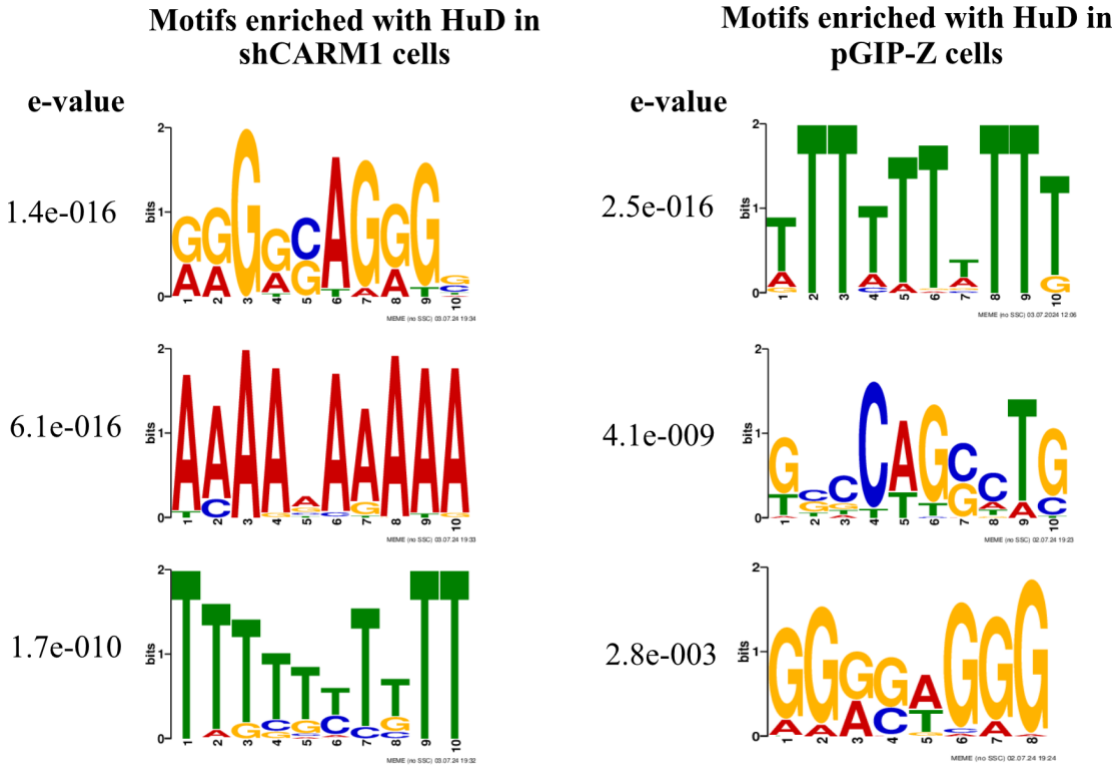

Figure 12: Motifs enriched in the 3'UTRs of protein coding genes coprecipitating with HuD in pGIP-Z or shCARM1 MN-1 cells.

The 3'UTRs of genes with GFOLD values of below -1.5 and above 1.5 were used to determine the motifs enriched with HuD in pGIP-Z and shCARM1 cells, respectively.

4.3.5 Gene ontology Analysis

Aim iii. Determine which roles within HuD mRNA targets are influenced by CARM1

Preserving the same criteria, the 90 genes and 101 genes falling above and below GFOLD values of 1.5 and -1.5, respectively, were used to investigate the GO terms influenced by CARM1 protein levels (Table 2, Table 3). The highlighted genes were compared to all genes identified within the pGIP-Z input sequencing dataset. The GO terms mentioned in the text are italicized.

4.3.5.1 *Molecular Function*

Molecular function terms enriched within the control group (pGIP-Z cells) highlight GO terms relating to protein signalling, such as *ligand activity*, *growth factor binding* and *signalling receptor binding*. Interestingly, signalling terms represent the majority of result from the gene list. In addition, two GO terms stood out in their direct relation to the investigation of CARM1 function within MN. First, *protein-arginine deiminase activity* was found to be enriched. As mentioned, Arg deamination or citrullination is a permanent modification that renders Arg unsuitable as a methylation substrate in addition to changing its chemical properties (Cuthbert et al., 2004). Most notably, the identification of this GO term in the context of CARM1 protein levels suggest a potential lasting downstream impact in global arginine methylation. Secondly, consistent with the model used for this investigation, genes taking part of *structural constituent of myelin sheath* were also enriched within this gene list. As myelination is a significant component of MN biology, the potential involvement of CARM1 in their function further suggests its involvement in this cell type.

On the other hand, genes found to be enriched within the experimental dataset (shCARM1 cells) reflected a very different type of molecular function. RNAPII regulation and DNA binding relating GO terms constitute the majority terms identified. For instance, terms such as *RNAPII regulatory region sequence-specific DNA binding* and *double stranded DNA binding* fell towards the top of the list. Together, these point towards a CARM1 dependent transcriptional influence, which agrees with its known roles. Other terms were highlighted as well, such as *cation binding*, its subgroup of *metal ion binding*, as well as *regulatory region nucleic acid binding*.

CARM1 protein levels appear to alter the molecular function of the pool of mRNAs bound by HuD. Lower levels of CARM1 correlated with the enrichment of RNAPII and DNA binding terms while higher levels of CARM1 correlated with protein signalling terms. The abundance of correlating terms brought forward by both gene groups put in evidence the distinct functional impact that CARM1 could impart through HuD.

4.3.5.2 *Biological Processes*

Biological processes enriched within each group are numerous and diverse in function. Given the experimental method, there is the expectation that the terms identified in both groups be relating to known HuD functions. In accordance with this, commonalities between the shCARM1 and pGIP-Z groups include terms relating to development, morphogenesis and the positive regulation of cell differentiation. However, to delineate the terms most relevant to this work, the focus was put on GO terms most influenced by CARM1 protein levels, and therefore the terms unique to only one dataset.

Accordingly, both groups were found to have unique biological functions. Within the shCARM1 cells, terms relating to the Wnt signalling pathway were found to be recurrent;

Canonical Wnt signaling pathway, *regulation of Wnt signaling pathway* and *cell-cell signaling by Wnt* are among the terms found to be enrichment. Meanwhile, no Wnt relating terms were identified within the control group. The repeated inclusion of these terms in the experimental group strongly suggest that Wnt signaling be a noteworthy component of CARM1's influence.

Relevant to the model investigated, the term *nervous system development* and *cell projection organization* were also identified within the shCARM1, but not within the pGIP-Z dataset. The implied regulation of HuD on CARM1 to bind mRNAs relating to neuronal development further implicates CARM1 in the mediation of neuronal development, consistent with the previous findings that CARM1 delineates cell fate through HuD (Fujiwara et al., 2006; Hubers et al., 2011).

Meanwhile, terms enriched within the pGIP-Z cells include *skeletal system development*, which is reminiscent of CARM1's known role in skeletal muscle health. The presence of this term in the context of MN is consistent with CARM1's strong association to myogenesis (Saber & Rudnicki, 2022). Furthermore, the presence of *peptidyl-arginine modification* within the list is also in a clear association to CARM1's primary function, and ties into the term *protein-arginine deiminase activity* identified in the molecular function. The reoccurrence of this process is corroborating the idea of an influence on Arg methylation beyond CARM1's immediate substrates.

As a whole, the terms highlighted are consistent with both HuD's known roles and CARM1's own. The identification of terms closely related to CARM1 known functions further suggest that CARM1's influence be at least in part occurring through HuD in MNs.

4.3.5.3 *Cellular Component*

MN are defined by their distinct structural features adapted for the rapid transduction and transmission of signal across a large distance (De Vos & Hafezparast, 2017). The regulation of axonal transport upon and after differentiation represents an additional layer of control particularly required of MNs. In the investigation of HuD and CARM1's roles in MN, the cellular component predominant of each gene group has potential to indicate which MN pathways are impacted.

Consistently with what was found in Biological Processes, the datasets had a commonality. In both groups, the extracellular region was an enriched cellular component. Since this term encompasses a broad range of genes, it is unsurprising that it can be found among both datasets. Interestingly, all other terms were unique to each dataset suggesting that CARM1's influence be targeting different cellular components. Most notably, *cellular anatomical entity*, was found to be most enriched within the shCARM1 dataset. In addition, terms more meaningful in the context of this study include *intracellular anatomical structure*, *extracellular region* and the *plasma membrane*. Overall, the shCARM1 dataset points towards structural features as a main area of influence.

On the other hand, terms highlighted only within the pGIP-Z datasets are limited to *endomembrane system*, *postsynapse* and *neuron part*. These terms are more apparently related to the specialized functions expected of a MN cell type. The fact that these terms were not found in the other dataset presents CARM1's influence on HuD's binding as being meaningful towards neuronal regulation.

While more inferences could be made from this dataset, the terms discussed so far give a clear insight on the contributions of CARM1 within this cell type. The molecular function subgroup identifies signaling, DNA binding, protein-arginine deamination and structural

constituents of myelin sheaths as being influenced by CARM1 protein levels. In terms of biological function, the data suggests that CARM1 be implicated in signaling, including Wnt signaling, neuron system development and skeletal system morphogenesis. Additionally, the cellular component ontology subgroup highlights CARM1's protein level as having influence on cellular structure and neuronal parts. These findings are consistent with a model where CARM1 alters HuD's gene pool towards the regulation of MN development and signalling pathways.

Table 2: GO terms associated with protein coding genes coprecipitating with HuD in shCARM1 MN-1 cells.

Protein coding genes with GFOLD values of above 1.5 were included for GO analysis and compared to protein coding gened identified in the total cell lysate of pGIP-Z cells. The green scale bars visually represent the significance of each GO term within the sample set.

(This table is continued on the next page.)

Molecular Function		
Term Name	**GO term ID**	**-log10 Adj. p Value**
cation binding	GO:0043169	2.173
RNA polymerase II regulatory region sequence-specific DNA binding	GO:0000977	2.130
RNA polymerase II regulatory region DNA binding	GO:0001012	2.114
double-stranded DNA binding	GO:0003690	2.090
metal ion binding	GO:0046872	1.850
transcription regulatory region sequence-specific DNA binding	GO:0000976	1.845
sequence-specific double-stranded DNA binding	GO:1990837	1.688
histone acetyltransferase binding	GO:0035035	1.584
RNA polymerase II proximal promoter sequence-specific DNA binding	GO:0000978	1.550
transcription regulatory region DNA binding	GO:0044212	1.449
proximal promoter sequence-specific DNA binding	GO:0000987	1.447
regulatory region nucleic acid binding	GO:0001067	1.435

Table 2 (Continued): GO terms associated with protein coding genes coprecipitating with HuD in shCARM1 MN-1 cells.

Biological Process

Term Name	GO term ID	-log10 Adj. p Value
tissue morphogenesis	GO:0048729	7.085
animal organ morphogenesis	GO:0009887	4.750
tissue development	GO:0009888	4.446
regulation of canonical Wnt signaling pathway	GO:0060828	4.131
tube morphogenesis	GO:0035239	4.116
anatomical structure morphogenesis	GO:0009653	4.082
positive regulation of developmental process	GO:0051094	4.015
morphogenesis of an epithelium	GO:0002009	3.855
system development	GO:0048731	3.805
multicellular organism development	GO:0007275	3.747
regulation of multicellular organismal development	GO:2000026	3.713
canonical Wnt signaling pathway	GO:0060070	3.545
regulation of Wnt signaling pathway	GO:0030111	3.477
mammary gland specification	GO:0060594	3.267
tube development	GO:0035295	3.248
positive regulation of multicellular organismal process	GO:0051240	3.209
epithelium development	GO:0060429	3.196
cellular response to growth factor stimulus	GO:0071363	3.176
regulation of transcription by RNA polymerase II	GO:0006357	3.174
regulation of morphogenesis of an epithelium	GO:1905330	3.164
nervous system development	GO:0007399	3.164
cellular response to BMP stimulus	GO:0071773	3.100
response to BMP	GO:0071772	3.100
cell differentiation	GO:0030154	3.082
response to growth factor	GO:0070848	2.994
positive regulation of cell differentiation	GO:0045597	2.957
regulation of multicellular organismal process	GO:0051239	2.956
transcription by RNA polymerase II	GO:0006366	2.935
animal organ development	GO:0048513	2.883
inner ear development	GO:0048839	2.802
semicircular canal development	GO:0060872	2.728
cellular developmental process	GO:0048869	2.658
epithelial tube morphogenesis	GO:0060562	2.656
Wnt signaling pathway	GO:0016055	2.554
response to endogenous stimulus	GO:0009719	2.550
cell-cell signaling by wnt	GO:0198738	2.535
regulation of developmental process	GO:0050793	2.486
regulation of cell differentiation	GO:0045595	2.427
mammary gland formation	GO:0060592	2.422
ear development	GO:0043583	2.422
response to organic substance	GO:0010033	2.378
positive regulation of macromolecule metabolic process	GO:0010604	2.349
regulation of transcription, DNA-templated	GO:0006355	2.332
cellular response to chemical stimulus	GO:0070887	2.294
sensory organ development	GO:0007423	2.268
cellular response to endogenous stimulus	GO:0071495	2.241
regulation of nucleic acid-templated transcription	GO:1903506	2.176
positive regulation of gene expression	GO:0010628	2.164
regulation of RNA biosynthetic process	GO:2001141	2.159
cell projection organization	GO:0030030	2.120
negative regulation of canonical Wnt signaling pathway	GO:0090090	2.104
anatomical structure formation involved in morphogenesis	GO:0048646	2.095
regulation of macromolecule biosynthetic process	GO:0010556	2.067
transcription, DNA-templated	GO:0006351	2.047
response to chemical	GO:0042221	2.036
transmembrane receptor protein serine/threonine kinase signaling pathway	GO:0007178	2.021
nucleobase-containing compound biosynthetic process	GO:0034654	2.012

Cellular Component

Term Name	GO term ID	-log10 Adj. p Value
cellular anatomical entity	GO:0110165	13.116
cellular_component	GO:0005575	11.868
intracellular anatomical structure	GO:0005622	3.544
cell periphery	GO:0071944	3.459
membrane	GO:0016020	3.277
extracellular space	GO:0005615	3.209
extracellular region	GO:0005576	2.755
plasma membrane	GO:0005886	2.659

Table 3: GO terms associated with protein coding genes coprecipitating with HuD in pGIP-Z MN-1 cells.

Protein coding genes with GFOLD values of -1.5 and smaller were included for the analysis and compared to protein coding gened identified in the total cell lysate of pGIP-Z cells. The green scale bars visually represent the significance of each GO term within the sample set.

Molecular Function		
Term Name	**GO term ID**	**-log10 Adj. p Value**
receptor ligand activity	GO:0048018	3.511
receptor regulator activity	GO:0030545	3.276
molecular function regulator	GO:0098772	2.466
growth factor binding	GO:0019838	2.072
insulin-like growth factor binding	GO:0005520	1.773
protein-arginine deiminase activity	GO:0004668	1.577
signaling receptor binding	GO:0005102	1.533
structural constituent of myelin sheath	GO:0019911	1.366
Biological process		
Term Name	**GO term ID**	**-log10 Adj. p Value**
signal transduction	GO:0007165	6.281
regulation of response to stimulus	GO:0048583	4.492
system development	GO:0048731	4.339
multicellular organism development	GO:0007275	4.258
positive regulation of developmental process	GO:0051094	4.043
regulation of signal transduction	GO:0009966	3.925
positive regulation of cell differentiation	GO:0045597	3.836
regulation of cell communication	GO:0010646	3.608
regulation of signaling	GO:0023051	3.564
regulation of developmental process	GO:0050793	3.374
regulation of signaling receptor activity	GO:0010469	3.129
regulation of multicellular organismal process	GO:0051239	2.634
animal organ development	GO:0048513	2.118
regulation of cell differentiation	GO:0045595	2.031
skeletal system morphogenesis	GO:0048705	1.969
regulation of multicellular organismal development	GO:2000026	1.935
cellular calcium ion homeostasis	GO:0006874	1.917
intracellular signal transduction	GO:0035556	1.888
cell surface receptor signaling pathway	GO:0007166	1.823
cell population proliferation	GO:0008283	1.805
calcium ion homeostasis	GO:0055074	1.793
cellular divalent inorganic cation homeostasis	GO:0072503	1.753
tissue development	GO:0009888	1.721
regulation of molecular function	GO:0065009	1.683
regulation of anatomical structure morphogenesis	GO:0022603	1.660
transport	GO:0006810	1.629
divalent inorganic cation homeostasis	GO:0072507	1.583
regulation of animal organ morphogenesis	GO:2000027	1.461
adrenomedullin receptor signaling pathway	GO:1990410	1.456
peptidyl-arginine modification	GO:0018195	1.440
growth	GO:0040007	1.383
establishment of localization	GO:0051234	1.364
anatomical structure morphogenesis	GO:0009653	1.362
positive regulation of cellular process	GO:0048522	1.327
cell-cell signaling	GO:0007267	1.313
hormone metabolic process	GO:0042445	1.308
Cellular Component		
Term Name	**GO term ID**	**-log10 Adj. p Value**
extracellular region	GO:0005576	4.153
endomembrane system	GO:0012505	1.490
postsynapse	GO:0098794	1.467
neuron part	GO:0097458	1.366

4.3.6 Abundant and Differentially Enriched Genes within the HuD RIP-seq Datasets

Aside from motif analysis and gene ontology, the identities of HuD mRNA targets influenced by CARM1 are needed to understand the mechanisms downstream of the CARM1 and HuD interaction. Accordingly, a series of genes were selected for experimental validation. As before, only protein coding genes were considered. In addition, genes with larger RPKM values (arbitrarily defined as 5 or above) in at least one condition were prioritized with the aim of promoting the discovery of major HuD interactors.

4.3.6.1 *Genes enriched within the pGIP-Z dataset*

CARM1

Interestingly, *CARM1* was found to fall within the threshold of differentially abundant genes (GFOLD -2.47) (Supplementary Table 1). Evidently, the differential expression of the CARM1 mRNA transcript was expected when exploring the RNAome of shCARM1 MN-1 cells. However, *CARM1* was never confirmed or highlighted as a HuD mRNA target, making its presence in the HuD RIP-seq dataset unexpected. Among the 123 genes identified as having different abundance between samples, *CARM1* was on the higher end of RPKM values in pGIP-Z cells (Supplementary Table 1). This suggests its interaction with HuD be notable when compared to its other interactors. Mechanistically, it also suggests a potential feedback loop between CARM1 protein levels and its mRNA levels, although this cannot be confirmed from this data alone.

Schip1 and Iqschfp

With GFOLD values of -8.57 and -8.44 for *Ship1* and *Iqschfp*, respectively, these genes are a stark contrast to the rest of the dataset. Iqschfp is a fusion protein of Schip1 and Iqcj (also

denoted as Iqcj-Schip1). As such, both Schip1 and Iqschfp share a 3'UTR. Knowing that HuD interacts in majority with 3'UTR, their proximity in the dataset suggest it interacts with the fusion protein, however, neither proteins are known HuD mRNA targets. Schip1 is a cytoskeleton associated protein defined by its interaction with the merlin protein (Goutebroze et al., 2000). Unlike Schip1, Iqschfp contains a calmodulin binding IQ motif (Kwaśnicka-Crawford et al., 2006) and contributes to cytoskeletal organization at the nodes of Ranvier (Martin et al., 2016).

Smarca2

With a GFOLD value of -4.74, *Smarca2* is the third most differentially enriched gene following *Schip1* and *Iqschfp*. Smarca2 is an ATPase member of the SWI/SNF chromatin remodelling complex (Li et al., 2024), and epigenetic regulator with a strong association with neuronal differentiation (Sokpor et al., 2021). To date, the *Smarca2* is not a confirmed HuD mRNA target and there is no clear direct association in the literature linking HuD and Smarca2. This is therefore a novel interaction which warrants further experimental validation.

Adra2B

In addition, *Adra2B* was a highlighted gene of relevance due to its high RPKM and large absolute GFOLD value (-2.14). *Adra2B*, once again, is not a defined HuD mRNA target. Adra2B is a transmembrane protein and one of three sub members of the α2 adrenoceptor family (α2-AR), a G-protein coupled receptor family. Adra2B is known to regulate neurotransmitter release within the sympathetic system, as well as adrenergic neurons in the central nervous system (Papageorgiou et al., 2022). For this reason, Adra2B's regulation is of interest in the regulation of MN.

Stc2

Stc2 was also found to stand out within the dataset with a GFOLD value of -2.73. Its canonical function relates to ER stress, where its overexpression acts as part of the cell response to unfolded or misfolded proteins, oxidative stress and hypoxia as a pro-survival factor (Byun et al., 2010; Ito et al., 2004; Zeiger et al., 2011). To date, it has not been identified as a HuD mRNA target.

4.3.6.2 *Genes Enriched Within the shCARM1 Dataset*

Overall, genes enriched in the shCARM1 dataset were fewer in number. As such only two genes of interest were selected in this subset; Ptger4 and Phox2B.

Ptger4

Ptger4, or EP4, was found to stand out from other genes within this dataset through its large GFOLD value of 2.15. It is a G protein-coupled receptor (GPCR) canonically acting downstream of PGE2 towards the increase of intracellular cAMP (Katsuyama et al., 1995; Sugimoto & Narumiya, 2007). It is also not a known HuD mRNA target.

Phox2B

Phox2B was found to have a GFOLD value of 2.19 and with high abundance within the samples. It is a transcription factor and regulator of neurogenesis, especially in the specification of motoneuron types (Brunet & Pattyn, 2002). *Phox2B*, like the other genes mentioned, is not a confirmed HuD mRNA target.

Taken together, *Schip1/Iqschfp*, *Smarca2*, *Adra2B*, *Stc2*, *Ptger4* and *Phox2B* are genes that stand out from the HuD RIP-seq dataset based on their large absolute GFOLD value;

suggesting a CARM1 dependence. Their high RPKM value also suggests they be prevalent HuD mRNA targets. To date, none of the genes listed above have been established as HuD mRNA targets. The novelty suggests that CARM1's influence on HuD might be through so far undescribed interactions.

4.3.6.3 *Known HuD mRNA Targets*

Based on the data presented here, it seems that most genes identified as being influenced by CARM1 have not previously been experimentally validated within the literature as *bona fide* HuD mRNA targets. However, the dataset is consistent with what is anticipated of HuD, as many of its known mRNA targets were prevalent within the samples (Figure 10, blue labels).

First, by far the most prevalent mRNA seen in the dataset was *β-actin* (Actb), a confirmed HuD target in MN (Akten et al., 2011; Kim et al., 2015; le et al., 2017). Actb is also recognized as a particularly abundant protein expressed ubiquitously (Condeelis & Singer, 2005; Vedula & Kashina, 2018). This is consistent with *Actb*'s distinctively high read count within the samples.

In addition to *Actb*, several other mRNA targets known as HuD mRNA targets were identified within the dataset. These include *p21* (Cdkn1a) (Fujiwara et al., 2006; Hubers et al., 2011; Joseph et al., 1998), *Marcks* (Wein et al., 2003), *HuD* (Elavl4) (Borgeson & Samson, 2005), *HuR* (Elavl1) (Dai et al., 2012; Mansfield & Keene, 2011), *App* (Kang et al., 2014), *Bdnf* (Allen et al., 2013; Vanevski & Xu, 2015), *Nova1* (Ratti et al., 2008) and *Ache* (Deschênes-Furry et al., 2007) and *GAP-43* (Mobarak et al., 2000) amongst others. As expected, these genes fell towards the higher RPKM values, consistent with their enrichment expected from a HuD-RIP. Interestingly, their affinity to HuD was not impacted by CARM1 protein levels according to the criteria defined above.

On the other hand, the genes highlighted above as being potentially impacted by CARM1 protein levels fall within the same RPKM range as the genes known as HuD mRNA targets (Figure 10, green labels). This suggests that the genes highlighted have a prevalence of interaction with HuD comparable to that of its other known mRNA targets. This implies a similar degree of interaction, although it cannot be concluded from this alone.

4.3.6.4 *Experimental validation of HuD's interactions in MNs*

To test if the findings derived from the sequencing data were replicated experimentally, the ability and replicability of CARM1 protein levels to alter gene enrichment yielding from a HuD RIP was tested.

Through biological replicates, the RNA product enriched from a HuD RIP performed in MN-1 pGIP-Z and shCARM1 cells was amplified via RT-PCR (Figure 13). As none of these genes are confirmed HuD mRNA targets, the specificity of the amplification is essential. For this purpose, cross exon primers were designed to ensure the specific amplification of the mRNA product. For the primer sequences, refer to Supplementary Table 3. Due to the nature of some of the highlighted genes, several elements are important to consider for interpretation of results.

First, as a fusion protein, the Schip1 and Iqschfp primers target a sequence contained within both of the genes. The Schip1 and Iqschfp datapoints highlighted in the dataset will therefore be considered together and without distinction for this analysis. Secondly, it is important to note that cross exon primers could not reliably be used for *Phox2B*. Similarly, as an intronless gene, Adra2B primers fall within the bounds of its only exon. As such, the targeted sequence for both genes can be found on both genomic DNA and mRNA transcripts. Genomic DNA should not be present in the RIP samples based on the methodology used for RNA extraction however, it is important to rule out its potential use as template source. For this

reason, an additional set of controls was included in the experimental design. In these control samples, the purified RNA product resulting from the RIP was used as template for PCR amplification without reverse transcription. This effectively prevents the amplification from RNA transcripts and limits amplification to DNA already present in the samples should it be a meaningful source of template.

An additional factor to consider is that only the signal coming from RIP was considered in the subsequent densitometry analysis. While the inputs serve as a visual assessment of the total, the normalization of the RIP yield to the total RNA may not be reflective of the impact CARM1 has on HuD. Since CARM1 is well known to alter gene expression through transcriptional regulation, it reasons that the total mRNA levels have the potential to be different in the two cell lines expressing different levels of CARM1. Additionally, as potential HuD mRNA targets, the mRNAs investigated here are also likely to have altered stability through their association with HuD. With these unknown variables, the normalization of the signal coming from the RIP to the input would not have interpretative value. Consequently, this approach was avoided. Instead, direct comparison of HuD RIP amplification signals was used as a snapshot of the impact of CARM1 protein levels on HuD's pool of mRNA targets.

Encouragingly, the RT-PCRs of *Schip1*/*Iqschfp*, *Smarca2*, *Stc2*, *Ptger4*, *Phox2B*, *Adra2B* and *CARM1* (Figure 13A-G) performed as described above showed to be replicable and consistent with the RIP-seq datasets. For, *Schip1*/*Iqschfp*, *Smarca2*, *Stc2*, *Ptger4*, *Phox2B*, *Adra2B (*Figure 13 A-F), the PCRs performed in the absence of reverse transcription showed no signal within HuD RIP samples confirming that their amplification stems from mRNA templates as opposed to residual genomic DNA. Importantly all of the genes tested were amplified beyond

background levels (IgG) following a HuD RIP for at least one of the two cell lines. This confirms the interaction of the mRNAs of interest with HuD.

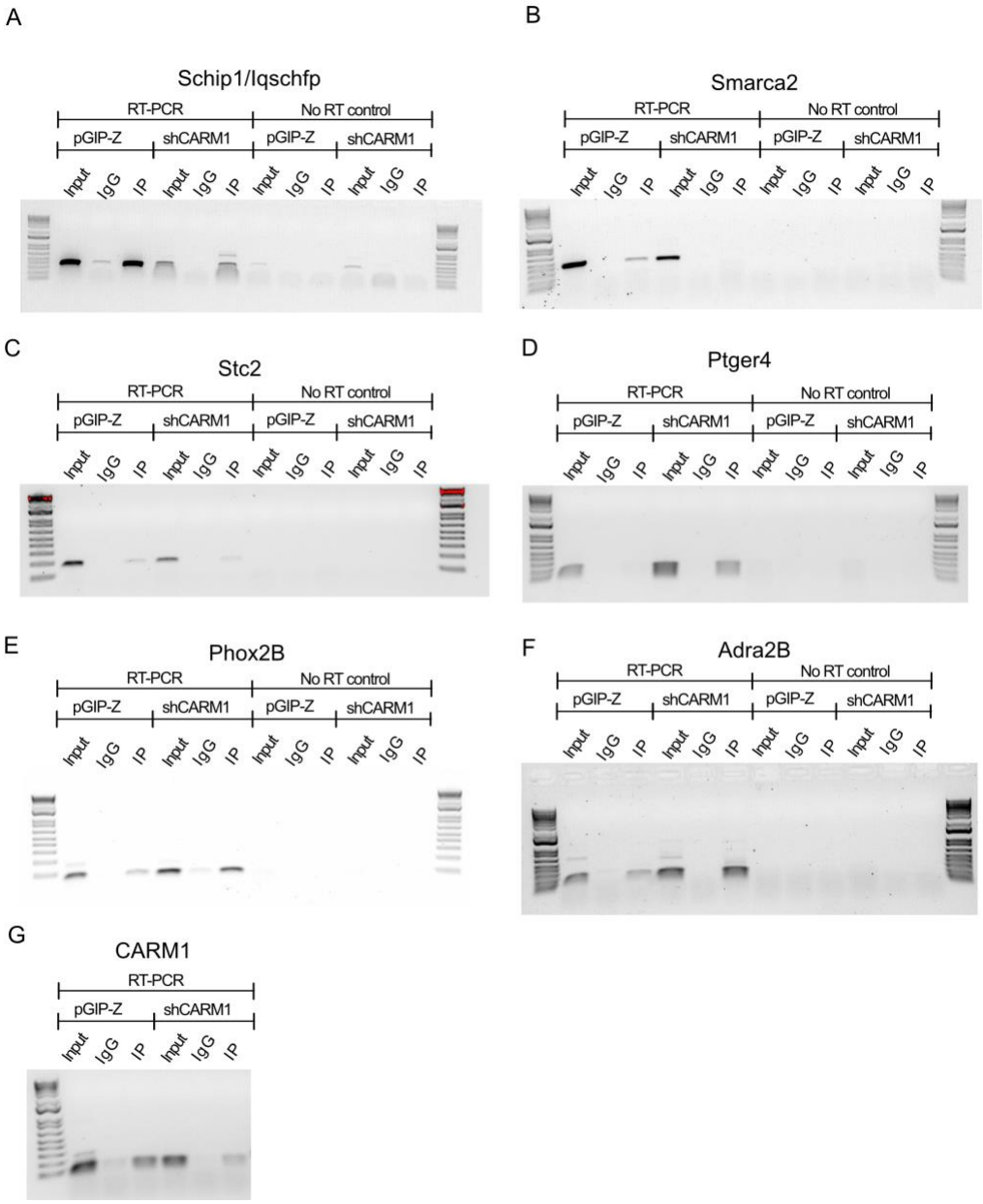

Figure 13: RT-PCR amplification of the genes of interest following a HuD RIP in pGIP-Z and shCARM1 MN-1 cells.

Schip1/*Iqschfp* (A), *Smarca2* (B), *Stc2* (C), *Ptger4* (D), *Phox2B* (E), *Adra2B* (F) and *CARM1* (G) were amplified through RT-PCR and the DNA product run on an agarose gel prior to imaging. "No RT control" samples were processed without reverse transcription. All inputs represent 10% of the total cell lysate. Images are representative of all replicates.

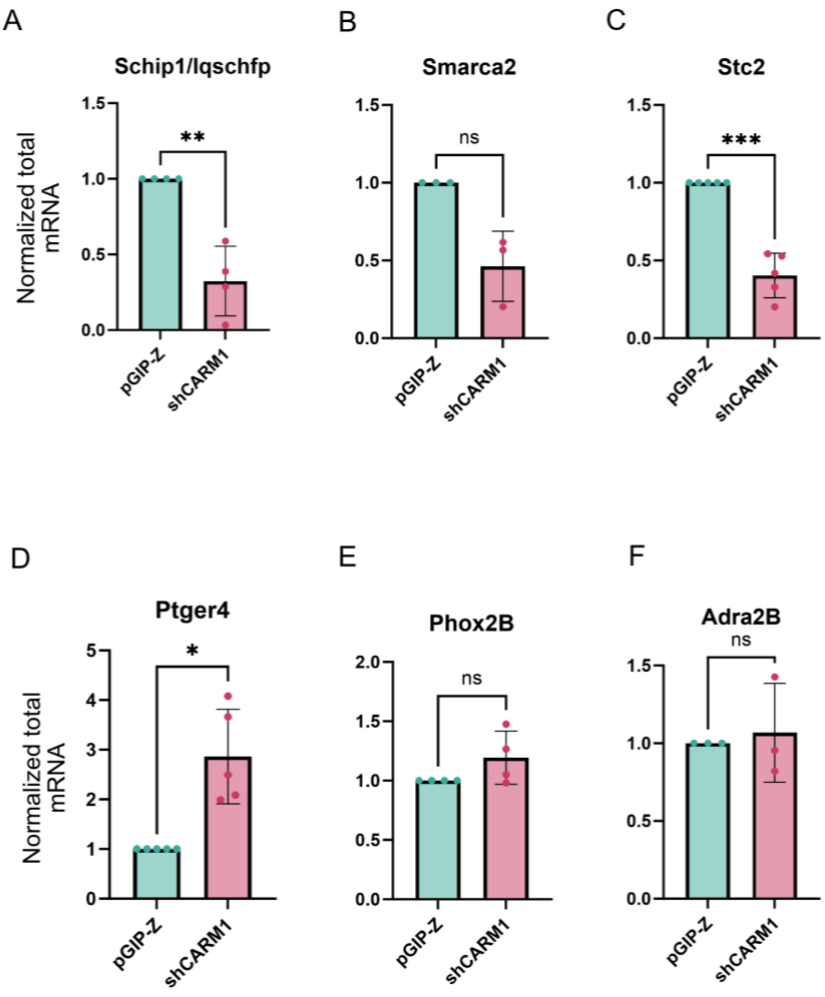

Figure 14: Quantification of the mRNA levels of the genes of interest in the inputs of pGIP-Z and shCARM1 MN-1 cells.

The RT-PCR amplification of *Schip1/lqschfp* (A), *Smarca2* (B), *Stc2* (C), *Ptger4* (D), *Phox2B* (E) and *Adra2B* (F) mRNA from inputs were quantified through densitometry analysis and normalized to the pGIP-Z sample. Each datapoint represent different biological replicates. Statistical analysis; Paired t-test $P<0.05$. N=3-5. Error bars represent SD.

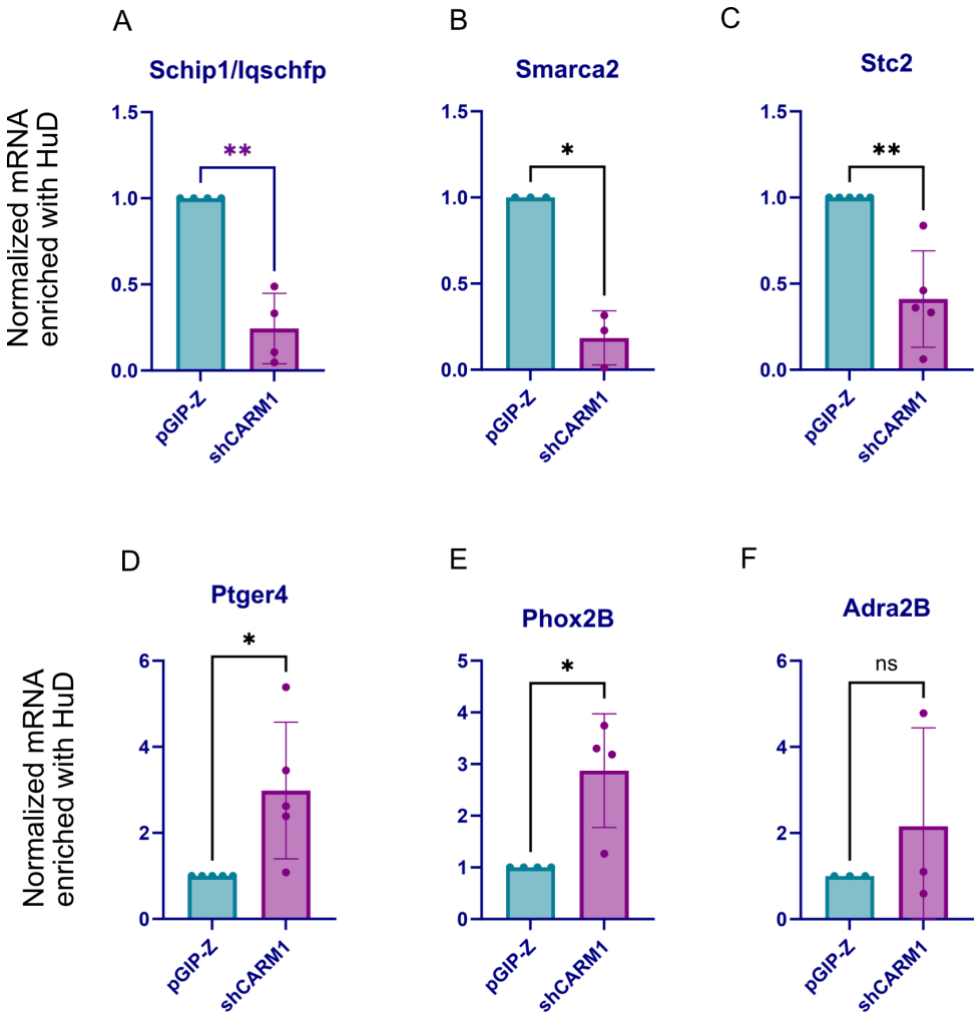

Figure 15: Quantification of the mRNA coprecipitating with HuD in pGIP-Z and shCARM1 MN-1 cells.

The RT-PCR amplification of *Schip1/Iqschfp* (A), *Smarca2* (B), *Stc2* (C), *Ptger4* (D), *Phox2B* (E) and *Adra2B* (F) from a HuD RIP were quantified through densitometry analysis and normalized to the pGIP-Z sample. Each datapoint represent different biological replicates. Statistical analysis; Paired t-test $P<0.05$. Error bars represent SD. N=3-5.

Beyond the confirmation of interaction, almost all genes tested here had significant changes in HuD interaction dependent on CARM1 protein levels. *Schip1/Iqschfp* and *Stc2* displayed the most significant change (Figure 15A, C, E), followed by *Smarca2*, *Ptger4*, and *Phox2B* (Figure 15 B, D, E). Of all mRNAs tested only *Adra2B* failed to reach significance (Figure 15F).

It is worth noting that, as seen in the quantification of the input lanes (Figure 14), the global levels of some of these mRNA targets are also dependent on CARM1. Here, *Schip1*/*Iqschfp*, *Stc2* and *Ptger4* levels are altered along with CARM1's protein levels (Figure 14A, C, D). Meanwhile, *Smarca2*, *Phox2B* and *Adra2B* did not reach significance (Figure 14B, E, F). On that account, CARM1 protein levels exert an influence on the global levels of these mRNAs. This could be reflected through changes in transcription, stability or degradation. Regardless, the significant changes of mRNA interaction with HuD between cell lines confirms that CARM1 protein levels can alter the composition of HuD's pool of mRNA targets.

In addition to the significant change in mRNA interacting with HuD, the direction of the change is consistent with the RIP-seq dataset (Figure 10). In other words, the dataset identified *Ptger4* and *Phox2B* as being enriched in HuD RIP samples of shCARM1 cells when compared to the control. Meanwhile, *Schip1*/*Iqschfp*, *Smarca2* and *Stc2* were found to be more enriched in the control as opposed to the shCARM1 cells. In all cases, the directional change agrees with the expectations of the RIP-seq dataset (Figure 15A-F, Figure 10).

In summary, it is clear that CARM1 protein levels have influence on the global levels of some of the mRNAs outlined. Still, all mRNAs could be amplified following a HuD RIP, which argues that the mRNAs of *Schip1/Iqschfp*, *Smarca2*, *Adra2B*, *Ptger4*, *Phox2b*, *Stc2 and CARM1* be true interactors of HuD. Additionally, except for *Adra2B*, HuD's interactions with the

outlined genes were found to be in dependence of CARM1 levels. For *Schip1/Iqschfp*, *Smarca2*, *Ptger4*, *Phox2b* and *Stc2,* the directional change of interaction with HuD in the two cell lines were significant and consistent with the RIP-seq dataset. This suggests that CARM1 protein levels alter the prevalence of *Schip1/Iqschfp*, *Smarca2*, *Ptger4*, *Phox2B* and *Stc2* within HuD's pool of mRNA interactors in MNs.

4.3.7 CARM1 Enzymatic Activity Impacts Ptger4 and Smarca2 Protein Levels

CARM1 function is heavily tied to its enzymatic activity, although not in complete overlap (Jayne et al., 2009; Kim et al., 2010; Sanchez et al., 2015; Yadav et al., 2003). It cannot be determined if effects observed within this chapter are a direct consequence of CARM1's enzymatic activity.

As briefly mentioned in Chapter 3, CARM1's methylation activity can be prevented through a point mutation. This mutant form of CARM1 is used within the next section of this chapter and throughout the rest of this work.

A pEGFP-N1 construct was used as the backbone for CARM1 insertion. Alone, the construct leads to free GFP expression. After CARM1 insertions, the pEGFP-N1 CARM1 construct expresses the CARM1-GFP fusion protein, while the CARM1-GFP E266Q construct expresses the enzymatically dead fusion protein (Figure 16 A). For the confirmation of the lack or presence of enzymatic activity stemming from these CARM1 constructs, refer to Supplementary data and Figure S5.

CARM1's protein levels have influence on the global mRNA levels of *Schip1/Iqschfp*, *Stc2* and *Ptger4* (Figure 14 A, C, D) and HuD's interaction with *Schip1/Iqschfp*, *Stc2*, *Ptger4*, *Smarca2*, and *Phox2B* mRNAs (Figure 15 A-E). As precursors of protein translation, it is plausible that CARM1's influence on these mRNAs results in their altered protein expression. As

such, the ability of CARM1's overexpression to incur a change in the expression of the genes highlighted was assessed by WB.

Once more, stable MN-1 shCARM1 and pGIP-Z cells were used as baselines of low or endogenous levels of CARM1, respectively. Endogenous levels of CARM1 expression could potentially stifle any exogenous effect through the saturation of its methylome. Therefore, the shCARM1 cell line is used to replicate a system unsaturated in CARM1 activity. The use of both cell lines should showcase the unstifled effect of transient CARM1 expression.

To discern between the consequences that are dependent or independent of CARM1's activity, the two cell lines were transfected to express CARM1-GFP or the aforementioned catalytically inactive CARM1-GFP E266Q mutant. After 48h incubation, the lysate was collected and used towards WB analysis. The expression of the exogenous and endogenous CARM1 protein was evaluated and confirmed prior to evaluating the protein levels of the highlighted genes (Figure 16A).

First, Adra2B protein levels 48h after CARM1-GFP or CARM1-GFP E266Q transfection show no significant changes within either the pGIP-Z or shCARM1 cells (Figure 16D). Since *Adra2B* was not experimentally found as having mRNA levels dependent on CARM1 (Figure 14F and Figure 15F), there was no strong basis supporting CARM1's ability to impact its protein levels. Accordingly, the absence of change is in line with what was observed from *Adra2B*'s mRNA experimentally.

Unlike *Adra2B*, the *Ptger4* mRNA levels interacting with HuD were found to be significantly dependent on CARM1. This does not guarantee a change at the protein level, but could be a plausible outcome of CARM1's influence. Importantly, the overexpression of the CARM1 constructs did not yield any significant changes in the pGIP-Z cells, but did reach

significance in shCARM1 cells (Figure 16B). More specifically, CARM1-GFP overexpression led to a decrease in Ptger4 protein levels. Interestingly, the overexpression of CARM1's catalytically inactive counterpart was unable to cause the same change. This demonstrates the dependence of Ptger4 protein levels on CARM1's enzymatic activity. Additionally, the absence of the same observations in the pGIP-Z cell line suggests that endogenous CARM1 expression is enough to saturate the methylome responsible for the change. By relating these findings with those of Figure 14D and Figure 15D, it can be concluded that the influence of CARM1 in Ptger4's mRNA is reflected at the protein level (Figure 16B).

Another gene of interest highlighted is Smarca2. Similarly to what is observed for Ptger4, the overexpression of CARM1-GFP was able to incur a change in Smarca2 protein levels in shCARM1 cells, but not in pGIP-Z cells (Figure 16C). The fact that Smarca2 protein levels are unaffected in pGIP-Z cells suggests that the function of CARM1 responsible for the change is saturated with its endogenous levels of expression. Interestingly, the overexpression of CARM1-GFP E266Q did not lead to a change of Smarca2 protein levels. The inability of the catalytically inactive form of CARM1 to cause the same change shows that the mechanisms at cause depend on its methylation activity. This data shows the ability of CARM1 to decrease Smarca2 protein levels in an enzymatically dependent manner.

Unfortunately, only Adra2B, Ptger4 and Smarca2 were evaluated here. Schip1/Iqschfp, Stc2, and Phox2B were omitted solely based on the absence of reliable IB antibodies. On that account, they cannot be ruled out as genes with or without a potential dependence on CARM1 at their protein level.

Altogether, this experiment demonstrates that CARM1 can alter the protein levels of genes identified within the HuD RIP-seq dataset to be dependent on CARM1. This suggests that CARM1's influence on HuD binding could contribute to changes in their expression.

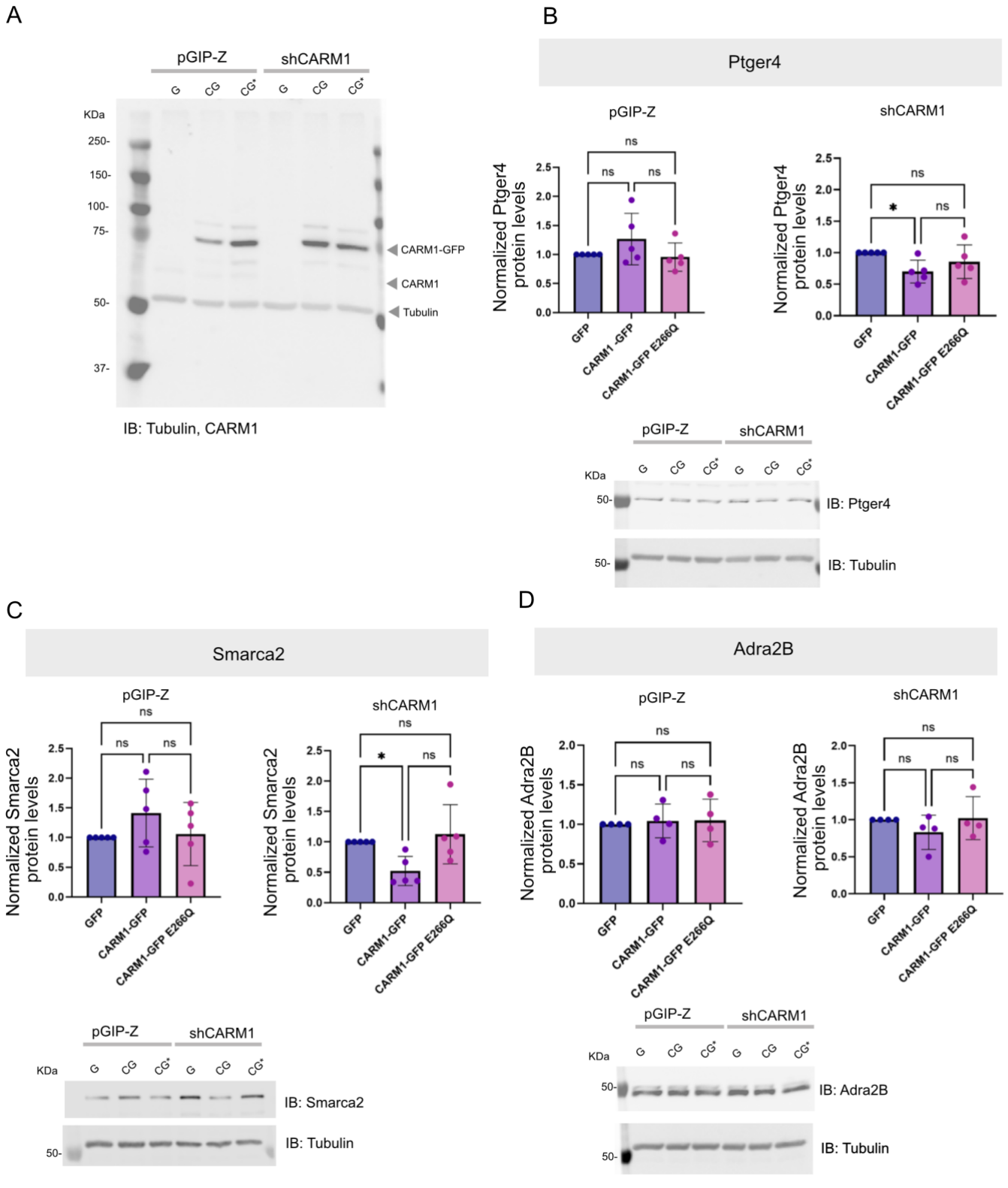
A
pGIP-Z
shCARM1
G
CG
CG*
KDa
250-
150-
100-
75-
50-
37-
CARM1-GFP
CARM1
Tubulin
IB: Tubulin, CARM1
B
Ptger4
pGIP-Z
shCARM1
Normalized Ptger4 protein levels
ns
*
GFP
CARM1 -GFP
CARM1-GFP E266Q
IB: Ptger4
IB: Tubulin
C
Smarca2
Normalized Smarca2 protein levels
IB: Smarca2
IB: Tubulin
D
Adra2B
Normalized Adra2B protein levels
IB: Adra2B
IB: Tubulin

Figure 16: Impact of CARM1 overexpression on the protein levels of Ptger4, Smarca2 and Adra2B.

(A) Stable MN-1 cells expressing either pGIP-Z control or shCARM1 were transfected with pEGFP-N1 (G), pEGFP-N1 CARM1 (CG) or mutant catalytically inactive CARM1 (CG*). The resulting immunoblots of Ptger4 (B), Smarca2 (C), and Adra2B (D) were quantified through densitometry analysis and normalized to their respective empty vector control. WB images are representative of each replicate. IB; Immunoblot. Statistical Analysis, One Way ANOVA with Tukey's multiple comparisons test. $P<0.05$, Error bars represent SD. N=4-5

4.4 Discussion

4.4.1 Identifying the Full Spectrum of HuD mRNA Targets Influenced by CARM1 in MNs

HuD is dynamic in nature, interacting with a plethora of proteins and complexes essential in RNA biology. To get a representative outlook of HuD in RNA biology, its discrimination among its protein interactors is essential. As such, stringency was prioritized in defining the experimental conditions surrounding this objective. When considering the total amount of HuD (input lane), it can be determined that the IP efficiency falls just below the 5% threshold (Figure 9). This represents a non-dominant portion of the total HuD protein. While it was found that another antibody did have a better IP efficiency, it was also determined that the IP efficiency did not necessarily correlate to the enrichment of known HuD mRNA targets (Figure S4). In fact, a more efficient HuD pull down leads to less *p21* and *GAP-43* mRNA isolated in the process. Moreover, the RT-PCR amplifications were more comparable to that of the IgG, indicating their inefficient affinity purification. Meanwhile, the lower efficiency IP led to the robust RT-PCR amplification of its known targets, especially for that of *p21*. For this reason, the conditions leading to a better RIP yield were prioritized.

It is worth noting that the p21 mRNA target, as emphasized throughout the investigative rationale of this objective, did not stand out from this dataset. Reflecting what was found by RT-PCR (Figure 9), its presence within the HuD RIP samples was confirmed in the dataset (Figure 10), but its GFOLD value (-0.14065) did not meet the threshold established in this work. As mentioned, this cell model was previously found by our group to replicate the initial finding that CARM1 methylation of HuD altered p21 mRNA affinity (Fujiwara et al., 2006; Hubers et al., 2011). The fact that it was not highlighted here suggests that other factors are involved in their interactions, such as the cell's commitment to cell differentiation. Consequently, the data presented here cannot be considered a comprehensive evaluation of CARM1 dependent HuD

mRNA targets in MN. However, 123 genes under the influence of CARM1 were identified within HuD interactors, answering to the purpose of this aim.

4.4.2 Determining Which Motifs within HuD's mRNA Targets are Influenced by CARM1

The second aim focused on the identification of motifs within HuD interactors that are influenced by CARM1. This was evaluated in two ways; first through the identification of the top motifs among the 123 genes with the largest absolute GFOLD values, and subsequently by comparing motif abundance between the pGIP-Z and shCARM1 cell lines.

As per the introduction, HuD's affinity to AREs is widely reported (Wang & TanakaHall, 2001), but U-rich motifs are now thought to be a more accurate reflection of its binding affinities (See Table 1).

When considering the motifs identified among the 123 genes highlighted, a high prevalence of U-rich sequences show consistency with the expectations of a HuD RIP. This agrees with the notion that the genes identified in this work are true interactors of HuD. Interestingly, an enriched motif, the 5-'ACACAC-3' motif, is very similar to the 5'-ACACCC-3' motif, which itself is found to precede the U-rich elements bound by HuD in the β-actin mRNA (Kim et al., 2015). Since this is not a known HuD binding site, its significance points towards a potential adjacent regulatory element.

On the other hand, when considering the motifs influenced by CARM1, poly(U) motifs were more significantly associated with HuD within the pGIP-Z cell line. This suggests that CARM1 acts positively towards the association of HuD and its highest affinity sequence (Park-Lee et al., 2003). This positive association is not in agreement with the only HuD mRNA target currently known to be regulated through CARM1. As a reminder, CARM1 was found to act negatively towards HuD's and p21's mRNA interaction (Fujiwara et al., 2006). Overall, there is

a discrepancy between the overall positive influence of CARM1 on HuD's highest affinity sequence, and its negative influence observed with the p21 mRNA. Nevertheless, this could be explained through other factors. Most importantly, the sequence targeted by HuD within the p21 mRNA is not strictly a poly(U) sequence. In fact, despite its high U content, *p21*'s sequence targeted by HuD is best described as an ARE sequence (Joseph et al., 1998). Accordingly, the poly(U) motif identified in this dataset does not necessarily represent the biology surrounding the p21 mRNA. This suggests that CARM1's influence on HuD acts beyond the ARE motif identified within the p21 mRNA and argues for an extended range of influence than what is currently described.

Within the shCARM1 cells only, a poly(A) sequence was identified as being enriched. The presence of a poly(A) sequence itself is expected in a HuD RIP as RRM3 it is known to bind polyadenylated sequences in the poly(A) tail (Beckel-Mitchener et al., 2002; Bolognani et al., 2010; Bolognani & Perrone-Bizzozero, 2008; Perrone-Bizzozero & Bird, 2013). The same motif was not found to reach the same significance in pGIP-Z cells, once again suggesting CARM1 acts negatively on its binding with HuD.

Aside from the poly(U) and poly(A) sequences, other motifs highlighted here are G-rich sequences. These G-rich sequences were found to be enriched within both cell lines, but with very different e-values. As mentioned, G-rich sequences are not associated with HuD's binding motifs but do align with their prevalence adjacent to polyadenylated regions (Kostadinov et al., 2005). Unlike the other motifs found to be under the influence of CARM1, this motif implies a means of influence outside of HuD's known binding motifs.

It is interesting that this specific motif be identified. G-rich sequences are known to form G-quartets; a secondary structure often associated with an increased RNA stability (Fay et al.,

2017). It cannot be concluded from this data alone that the G-rich sequence described here does adopt the G-quartet secondary structure *in vivo*. However, the sequence associated with this structure is closely related to those found here (Kamura et al., 2020). G-quartets have been shown to be recognized by FMRP, an RBP associated with neuronal development (Didiot et al., 2008). This structure is also associated with translation regulation (Didiot et al., 2008; Fay et al., 2017), and splicing (Georgakopoulos-Soares et al., 2022). The presence of the G-rich motif in both conditions is therefore consistent with their regulatory role in mRNA biology beyond HuD's direct binding motifs.

Most relevant to this work is the involvement of RNA G-quartets in PRMT biology. For instance, PRMT5's methylation of the RBP FXR1 was required for its binding of G-quartets, leading to increased oncogene expression (Vijayakumar et al., 2024). Meanwhile, PRMT1's methylation of FMRP led to a decrease in binding with its G-quartet containing RNA (Stetler et al., 2006). Additional regulatory elements of G-quartet containing mRNAs have emerged from such methylation events. The RGG motif, a major site of Arg methylation for most PRMTs, has the ability to interact with G-quartet containing mRNAs as described in the apoptotic inhibitor Aven. The motif's association with G-quartet containing mRNAs occured independently of its methylation. However, its methylation by PRMT1 was required for the association of methyl sensing proteins TDRD3 and SMN, which recruited the complex to polysomes. The recruitment effectively led to increased protein translation, establishing RGG motif methylation as a regulatory element in G-quartet containing mRNA expression (Thandapani et al., 2015). As such, PRMT methylation of RBPs can lead to their altered interaction with the G-quartet motif. While HuD has no evidence of being one of these proteins, it is plausible that HuD's CARM1 dependent differential affinity to mRNAs containing this G-rich motif carries a functional impact

on other RBPs and substrates of other PRMTs. As such, the regulation of this subset of mRNAs could lend CARM1 translational control beyond HuD's direct influence.

Overall, the data presented here argues that CARM1 has an expanded range of influence on HuD. For one, CARM1's influence on the mRNAs interacting with HuD reveals a positive influence on HuD and poly(U) motif interaction. On the other hand, CARM1's was found to carry a negative influence on HuD's poly(A) motif interaction. The data also reveals an influence beyond HuD's canonical binding motifs; the G-rich motif. This motif was prevalent in both groups but represented the most significant motif in shCARM1 cells. This suggests that CARM1 represses HuD's interaction with RNAs containing this motif, potentially as an additional indirect influence on the translation regulation of HuD's mRNA targets.

4.4.3 Determining the CARM1 Dependent Roles of HuD's mRNA Targets

Through gene ontology analysis, the combination of the molecular functions, biological processes and cellular components identified as being dependent on CARM1 within HuD's mRNA targets highlights a broad range of influence.

Key molecular function terms involve the recurrent Wnt pathway related terms found to be enriched within the HuD-RIP performed in the shCARM1 MN-1 cells. The functional relevance of the Wnt pathway has been extensively reported through its heavy involvement in neurogenesis (Arredondo et al., 2020; Galli et al., 2014; Lie et al., 2005; Rosso & Inestrosa, 2013; Teo & Salinas, 2021). The prevalence of Wnt related terms in a HuD-RIP of MN-1 cells is therefore consistent with the pathways expected to be at work. Coincidingly, a HuD-RIP performed in the forebrain tissue of transgenic human HuD expressing mice identified a high prevalence of genes within Wnt signalling pathways (Bolognani et al., 2010; Tanner et al., 2008).

On the other hand, no Wnt related terms were identified in the HuD-RIP performed in the control group. This shows that Wnt related genes are under the influence of CARM1 for their interaction with HuD, more specifically, that CARM1 expression acts negatively towards their association with HuD. It is unclear what functional impact could stem from the altered interaction of Wnt related genes with HuD. Nevertheless, as mentioned, transient knockdown of CARM1 has been shown to be sufficient to induce MN-1 cell differentiation (Hubers et al., 2011), and Wnt signalling contribute to neurogenesis (Arredondo et al., 2020; Galli et al., 2014; Teo & Salinas, 2021). This points towards a model where the reduction of CARM1 protein levels associated with MN-1 cell differentiation promotes HuD's interaction with Wnt associated genes, enabling their downstream contributions to neural differentiation events. The identification of terms such as *nervous system development*, *cell differentiation* and *cell projection organisation* enriched in the HuD-RIP shCARM1 sample (but not the control sample) is consistent with this hypothesis.

The identification of Wnt genes as acting downstream of CARM1 is not novel. CARM1 has previously been shown to promote the expression of Wnt signalling, albeit in colorectal cancer cells known for their aberrant Wnt gene expression and activation. In this study, CARM1 was found to promote Wnt gene expression through its coactivator function (Ou et al., 2011). The context of this interaction is not likely equivalent in MNs, however this finding is consistent with CARM1's influence on Wnt genes, and points towards HuD as an intermediate in its effect in MNs.

4.4.4 Determining CARM1's Impact on Novel HuD mRNA Targets

So far, CARM1's influence on HuD has been discussed in the scope of mRNA motif and gene ontology term enrichment. Several genes were highlighted and validated as being HuD

mRNA targets under the influence of CARM1. *Schip1/Iqschfp*, *Smarca2*, *Adra2B*, *Stc2*, *Ptger4* and *Phox2B* were confirmed as HuD mRNA targets, and for the exception of *Adra2B*, all were confirmed to be dependent on CARM1 for their interaction with HuD. Their canonical functions were briefly addressed above, however, their relevance in the context of neural and MN biology was not explored. The roles and potential ramifications stemming from their identification will be expanded on below.

4.4.4.1 *Schip1 and Iqschfp*

As mentioned, the Schip1 and Iqschfp datapoints are clear standouts from the dataset. Schip1, or schwannomin interacting protein 1, as the name suggests, is an interactor of the schwannomin protein (also denoted as NF2 or merlin). The fusion protein Iqschfp was also found to interact with NF2, Ankyrin-G (AnkG) (Martin et al., 2008) and Ankyrin-B (AnkB) (Martin et al., 2017). Schip1 is strongly expressed in the heart and skeletal muscles, while both Iqschfp and Schip1 are strongly expressed in the brain (Goutebroze et al., 2000; Kwaśnicka-Crawford et al., 2006).

Consistent with their cytoskeletal associations, Iqschfp, as well as Schip1 are established neuronal contributors, most notably through their importance in neurites. For instance, Schip1's expression coincides with axonogenesis stages in brain tissues. Adult and embryonic mice expressing Schip1Δ10, a frameshift mutant with a premature stop codon, displayed decreased size of the anterior commissure anterior branch and posterior branch consistent with axonal loss. Primary neurons from the anterior commissure showed defects in axon elongation and guidance (Klingler et al., 2015). The events leading to these defects are still unelucidated.

While Iqschfp shares a portion of its sequence with Schip1, its role appears to be distinct. In fact, Iqschfp's role is reportedly of most consequence in the long-term maintenance and

regulation of mature axonal structures. Unlike Schip1, Iqschfp is known to accumulate at axon initial segments (AISs) as well as nodes of Ranvier (Martin et al., 2008). In myelinated neurons, AISs and nodes of Ranvier are rich in voltage-gated ion channels, key for the rapid voltage changes required of action potentials (Nelson & Jenkins, 2017). Iqschfp's recruitment to these regions showed to be dependent on βIV-spectrin (P. M. Martin et al., 2008); a key node of Ranvier component requirement for normal sodium channel clustering in neurons (Komada & Soriano, 2002). Including βIV-spectrin and AnkG, Iqschfp also interacts with potassium channels (Kv7.2, Kv7.3). Mutations in Iqschfp in mice led to ataxia and reduced pain sensitivity, coinciding with the abnormal shape of cytoskeletal structures in the nodes of Ranvier (Martin et al., 2016). While the nature of these defects are yet to be fully elucidated, it suggests that Iqschfp be a structural contributor of nodal architecture.

In proliferating PC12 cells, Iqschfp was found to have a diffuse expression while differentiated cells showed it to concentrate in neurite extensions and growth cones. Moreover, it was found to colocalize to F-actin rich regions. Its punctate appearance suggests an association to organelles and active transport towards growth cones (Kwaśnicka-Crawford et al., 2006). Taken as a whole, Iqschfp's association to cytoskeletal structures in neurites emphasizes the importance of its localized recruitment for normal neuronal function in differentiated cells.

As a novel HuD interactor, this is in line with the RBP's established functions. As per the introduction, HuD is known to act towards axonal transport of its mRNA targets through its recruitment to RNA granules (Fallini et al., 2011). GAP-43 is the best example of a growth cone associated protein with a dependence on HuD for its localization. Akin to Iqschfp, GAP-43 concentrates in neurites and growth cones (Yoo et al., 2013), and colocalizes with F-actin due to

its direct interaction (Nguyen et al., 2009). Their similarity suggests a potential common method of transportation matching HuD's roles.

It is clear that Schip1 and Iqschfp have essential roles for neuron development and maintenance fitting under HuD's regulatory umbrella. This work cannot confirm that Schip1 or Iqcshfp mRNAs are direct targets of HuD. However, Schip1 was identified as being downregulated in the striatum of a HuD KO mice model (Dell'orco et al., 2021). This association suggests that HuD has a non-redundant influence on Schip1 protein levels. This could be mediated through HuD's regulation of Ship1's mRNA as the data presented here suggests. Nevertheless, other interactors are likely involved, and CARM1's influence on Schip1/Iqschfp function independently or through HuD is still unknown.

Lastly, the data presented here is the first evidence implicating CARM1, HuD and Schip1/Iqschfp in MN biology. It is clear that this association has the potential to impact MN health. For this reason, more exploration of the contributions of this pathway is needed.

4.4.4.2 *Ptger4*

Ptger4 is often viewed through the lens of PGE2 as one of its receptor subtype which also includes EP1, EP2 and three EP3 splice variants (A, B and C) (Palikhe et al., 2012; Sugimoto & Narumiya, 2007). However, each subtype differs in the type of signal transduced resulting in varied biological roles (Sugimoto & Narumiya, 2007). As the only EP receptor subtype identified within the dataset presented here, the unique roles of Ptger4 are of particular interest.

Ptger4 specifically has been linked to several diseases. Topics reoccurring in its study surround a variety of cancer types, including colorectal, lung, breast, prostate and ovarian cancer. For the most part, Ptger4's role in the aforementioned cancers contributed to disease through increased proliferation, invasion and migration (Yokoyama et al., 2013).(De et al.,

2021)(Bacabac et al., 2024)(Yokoyama et al., 2013) Interestingly, CARM1 and Ptger4's common effect on breast cancer tissue appears to be more than a coincidence, as Ptger4 can act upstream of CARM1 thereby altering its role (Hiken et al., 2016). (Johnston & Dowsett, 2003)(Hiken et al., 2016)In ligand independent growth, Ptger4 was found to be overexpressed, as well as required for growth to persist. Concurrently to Ptger4 overexpression, the intracellular concentration of cAMP was found to increase (Hiken et al., 2016), in line with its canonical function (Katsuyama et al., 1995). PKA is well known to be activated through cAMP signalling (Das et al., 2007; Koschinski & Zaccolo, 2017). PKA is also known to phosphorylate CARM1, promoting its direct binding and transcriptional activity at ERα in a ligand independent manner (Carascossa et al., 2010). Consistent with these findings, CARM1 direct interaction with ERα was found to be dependent on Ptger4 activity.To that end, the Ptger4 and CARM1 interaction was suggested to influence the transcriptional biology contributing together to breast cancer progression (Hiken et al., 2016).

Ptger4's role in neurons is less defined than in cancer biology. Consequently, its downstream impact on CARM1 is not necessarily equivalent in MNs. Nevertheless, ERα carries functions outside of breast tissues or the female reproductive system. In fact, ERα was found to be enriched within MNs (McLeod et al., 2020). Estrogen signalling was also found to enhance MN axonal regeneration after peripheral nerve injury (Acosta et al., 2017) and promote dendrite growth of steroid-sensitive MNs in a male specific subset of muscles (Rudolph & Sengelaub, 2012). The ERα pathway linking Ptger4 and CARM1 is therefore not to be excluded from MN biology.

(Li et al., 2008)(Southall & Vasko, 2001)(Echeverria et al., 2005)(Ahmad et al., 2005)Here, Ptger4 mRNA is identified as a HuD interactor in MN. Through its association with

HuD, the Ptger4 mRNA has potential to be regulated in its stability, translation and localization. Under HuD's neuronal regulatory umbrella, Ptger4 could be contributing to known and novel functions associated with HuD.

Nevertheless, the Ptger4 mRNA interaction with HuD was found to be dependent on CARM1 protein levels. Functionally, CARM1 decreased Ptger4 mRNA interaction with HuD. The decrease in interaction between the mRNA and HuD suggests a loss of overall mRNA stability that could expand to an altered Ptger4's protein levels. In line with this, Ptger4 protein levels were found to decrease upon CARM1 overexpression, but not the overexpression of the methyl dead mutant. As such, Ptger4 protein level regulation by CARM1 is mediated through its enzymatic activity. This suggests a mechanism through which CARM1's methylation of HuD influences Ptger4's mRNA stability which could at least in part contribute to its decrease in protein levels. Of course, this is only one possibility, and more work is required to test this mechanism. Most notably, it remains to be determined if HuD is required or sufficient to carry out CARM1's impact on Ptger4 protein expression.

Regardless of if HuD is an intermediate to CARM1's regulatory role on Ptger4 protein levels, this work demonstrates that in addition to Ptger4's ability to act upstream of CARM1, CARM1 can act upstream of Ptger4's expression. This is the first suggestion of a feedback mechanism occurring between Ptger4 and CARM1. What is known of how both proteins interact suggests that the ERα pathway might carry further relevance in MN, although more exploration is needed. (Ahmad et al., 2005; Echeverria et al., 2005)Since Ptger4's role in neuronal cell types is still largely unexplored, the full scale of its importance is still unreported. CARM1's influence on Ptger4 protein level could have broader implications in MN function.

4.4.4.3 *Stc2*

Stc2 is of interest in cancer research as it was found to be upregulated in a variety of tumours, correlating with increased proliferation and invasion (Qie & Sang, 2022). It is considered a hormonal protein, as it is secreted out of the cell in response to cellular stress such as nutrient insufficiency (Qie et al., 2024). In addition to its role in ER stress response, Stc2 has been shown to carry relevance in a neuronal setting, more particularly in the context of axonal injury.

In a recent study, Stc2 mRNA levels were found to increase 5.5 fold following axonomy of DRG neurons, coinciding with an increase in Stc2 protein secretion. Mechanistically, this upregulation was determined to occur via epigenetic control, specifically through HDAC5. In a sciatic nerve injury Stc2 knockout mice model, axon regeneration was found to be lacking, as reflected by a decrease in the regenerative axonal marker SCG10. Importantly, Stc2 gene delivery rescued axonal regenerative defects (Jeon et al., 2021), highlighting its requirement in this setting.

Beyond the context of axonal injury, Stc2 protein expression is linked to regulation of skeletal muscle mass. A transgenic hSTC2 mice model displayed dwarfism as a phenotype, in part through a significant reduction of skeletal muscle mass (Gagliardi et al., 2005). In humans, Stc2 was found to be a muscle mass modifier through a genome-wide association study. This finding was reflected in C2C12 cell culture, where Stc2 knockdown led to an increase in myotube length establishing the protein as a regulator of myogenesis (Hernandez Cordero et al., 2019). Additionally, Stc2 knockout mice model showed increased muscle mass, more specifically through an increase in muscle fiber hypertrophy as opposed to an increase in number (Lionikas et al., 2023). Stc2's proper regulation is therefore essential for skeletal muscle function.

In vivo studies found that the loss of Stc2 prevented recovery following axonomy (Jeon et al., 2021), and in a different study, caused an increased muscle mass (Lionikas et al., 2023). These neuronal and muscular functions shape Stc2's as having a hand in neuromuscular biology. Coincidently, Stc2's prevalence in the HuD RIP-seq dataset obtained from a MN model offers a potential avenue through which Stc2's most novel functions overlap.

(Jiang et al., 2023)Furthermore, Stc2's protein expression was found to be estrogen receptor dependent (Bouras et al., 2002). As mentioned, CARM1 acts towards estrogen receptor transcriptional activation. The finding that Stc2's mRNA levels decrease along with CARM1 protein levels (Figure 14C, Figure 15C) is consistent with what is known of Stc2's transcriptional regulation. In addition, in the context of this work, it suggests that CARM1's regulation of Stc2 mRNA be at least in part carried through at transcription, if not also through HuD.

The prevalence of Stc2 as a HuD mRNA further hints at Stc2's influence in MN. Stc2's mRNA dependence on CARM1 for HuD interaction implies a downstream influence on its mRNA's stability and/or localization. Given Stc2's role in axon regeneration (Jeon et al., 2021), this range of influence broadens the means through which CARM1 could take part of MN health. Once again, more work is required to confirm CARM1's influence beyond Stc2's interaction with HuD. The CARM1, Stc2 mRNA and HuD interaction should be considered for further investigation.

4.4.4.4 *Adra2B*

The α2-AR family was linked to actin dynamics, as their activation increased the length and number of dendritic spines in cortical neurons. This was found to occur through an increase in Spinophilin expression (J. Hu et al., 2008), an actin binding protein enriched in dendritic

spines (Hsieh-Wilson et al., 2003) and regulator of NMJ synaptic vesicle release (Muhammad et al., 2015). Adra2B is therefore a notable gene in neuronal biology.

Regarding Adra2B, the sequencing data presented here (Figure 10) identifies its mRNA as potential HuD target impacted by CARM1 protein levels. However, the CARM1 dependence did not reach significance experimentally. As mentioned, this suggests that Adra2B mRNA is not impacted by CARM1 in its levels. However, it does not rule it out as a HuD mRNA target. In fact, through RT-PCR following a HuD RIP, Adra2B was amplified suggesting an interaction. The data presents Adra2B as being a novel HuD mRNA target. That alone brings insight to MN biology, a cell type for which HuD mRNA targets have yet to be explored. It goes without saying that Adra2B and its downstream function have clear ties to neuron biology. Current investigation found it tied to several cognitive processes; memory (Fairfield et al., 2019; Rasch et al., 2009), emotional information processing (Mammarella et al., 2016; Xie et al., 2018) being clinically its main area of interest. At a molecular level, the Adra2B's distinction from other α2-ARs adrenergic receptors is still in its early stages of investigation. The potential implications of HuD in neuron biology should be considered in further explorations of Adra2B.

Adra2B is the only mRNA target identified within the RIP-seq dataset whose affinity with HuD appeared to be influenced by CARM1 but that was not validated experimentally. For this reason, Adra2B will not be emphasized in the rest of this work since it does answer this work's hypothesis.

4.4.4.5 *Phox2B*

Phox2B is a transcription factor found to mediate the expression of neural specification genes. In the three main subtypes of MNs; branchial, visceral and somatic, Phox2B is required for the formation of the former two, but not the somatic subtype (Dubreuil et al., 2000, 2002).

Without Phox2B, mice embryos did not have the branchial and visceral nuclei expected of this developmental stage of the hindbrain. Further investigation found that the absence of Phox2B did not impair MN progenitor cell prevalence but blocked their ability to differentiate and form axons (Pattyn et al., 2000). Overall, the timed regulation of Phox2B in the early development of branchial and visceral MNs is required for a normal phenotype.

Aside from its key role for normal development, its abnormal expression is also enough to alter cell fate. For instance, forced expression of Phox2B in chick embryonic spinal cord, led to ectopic neurons with abnormal MN-like phenotype. In other words, these ectopic neurons expressed Islet1 and ChAT, but not Islet2, consistent with the markers associated with branchial and visceral MNs (Dubreuil et al., 2000). Therefore, abnormal expression of Phox2B is sufficient to promote atypical neural differentiation with a likeness to branchial and visceral MN subtypes.

As mentioned, Phox2B is a transcription factor with a hand in neural specification gene expression, consistent with its influence on MN lineage. Notably, Phox2B can upregulate Ngn2 (Neurogenin2) (Dubreuil et al., 2002), a proneuronal factor, which depends on other transcription factors to specify neuron identity (Ma et al., 2008). Phox2B can also repress Pax6 and Olig2 (Dubreuil et al., 2002). In the spinal cord, Pax6 is a transcription factor which activates Ngn2 expression (Scardigli et al., 2003), which in turns represses Pax6 towards MN differentiation (Bel-Vialar et al., 2007). In addition to its Phox2B dependent downregulation, Olig2 is also downregulated by Ngn2 to promote MN lineages over those of astrocyte or oligodendrocytes (Hulme et al., 2021; S. K. Lee et al., 2005). Islet1, a required gene for specification of MN lineages (Pfaff et al., 1996), also acts downstream of Phox2B in sympathoadrenal neurons (Huber et al., 2013). Since the mechanisms surrounding lineage specification are complex, they cannot in their entirety be reviewed here. Nevertheless, Phox2B's impact on Ngn2, Pax6, Olig2

and Islet1's biological function is a clear indicator to its particular relevance in MN lineage determination and the premise of this work.

As a novel HuD mRNA target whose interaction is dependent on CARM1, this new avenue of regulation suggests CARM1 could have a hand in these biological functions. According to the HuD RIP dataset, Phox2B's mRNA interacted with HuD more in the experimental condition, suggesting CARM1 negatively impacted the association. Should CARM1's impact on Phox2B's mRNA be reflected at the protein level, this could reflect a novel way through which CARM1 could influence MN health. Needless to say, more work needs to be done to test this hypothesis. However, deregulation in Phox2B's mRNA stability is already pathologically relevant in MN disease, as investigated by Mitsuzawa *et al*. Since this is closely related to the work presented here, this will be expanded on below.

In a familial ALS iPSC model (TARDBP p.G376D mutation), Phox2B mRNA levels were found to be downregulated. Further investigation into the impact of pathological TDP-43 found that it lacked WT TDP-43's ability to bind Phox2B mRNA and localize to neurites, coinciding with a decrease in neurite length. They also reported a decrease in global Phox2B mRNA stability, although pathological TDP-43's interaction with the Phox2B mRNA was unchanged. This leaves the cause behind its decreased stability unresolved. The authors suggest there is a distinction to be made between two Phox2B isoforms that could account for the loss of stability (Mitsuzawa et al., 2021). While certainly plausible, it also leaves the possibility of other regulatory elements impacting Phox2B's mRNA levels. Based on this work, HuD, and by extension, CARM1, could be one of those elements. Both HuD and CARM1 have been involved in ALS, and fit within the scope of its pathology (De Santis et al., 2019; Dell'Orco et al., 2021; Liu et al., 2018). Deregulations stemming from their interactions should not be ruled out.

In any case, the work presented here identifies Phox2B as being a member of HuD's pool of mRNA interactors under the influence of CARM1. The novel interaction of these three genes supports the idea that they take part in MN health. The interaction of CARM1, HuD and Phox2B should therefore be considered for further investigation.

4.4.4.6 *Smarca2*

Smarca2, also known as BRM, is a core component of the SWI/SNF chromatin remodeling complex. Alike to its homologous counterpart, Smarca4 (or BRG), it functions as an ATPase subunit, hydrolysing ATP towards nucleosomal disassembly (Kim et al., 2024; Li et al., 2024). The complex has transcriptional control leading to gene activation or repression (Martens & Winston, 2003). The transcriptional changes yielding from this chromatin remodeling are understood to be tightly regulated to maintain cellular health, as more than 20% of all cancers were reported to have mutations within SWI/SNF subunits (Church et al., 2023; Wang & Tang, 2023).

The SWI/SNF complex subunits are interchangeable, providing distinguishable compositions and functionalities. Smarca2 is found in what is termed the BAF (BRG/BRM Associated Factors) complex. In addition to its association to cancer biology as a member of the SWI/SNF complex (Wang & Tang, 2023; Wang et al., 2014), the BAF complex has been shown as necessary to normal neuronal function.

The complete ablation of the BAF complex in the cortex of developing mice revealed it to be required for correct neuron morphogenesis. In its absence, deficiencies in excitatory neuron projection were prominent as seen through defects in cell adhesion, polarization and Wnt signalling (Sokpor et al., 2021). Additionally, the presence of the complex is not enough to guarantee proper neural development. Since its subunits are interchangeable, its control is also

mediated through the spatiotemporal distributions of the complex and its subunit composition (Ho et al., 2019; Lessard et al., 2007). Without adapting its subunits from the neural progenitor BAF (termed npBAF) to the neural BAF (nBAF), the transition from neural stem cell progenitor to post mitotic neurons is blocked (Lessard et al., 2007). The BAF complex is also required for forebrain development, with proliferation, differentiation and survival of neural progenitor cells being dependent on its function (Narayanan et al., 2015). The BAF complex is therefore undeniably linked to neural development, and the identity of its components is required if one is to understand its functionality.

Admittedly, the BAF complex is composed of mutually exclusive Smarca2 or Smarca4 (Gao et al., 2019; Jelinic et al., 2014), and as above (Lessard et al., 2007; Sokpor et al., 2021), the distinction between the ATPases is not always made. It is possible that one of the ATPases be specifically required to drive neural development in addition to the other subunits mentioned, however this remains to be investigated.

Smarca2 has clear clinical roots in neural pathology. The Nicolaides-Baraister Syndrome (NCBRS) is caused by pathogenic variants of Smarca2, with an initial onset of neurological symptoms, such as seizures, as early as 7 months old (Zhang et al., 2022). The syndrome is further characterized by its high prevalence of intellectual disability, as well as cognitive delay, limited speech and microcephaly (Pretegiani et al., 2016).

The specifics of how these symptoms come to be are still an ongoing point of interest, but investigations into this field found that the pathological variants of Smarca2 are structurally sound, retaining the ability to gather in the BAF complex, but with altered functional role (Gao et al., 2019; Van Houdt et al., 2012).

Interestingly, most mutations associated with the syndrome localize to areas of DNA contact but are not an apparent cause of altered affinity to DNA (Gao et al., 2019). Nevertheless, the expression of pathological Smarca2 variants caused widespread gain and losses of chromatin accessibility, in addition to defects in neurogenesis. More specifically, hESC expressing pathological Smarca2 variants showed defects in neural progenitor cell differentiation, failing to express key neural progenitor markers Pax6 and SOX2, and having reduced expression of neural-specific transcription factor SOX3. In addition, increased chromatin accessibility caused the recruitment and colocalization of Smarca2 and Smarca4, and *de novo* activation of astrocyte enhancers (Gao et al., 2019). As such, the epigenetic impact yielding from Smarca2 is of relevance in the context of neurogenesis and determination of cell lineage.

Curiously, conditional knockout of Smarca2 in mature rats is viable, with no toxicities associated with its loss (Maher et al., 2023). This is a stark contrast to the pathologies observed in NCBRS. The early onset of neurological symptoms associated with the syndrome, combined with the experimentally validated requirement of Smarca2 for normal neural differentiation suggests it is likely to be relevant throughout development, whereas the viability of its loss thereafter suggests its role be redundant past maturity.

4.4.5 CARM1, HuD and Smarca2

The identification of a prominent ATPase from the SWI/SNF chromatin remodeling pathway also builds on the premise that CARM1 takes part of the chromatin remodeling it causes. CARM1 has already been shown to methylate BAF155 (or SMARCC1), a subunit of the BAF complex. The methylation strengthened the colocalization of BAF155 and Smarca4 and promoted the expression of the NANOG pluripotency marker (Panamarova et al., 2016). Additionally, in the context of breast cancer the same methylation equipped BAF155 with the

means to increase proliferation and metastasis (Wang et al., 2014). It is worth noting that CARM1 was the only canonical PRMT able to methylate BAF155 *in vitro* (Wang et al., 2014). Moreover, it was found that Smarca4's ATPase activity was activated through a direct interaction with CARM1 and promoted ER-dependent transcription (Roberts, 2014; Xu et al., 2004), although Smarca4 is not a CARM1 substrate. Instead, Smarca4 acts as an intermediate between BAF155 and CARM1 (Xu et al., 2004). CARM1's influence towards pluripotency and proliferation through BAF155 and Smarca4 in the SWI/SNF complex corroborates to its epigenetic impact beyond that of histone methylation, with a strong influence on cell lineage.

It is interesting that the methylation of BAF155 incurs a stronger colocalization with Smarca4, and that CARM1 interacts with Smarca4. While the same studies did not investigate if Smarca2 is impacted similarly, (Panamarova et al., 2016; Xu et al., 2004), the fact that the two ATPases of the SWI/SNF complex are mutually exclusive (Gao et al., 2019; Jelinic et al., 2014) suggests a potential inverse correlation between CARM1 activity and Smarca2 recruitment to the SWI/SNF complex.

Functionally, the two proteins are established opposites in their influence over the cell cycle. As expanded upon earlier, CARM1 has a strong association with pluripotency and proliferation. In addition, as demonstrated by our group in the MN-1 cell model, CARM1 is quickly downregulated at the protein level upon differentiation. Knocking down CARM1 is also sufficient to induce an increase in differentiation (Hubers et al., 2011). Accordingly, the downstream impact of CARM1 is significant in the determination of cell fate, and its protein expression is associated with the outcome.

Meanwhile, Smarca2 upregulation within various cell models (P19, F9, C2C12) was found to be synonymous with differentiation, with its protein levels strongly increasing

throughout the process (Itoh et al., 2008). In a neuronal setting, Smarca2 protein was found to be lowly expressed in neural progenitor cells but was strongly induced after initiation of differentiation (Machida et al., 2001). Smarca2 was also found to have increased protein expression upon neuronal differentiation coinciding with the transition from npBAF to nBAF (Staahl et al., 2013).

While the protein levels of CARM1 and Smarca2 were not evaluated together, these findings are consistent with a model where CARM1 and Smarca2 protein levels inversely correlate, to promote either proliferation or differentiation. The apparent necessity of an increase in Smarca2 protein levels during differentiation emphasizes the significance of the elements mediating its protein expression. Prior to this work, the HuD and *Smarca2* interaction had yet to be defined. This alone, brings interest on potential new additions to HuD's functions, but the influence of CARM1 protein levels on HuD's binding ability towards *Smarca2* highlights a potential regulatory pathway through which Smarca2 protein levels could be at least in part modulated.

Based on the data presented here, CARM1 does not significantly alter Smarca2's total mRNA levels (Figure 14B). However, there is a CARM1 dependent increase in interaction between HuD and *Smarca2* mRNA (Figure 15B). While not exclusively the case, HuD is mostly known to promote the active translation of its mRNA targets (Kullmann et al., 2002; Tebaldi et al., 2018). If taken at face value, this would suggest that Smarca2 protein levels would increase to reflect a stronger association with HuD and subsequent increased translation. However, the data presented here also determined that transient expression of active CARM1, but not its inactive form, decreased Smarca2 expression (Figure 16C). This demonstrates that additional regulatory elements are present and contribute to lower Smarca2 protein levels, and that the same

regulatory elements are dependent on CARM1's activity. This suggests that CARM1's enzymatic function has post-transcriptional control on Smarca2, although the mechanisms potentially at cause are unknown.

As above, Smarca2 is linked to neuronal health. Its identification as a HuD mRNA target is consistent with what is already known of HuD's function. It reasons that a major neurogenesis RBP regulates the mRNA of an epigenetic factor associated with neuronal development. Furthermore, HuD function is known to be modulated by CARM1 methylation. The potential dependence of *Smarca2* mRNA stability on HuD's methylation would be consistent with its known attributes.

Having established that CARM1 increases *Smarca2* mRNA binding with HuD while repressing its protein expression, the data points towards a model where CARM1 is a regulator of Smarca2 protein expression in MNs. Considering what is known of each protein, the molecular shift between proliferation and differentiation could potentially be a particularly relevant process. With the understanding that the interactions are not fully resolved yet, the literature and data shown here is consistent with the following model.

It is consistently reported that Smarca2 protein levels increase rapidly in the transition from proliferation to differentiation. As such, the regulation of its mRNA transcript is likely to be closely tied to the events leading the transition. In a proliferative state, abundant CARM1 could act through HuD to stabilize Smarca2's transcript while also acting downstream to repress its expression. At this stage, Smarca2 protein levels are low and its mRNA protected by HuD.

At differentiation onset, when CARM1 levels drop, its repression on Smarca2 protein dwindles resulting in a rise in its expression. At this stage, HuD's abundant interaction with

Smarca2 contributes to its upregulation. As a contributor to neuronal differentiation, Smarca2 would drive and/or further the differentiation until its completion (Figure 17).

Moreover, since Arg methylation is a stable modification, the drop in CARM1 protein levels at differentiation would not cause the immediate loss of HuD's interaction with *Smarca2*, maintaining its increased transcript interaction until protein turnover restores it to its basal methylation state. Such a mechanism could then restore Smarca2 to basal levels after the transition is complete. Of course, more work needs to be done to test if this model is corroborated in the cell model.

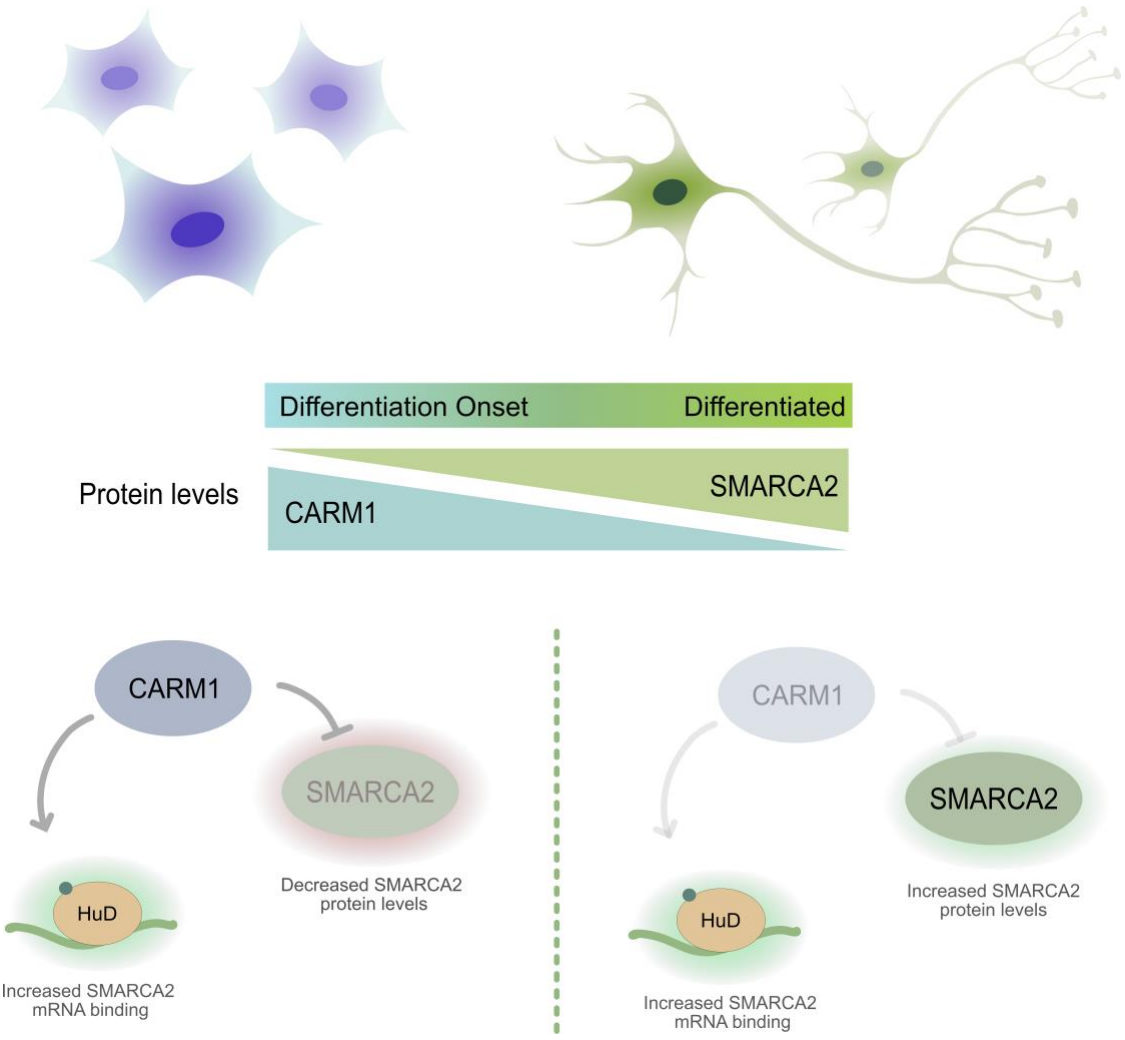

Figure 17: Proposed model of the interactions linking CARM1, Smarca2 and HuD in MN differentiation.

Lastly, Smarca2 also has a transcriptional influence on a known CARM1 substrate. As mentioned, hESC expressing pathological Smarca2 failed to express the transactivator SOX2 (Gao et al., 2019), a marker of neural stem cells, stemness and pluripotency (Bareiss et al., 2013; Ellis et al., 2004; Schaefer & Lengerke, 2019). SOX2 is a known substrate of CARM1. Its methylation impacts SOX2's ability to self-associate and act as a transactivator (Zhao et al., 2011). Akin to CARM1, SOX2's expression was found to be aberrant in various forms of cancer, including breast and ovarian cancer (Bareiss et al., 2013; Leis et al., 2012; Lengerke et al., 2011). The ability of Smarca2 to regulate SOX2 could also have a downstream impact on CARM1 function. The novel link between CARM1 and Smarca2 protein levels described in this work implies a potentially functional mechanism through which CARM1, Smarca2 and SOX2 intersect. In any case, more exploration is required to test if such an interaction is reflected in the MNs.

To conclude, the work described here establishes the first links between CARM1, HuD and Smarca2 in MNs; first, that the CARM1 protein promotes HuD's interaction with *Smarca2* mRNA, and second, that CARM1's activity can decrease Smarca2 protein levels. The bigger picture surrounding these interactions is undetermined. The premise of a CARM1, HuD and Smarca2 interaction is a strong incentive to research how three independently major regulators of cell function can act in conjunction towards MN regulation.

4.4.6 Limitations and Future Directions

The conclusions drawn from the data shown here offer many other lines of investigation to pursue. First and foremost, there are missing elements relating to the methodology used here. Evaluating if Schip1, Iqschfp, Stc2 and Phox2b protein levels are dependent on CARM1's enzymatic activity, akin to Smarca2 and Ptger4, would be of value to complete this preliminary

line of investigation. As mentioned, a CARM1 dependent protein level change does not necessarily equate to HuD's involvement. However, identifying such a dependence does give direction to the next steps of investigation of HuD and mRNAs of interest.

There remains to make a distinction between direct HuD mRNA targets or interacting mRNAs. IPs do not discriminate against indirect interactors. It cannot be argued that the HuD IPs presented did not also pull-down unintentional targets. Nevertheless, the conditions maintained throughout these experiments were purposely carried through with high stringency to avoid the discovery of confounding mRNAs. As such, while this limitation must be considered, the data presented here is brought forward through conditions most favorable to promote the discovery of direct HuD mRNA targets. As mentioned, the comparable abundance between the confirmed HuD mRNA targets and the novel targets identified here (Figure 10) suggest a direct interaction. Still, confirmation is required in order to properly characterize the interactions.

A Clip-seq experiment would be an ideal tool to determine HuD's footprint for each of its mRNA targets in MNs. In addition to making a stronger argument for a direct interaction, this method narrows the location of the interaction.

The premise of this work focuses on the ability of CARM1 to alter the landscape of HuD's mRNA binding. The methodology used does not discriminate between HuD and methylated HuD (HuD*) and instead relies on altered CARM1 protein levels. As such, the findings outlined here do not differentiate between what is a consequence of methylation dependent affinity with HuD or a CARM1 dependent change in target mRNA levels through other pathways. Overall, while the changes described are dependent on CARM1, it cannot be argued that it is necessarily through HuD's methylation. The involvement of HuD in the process can be tested through two *in vitro* experiments. First, an RNA mobility shift assay would test the

ability of HuD or HuD* to bind to the mRNA target of interest and alter the complex's ability to migrate through a native gel. Secondly, a filter binding assay would give quantifiable mean to assess the binding affinity of HuD or HuD* to the mRNA of interest.

As mentioned, CARM1's methylation of HuD allowed its binding with SMN and concurrent recruitment to RNA granules for axonal transport (Hubers et al., 2011). These mRNAs could also be dependent on CARM1 for axonal transport. Among the genes listed, Iqschfp particularly has functions tied to its axonal localization (Martin et al., 2008, 2016). It is of interest to determine if CARM1 is a determining factor in its localization of other highlighted genes.

Furthermore, in terms of data analysis, the investigation focused on protein coding RNAs, so while HuD is known to bind many types of RNAs, only mRNAs were considered here. Accordingly, the conclusions made through this work does not encompass the full scope of RNA biology that may be impacted. Additional bioinformatic analyses with the current dataset could also be further expanded on. Lastly, there are limitations associated with the use of the MN-1 cell model. Since this relates to more than this chapter, these limitations will be discussed in Chapter 6.

4.4.7 Conclusion

In this chapter, CARM1's influence on HuD's interaction with its mRNA targets in MNs was investigated, which so far had not been explored. Here, a HuD RIP-seq found that CARM1 heavily influenced the G-rich motifs, although they are not known to be HuD binding motifs. The data here also suggest that CARM1 acts positively towards the association of HuD and the poly(U) motif. In terms of GO, the data reinforces CARM1's influence on differentiation through HuD, but also suggest additional neuronal roles. At the gene level, *Schip1/Iqschfp*,

Ptger4, *Stc2*, *Phox2B* and *Smarca2* are identified as novel HuD mRNA targets, all of which are dependent on CARM1 for their association to HuD. Ptger4 and Smarca2 are also found to be dependent on CARM1 at their protein levels, although the importance of HuD in this process was not investigated.

As a whole, this investigation identified several means of influence deriving from CARM1 in MNs. When considering the genes highlighted in this study, none were previously established as HuD mRNA targets. Through this novelty, it is clear that the full extent of CARM1's influence in MNs is not fully defined. This suggests that CARM1's role in MNs takes part of pathways so far undescribed in the cell type. In this regard, this work establishes CARM1 as an emerging player in MN biology, prompting for more investigation of its contributions to the MN cell type.

Chapter 5 CARM1 Interactions in Motoneurons

The identity of CARM1 substrates has been proven to be biologically relevant in both normal cell function and disease. The cell type specific roles it may carry has the potential to have therapeutic value beyond the scope of its predominant study in cancer research. In neuronal cell types, CARM1 has an established function, but there has been little furthering of this field of study throughout the years. This chapter aims to explore CARM1 neuronal substrates with the objective of shaping the general outlook of this ubiquitous protein within the frame of the MN cell type.

5.1 Experimental Overview

MN-1 cells stably expressing GFP, CARM1-GFP or CARM1-GFP E266Q were generated and used in an GFP-AP/MS experiment towards the isolation of interacting partners. The proteins of interest were validated through an *in vitro* methylation assay. The AP/MS methodology is based on co-authored paper (Morettin et al., 2019).

5.2 Results

5.2.1 Generation of CARM1-GFP Stable Cell Lines

Using the GFP, CARM1-GFP or CARM1-GFP E266Q constructs described above, MN-1 cells were transfected and selected for stable genomic integration. After selection, the three cell lines were further selected by flow cytometry using GFP fluorescence as a selection tool towards the isolation of cell populations expressing it in equal intensity. Accordingly, the expression levels of GFP, CARM1-GFP and CARM1-GFP E266Q were further investigated by WB. The resulting blots show bands at a MW of ~90 kDa for the CARM1 constructs, and a ~27 kDa band for the GFP alone construct (Figure 3A). This is consistent with the expression of the intended

protein product. There was however a visible decrease in signal coming from the CARM1-GFP E266Q protein when compared to its enzymatically active counterpart. This is unexpected given the population selection for equal expression of GFP constructs. Although this could suggest an inherent lower expression level, the evidence of free GFP in the mutant lane (Figure 3A) points towards the degradation of the protein product. Since CARM1 is largely dependent on its catalytic activity to carry out its roles (Yadav et al., 2003), it can be expected that the cell's response to its accumulation lead to its cleavage or degradation (Trinkle-Mulcahy, 2019). This experimental artefact should be considered in the downstream applications of these cell lines but given the sustained expression of the mutant fusion protein, the cells were subsequently used for interactor identification. Importantly, the endogenous levels of CARM1 remain unaffected by the expression vectors, suggesting that its effect be consistent among all cell lines.

5.2.2 CARM1 Localization

The localization of CARM1 within the stable cell lines was evaluated by fluorescence microscopy to determine if the exogenous CARM1 interactions are representative of the endogenous protein. As mentioned, CARM1 localization is dependent on cell type, and not strictly considered either nuclear and/or cytoplasmic (Herrmann et al., 2009). In MN-1 WT cells, CARM1 signal is specular and dispersed within the cytoplasmic compartment of the cell with noticeable perinuclear accumulation (Figure 18). CARM1 signal is also consistent with nuclear localization, suggesting it localizes to both compartments in this cell type. The same observations are made of the free GFP expressing MN-1 cells (Figure 19). The perinuclear CARM1 accumulation is more contrasting in MN-1s expressing the fusion protein, but this finding is consistent with CARM1's overexpression (Figure 20, Figure 21). GFP localization is diffuse in the free GFP expressing cells, but colocalized with CARM1 in the fusion protein

expressing cells, consistent with the expected signal. Taken together, CARM1's distribution is conserved within all cell lines, suggesting that exogenous CARM1 interactions are representative of endogenous CARM1.

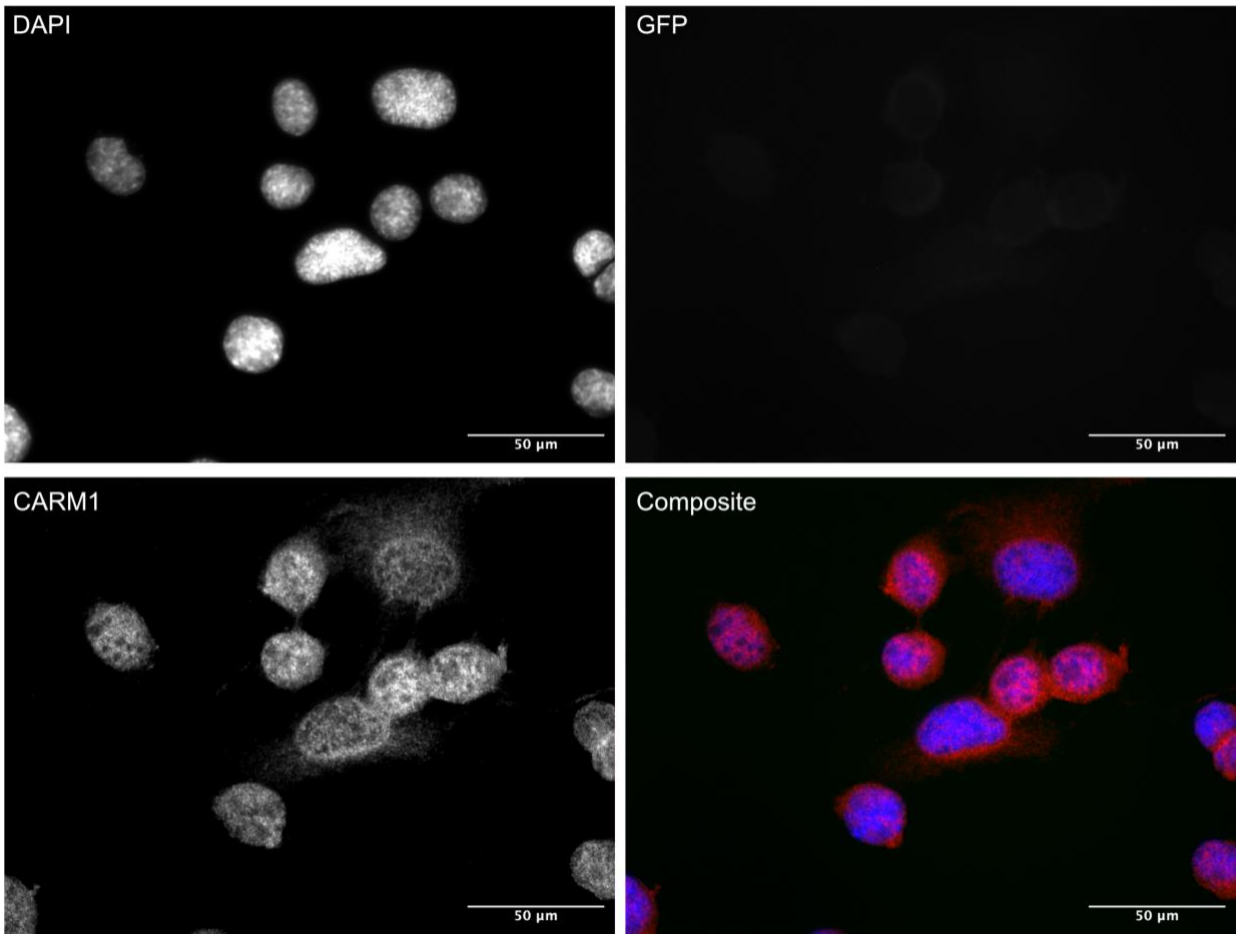

Figure 18: Fluorescence microscopy of WT MN-1 cells.

Proliferating MN-1 cells were fixed, probed for CARM1 and stained with DAPI. All images are representative and taken in random fields of view. Composite image shows DAPI (blue), CARM1 (red) and GFP (green). Scale bar represents 50 µm.

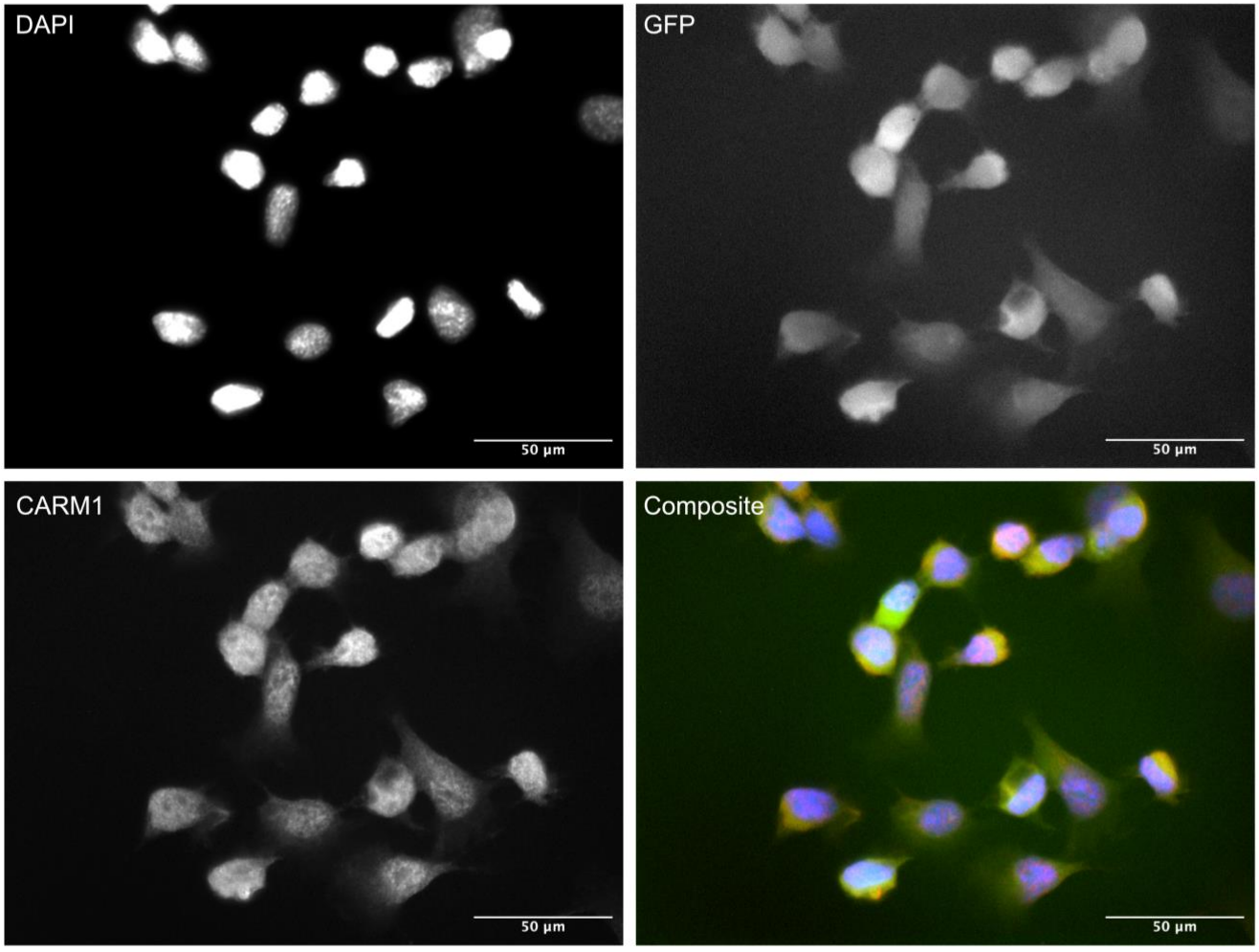

Figure 19: Fluorescence microscopy of stable MN-1 cells expressing pEGFP-N1.
Proliferating MN-1 cells were fixed, probed for CARM1 and stained with DAPI. All images are representative and taken in random fields of view. Composite image shows DAPI (blue), CARM1 (red) and GFP (green). Scale bar represents 50 µm.

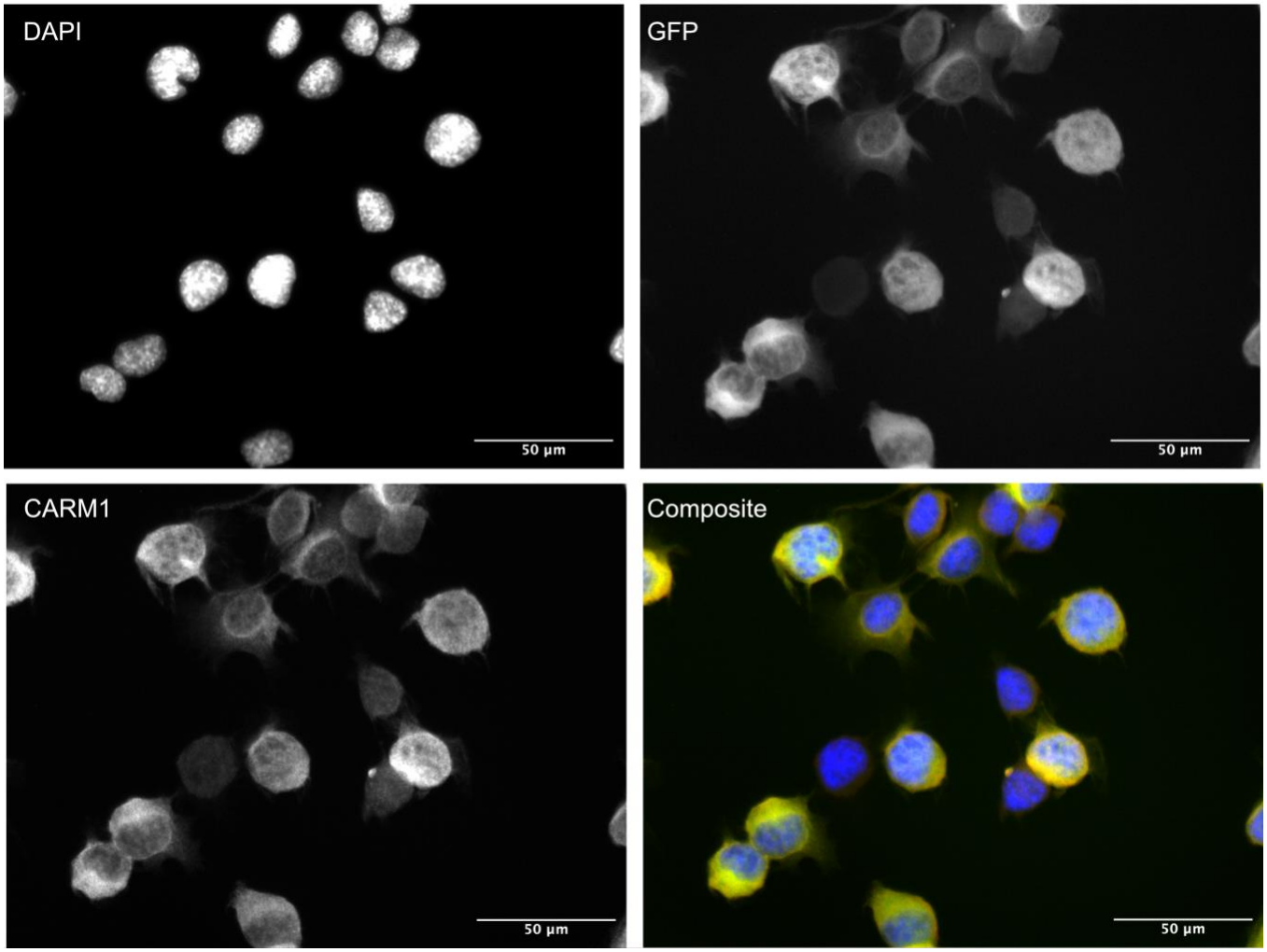

Figure 20: Fluorescence microscopy of stable MN-1 cells expressing pEGFP-N1 CARM1. Proliferating MN-1 cells were fixed, probed for CARM1 and stained with DAPI. All images are representative and taken in random fields of view. Composite image shows DAPI (blue), CARM1 (red) and GFP (green). Scale bar represents 50 µm.

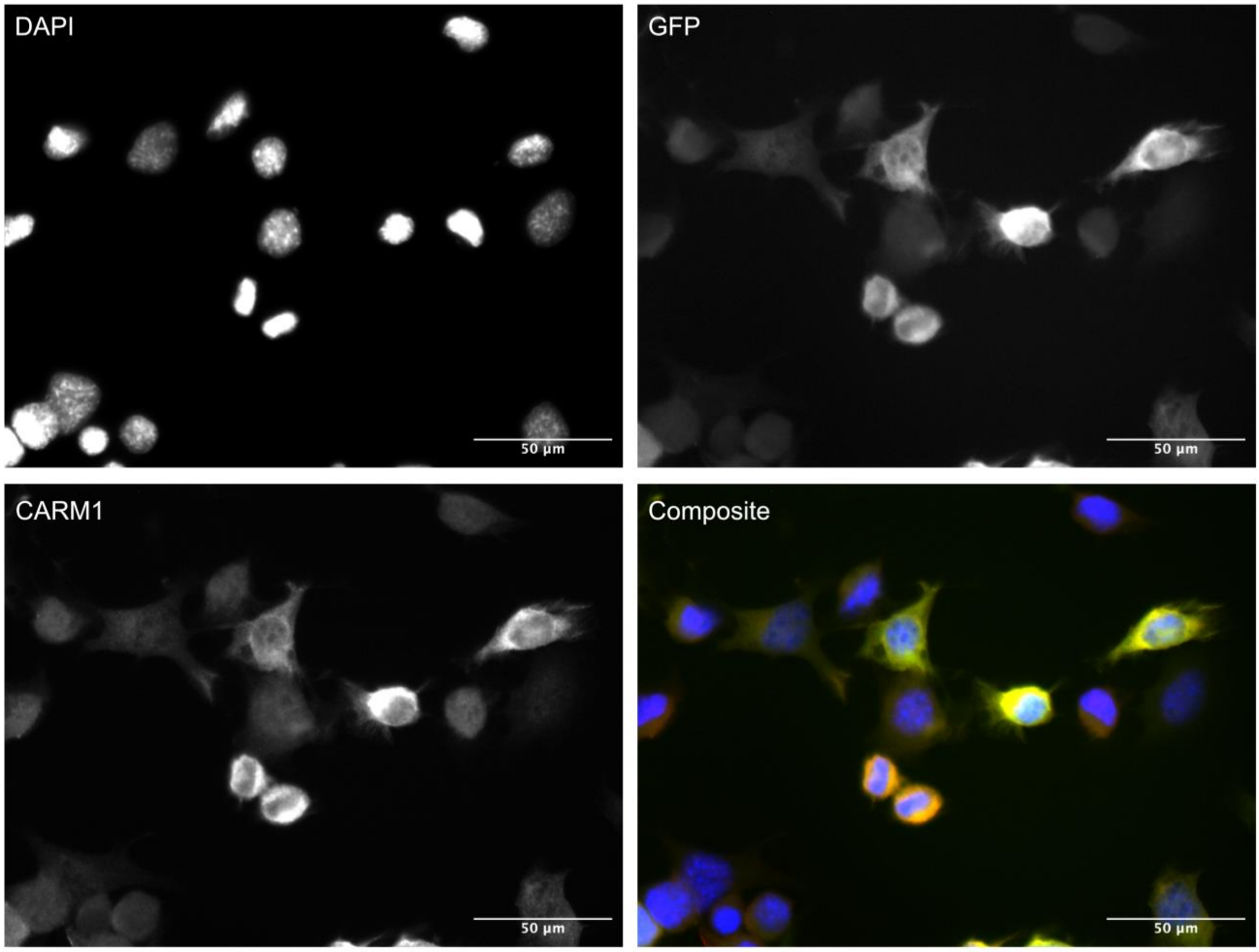

Figure 21: Fluorescence microscopy of stable MN-1 cells expressing pEGFP-N1 CARM1-E266Q. Proliferating MN-1 cells were fixed, probed for CARM1 and stained with DAPI. All images are representative and taken in random fields of view. Composite image shows DAPI (blue), CARM1 (red) and GFP (green). Scale bar represents 50 µm.

5.2.3 GFP Affinity Purification

The affinity purification of CARM1 and interacting partners was done through GFP-trap beads, which were incubated with the lysate of the stable MN-1 cells expressing GFP, CARM1-GFP or the E266Q mutant. After incubation with GFP-trap beads and washes, the affinity product was eluded and used for MS analysis. Given the unique properties of CARM1 outlined in Chapter 3 (Bourassa et al., 2024), an affinity purification approach does go in opposition to the optimal conditions called for by CARM1. For this reason, several elements had to be taken into consideration in the methodology used. These will be discussed below.

First of all, as described in Chapter 3, factors promoting CARM1 aggregation include heat denaturation, high CARM1 concentration as well as DTT. Coincidingly, steps often used towards AP-MS bead elution make use of heat denaturation and DTT for sample preparation. Of course, this is not a universal rule but is part of established protocols which were used as the baseline of this objective (Morettin et al., 2019; Trinkle-Mulcahy, 2012; Trinkle-Mulcahy et al., 2008). In the exploration of CARM1 aggregation following the methodology of those established protocols, even the avoidance of heat denaturation failed to prevent CARM1 aggregation following AP (Figure S6). This further emphasizes CARM1's own concentration as a driving factor of its aggregation. It also suggests that a CARM1 AP approach is bound to be conducive to its aggregation.

There is little precedent on the impact of aggregations in MS analysis outside the scope of pathological aggregates (Pukala, 2023), which arguably are not of the same nature as those observed of CARM1 at sample preparation. As such, the impact aggregates could have on this type of experimental design is also unknown. Some degree of CARM1 aggregation was anticipated to be unavoidable using this approach. Nevertheless, since CARM1 appears to be an

exception to most in its biochemical properties, the conditions following the AP should not impede interactor detection.

5.2.4 GFP-AP/MS Results

Aim iv. Identify CARM1 substrates in MNs

The MS data stemming from the AP of GFP, CARM1-GFP and CARM1-GFP E266Q was compared three ways to distinguish outstanding genes between all samples.

5.2.4.1 *CARM1-GFP vs GFP*

In the first analysis, the comparison of gene enrichment between the CARM1-GFP and free GFP highlights interactors specific to CARM1 as opposed to those of GFP or unspecific bead binding (Figure 22). Unsurprisingly, CARM1 itself was by far the most prevalent gene identified within the dataset. This was anticipated since CARM1 is well known to dimerize (Troffer-Charlier et al., 2007). Outstandingly, only one other gene reached significance. This gene is Pdcd6ip, also known as Alix. Since Alix is a clear stand out from the other data points both in terms of signal intensity and p-value, it suggests that it is a primary interactor of CARM1.

Alix was first identified as an ALG-2 interacting protein, whose interaction with the latter is calcium dependent and involved in pro-apoptotic signaling (Missotten et al., 1999). More recently, Alix's interaction with ALG-2 acts as a mediator of calcium induced caspase 9 activation (Strappazzon et al., 2010). Nonetheless, key contributions of Alix were found to relate to other molecular mechanisms such as endocytosis, viral budding and focal adhesions (Odorizzi, 2006). Due to its broad involvement, its identification as a potential CARM1 substrate could be biologically impactful.

According to the criteria defined, CARM1 and Alix are the only genes found to be significantly enriched within the CARM1-GFP AP sample. As an enzyme with other well defined substrates, it is surprising that no other genes were found as enriched. This could be at least in part explained by the transient nature of PRMT's catalytic activity (Feng et al., 2011; Hu et al., 2016; Kölbel et al., 2009; Van Haren et al., 2017). It is expected that the interaction between CARM1 and its substrates be brief, which could explain lower intensities of other peptide sequences. For the purpose of CARM1 substrate exploration, the genes below the significant threshold were also considered for further investigation.

Expectedly, OGT was found to be another standout gene from the dataset. As discussed in Chapter 1, CARM1 is O-GlcNAcylated by OGT, a modification which altered CARM1's ability to methylate H3R17, prevented its phosphorylation and altered its localization in mitotic cells (Sakabe & Hart, 2010). Moreover, OGT was found to be methylated by CARM1 (R348) increasing its stability and global O-GlcNAcylation levels (Lin et al., 2024). As an interactor and substrate of CARM1, its identification is consistent with the literature surrounding the two enzymes.

Another protein of interest identified within this dataset is RPS7. RPS7, is a component of the small ribosomal subunit 40S (Nakao et al., 2004). It is one of numerous ribosomal proteins identified in this dataset as seen in the (Figure 22, bottom panel). RPS7 specifically was not empirically validated as a CARM1 interactor but was identified in CARM1 interactor datasets (Wei et al., 2021). Since CARM1 is known to interact and methylate ribosomal proteins (Wei et al., 2021), the high visibility of ribosomal proteins in this work is consistent with the literature.

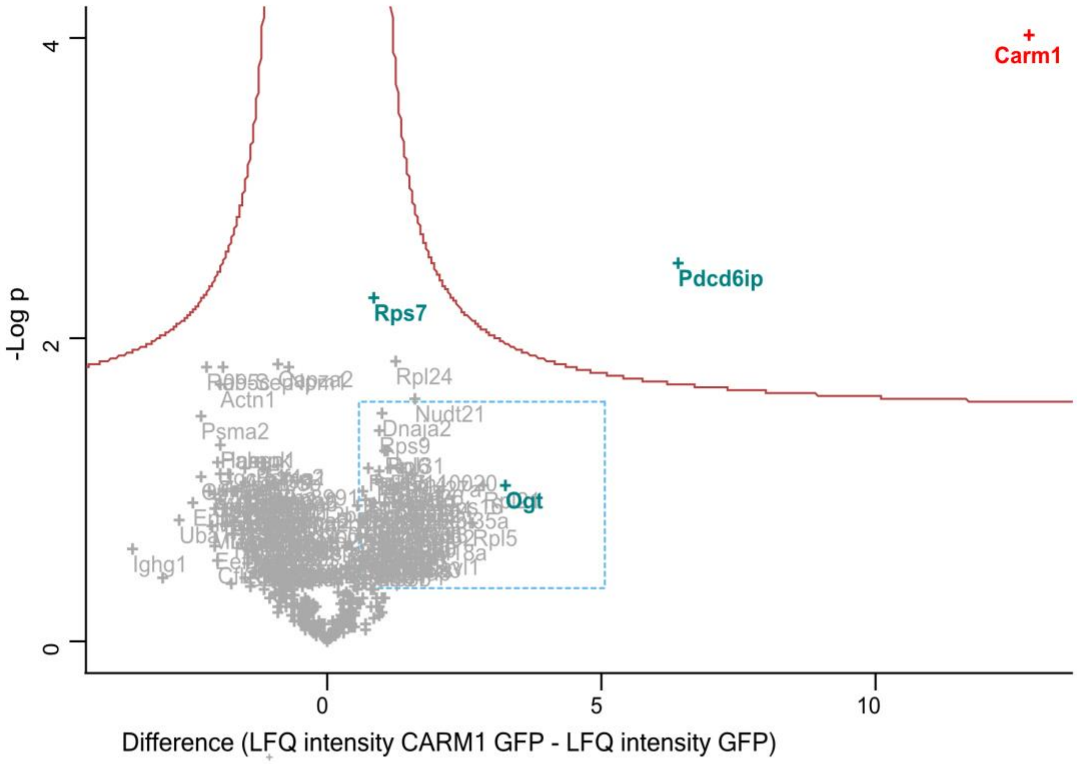
Carm1
Pdcd6ip
Rps7
Ogt
Rpl24
Actn1
Nudt21
Dnaja2
Psma2
Rps9
Rpl5
Ighg1
-Log p
0
2
4
0
5
10
Difference (LFQ intensity CARM1 GFP - LFQ intensity GFP)

Zoom:

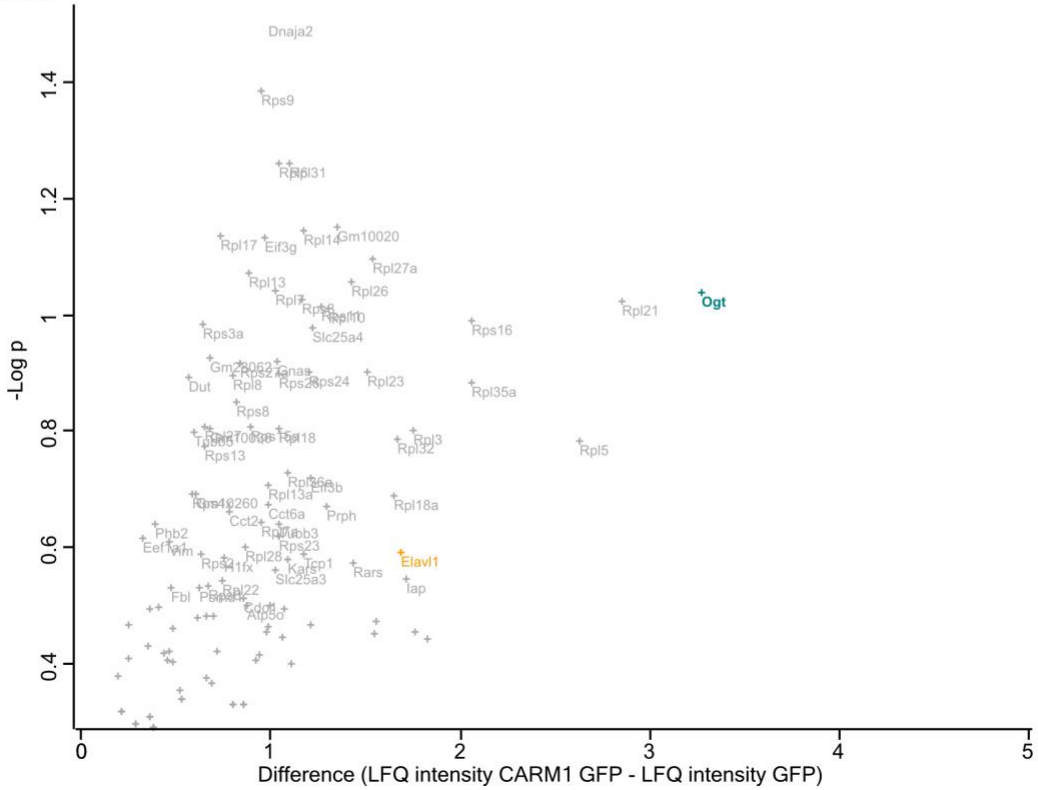
Dnaja2
Rps9
Rpl31
Rpl17
Eif3g
Rpl14
Gm10020
Rpl27a
Rpl13
Rpl26
Rpl7
Ogt
Rpl21
Rps16
Rps3a
Slc25a4
Dut
Rpl8
Rps24
Rpl23
Rpl35a
Rps8
Rps13
Rpl3
Rpl32
Rpl5
Rpl18a
Cct2a
Prph
Phb2
Rps23
Elavl1
Rps11fx
Rars
Slc25a3
Fbl
Rpl22
-Log p
0.4
0.6
0.8
1
1.2
1.4
0
1
2
3
4
5
Difference (LFQ intensity CARM1 GFP - LFQ intensity GFP)

Figure 22: Interactions of CARM1-GFP in MN-1 cells.

A GFP affinity purification and mass spectrometry approach was used to identify CARM1-GFP's interacting partners. The volcano plot illustrates the difference of interactions between CARM1-GFP and GFP (top panel) as a function of statistical significance. The dotted square in the top panel outlines the zoomed in area shown in the bottom panel. Solid line represent FDR (0.05, s0:0.3). CARM1, and HuR (Elavl1) are highlighted in red and orange, respectively. Other genes of interest are highlighted in green. LFQ; Label-Free Quantification. N=3. Paired t-test $P<0.05$.

5.2.4.2 *CARM1-GFP E266Q vs GFP*

As a second method of analysis, the gene enrichment between CARM1-GFP E266Q and the free GFP AP was evaluated (Figure 23). Once again, CARM1 itself was by far the most significant and prominent gene identified within this dataset, consistent with CARM1's dimerized nature (Troffer-Charlier et al., 2007).

In this instance, CARM1 is the only significantly enriched gene. Surprisingly, Pdcd6ip/Alix was not enriched within this dataset. In fact, the CARM1 and Alix interaction was eliminated, falling below Alix detection levels in the control sample. This is a drastic contrast to the interaction found for CARM1's active form. Accordingly, this strongly suggests that Alix's interaction with CARM1 is dependent on its activity.

On the other hand, OGT remains a standout gene in this dataset. This is consistent with the active form of CARM1. This suggests that this interaction is independent of CARM1's enzymatic activity. The persistent interaction between OGT and the enzymatically dead CARM1 supports the notion of an interaction independent of CARM1 activity.

Lastly, RPS7 was also evaluated in this dataset. Unlike CARM1's active form, RPS7 falls well within the bulk of the datapoints, suggesting its enrichment to be negligible when compared to OGT's and CARM1's enrichment. As such, RPS7 interaction with CARM1 appears to be dependent on its enzymatic activity.

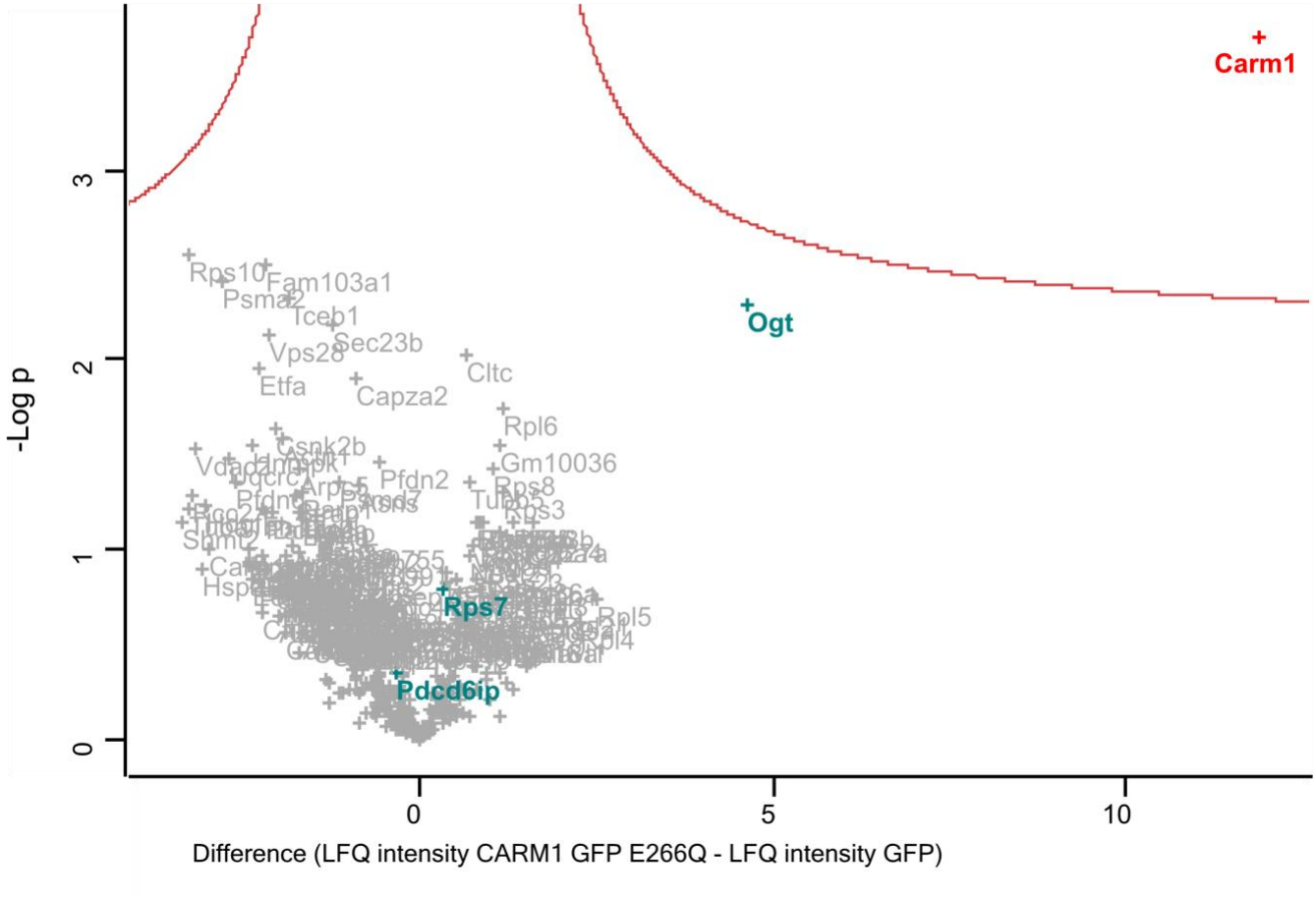

Figure 23: Interactions of CARM1-GFP E266Q in MN-1 cells.

A GFP affinity purification and mass spectrometry approach was used to identify CARM1-GFP E266Q's interacting partners. The volcano plot illustrates the difference of interactions between CARM1-GFP E266Q and GFP as a function of statistical significance. Solid line represent FDR (0.05, s0:0.3). CARM1 is highlighted in red. Other genes of interest are highlighted in green. LFQ; Label-Free Quantification. N=3. Paired t-test P<0.05.

5.2.4.3 *CARM1-GFP vs CARM1-GFP E266Q*

Finally, gene enrichment between the two CARM1 constructs were compared to directly assess the impact of its enzymatic activity on its interactions (Figure 24). Overall, the comparison of these two groups reveals that no gene enrichment reached significance. Nevertheless, with its datapoint falling just below the threshold of significance, only Pdcd6ip/Alix stood out from the comparison. As mentioned, the previous plots suggested that Alix's interaction with CARM1 is dependent on its enzymatic activity. This figure further corroborates this assessment, and highlights Alix as the protein whose interaction with CARM1 is by far the most dependent on its activity.

Aside from Alix, CARM1 itself and OGT were other notable genes as defined in Figure 22, Figure 23). Consistent with the finding that both CARM1 constructs had strong interactions with CARM1 and OGT, neither are particularly outstanding in this plot (Figure 24). OGT is more enriched in the CARM1-GFP E266Q sample while CARM1 is more enriched in the CARM1-GFP sample, however these changes are below statistical significance and might not be biologically relevant. Lastly, RPS7 is more enriched within the CARM1-GFP sample when compared to the mutant construct. This suggests that RPS7 has a stronger interaction with active CARM1 but retains some ability to interact with the catalytically dead CARM1.

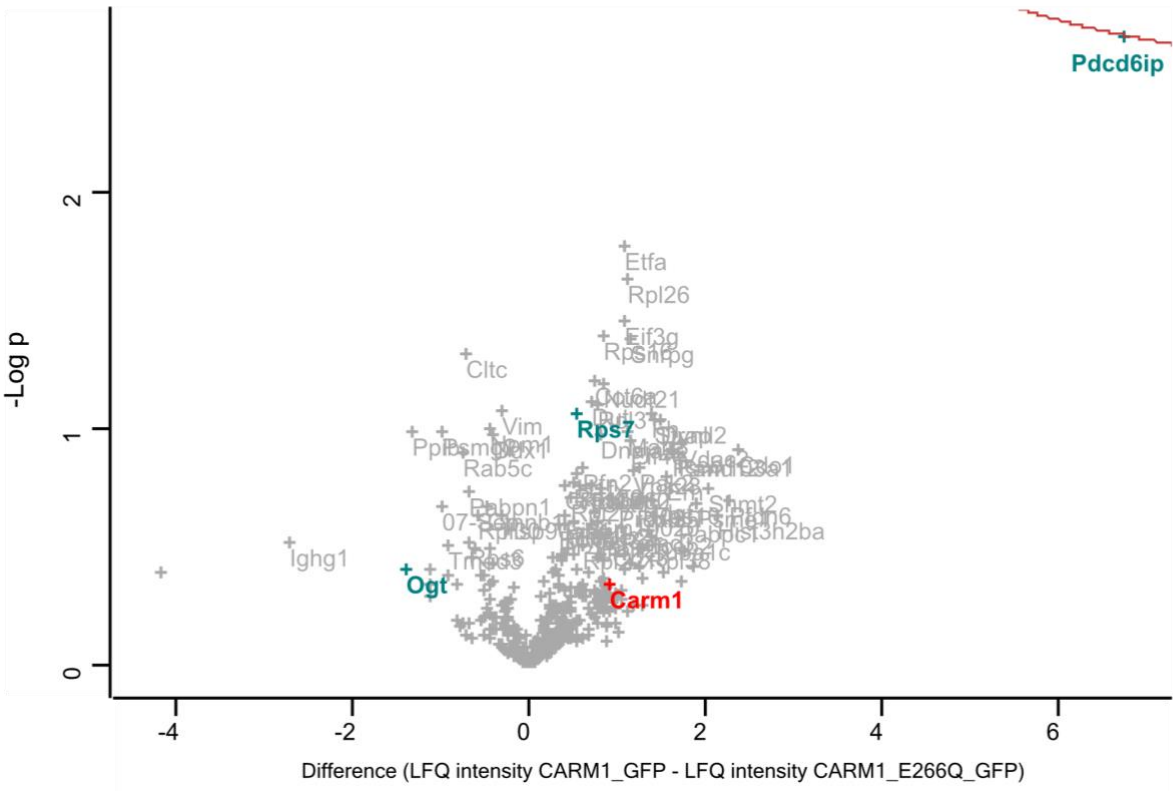

Figure 24: The enzymatic activity of CARM1-GFP alters its interactions.

A GFP affinity purification and mass spectrometry approach was used to compare the interactions of CARM1-GFP and CARM1-GFP E266Q. The volcano plot illustrates the difference of interactions between CARM1-GFP and CARM1-GFP E266Q as a function of statistical significance. CARM1 is highlighted in red. Other genes of interest are highlighted in green. Solid line represent FDR (0.05, s0:0.3) LFQ: Label-Free Quantification. N=3. Paired t-test $P<0.05$.

5.2.5 CARM1 Methylates RPS7.

Having identified Alix, OGT and RPS7 as potential interactors of CARM1, the nature of the interaction was further investigated. As expanded on in the introduction, CARM1's role is heavily tied to its enzymatic activity but not fully encompassed by it. For this reason, Alix, OGT and RPS7 were used in a radiolabelled *in vitro* methylation assay to test if they are part of CARM1's pool of substrates (Figure 25).

Using recombinant CARM1 as an enzyme source, its ability to methylate purified histones, HuD, Alix, OGT, and RPS7 was assessed. Here, histones and GST-HuD were used as positive controls since they are both known CARM1 substrates. Since HuD is GST tagged, CARM1's ability to methylate the tag alone was also included to account for any potential methylation outside HuD's sequence. Due to peptide availability, OGT was tested through two partial peptides covering most of the full length sequence. Lastly, since CARM1 has the ability to automethylate, the presence of CARM1 itself is expected to be sufficient to cause some methylation reactions. Hence, all methylation reactions were normalized to a sample containing no other substrate (denoted as CARM1 alone). For interpretation, this means that this assay measures CARM1's ability to methylate each substrate beyond its automethylation, as opposed to being a measure of total methylation.

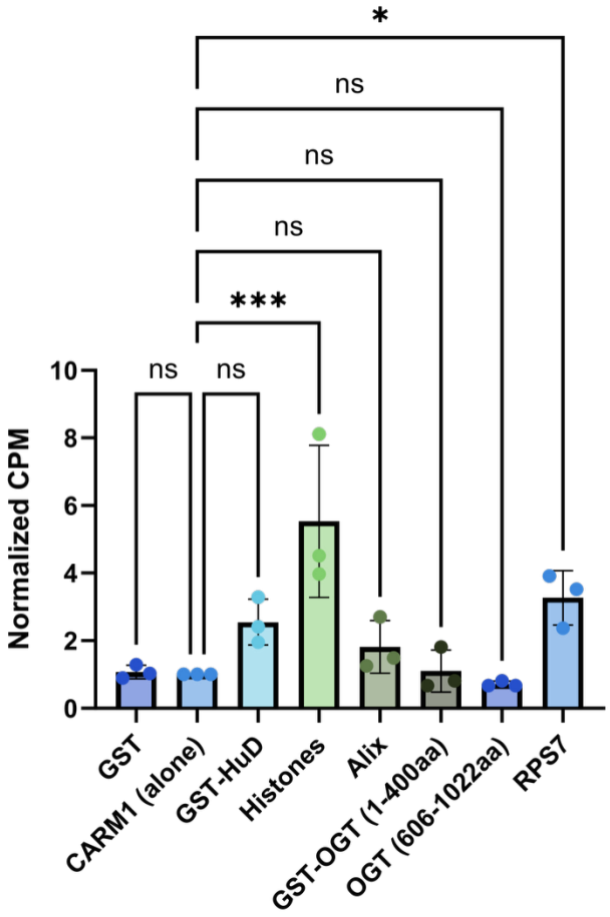

Figure 25: In vitro methylation assay of CARM1 interactors.

The incorporation of radiolabelled SAM[^{3}H] was measured by CPM following incubation of each interactor with active recombinant CARM1 and represented as fold change. The CPM values were normalized to CARM1 (alone) to account for potential automethylation. Statistical analysis; One Way ANOVA with Dunnett's multiple comparisons test. $P<0.05$, Error bars represent SD. N=3.

Taken together, the *in vitro* methylation assay reveals histones to be by far the most methylated substrates among all samples. This is consistent with the notion that CARM1 methylates H3 at multiple sites; H3R2, H3R17 and H3R26 (Bedford & Clarke, 2009; Cheng et al., 2007; Feng et al., 2006). Interestingly GST-HuD was not significantly methylated, although there was a non-significant increase in methylation, suggesting that some methylation occured. As covered at length, CARM1 is well known to methylate HuD. The lack of statistical significance suggests a need for increased sensitivity to confirm the methylation of substrates with similar levels of methylation. Since HuD is methylated by CARM1 at only one site (R248) (Hubers et al., 2011), as compared to the three sites in H3 (Bedford & Clarke, 2009; Cheng et al., 2007; Feng et al., 2006), it reasons that the methylation signal be lower in this assay. Therefore, it should be understood that this methodology may not validate substrates with lower, or comparable, methylation rates to HuD.

In the same line of thought, OGT was found to be methylated by CARM1 (Lin et al., 2024). Since this finding had not yet been published when this experiment took place, OGT was tested with two peptide sequences covering most of the full length protein. With the two peptides (1-400 aa, and 606-1022 aa) the objective was to explore whether CARM1 could methylate OGT, and if so, narrow down the location of the methylated Arg. Nevertheless, CARM1 is expected to methylate at site R348 (Lin et al., 2024), or in the first peptide sequence (1-400aa) used in this methylation assay.

Under the condition tested, the methylation assay reveals no significant methylation between CARM1 and either OGT peptide. This contrasts with the aforementioned publication. This discrepancy could be explained in many ways, first of which is the sensitivity of the assay. Visually, the CPM count of both peptides fall below that of HuD, suggesting that

OGT's methylation rate be lower than HuD's. Should it be a true substrate, this method is likely not sufficient to discern OGT's methylation from CARM1's automethylation. On the other hand, if OGT is not methylated in this assay as the CPM values suggest, it is plausible that other factors be required for OGT methylation to occur. In any case, this cannot be confirmed from this assay.

Pdcd6ip, or Alix, is another protein identified in this work, and a clear stand out from the MS datasets. Interestingly, Alix is known to contain a PRD (Elias et al., 2020) where approximately 30% of all residues are prolines. As mentioned, CARM1's methylation sites are well known to be proline rich motifs (Shishkova et al., 2017), making this particular region of Alix a promising target sequence. The methylation assay reveals Alix to not be significantly methylated by CARM1. Nevertheless, its CPM values were more comparable to those of HuD, suggesting that some methylation may have occurred. Importantly, the Alix purified protein was from a mammalian host. Consequently, the protein might already have been methylated by endogenous CARM1 prior to the assay, dampening any signal. Evidently, this cannot be confirmed from this assay, but the data does prompt for further investigation of this interaction.

Lastly, RPS7 is the last protein identified in the MS dataset selected for experimental validation. Here, the methylation assay shows RPS7 to be significantly methylated by CARM1. This confirms RPS7 as an *in vitro* substrate of CARM1. While RPS7 was identified as a potential interactor of CARM1 in proteomic studies (Wei et al., 2021), RPS7 had yet to be experimentally validated as a CARM1 substrate. It remains to be determined if the methylation also occurs *in vivo*, but its identification is consistent with CARM1's strong affinity with ribosomal proteins and biological functions (Wei et al., 2021).

5.2.6 CARM1 in MN Ribosomal Protein Biology

Finally, the last analysis performed in this objective aimed to identify GO terms associated with CARM1's top interactors (Table 4). Since only CARM1 and Alix were significantly enriched from the comparison of the AP-MS of CARM1-GFP and GFP, the inclusion criteria for this analysis was expanded to include the top 74 genes enriched within the CARM1-GFP sample set. The selection was then compared to all identified genes, within the GFP, CARM1-GFP, and CARM1-GFP E266Q datasets.

While RPS7 is the only ribosomal protein investigated in this work, it is clear that ribosomal proteins are prevalent in this sample, as seen in Figure 22 (bottom panel). This visual assessment is reflected in the abundance of ribosomal functional annotation terms. The same applied to other subontologies. At the level of molecular function, *structural constituent of ribosome* is the most significant. The top biological process was *cytoplasmic translation* and was followed but other terms heavily associated with translation biology. These include *peptide biosynthetic and metabolic process*, *ribosome biogenesis* and *ribonucleoprotein complex biogenesis*. Furthermore, *translation at presynapse* and *postsynapse* were also found to be enriched. Lastly, the cellular component term most enriched in the same dataset expectedly includes *cytosolic ribosomes* but further expands to the *postsynapse.*

As previously described, ribosomal proteins were found to be extensively methylated by PRMTs (Wei et al., 2021). The prevalence of translation terms is in line with what is known of CARM1's proteome. Nevertheless, the GO analysis performed here makes further distinction to CARM1's translation impact and brings forward its potential role in neuronal biology. At both molecular function and cellular component subontology levels, CARM1's translational influence is narrowed down to both the pre- and postsynapse. While more investigation is needed, this

assessment implies that CARM1 may contribute to the regulation of the synaptic proteome in MNs; the first insight into CARM1's biology in this cell type.

Table 4: GO terms enriched within the top 74 genes found to interact with CARM1

The top 74 protein coding genes enriched with CARM1-GFP underwent GO analysis and were compared to all protein coding genes identified within the GFP, CARM1-GFP and CARM1-GFP E266Q datasets. Green scale bars visually represent the terms's significance. Analysis performed in g:profiler.

Molecular Function		
Term Name	**GO term ID**	**-log10 Adj. p Value**
structural constituent of ribosome	GO:0003735	9.776979616
structural molecule activity	GO:0005198	7.103441226
Biological Process		
Term Name	**GO term ID**	**-log10 Adj. p Value**
cytoplasmic translation	GO:0002181	8.719344108
peptide biosynthetic process	GO:0043043	7.365256383
translation	GO:0006412	7.365256383
peptide metabolic process	GO:0006518	6.79650754
amide biosynthetic process	GO:0043604	6.612589124
amide metabolic process	GO:0043603	5.732658641
translation at presynapse	GO:0140236	4.508309614
translation at postsynapse	GO:0140242	4.186436749
translation at synapse	GO:0140241	4.186436749
organonitrogen compound biosynthetic process	GO:1901566	3.985966867
protein metabolic process	GO:0019538	2.022403564
ribosome biogenesis	GO:0042254	1.973166895
ribonucleoprotein complex biogenesis	GO:0022613	1.597438466
cellular nitrogen compound biosynthetic process	GO:0044271	1.533861636
Cellular Component		
Term Name	**GO term ID**	**-log10 Adj. p Value**
cytosolic ribosome	GO:0022626	10.91294649
ribosome	GO:0005840	9.63937763
ribosomal subunit	GO:0044391	9.462807854
cytosolic large ribosomal subunit	GO:0022625	4.846785712
ribonucleoprotein complex	GO:1990904	4.260508942
large ribosomal subunit	GO:0015934	4.186436749
postsynapse	GO:0098794	3.273985087
intracellular non-membrane-bounded organelle	GO:0043232	2.238300963
non-membrane-bounded organelle	GO:0043228	2.238300963

5.3 Discussion

This objective aimed to explore CARM1's methylome in MNs, a cell type in which CARM1 research remains limited. Here, an AP-MS approach is used to uncover CARM1 interactors in the MN-1 cell model. A proteomic analysis reveals Alix, OGT and RPS7 as genes of interest in this study, and an *in vitro* methylation assay confirms RPS7 to be a novel CARM1 substrate (Figure 26). Each finding will be considered and elaborated on below.

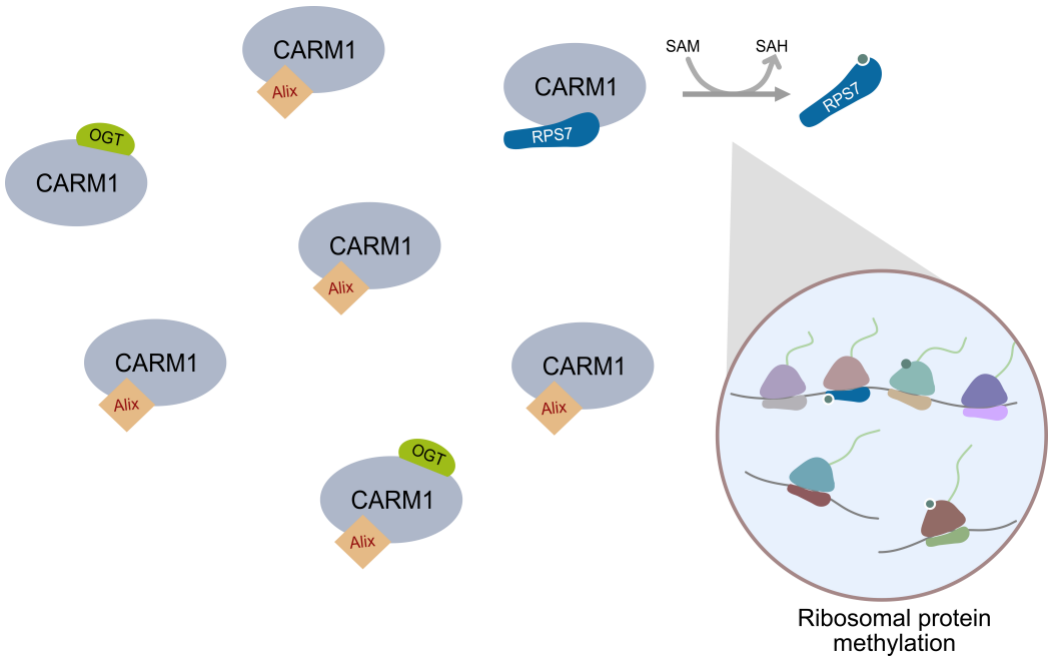

Figure 26: Suggested interactions of CARM1 in MNs.

CARM1's predominant interactor in MNs is Alix, which occupies its catalytic site. CARM1 also interacts with OGT independently of its catalytic site. CARM1 methylates RPS7 and other ribosomal proteins in the MN proteome towards downstream translation regulation.

5.3.1 OGT as an Interactor of CARM1 in MNs

In this work, OGT is identified as one of CARM1's most prevalent interactors. While OGT was not significantly enriched, it stood out from other datapoints. As mentioned, OGT is known to modify CARM1 through an O-GlcNAc modification (Sakabe & Hart, 2010). Furthermore, OGT itself was recently found to be a CARM1 substrate (Lin et al., 2024). This suggests that the interaction observed here is representative of their biological interaction. While OGT was not significantly enriched in this dataset, the literature on both proteins suggest that the CARM1 and OGT interaction occurs in the MN cell type as well.

Furthermore, OGT's strong detection was observed in both the catalytically active and inactive form of CARM1. The fact that OGT interaction with CARM1 is independent of its enzymatic activity suggests that the interaction takes place outside of CARM1's catalytic site. This is consistent with the notion that the interaction of CARM1 and OGT observed is the consequence of CARM1 acting as a substrate of OGT, but not OGT acting as substrate of CARM1.

An *in vitro* methylation assay shows no convincing evidence of OGT methylation by CARM1. This does contrast the previous report of OGT as a CARM1 substrate however, this methylation event was reported to be dependent on extracellular glucose concentrations (Lin et al., 2024). Therefore, the conditions leading to OGT methylation by CARM1 are unlikely to be relevant to the conditions tested. This supports the idea that, at least in the absence of atypical glucose concentrations, CARM1 is a substrate of OGT but not the other way around in MNs.

As an OGT substrate, CARM1's role in MNs could have biological meaning. Functionally, the O-GlcNAcylation of CARM1 was shown to alter its ability to modify H3R17, its localization and phosphorylation in the mitotic process (Sakabe & Hart, 2010). The same was not observed outside from the mitotic process (Charoensuksai et al., 2015). Nevertheless, OGT

was found to influence CARM1's substrate specificity. The investigation of CARM1's methylome identifies 840 putative substrates potentially regulated by CARM1's modification by OGT. Interestingly, RPS7 was identified within that list, suggesting that OGT act upstream of its methylation by CARM1 (Charoensuksai et al., 2015). Importantly, since RPS7 was not a confirmed CARM1 substrate before this work, OGT's influence on its methylation by CARM1 has not been experimentally tested.

As a known interactor and substrate of CARM1, OGT's identification in the MN model is consistent with that of other investigations performed in different models. The consistency between cell types suggests a role that is not specific to MNs. OGT does have neuronal functions and is found to be neuroprotective towards certain neurodegenerative diseases, including ALS (Han et al., 2024; Lee et al., 2021; Shen et al., 2021; Su & Schwarz, 2017; Zhao et al., 2021). As an emerging research field, the mechanisms surrounding OGT's role in neurons are not fully elucidated. It is possible that OGT's neuronal roles be carried through at least in part by CARM1, but this cannot be confirmed here.

5.3.2 Alix is CARM1's Strongest Interactor in MNs

The data presented here suggests a unique affinity of Alix with CARM1. In fact, aside from CARM1 itself, Alix was the only protein identified within the threshold of statistical significance. Alix's identification in the dataset is consistent with the literature, as Alix was found to associate with CARM1 in 293T cells in a wide scale proteome interaction investigation. The interaction however was not tested experimentally in the same work (Huttlin et al., 2021). Additionally, another investigation into CARM1's proteome in a breast cancer model further corroborates the findings described here. Through an IP-MS approach, the most prevalent CARM1 interactors was revealed to be CARM1 itself, as well as Alix (Suresh, 2021). Akin to

what is seen here, both genes were clear standouts from the rest of the dataset. This replicable interaction in this work and that of others suggests that Alix is a true interactor of CARM1.

In this work, the interaction between CARM1 and Alix was found to be dependent on CARM1's enzymatic activity as reflected in the complete loss of interaction between Alix and the CARM1-GFP E266Q fusion protein. This drastic change in interaction suggests that Alix interacts with CARM1 at its catalytic site.

The same conclusion is drawn from another group. In the work of Suresh (2021), the CARM1 and Alix interaction was further investigated based on their distinctively strong interaction in breast cancer cells. In their work, the interaction between Alix and active CARM1-Flag was lost with CARM1-Flag E266Q (Suresh, 2021). The consistency between both works highlights the importance of the E266 site, or the double E loop in the catalytic site, for Alix binding. It also further corroborates the need of CARM1's active form for its interaction with Alix.

Due to the transient nature of PRMT methylation reactions, an AP or IP approach is understood to be a snapshot of the total interactions occurring in the cell. In other words, the short-term methylation interactions are likely to be detected at lower levels than that of a stable interaction. For this reason, the globally low detection levels in the AP-MS experiment is consistent with the transient nature of CARM1's interaction. For instance, HuR, a known CARM1 substrate, is enriched in the dataset but not an outlier akin to Alix (Figure 22, bottom panel). As the only significant interaction, the high prevalence of Alix peptide detection suggests that it be the predominant interactor of CARM1 in MNs. It also hints at a more stable interaction, with function potentially distinct from a methylation event.

The same suggestion was made by Suresh et al., 2021 regarding the Alix and CARM1 interaction in breast cancer cells. In their work, the author suggests a stable interaction between Alix and CARM1 and hypothesizes that Alix is the main interactor of CARM1 in breast cancer cells. Since this was replicated here, this hints at a ubiquitous interaction between the two proteins across cell types.

As discussed, Alix interacts with CARM1 at its catalytic site. As a potential stable interaction, Alix could block any further methylation events by CARM1. If biologically relevant, this interaction could act as a CARM1 regulatory tool. There is little precedent to such an interaction. PRMT regulation is most reported to be done though PTMs, degradation and splicing (Bedford & Clarke, 2009; Goulet et al., 2007; Hartley & Lu, 2020; Wang et al., 2013). Stable interactions at the catalytic site are typically inhibitory. Synthetic small molecules are often used to inhibit PRMTs (Ferreira de Freitas et al., 2019; Wu et al., 2021; Xie et al., 2023), but differ in nature as they are not endogenous proteins. This leaves a lot of questions to be answered and more investigation is needed before making conclusions on the nature of the Alix and CARM1 interaction.

Structurally, Alix has a PRD domain (Elias et al., 2020). As the only PRMT with a proline rich motif preference, this domain is of interest when investigating potential CARM1 methylation sites. An *in vitro* methylation assay reveals that Alix is not significantly methylated by CARM1, but comparable to HuD's signal. As discussed, the assay's sensitivity was likely insufficient to distinguish non-substrates from those of lower methylation rates. For this reason, Alix cannot be excluded as a CARM1 substrate in MNs.

Once again, Suresh et al., 2021 investigated CARM1's ability to methylate Alix and further characterized their interaction. In their work, the ability of CARM1 to interact with Alix

was found to be through the PRD. Using synthetic peptides, they also identify two sites that are methylated by CARM1 *in vitro* (Arg745 and Arg757), both replicating potential methylation sites within the PRD (Suresh, 2021). This strongly suggests that CARM1 has the ability to methylate Alix in MNs. Here, the full-length protein was used in an *in vitro* methylation assay. While admittedly not significant, the methylation assay in Figure 25 suggests that some methylation reactions may have occurred.

Overall, this work shows Alix to be CARM1's most prominent interactor in MN but there is very little literature on the role of their interaction in cellular biology. Alix is known for its proapoptotic properties mediated through its interaction with the ALG-2 protein and is a regulator of the endolysosomal system through ESCRT proteins (Larios et al., 2020; Mahul-Mellier et al., 2006). In Hela cells, both CARM1 and Alix localize to the abscission site during cytokinesis. Depletion of either led to an increase in binucleated cells and defects in ESCRT-III protein recruitment (Suresh, 2021). Therefore, CARM1 and Alix interaction appear to have a biological function but the mechanisms surrounding it are unelucidated. Aside from what was described above, there is very little information on the nature of the interaction. For this reason, giving context to their interaction in a MN setting is difficult.

Mechanistically, since the PRD contains CARM1's methylation sites and is its site of interaction (Suresh, 2021) its function is most likely to be impacted. Coincidingly, the PRD domain is a major site of interactions required for Alix's function, which includes ALG-2 and TSG101 (a member of the ESCRT-I complex). It was found that Alix interaction with ALG-2 and TSG101 proteins were required for neuronal death *in vivo*. Deletion of these binding domains could also protect against naturally occurring cell death (Mahul-Mellier et al., 2006). Based on this, the PRD domain is an essential part of Alix for its apoptotic role. This suggests

that CARM1 may take part of these processes. Nevertheless, other functions could also be impacted.

The role of Alix in neurons has been investigated for its apparent relevance in synaptic regulation. Alix concentrates at synapses during synaptogenesis. It also concentrates at the presynaptic ends in a manner dependent on its ALG-2 interaction. A mouse Alix KO model reveals its loss to be viable, but not without a phenotype. In fact, despite its vesicular function, Alix is not required for synaptogenesis. However, a decrease in synaptic vesicle number was identified in the KO animals (Laporte et al., 2022). These animals also have a reduction in their brain volume, and a decrease in neural progenitor cells at embryonic stages. Alix KO neurons displayed a decrease in dendrite and axonal length, and growth cone area (Laporte et al., 2017).

In summary, a CARM1 influence on Alix biology could contribute to a series of biological functions. With a significant role in apoptosis, endocytosis and synaptic health, Alix is a promising contributor to MN biology under CARM1's influence. Still, Alix appears to have a unique type of interaction with CARM1, of which there is no concrete understanding. CARM1's main interactor appears to be Alix, but the inverse is suggested to not be true (Suresh, 2021). As such, the interaction could be involved in only a subset of Alix's function. This leaves a great deal of questions that need to be answered before the purpose of the interaction is clear.

5.3.3 RPS7 is a Novel CARM1 Substrate

Ribosomal proteins have been particularly prevalent in the AP-MS of CARM1-GFP. Ribosomal biology has been known to be within PRMT's realm of interaction, but only recently was this solidified into one of their core functions. A recent investigation of PRMT proteomes reveal ribosomal proteins as being overrepresented among their pool of interactors. PRMT1 and CARM1 particularly stood out from other PRMTs as their inhibition was sufficient to decrease

global translation coinciding with a decrease in polysome abundance (Wei et al., 2021). As one of the two PRMTs found to be most influential in translation biology, the data presented here is consistent with this notion.

Here, RPS7 was selected to be further investigated. An AP-MS approach reveals its strong affinity with CARM1-GFP, which was lost in the CARM1-GFP E266Q catalytically inactive protein. This drastic change in interaction suggests that RPS7 interacts with CARM1 through its catalytic site, implying RPS7 to be one of CARM1's substrates. This is reflected in an *in vitro* methylation assay, thereby confirming it to be a CARM1 substrate, although the validity of this interaction remains to be determined *in vivo*. Nevertheless, the high level of interaction of RPS7 with the active CARM1 taken in combination with its ability to be methylated suggests a biological relevance. As a CARM1 substrate, RPS7 methylation could act as a modulator of translation, promoting or inhibiting the translation of a subset of genes towards a functional goal.

As mentioned, CARM1 inhibition led to a decrease in global translation reflecting its contributions in translation (Wei et al., 2021). Moreover, SMN is a well-known effector protein of CARM1 (Hubers et al., 2011) and an interactor of ribosomal proteins acting towards the translation of mRNA contributing to MN function and stability (Lauria et al., 2020). On that premise, the methylation of RPS7 by CARM1 suggests an interaction with SMN that may impact MN gene translation. However, there is no evidence of RPS7 being one of SMN's interacting ribosomal proteins (Sharma et al., 2024). SMN has been the methyl reader most relevant to this work but is also not the sole reader of methyl marks. This leaves the door open for other potential effector proteins to detect RPS7's methylation by CARM1.

On its own, RPS7 deregulation has been found to contribute to cancer biology. For instance, aberrant RPS7 expression correlated to increased ovarian cancer development (Wang et

al., 2013), a poorer prognosis in prostate cancer (Wen et al., 2019), lung adenocarcinoma (Wu et al., 2021), and hepatocellular carcinoma (Zhou et al., 2024). It is worth noting that this is reminiscent of CARM1's own proliferative properties, although there is no evidence of the CARM1-RPS7 interaction taking part of it.

Interestingly, RPS7 is among several ribosomal proteins to regulate MDM2 and p53 interactions. MDM2, an E3 Ligase directly binds and promotes degradation of p53. In this pathway, RPS7 directly interacts with MDM2 resulting in the protection of p53 (Chen et al., 2007; Zhu et al., 2009). Needless to say, as the "*guardian of the genome*" p53 has been and continues to be central to cancer biology through its tumor suppressor properties. P53 mutations are notable contributing factors to tumor progression and its targeting is a promising therapeutic target (Peuget et al., 2024). As a whole, RPS7's interactions with MDM2 have been of interest for its apparent value in cancer biology.

As a CARM1 substrate, it remains to be determined if RPS7 methylation can alter its known interactions *in vivo*. For instance, it is clear that a change in interaction between RPS7 and MDM2 has the potential to influence p53 biology. The examples given above all relate to a cancer setting, but regardless of if this interaction occurs in cancer or in healthy cells, the elements leading to its regulation are biologically relevant. Despite its strong association to cancer, p53 is also attributed neuronal roles. p53 has widespread expression in brain tissues and has been found to take part of neuronal functions through its transcriptional targets. For instance, in PC12 cells, p53 induced the expression of wnt7b, Coronin 1b and Rad13 to contribute to neurite outgrowth after NGF mediated differentiation (Brynczka & Merrick, 2008; Di Giovanni et al., 2006). P53 was also found to be required for GAP-43 expression during neurite and axon outgrowth through its acetylation and p300/CBP mediated signalling (Tedeschi et al., 2008).

Beyond normal cell function, p53 mutations or deregulations are also associated with nervous system diseases. Notably, p53 takes part in Parkinson disease, Alzheimer, epilepsy and spinocerebellar ataxia (Li et al., 2023), emphasizing the requirement of its regulation for neuronal health. MN diseases are not exempt from p53 influence. In the context of SMA, the loss of SMN has been reported to cause p53 upregulation (Courtney et al., 2019). In SMA mice, p53 activation contributed to MN death, driving MN degeneration. P53 activation and phosphorylation was also found to be a marker of vulnerable MNs (Simon et al., 2017). Furthermore, inhibition of p53 signalling reduced the NMJ loss experienced in SMA mice (Courtney et al., 2019). In ALS iPSCs derived MNs and mice, p53 protein level reduction rescued axonal degeneration and increased survival (Maor-Nof et al., 2021). Therefore, in multiple instances p53 deregulation was found to take part of MN disease. As a p53 regulator, RPS7 could equally be involved in these pathways.

To conclude, with its identification as a CARM1 substrate, RPS7 interactions are now particularly relevant in the MN setting. Whether through p53, its translational role, or even an undescribed one, it is clear that RPS7 methylation by CARM1 could play a role in its downstream functions. Needless to say, more exploration of the CARM1 and RPS7 interaction is required to fully grasp its implications. This exploration of CARM1's MN interactors identifies RPS7 as one of its substrate, attesting to CARM1's ability to contribute to the MN methylome beyond HuD.

5.3.4 HuD as a Distinctive Neuronal Substrate

In this work, CARM1's interaction with HuD has been the main motivation in pursuing CARM1's exploration in MN. As per this project's rationale, HuD is a known CARM1 substrate and effector protein (Fujiwara et al., 2006; Hubers et al., 2011). Interestingly, HuD was not a

significant or outstanding interactor of CARM1 in this study. Several reasons could explain its absence. First of all, as discussed above, the transient nature of CARM1's interactions results in a generally low peptide count. While HuD's methylation by CARM1 in MN-1 cells was found to have a functional impact (Hubers et al., 2011), the level of interaction between the two proteins is likely to be temporary and lesser than the interactors identified here. Moreover, the cells were maintained in a proliferative state and therefore CARM1's interaction with HuD so far associated with the transition to differentiation (Fujiwara et al., 2006; Hubers et al., 2011) may not be as apparent here. The limitations associated with the cell model used here are expanded on in Chapter 6.

Interestingly, no uniquely neuronal proteins were identified. Of course, as discussed, those identified have the ability to contribute to neuronal biology, but they are not predominantly neuronal in function or expression. This investigation of CARM1's proteome in MNs suggests that HuD is its only predominantly neuronal substrate. This in itself is indicative of CARM1's role and points towards non-tissue specific interactors as the majority of its functional intermediates. Further supporting this is the prevalence of HuR as a CARM1 interactor (Figure 22).

HuR is a protein of the same family as HuD and known CARM1 substrate (Li et al., 2002; Pang et al., 2013; Ravel-Chapuis et al., 2022). Unlike HuD, HuR is ubiquitously expressed but both RBPs are structurally conserved (Clark et al., 2025; Ma et al., 1996). HuR was found to be among the most enriched interactors identified in the AP-MS of CARM1-GFP, suggesting that in MN, HuR interaction in CARM1 is more prevalent than HuD's. As such, while HuD is a well-known CARM1 MN substrate, the data suggests that HuR's interaction is more abundant.

This notion further supports the idea that CARM1's role in MN is not limited to HuD as its only specifically neuronal substrate but occurs through other broadly expressed intermediates.

5.3.5 Limitations and Future directions

The absence of HuD highlighted the limitation of an AP-MS approach for transient interactions. The temporary nature of the interaction could be reflected in a generally lower peptide count. As is currently the case with HuD, some true CARM1 substrates were likely not identified in this dataset. For this reason, this is unlikely to be a complete list of interactors. Other methods such as BioID, which use a covalent label to mark protein interactions, could be used as a complementary approach. This method would remove the barrier brought forward by AP for transient interactions and could highlight interactors of low prevalence.

Still, the data presented here identified RPS7 as a novel CARM1 substrate. In order to further this finding, the biological relevance of the RPS7 interaction needs to be characterized.

To this effect, an *in vitro* methylation assay coupled with a MS analysis would narrow down which site(s) within RPS7 is or are methylated by CARM1. With this information in hand, each methylated Arg site(s) can be mutated to assess the role of each PTM. Through comparison of WT RPS7 and mutant(s), the impact of the methylation(s) by CARM1 on RPS7 interactome can be assessed through a Co-IP approach. This would reveal if its modification by CARM1 disrupts or promotes its known interactions.

Lastly, it would be of value to determine if SMN interacts directly or indirectly with RPS7 in MNs, and if so, if its methylation by CARM1 takes part or modulates the interaction. Since SMN's direct association to ribosomes contributes to the translation of genes involved in neurogenesis (Lauria et al., 2020), it would be relevant to determine if RPS7 contributes to the process.

Overall, these methods would be a clear outlook to the CARM1 and RPS7 interaction through its interactome and translation influence. Other avenues of investigation can be considered based on the data presented here. Alix is clearly a protein of note in CARM1 biology, although very little about the interaction is known. As discussed, its apparent stable association with CARM1 suggests a role not limited to its methylation. Consequently, Alix may have a broader impact on CARM1's function than its other interactors. Here, the possibility of it acting as a potential inhibitor is hypothesized, although there is little precedent to this type of interaction. Determining the accuracy of this hypothesis would be the first step in understanding the biological relevance of the interaction as well as its implication in MNs.

5.4 Conclusion

In summary, this Chapter aimed to determine if CARM1 contributed to the MN methylome. In this work, OGT, Alix and RPS7 were highlighted for their apparent abundant interaction with active CARM1. Under the conditions tested, OGT and Alix were not significantly methylated by CARM1 *in vitro* although previous publications support a model where both are CARM1 substrates. Lastly, RPS7 was found to co-purify with CARM1 in MN in an enzymatically dependent manner and was confirmed as a novel CARM1 substrate *in vitro*. Therefore, CARM1 contributes to the MN methylome, answering to the hypothesis premised by this work.

Chapter 6 General Discussion

6.1 CARM1 as a Contributor to MN biology

Previous work by our group identified CARM1 as a contributor to MN biology through its methylation of HuD. In this investigation, CARM1's MN roles were further explored with the goal of answering our hypothesis;

CARM1 can alter HuD's landscape of mRNA targets and contribute to MN proteome methylation.

The influence of CARM1 protein levels on HuD's interaction with its mRNA targets was narrowed to the identification of six genes; Schip1/Iqschfp, Smarca2, Stc2, Ptger4 and Phox2B. Each of these genes were found to be dependent on CARM1 protein levels for their mRNA interaction with HuD. None of these genes were confirmed HuD mRNA targets prior to this work, bringing novelty to what is known of each protein. Ptger4 and Smarca2 protein levels were found to be dependent on CARM1's enzymatic activity. Without precedent for these interactions, CARM1 brings a novel facet of HuD biology and broadens its scope of neuronal influence.

On the other hand, the exploration of CARM1 interactors in MN is found to be consistent with other investigations, even those based in other cell types and disease models. Corroborating with literature, translation proteins are overrepresented in the list of its interactors suggesting a broad influence in the process. RPS7 is a novel substrate of CARM1 experimentally validated in this work consistent with its identification as a putative substrate in other studies (Charoensuksai et al., 2015; Wei et al., 2021). Still, GO analysis does identify neuronal terms, most relating to translation and postsynaptic components. As a whole, CARM1's neuronal influence appears to take place indirectly via other regulatory processes, such as translation.

Taken as a whole, there is evidence for a stronger CARM1 influence in MNs than what is currently attributed to it. These findings answer the hypothesis premised in this work. In MNs, CARM1 alters HuD's mRNA landscape and contributes to the methylation of its proteome.

6.2 Limitations

What is known of CARM1 in MNs places its influence as being at least in part contributing to the events leading to differentiation since its downregulation was sufficient to promote the latter (Hubers et al., 2011). Consequently, the sequence of events leading and driving differentiation must be faithfully represented to fully contextualize its function.

As with the use of any cell line, the limitations of the MN-1 line used here must be considered. This model has been made and used towards the study of MNs (Awad et al., 2018; Gopinath et al., 2016; Mi et al., 2007; Salazar-Grueso et al., 1991; Taga et al., 2022). However, MN-1 cells are in a proliferative state unless induced to differentiate through the addition of retinoic acid and GDNF (Hubers et al., 2011). Prior to differentiation, the cells are already committed to the MN lineage as they express ChAT; a MN marker (Salazar-Grueso et al., 1991). As such, the cells already display specialized MN properties, while preserving their proliferative ability. This "in between" state makes their practicality an asset but comes with the drawback of not being fully representative of the target model. This is particularly true for the events leading to or involved in MN differentiation, which as discussed, are particularly relevant to CARM1. For this reason, the MN-1 cell line cannot fully replicate the differentiation process and are not ideal for the next steps of CARM1 research in MNs.

In recent years, iPSC derived MNs have been extensively characterized and used to replicate the properties canonical to the MN cell type (Bianchi et al., 2018; Du et al., 2015; Johns & Maragakis, 2022; Solomon et al., 2021; Thiry et al., 2020). In addition to their fidelity to the

cell type of interest, iPSCs allow the exploration of the events involved in the differentiation of neuron progenitor cells to fully differentiated MNs (Solomon et al., 2021). For this reason, iPSCs bridge the gap left by the MN-1 cell model and should be considered as a model for the next steps of the investigation of CARM1 in MNs.

6.3 Lessons from CARM1

CARM1's neuronal contributions are not within its primary research topics. With its deregulation being strongly associated with cancers, CARM1 research is broadly focused on its role in disease models. Still, CARM1 is ubiquitously expressed and a regulator of essential biological processes. Its role in MN was found to be a promising facet of its function as previously demonstrated by its impact on HuD, but little more was uncovered since then (Hubers et al., 2011).

Throughout these chapters, novel CARM1 interactions or CARM1-dependent interactions were identified. The implications of each finding were discussed in detail, each offering plausible means through which CARM1 could further take part of MN biology. Even so, other assessments can be made from the combined conclusions of each chapter.

Notably, there was a strikingly different degree of novelty brought forward by each objective. In the exploration of HuD interactions, it was clear that CARM1's influence so far centered on so far unidentified targets. In fact, HuD's known targets were relatively unaffected by CARM1's protein levels. Meanwhile, CARM1's interactome was consistent with other similar studies, with very little novelty observed from this dataset.

When starting this work, the notion of HuD being a substrate of CARM1 suggested other prominent neuronal regulators might also be identified. Contradicting this, no other specialized neuronal health contributors were highlighted to be interactors of CARM1. In other words, any

neuronal influence stemming from these proteins are not representative of their canonical function as is the case with HuD. CARM1's influence on HuD therefore appears to be an exception to a generally conserved interactome between cell types. As such, this work suggests that CARM1's neuronal roles are carried through means already established to be within CARM1's realm of interaction. This in itself is a telling assessment of CARM1 biology.

Still, although CARM1's interactome appears to be conserved between cell types, its role in MN is not, indicating that a conserved interactome does not equate to a conserved function. Different MN roles may exist through other indirect mechanisms. Evidently, not all aspects of CARM1 functions were explored here. In Chapter 1, CARM1's extensive influence on transcription and translation was described, both of which are at the core of CARM1 function. The findings of Chapter 4 and 5 argue that both of these facets act downstream of CARM1 towards a functional role in MNs.

In Chapter 4, Smarca2, an ATPase subunit of the SWI/SNF chromatin remodelling pathway was found to be regulated by CARM1 in both its mRNA's association with HuD and its total protein level. As discussed above, the transcriptional influences of CARM1 and Smarca2 are part of their core functions and are associated with opposing roles; proliferation and differentiation, respectively. The antagonistic influence of CARM1 activity on Smarca2 protein levels implies a downstream influence, plausibly associated with the transition between proliferation and differentiation. On the other hand, in Chapter 5, ribosomal proteins were found to be overrepresented in CARM1's MN interactions. The functional impact of those interactions are not defined, but it strongly suggests that translation biology remains a core facet of CARM1 function in MNs. Taken together, this suggests that CARM1's MN specific influence may be extended to transcriptional and translational regulation. Both processes are dynamic and

complex, for these reasons a comprehensive approach is required in the next steps of this investigation.

In their respective chapters, the future directions were described with the goal of characterizing and solidifying each interaction as *bona fide* interactions. Here, the notion that CARM1 contributes to MN function through a broader transcriptional and translational control will be explored.

6.4 Future Directions

6.4.1 Defining the Transcriptional Influences of CARM1 in MNs

Here, it is suggested that CARM1 regulates Smarca2 protein levels, potentially through HuD methylation, and contributes to the chromatin remodelling changes occurring throughout MN differentiation (Figure 17). In order to test these interactions, iPSC derived MNs expressing HuD or HuD R248K (a mutant that cannot be methylated by CARM1 (Hubers et al., 2011)) could be used to determine the impact of CARM1 inhibition on Smarca2 protein levels. This would specify if Smarca2 protein levels are regulated through HuD, or other CARM1 dependent avenues. Additionally, a Smarca2 ChIP-seq approach could assess which genes fall under the transcriptional influence of HuD's methylation and/or CARM1 activity. In parallel, it would be of interest to determine if Smarca2 downregulation impacts the MN's ability to differentiate. Collectively, these experiments would define the transcriptional impact that CARM1, Smarca2 and potentially HuD have on MN differentiation.

6.4.2 Defining the Potential Influence of CARM1 on Translation in MNs

Following CARM1 inhibition in iPSC derived MNs, a Ribo-seq experiment would be a great method to define the mRNAs under the influence of CARM1's methyl transfers. Based on

the data here, it is plausible that CARM1 inhibition alters the pool of genes being actively translated, potentially promoting the translation of genes involved in neurogenesis.

In addition, a polysome profiling assay will define the translation dynamics impacted. Based on literature, it is expected that CARM1 inhibition will decrease global translation and polysome assembly (Wei et al., 2021). However, the distribution of known CARM1 ribosomal protein substrates among monosomes, polysomes or free protein in MNs has not been evaluated. It would be of interest to determine if ribosomal proteins, such as RPS7, depend on their methylation by CARM1 for their assembly. With the Ribo-seq experiment, these should give insight into which processes are translationally regulated through CARM1.

6.4.3 Defining CARM1's impact on MN development

Lastly, *in vivo* work is required to determine the importance of CARM1 in MNs in its full biological context. As discussed throughout this work, CARM1 is suggested to contribute to MN biology, although the full extent of its role is not defined. For these reasons, establishing a mice model with a MN specific CARM1 knockout would highlight if it is required for MN development, and if its loss is grounds for neuromuscular defects. Taken in combination with the other proposed experiments, these answers would solidify the breadth of impact that CARM1 carries in the cell type.

6.4.4 CARM1 as a Therapeutic Target in MNs

It is argued here that CARM1 could have functional relevance in the MN cell type. As such, CARM1's regulation in MNs could potentially be used as a therapeutic approach in neuromuscular diseases. In this work, SMA was brought forward as a disease of interest due to the involvement of CARM1 and HuD in the biology surrounding its causative gene; SMN.

SMA is a neurodegenerative disease known for the particular vulnerability of MNs. Intervention at pre-symptomatic or early stages of the disease is the best way to prevent MN degeneration (Chaytow et al., 2024; Dangouloff & Servais, 2019). Later intervention is still beneficial but limited (Wood, 2018). SMA MNs have been suggested to display developmental delays, including an altered proteome and delayed neurite outgrowth (Fuller et al., 2016; Varderidou-Minasian et al., 2021). For these reasons, targeting contributors of MN differentiation could be beneficial to their overall function. CARM1's inhibition in SMA could promote MN differentiation and rescue/prevent developmental delays.

Therefore, CARM1 could prove itself to be of therapeutic value in SMA and other neurodegenerative diseases. As an enzyme, CARM1 has the advantage of being targetable through inhibitors (Iannelli et al., 2022; Nakayama et al., 2018; Peng et al., 2024; Vhuiyan et al., 2013). Should its inhibition be beneficial to MN health, its targeting could be an accessible and much needed therapeutic tool in neuromuscular diseases.

6.5 Conclusion

CARM1's current literature frames its function in proliferative roles giving the impression that its influence is narrowed to the process. Here, the scope of CARM1 function is expanded and provides evidence supporting a broader involvement in MN biology. This study brings attention to the emerging contributions of CARM1 in specialized cells such as MNs. The complete picture of CARM1's role in MN is still at its introduction. These findings described here bring forward several investigative avenues. This exploration of CARM1 in MNs should therefore be considered in guiding further efforts.

References

Abueg, L. A. L., Afgan, E., Allart, O., Awan, A. H., Bacon, W. A., Baker, D., Bassetti, M., Batut, B., Bernt, M., Blankenberg, D., Bombarely, A., Bretaudeau, A., Bromhead, C. J., Burke, M. L., Capon, P. K., Čech, M., Chavero-Díez, M., Chilton, J. M., Collins, T. J., … Zoabi, R. (2024). The Galaxy platform for accessible, reproducible, and collaborative data analyses: 2024 update. *Nucleic Acids Research*, *52*(W1), W83–W94. https://doi.org/10.1093/NAR/GKAE410

Acosta, M. C., Copley, P. A., Harrell, J. R., & Wilhelm, J. C. (2017). Estrogen signaling is necessary for exercise-mediated enhancement of motoneuron participation in axon regeneration after peripheral nerve injury in mice. *Developmental Neurobiology*, *77*(10), 1133–1143. https://doi.org/10.1002/DNEU.22501

Akamatsu, W., Okano, H. J., Osumi, N., Inoue, T., Nakamura, S., Sakakibara, S. I., Miura, M., Matsuo, N., Darnell, R. B., & Okano, H. (1999). Mammalian ELAV-like neuronal RNA-binding proteins HuB and HuC promote neuronal development in both the central and the peripheral nervous systems. *Proceedings of the National Academy of Sciences of the United States of America*, *96*(17), 9885. https://doi.org/10.1073/PNAS.96.17.9885

Akten, B., Kye, M. J., Hao, L. T., Wertz, M. H., Singh, S., Nie, D., Huang, J., Merianda, T. T., Twiss, J. L., Beattie, C. E., Steen, J. A. J., & Sahin, M. (2011). Interaction of survival of motor neuron (SMN) and HuD proteins with mRNA cpg15 rescues motor neuron axonal deficits. *Proceedings of the National Academy of Sciences*, *108*(25), 10337–10342. https://doi.org/10.1073/pnas.1104928108

Allen, M., Bird, C., Feng, W., Liu, G., Li, W., Perrone-Bizzozero, N. I., & Feng, Y. (2013). HuD promotes BDNF expression in brain neurons via selective stabilization of the BDNF long 3'UTR mRNA. *PloS One*, *8*(1). https://doi.org/10.1371/JOURNAL.PONE.0055718

Amaral, P., Carbonell-Sala, S., De La Vega, F. M., Faial, T., Frankish, A., Gingeras, T., Guigo, R., Harrow, J. L., Hatzigeorgiou, A. G., Johnson, R., Murphy, T. D., Pertea, M., Pruitt, K. D., Pujar, S., Takahashi, H., Ulitsky, I., Varabyou, A., Wells, C. A., Yandell, M., … Salzberg, S. L. (2023). The status of the human gene catalogue. *Nature*, *622*(7981), 41–47. https://doi.org/10.1038/s41586-023-06490-x

An, W., Kim, J., & Roeder, R. G. (2004). Ordered cooperative functions of PRMT1, p300, and CARM1 in transcriptional activation by p53. *Cell*, *117*(6), 735–748. https://doi.org/10.1016/j.cell.2004.05.009

Anders, S., Pyl, P. T., & Huber, W. (2014). HTSeq – A Python framework to work with high-throughput sequencing data. *BioRxiv*, 002824. https://doi.org/10.1101/002824

Anfinsen, C. B. (1973). Principles that govern the folding of protein chains. *Science*, *181*(4096), 223–230. https://doi.org/10.1126/SCIENCE.181.4096.223/ASSET/1A648F0F-E322-4108-98DD-B0857103738D/ASSETS/SCIENCE.181.4096.223.FP.PNG

Antic, O., & Keene, J. D. (1998). Messenger ribonucleoprotein complexes containing human ELAV proteins: interactions with cytoskeleton and translational apparatus. *Journal of Cell Science*, *111*(2), 183–197. https://doi.org/10.1242/JCS.111.2.183

Aranda-Abreu, G. E., Behar, L., Chung, S., Furneaux, H., & Ginzburg, I. (1999). Embryonic lethal abnormal vision-like RNA-binding proteins regulate neurite outgrowth and tau expression in PC12 cells. *The Journal of Neuroscience : The Official Journal of the Society for Neuroscience*, *19*(16), 6907–6917. http://www.ncbi.nlm.nih.gov/pubmed/10436048

Ardito, F., Giuliani, M., Perrone, D., Troiano, G., & Muzio, L. Lo. (2017). The crucial role of protein phosphorylation in cell signaling and its use as targeted therapy (Review). *International Journal of Molecular Medicine*, *40*(2), 271. https://doi.org/10.3892/IJMM.2017.3036

Arredondo, S. B., Valenzuela-Bezanilla, D., Mardones, M. D., & Varela-Nallar, L. (2020). Role of Wnt Signaling in Adult Hippocampal Neurogenesis in Health and Disease. *Frontiers in Cell and Developmental Biology*, *8*, 565112. https://doi.org/10.3389/FCELL.2020.00860/PDF

Awad, H., Bratasz, A., Nuovo, G., Burry, R., Meng, X., Kelani, H., Brown, M., Ramadan, M. E., Williams, J., Bouhliqah, L., Popovich, P. G., Guan, Z., Mcallister, C., Corcoran, S. E., Kaspar, B., Michele Basso, D., Otero, J. J., Kirsch, C., Davis, I. C., … Tili, E. (2018). MiR-155 deletion reduces ischemia-induced paralysis in an aortic aneurysm repair mouse model: Utility of immunohistochemistry and histopathology in understanding etiology of spinal cord paralysis. *Annals of Diagnostic Pathology*, *36*. https://doi.org/10.1016/j.anndiagpath.2018.06.002

Bacabac, M., Liu, P., & Xu, W. (2024). Protein Arginine Methyltransferase CARM1 in Human Breast Cancer. *Endocrinology*, *165*(8). https://doi.org/10.1210/ENDOCR/BQAE068

Bah, A., & Forman-Kay, J. D. (2016). Modulation of Intrinsically Disordered Protein Function by Post-translational Modifications. *The Journal of Biological Chemistry*, *291*(13), 6696. https://doi.org/10.1074/JBC.R115.695056

Bailey, T. L., & Elkan, C. (1994). Fitting a mixture model by expectation maximization to discover motifs in biopolymers [Article]. *Proceedings. International Conference on Intelligent Systems for Molecular Biology*, *2*, 28.

Bannister, A. J., & Kouzarides, T. (2011). Regulation of chromatin by histone modifications. In *Cell Research* (Vol. 21, Issue 3, pp. 381–395). https://doi.org/10.1038/cr.2011.22

Bao, J., Lorenzo, A. Di, Lin, K., Lu, Y., Zhong, Y., Sebastian, M. M., Muller, W. J., Yang, Y., & Bedford, M. T. (2019). Mouse models of overexpression reveal distinct oncogenic roles for different type I protein arginine methyltransferases. *Cancer Research*, *79*(1), 21–32. https://doi.org/10.1158/0008-5472.CAN-18-1995/653473/AM/MOUSE-MODELS-OF-OVEREXPRESSION-REVEAL-DISTINCT

Bao, J., Rousseaux, S., Shen, J., Lin, K., Lu, Y., & Bedford, M. T. (2018). The arginine methyltransferase CARM1 represses p300•ACT•CREMτ activity and is required for spermiogenesis. *Nucleic Acids Research*, *46*(9), 4327–4343. https://doi.org/10.1093/NAR/GKY240

Bareiss, P. M., Paczulla, A., Wang, H., Schairer, R., Wiehr, S., Kohlhofer, U., Rothfuss, O. C., Fischer, A., Perner, S., Staebler, A., Wallwiener, D., Fend, F., Fehm, T., Pichler, B., Kanz, L., Quintanilla-Martinez, L., Schulze-Osthoff, K., Essmann, F., & Lengerke, C. (2013). SOX2 expression associates with stem cell state in human ovarian carcinoma. *Cancer Research*, *73*(17), 5544–5555. https://doi.org/10.1158/0008-5472.CAN-12-4177

Bauer, K. E., de Queiroz, B. R., Kiebler, M. A., & Besse, F. (2023). RNA granules in neuronal plasticity and disease. *Trends in Neurosciences*, *46*(7), 525–538. https://doi.org/10.1016/J.TINS.2023.04.004/ASSET/8A562242-1053-4B5F-8291-AE69568D6003/MAIN.ASSETS/GR3.JPG

Bauer, U. M., Daujat, S., Nielsen, S. J., Nightingale, K., & Kouzarides, T. (2002). Methylation at arginine 17 of histone H3 is linked to gene activation. *EMBO Reports*, *3*(1), 39–44. https://doi.org/10.1093/EMBO-REPORTS/KVF013

Beckel-Mitchener, A. C., Miera, A., Keller, R., & Perrone-Bizzozero, N. I. (2002a). Poly(A) Tail Length-dependent Stabilization of GAP-43 mRNA by the RNA-binding Protein HuD. *Journal of Biological Chemistry*, *277*(31), 27996–28002. https://doi.org/10.1074/JBC.M201982200

Beckel-Mitchener, A. C., Miera, A., Keller, R., & Perrone-Bizzozero, N. I. (2002b). Poly(A) tail length-dependent stabilization of GAP-43 mRNA by the RNA-binding protein HuD. *Journal of Biological Chemistry*, *277*(31), 27996–28002. https://doi.org/10.1074/jbc.M201982200

Bedford, M. T., & Clarke, S. G. (2009). Protein arginine methylation in mammals: who, what, and why. *Molecular Cell*, *33*(1), 1–13. https://doi.org/10.1016/j.molcel.2008.12.013

Bel-Vialar, S., Medevielle, F., & Pituello, F. (2007). The on/off of Pax6 controls the tempo of neuronal differentiation in the developing spinal cord. *Developmental Biology*, *305*(2), 659–673. https://doi.org/10.1016/J.YDBIO.2007.02.012

Bhuyan, A. K. (2010). On the mechanism of SDS-induced protein denaturation. *Biopolymers*, *93*(2), 186–199. https://doi.org/10.1002/bip.21318

Bianchi, F., Malboubi, M., Li, Y., George, J. H., Jerusalem, A., Szele, F., Thompson, M. S., & Ye, H. (2018). Rapid and efficient differentiation of functional motor neurons from human iPSC for neural injury modelling. *Stem Cell Research*, *32*, 126–134. https://doi.org/10.1016/J.SCR.2018.09.006

Biggar, K. K., & Li, S. S. C. (2015). Non-histone protein methylation as a regulator of cellular signalling and function. In *Nature Reviews Molecular Cell Biology* (Vol. 16, Issue 1, pp. 5–17). Nature Publishing Group. https://doi.org/10.1038/nrm3915

Blanc, R. S., & Richard, S. (2017). Arginine Methylation: The Coming of Age. *Molecular Cell*, *65*(1), 8–24. https://doi.org/10.1016/j.molcel.2016.11.003

Blasi, R. Di, Blyuss, O., Timms, J. F., Conole, D., Ceroni, F., & Whitwell, H. J. (2021). Non-Histone Protein Methylation: Biological Significance and Bioengineering Potential. *Cite This: ACS Chem. Biol*, *16*, 250. https://doi.org/10.1021/acschembio.0c00771

Bolognani, F., Contente-Cuomo, T., & Perrone-Bizzozero, N. I. (2010). Novel recognition motifs and biological functions of the RNA-binding protein HuD revealed by genome-wide identification of its targets. *Nucleic Acids Research*, *38*(1), 117–130. https://doi.org/10.1093/NAR/GKP863

Bolognani, F., & Perrone-Bizzozero, N. I. (2008). RNA–protein interactions and control of mRNA stability in neurons. *Journal of Neuroscience Research*, *86*(3), 481–489. https://doi.org/10.1002/JNR.21473

Bonnici, J., Oueini, R., Salah, E., Johansson, C., Schofield, C. J., & Kawamura, A. (2023). The catalytic domains of all human KDM5 JmjC demethylases catalyse N-methyl arginine demethylation. *FEBS Letters*, *597*(7), 933–946. https://doi.org/10.1002/1873-3468.14586

Borgeson, C. D., & Samson, M. L. (2005). Shared RNA-binding sites for interacting members of the Drosophila ELAV family of neuronal proteins. *Nucleic Acids Research*, *33*(19), 6372. https://doi.org/10.1093/NAR/GKI942

Böttger, A., Islam, M. S., Chowdhury, R., Schofield, C. J., & Wolf, A. (2015). The oxygenase Jmjd6–a case study in conflicting assignments. *Biochemical Journal*, *468*(2), 191–202. https://doi.org/10.1042/BJ20150278

Boumpas, P., Merabet, S., & Carnesecchi, J. (2023). Integrating transcription and splicing into cell fate: Transcription factors on the block. *Wiley Interdisciplinary Reviews: RNA*, *14*(2), e1752. https://doi.org/10.1002/WRNA.1752

Bouras, T., Southey, M. C., Chang, A. C., Reddel, R. R., Willhite, D., Glynne, R., Henderson, M. A., Armes, J. E., & Venter, D. J. (2002). Stanniocalcin 2 Is an Estrogen-responsive Gene Coexpressed with the Estrogen Receptor in Human Breast Cancer 1. *CANCER RESEARCH*, *62*, 1289–1295. http://www.graphpad.com.

Bourassa, J., Paris, G., Trinkle-Mulcahy, L., & Côté, J. (2024). Biochemical Properties of CARM1: Impact on Western Blotting and Proteomic Studies. *ACS Omega*. https://doi.org/10.1021/ACSOMEGA.4C06360

Bowerman, M., Murray, L. M., Beauvais, A., Pinheiro, B., & Kothary, R. (2012). A critical smn threshold in mice dictates onset of an intermediate spinal muscular atrophy phenotype associated with a distinct neuromuscular junction pathology. *Neuromuscular Disorders*, *22*(3), 263–276. https://doi.org/10.1016/j.nmd.2011.09.007

Boyer, J. G., Bowerman, M., & Kothary, R. (2010). The many faces of SMN: Deciphering the function critical to spinal muscular atrophy pathogenesis. *Future Neurology*, *5*(6), 873–890. https://doi.org/10.2217/fnl.10.57

Bronicki, L. M., & Jasmin, B. J. (2013). Emerging complexity of the HuD/ELAVl4 gene; Implications for neuronal development, function, and dysfunction. *Rna*, *19*(8), 1019–1037. https://doi.org/10.1261/rna.039164.113

Brunet, J. F., & Pattyn, A. (2002). Phox2 genes — from patterning to connectivity. *Current Opinion in Genetics & Development*, *12*(4), 435–440. https://doi.org/10.1016/S0959-437X(02)00322-2

Brynczka, C., & Merrick, B. A. (2008). The p53 transcriptional target gene wnt7b contributes to NGF-inducible neurite outgrowth in neuronal PC12 cells. *Differentiation; Research in Biological Diversity*, *76*(7), 795. https://doi.org/10.1111/J.1432-0436.2007.00261.X

Burghes, A. H. M., & Beattie, C. E. (2009). Spinal Muscular Atrophy: Why do low levels of SMN make motor neurons sick? *Nature Reviews. Neuroscience*, *10*(8), 597. https://doi.org/10.1038/NRN2670

Burry, R. W., & Smith, C. L. (2006). HuD Distribution Changes in Response to Heat Shock but Not Neurotrophic Stimulation. *Journal of Histochemistry and Cytochemistry*, *54*(10), 1129. https://doi.org/10.1369/JHC.6A6979.2006

Byun, J. S., Lee, J. W., Kim, S. Y., Kwon, K. J., Sohn, J. H., Lee, K., Oh, D., Kim, S. S., Chun, W., & Lee, H. J. (2010). Neuroprotective effects of stanniocalcin 2 following kainic acid-induced hippocampal degeneration in ICR mice. *Peptides*, *31*(11), 2094–2099. https://doi.org/10.1016/J.PEPTIDES.2010.08.002

Carascossa, S., Dudek, P., Cenni, B., Briand, P. A., & Picard, D. (2010). CARM1 mediates the ligand-independent and tamoxifen-resistant activation of the estrogen receptor α by cAMP. *Genes & Development*, *24*(7), 708. https://doi.org/10.1101/GAD.568410

Chang, B., Chen, Y., Zhao, Y., & Bruick, R. K. (2007). JMJD6 Is a Histone Arginine Demethylase. *Science*, *318*(5849), 444–447. http://www.jstor.org.proxy.bib.uottawa.ca/stable/20051401

Chang, N. C., Sincennes, M.-C., Chevalier, F. P., Brun, C. E., Lacaria, M., Segalés, J., Muñoz-Cánoves, P., Ming, H., & Rudnicki, M. A. (2018). The Dystrophin Glycoprotein Complex Regulates the Epigenetic Activation of Muscle Stem Cell Commitment [Article]. *Cell Stem Cell*, *22*(5), 755-768.e6. https://doi.org/10.1016/j.stem.2018.03.022

Charoensuksai, P., Kuhn, P., Wang, L., Sherer, N., & Xu, W. (2015). O-GlcNAcylation of co-activator-associated arginine methyltransferase 1 regulates its protein substrate specificity. *Biochemical Journal*, *466*(3), 587–599. https://doi.org/10.1042/BJ20141072

Chaytow, H., Motyl, A. A. L., Huang, Y. T., Wong, C., Currie, G. L., Bahor, Z., Sena, E., & Gillingwater, T. H. (2024). Timing of SMN replacement therapies in mouse models of spinal muscular atrophy: a systematic review and meta-analysis. *Brain Communications*, *6*(4). https://doi.org/10.1093/BRAINCOMMS/FCAE267

Chen, D., Huang, S. M., & Stallcup, M. R. (2000). Synergistic, p160 coactivator-dependent enhancement of estrogen receptor function by CARM1 and p300. *Journal of Biological Chemistry*, *275*(52), 40810–40816. https://doi.org/10.1074/jbc.M005459200

Chen, D., Ma, H., Hong, H., Koh, S. S., Huang, S.-M., Schurter, B. T., Aswad, D. W., & Stallcup, M. R. (1999). Regulation of Transcription by a Protein Methyltransferase. *Science*, *284*(5423), 2174–2174. https://go-gale-com.proxy.bib.uottawa.ca/ps/i.do?p=AONE&sw=w&issn=00368075&v=2.1&it=r&id=GALE%7CA55175579&sid=googleScholar&linkaccess=fulltext

Chen, D., Zhang, Z., Li, M., Wang, W., Li, Y., Rayburn, E. R., Hill, D. L., Wang, H., & Zhang, R. (2007). Ribosomal protein S7 as a novel modulator of p53–MDM2 interaction: binding to MDM2, stabilization of p53 protein, and activation of p53 function. *Oncogene 2007 26:35*, *26*(35), 5029–5037. https://doi.org/10.1038/sj.onc.1210327

Chen, X., Huang, M. F., Fan, D. M., He, Y. H., Zhang, W. J., Ding, J. C., Peng, B. L., Pan, X., Liu, Y., Du, J., Li, Y., Liu, Z. Y., Xie, B. L., Kuang, Z. J., Yi, J., & Liu, W. (2024). CARM1 hypermethylates the NuRD chromatin remodeling complex to promote cell cycle

gene expression and breast cancer development. *Nucleic Acids Research*, *52*(12), 6811. https://doi.org/10.1093/NAR/GKAE329

Cheng, D., Côté, J., Shaaban, S., & Bedford, M. T. (2007a). The Arginine Methyltransferase CARM1 Regulates the Coupling of Transcription and mRNA Processing. *Molecular Cell*, *25*(1), 71–83. https://doi.org/10.1016/j.molcel.2006.11.019

Cheng, D., Côté, J., Shaaban, S., & Bedford, M. T. (2007b). The Arginine Methyltransferase CARM1 Regulates the Coupling of Transcription and mRNA Processing. *Molecular Cell*, *25*(1), 71–83. https://doi.org/10.1016/j.molcel.2006.11.019

Cheng, D., Gao, G., Lorenzo, A. DI, Jayne, S., Hottiger, M. O., Richard, S., & Bedford, M. T. (2020). Genetic evidence for partial redundancy between the arginine methyltransferases CARM1 and PRMT6. *Journal of Biological Chemistry*, *295*(50), 17060–17070. https://doi.org/10.1074/JBC.RA120.014704

Cheng, H., Qin, Y., Fan, H., Su, P., Zhang, X., Zhang, H., & Zhou, G. (2013). Overexpression of CARM1 in breast cancer is correlated with poorly characterized clinicopathologic parameters and molecular subtypes. *Diagnostic Pathology*, *8*(1), 1. https://doi.org/10.1186/1746-1596-8-129

Chevillard-Briet, M., Trouche, D., & Vandel, L. (2002a). Control of CBP co-activating activity by arginine methylation. *The EMBO Journal*, *21*(20), 5457. https://doi.org/10.1093/EMBOJ/CDF548

Chevillard-Briet, M., Trouche, D., & Vandel, L. (2002b). Control of CBP co-activating activity by arginine methylation. *The EMBO Journal*, *21*(20), 5457. https://doi.org/10.1093/EMBOJ/CDF548

Cho, Y., Song, D. G., Kim, S. N., & Kim, Y. K. (2025). CARM1 S217 phosphorylation by CDK1 in late G2 phase facilitates mitotic entry. *Cell Death & Disease 2025 16:1*, *16*(1), 1–10. https://doi.org/10.1038/s41419-025-07533-z

Chowdhury, M. N., & Jin, H. (2023). The RGG motif proteins: Interactions, functions, and regulations. *Wiley Interdisciplinary Reviews. RNA*, *14*(1). https://doi.org/10.1002/WRNA.1748

Chuikov, S., Kurash, J. K., Wilson, J. R., Xiao, B., Justin, N., Ivanov, G. S., McKinney, K., Tempst, P., Prives, C., Gamblin, S. J., Barlev, N. A., & Reinberg, D. (2004). Regulation of p53 activity through lysine methylation. *Nature*, *432*(7015), 353–361. https://doi.org/10.1038/NATURE03117

Chumanov, R. S., Kuhn, P. A., Xu, W., & Burgess, R. R. (2011). Expression and purification of full-length mouse CARM1 from transiently transfected HEK293T cells using HaloTag technology. *Protein Expression and Purification*, *76*(2), 145–153. https://doi.org/10.1016/j.pep.2010.11.010

Chung, S., Jiang, L., Cheng, S., & Furneaux, H. (1996). Purification and Properties of HuD, a Neuronal RNA-binding Protein. *Journal of Biological Chemistry*, *271*(19), 11518–11524. https://doi.org/10.1074/JBC.271.19.11518

Church, M. C., Price, A., Li, H., & Workman, J. L. (2023). The Swi-Snf chromatin remodeling complex mediates gene repression through metabolic control. *Nucleic Acids Research*, *51*(19), 10278–10291. https://doi.org/10.1093/NAR/GKAD711

Clark, M. E., Farinha, A., Morrison, A. R., & Lisi, G. P. (2025). Structural, biological, and biomedical implications of mRNA interactions with the master regulator HuR. *NAR Molecular Medicine*, *2*(1). https://doi.org/10.1093/NARMME/UGAF002

Condeelis, J., & Singer, R. H. (2005). How and why does β-actin mRNA target? *Biology of the Cell*, *97*(1), 97–110. https://doi.org/10.1042/BC20040063

Cornett, E. M., Ferry, L., Defossez, P. A., & Rothbart, S. B. (2019). Lysine methylation regulators moonlighting outside the epigenome. *Molecular Cell*, *75*(6), 1092. https://doi.org/10.1016/J.MOLCEL.2019.08.026

Courtney, N. L., Mole, A. J., Thomson, A. K., & Murray, L. M. (2019). Reduced P53 levels ameliorate neuromuscular junction loss without affecting motor neuron pathology in a mouse model of spinal muscular atrophy. *Cell Death & Disease 2019 10:7*, *10*(7), 1–14. https://doi.org/10.1038/s41419-019-1727-6

Culjkovic-Kraljacic, B., & Borden, K. L. B. (2013). Aiding and Abetting Cancer: mRNA export and the nuclear pore. *Trends in Cell Biology*, *23*(7), 328. https://doi.org/10.1016/J.TCB.2013.03.004

Cuthbert, G. L., Daujat, S., Snowden, A. W., Erdjument-Bromage, H., Hagiwara, T., Yamada, M., Schneider, R., Gregory, P. D., Tempst, P., Bannister, A. J., & Kouzarides, T. (2004). Histone Deimination Antagonizes Arginine Methylation. *Cell*, *118*(5), 545–553. https://doi.org/10.1016/J.CELL.2004.08.020

Dai, W., Zhang, G., & Makeyev, E. V. (2012). RNA-binding protein HuR autoregulates its expression by promoting alternative polyadenylation site usage. *Nucleic Acids Research*, *40*(2), 787–800. https://doi.org/10.1093/NAR/GKR783

Dangouloff, T., & Servais, L. (2019). Clinical Evidence Supporting Early Treatment Of Patients With Spinal Muscular Atrophy: Current Perspectives. *Therapeutics and Clinical Risk Management*, *15*, 1153. https://doi.org/10.2147/TCRM.S172291

Das, R., Esposito, V., Abu-Abed, M., Anand, G. S., Taylor, S. S., & Melacini, G. (2007). cAMP activation of PKA defines an ancient signaling mechanism. *Proceedings of the National Academy of Sciences of the United States of America*, *104*(1), 93–98. https://doi.org/10.1073/PNAS.0609033103/SUPPL_FILE/09033FIG6.PDF

De Santis, R., Alfano, V., de Turris, V., Colantoni, A., Santini, L., Garone, M. G., Antonacci, G., Peruzzi, G., Sudria-Lopez, E., Wyler, E., Anink, J. J., Aronica, E., Landthaler, M., Pasterkamp, R. J., Bozzoni, I., & Rosa, A. (2019). Mutant FUS and ELAVL4 (HuD) Aberrant Crosstalk in Amyotrophic Lateral Sclerosis. *Cell Reports*, *27*(13), 3818-3831.e5. https://doi.org/10.1016/J.CELREP.2019.05.085

De Vos, K. J., & Hafezparast, M. (2017). Neurobiology of axonal transport defects in motor neuron diseases: Opportunities for translational research? *Neurobiology of Disease*, *105*, 283. https://doi.org/10.1016/J.NBD.2017.02.004

Dell'orco, M., Elyaderani, A., Vannan, A., Sekar, S., Powell, G., Liang, W. S., Neisewander, J. L., & Perrone-Bizzozero, N. I. (2021a). HuD regulates mRNA-circRNA-miRNA networks in the mouse striatum linked to neuronal development and drug addiction. *Biology*, *10*(9), 939. https://doi.org/10.3390/BIOLOGY10090939/S1

Dell'orco, M., Elyaderani, A., Vannan, A., Sekar, S., Powell, G., Liang, W. S., Neisewander, J. L., & Perrone-Bizzozero, N. I. (2021b). HuD regulates mRNA-circRNA-miRNA networks in the mouse striatum linked to neuronal development and drug addiction. *Biology*, *10*(9), 939. https://doi.org/10.3390/BIOLOGY10090939/S1

Dell'Orco, M., Oliver, R. J., & Perrone-Bizzozero, N. (2020a). HuD Binds to and Regulates Circular RNAs Derived From Neuronal Development- and Synaptic Plasticity-Associated

Genes. *Frontiers in Genetics*, *11*, 555944. https://doi.org/10.3389/FGENE.2020.00790/BIBTEX

Dell'Orco, M., Oliver, R. J., & Perrone-Bizzozero, N. (2020b). HuD Binds to and Regulates Circular RNAs Derived From Neuronal Development- and Synaptic Plasticity-Associated Genes. *Frontiers in Genetics*, *11*. https://doi.org/10.3389/FGENE.2020.00790

Dell'Orco, M., Sardone, V., Gardiner, A. S., Pansarasa, O., Bordoni, M., Perrone-Bizzozero, N. I., & Cereda, C. (2021). HuD regulates SOD1 expression during oxidative stress in differentiated neuroblastoma cells and sporadic ALS motor cortex. *Neurobiology of Disease*, *148*, 105211. https://doi.org/10.1016/J.NBD.2020.105211

Deschênes-Furry, J., Mousavi, K., Bolognani, F., Neve, R. L., Parks, R. J., Perrone-Bizzozero, N. I., & Jasmin, B. J. (2007). The RNA-Binding Protein HuD Binds Acetylcholinesterase mRNA in Neurons and Regulates its Expression after Axotomy. *Journal of Neuroscience*, *27*(3), 665–675. https://doi.org/10.1523/JNEUROSCI.4626-06.2007

Deschênes-Furry, J., Perrone-Bizzozero, N., & Jasmin, B. J. (2006). The RNA-binding protein HuD: A regulator of neuronal differentiation, maintenance and plasticity. *BioEssays*, *28*(8), 822–833. https://doi.org/10.1002/BIES.20449

Dhang, S., Mondal, A., Das, C., & Roy, S. (2025). Metformin inhibits the histone methyltransferase CARM1 and attenuates H3 histone methylation during gluconeogenesis. *Journal of Biological Chemistry*, *301*(3), 108271. https://doi.org/10.1016/J.JBC.2025.108271

Dhar, S., Vemulapalli, V., Patananan, A. N., Huang, G. L., Di Lorenzo, A., Richard, S., Comb, M. J., Guo, A., Clarke, S. G., & Bedford, M. T. (2013). Loss of the major Type I arginine

methyltransferase PRMT1 causes substrate scavenging by other PRMTs. *Scientific Reports*, *3*. https://doi.org/10.1038/SREP01311

Di Giovanni, S., Knights, C. D., Rao, M., Yakovlev, A., Beers, J., Catania, J., Avantaggiati, M. L., & Faden, A. I. (2006). The tumor suppressor protein p53 is required for neurite outgrowth and axon regeneration. *The EMBO Journal*, *25*(17), 4084. https://doi.org/10.1038/SJ.EMBOJ.7601292

Didiot, M. C., Tian, Z., Schaeffer, C., Subramanian, M., Mandel, J. L., & Moine, H. (2008). The G-quartet containing FMRP binding site in FMR1 mRNA is a potent exonic splicing enhancer. *Nucleic Acids Research*, *36*(15), 4902–4912. https://doi.org/10.1093/NAR/GKN472

Dilworth, D., & Barsyte-Lovejoy, D. (2019). Targeting protein methylation: from chemical tools to precision medicines. In *Cellular and Molecular Life Sciences* (Vol. 76, Issue 15, pp. 2967–2985). Birkhauser Verlag AG. https://doi.org/10.1007/s00018-019-03147-9

Dobin, A., Davis, C. A., Schlesinger, F., Drenkow, J., Zaleski, C., Jha, S., Batut, P., Chaisson, M., & Gingeras, T. R. (2012). STAR: ultrafast universal RNA-seq aligner. *Bioinformatics*, *29*(1), 15. https://doi.org/10.1093/BIOINFORMATICS/BTS635

Du, Z. W., Chen, H., Liu, H., Lu, J., Qian, K., Huang, C. T. L., Zhong, X., Fan, F., & Zhang, S. C. (2015). Generation and expansion of highly pure motor neuron progenitors from human pluripotent stem cells. *Nature Communications 2015 6:1*, *6*(1), 1–9. https://doi.org/10.1038/ncomms7626

Dubreuil, V., Hirsch, M. R., Jouve, C., Brunet, J. F., & Goridis, C. (2002). The role of Phox2b in synchronizing pan-neuronal and type-specific aspects of neurogenesis. *Development*, *129*(22), 5241–5253. https://doi.org/10.1242/DEV.129.22.5241

Dubreuil, V., Hirsch, M. R., Pattyn, A., Brunet, J. F., & Goridis, C. (2000). The Phox2b transcription factor coordinately regulates neuronal cell cycle exit and identity. *Development*, *127*(23), 5191–5201. https://doi.org/10.1242/DEV.127.23.5191

Elbaum-Garfinkle, S. (2019). Matter over mind: Liquid phase separation and neurodegeneration. *The Journal of Biological Chemistry*, *294*(18), 7160. https://doi.org/10.1074/JBC.REV118.001188

Elbaum-Garfinkle, S., Kim, Y., Szczepaniak, K., Chen, C. C. H., Eckmann, C. R., Myong, S., & Brangwynne, C. P. (2015). The disordered P granule protein LAF-1 drives phase separation into droplets with tunable viscosity and dynamics. *Proceedings of the National Academy of Sciences of the United States of America*, *112*(23), 7189–7194. https://doi.org/10.1073/PNAS.1504822112/SUPPL_FILE/PNAS.201504822SI.PDF

Elias, R. D., Ma, W., Ghirlando, R., Schwieters, C. D., Reddy, V. S., & Deshmukh, L. (2020). Proline-rich domain of human ALIX contains multiple TSG101-UEV interaction sites and forms phosphorylation-mediated reversible amyloids. *Proceedings of the National Academy of Sciences of the United States of America*, *117*(39), 24274–24284. https://doi.org/10.1073/PNAS.2010635117/-/DCSUPPLEMENTAL

Ellis, P., Fagan, B. M., Magness, S. T., Hutton, S., Taranova, O., Hayashi, S., McMahon, A., Rao, M., & Pevny, L. (2004). SOX2, a persistent marker for multipotential neural stem cells derived from embryonic stem cells, the embryo or the adult. *Developmental Neuroscience*, *26*(2–4), 148–165. https://doi.org/10.1159/000082134

Eshraghi, M., McFall, E., Gibeault, S., & Kothary, R. (2016). Effect of genetic background on the phenotype of the Smn 2B/- mouse model of spinal muscular atrophy . *Human Molecular Genetics*, *25*(20), ddw278. https://doi.org/10.1093/hmg/ddw278

Fairfield, B., Mammarella, N., Fontanella, L., Sarra, A., D'Aurora, M., Stuppia, L., & Gatta, V. (2019). Aging and the Combined effects of ADRA2B and CB1 deletions on Affective Working Memory. *Scientific Reports 2019 9:1*, *9*(1), 1–10. https://doi.org/10.1038/s41598-019-40108-5

Fallini, C., Zhang, H., Su, Y., Silani, V., Singer, R. H., Rossoll, W., & Bassell, G. J. (2011). The Survival of Motor Neuron (SMN) Protein Interacts with the mRNA-Binding Protein HuD and Regulates Localization of Poly(A) mRNA in Primary Motor Neuron Axons. *The Journal of Neuroscience*, *31*(10), 3914. https://doi.org/10.1523/JNEUROSCI.3631-10.2011

Fay, M. M., Lyons, S. M., & Ivanov, P. (2017). RNA G-quadruplexes in biology: principles and molecular mechanisms. *Journal of Molecular Biology*, *429*(14), 2127. https://doi.org/10.1016/J.JMB.2017.05.017

Feige, M. J., & Hendershot, L. M. (2010). Disulfide bonds in ER protein folding and homeostasis. *Current Opinion in Cell Biology*, *23*(2), 167. https://doi.org/10.1016/J.CEB.2010.10.012

Feng, J., Meyer, C. A., Wang, Q., Liu, J. S., Liu, X. S., & Zhang, Y. (2012). GFOLD: A generalized fold change for ranking differentially expressed genes from RNA-seq data. *Bioinformatics*, *28*(21), 2782–2788. https://doi.org/10.1093/bioinformatics/bts515

Feng, Q., He, B., Jung, S. Y., Song, Y., Qin, J., Tsai, S. Y., Tsai, M. J., & O'Malley, B. W. (2009a). Biochemical Control of CARM1 Enzymatic Activity by Phosphorylation. *Journal of Biological Chemistry*, *284*(52), 36167–36174. https://doi.org/10.1074/JBC.M109.065524

Feng, Q., He, B., Jung, S. Y., Song, Y., Qin, J., Tsai, S. Y., Tsai, M. J., & O'Malley, B. W. (2009b). Biochemical control of CARM1 enzymatic activity by phosphorylation. *Journal of Biological Chemistry*, *284*(52), 36167–36174. https://doi.org/10.1074/jbc.M109.065524

Feng, Q., Yi, P., Wong, J., & O'Malley, B. W. (2006). Signaling within a Coactivator Complex: Methylation of SRC-3/AIB1 Is a Molecular Switch for Complex Disassembly [Article]. *Molecular and Cellular Biology*, *26*(21), 7846–7857. https://doi.org/10.1128/MCB.00568-06

Feng, Y., Xie, N., Jin, M., Stahley, M. R., Stivers, J. T., & Zheng, Y. G. (2011). A Transient Kinetic Analysis of PRMT1 Catalysis. *Biochemistry*, *50*(32), 7033. https://doi.org/10.1021/BI200456U

Ferreira de Freitas, R., Ivanochko, D., & Schapira, M. (2019). Methyltransferase inhibitors: Competing with, or exploiting the bound cofactor. In *Molecules* (Vol. 24, Issue 24). https://doi.org/10.3390/molecules24244492

Friesen, W. J., Massenet, S., Paushkin, S., Wyce, A., & Dreyfuss, G. (2001). SMN, the product of the spinal muscular atrophy gene, binds preferentially to dimethylarginine-containing protein targets. *Molecular Cell*, *7*(5), 1111–1117. https://doi.org/10.1016/S1097-2765(01)00244-1

Fujiwara, T., Mori, Y., Chu, D. L., Koyama, Y., Miyata, S., Tanaka, H., Yachi, K., Kubo, T., Yoshikawa, H., & Tohyama, M. (2006). CARM1 Regulates Proliferation of PC12 Cells by Methylating HuD. *Molecular and Cellular Biology*, *26*(6), 2273–2285. https://doi.org/10.1128/MCB.26.6.2273-2285.2006

Fukao, A., Sasano, Y., Imataka, H., Inoue, K., Sakamoto, H., Sonenberg, N., Thoma, C., & Fujiwara, T. (2009). The ELAV Protein HuD Stimulates Cap-Dependent Translation in a Poly(A)- and eIF4A-Dependent Manner. *Molecular Cell*, *36*(6), 1007–1017. https://doi.org/10.1016/J.MOLCEL.2009.11.013

Fuller, H. R., Mandefro, B., Shirran, S. L., Gross, A. R., Kaus, A. S., Botting, C. H., Morris, G. E., & Sareen, D. (2016). Spinal Muscular Atrophy Patient iPSC-Derived Motor Neurons Have Reduced Expression of Proteins Important in Neuronal Development. *Frontiers in Cellular Neuroscience*, *9*(JAN2016), 506. https://doi.org/10.3389/FNCEL.2015.00506

Gagliardi, A. D., Kuo, E. Y. W., Raulic, S., Wagner, G. F., & DiMattia, G. E. (2005). Human stanniocalcin-2 exhibits potent growth-suppressive properties in transgenic mice independently of growth hormone and IGFs. *American Journal of Physiology - Endocrinology and Metabolism*, *288*(1 51-1), 92–105. https://doi.org/10.1152/AJPENDO.00268.2004/ASSET/IMAGES/LARGE/ZH1001051945 0009.JPEG

Galli, S., Lopes, D. M., Ammari, R., Kopra, J., Millar, S. E., Gibb, A., & Salinas, P. C. (2014). Deficient Wnt signalling triggers striatal synaptic degeneration and impaired motor behaviour in adult mice. *Nature Communications 2014 5:1*, *5*(1), 1–13. https://doi.org/10.1038/ncomms5992

Gao, F., Elliott, N. J., Ho, J., Sharp, A., Shokhirev, M. N., & Hargreaves, D. C. (2019). Heterozygous Mutations in SMARCA2 Reprogram the Enhancer Landscape by Global Retargeting of SMARCA4. *Molecular Cell*, *75*(5), 891-904.e7. https://doi.org/10.1016/J.MOLCEL.2019.06.024

Gao, W. W., Xiao, R. Q., Peng, B. L., Xu, H. T., Shen, H. F., Huang, M. F., Shi, T. T., Yi, J., Zhang, W. J., Wu, X. N., Gao, X., Lin, X. Z., Dorrestein, P. C., Rosenfeld, M. G., & Liu, W. (2015). Arginine methylation of HSP70 regulates retinoid acid-mediated RARβ2 gene activation. *Proceedings of the National Academy of Sciences of the United States of*

America, *112*(26), E3327–E3336. https://doi.org/10.1073/PNAS.1509658112/-/DCSUPPLEMENTAL

Garone, M. G., Birsa, N., Rosito, M., Salaris, F., Mochi, M., de Turris, V., Nair, R. R., Cunningham, T. J., Fisher, E. M. C., Morlando, M., Fratta, P., & Rosa, A. (2021). ALS-related FUS mutations alter axon growth in motoneurons and affect HuD/ELAVL4 and FMRP activity. *Communications Biology 2021 4:1*, *4*(1), 1–17. https://doi.org/10.1038/s42003-021-02538-8

Gayatri, S., & Bedford, M. T. (2014a). Readers of Histone Methylarginine Marks. *Biochimica et Biophysica Acta*, *1839*(8), 702. https://doi.org/10.1016/J.BBAGRM.2014.02.015

Gayatri, S., & Bedford, M. T. (2014b). Readers of histone methylarginine marks. In *Biochimica et Biophysica Acta - Gene Regulatory Mechanisms* (Vol. 1839, Issue 8, pp. 702–710). Elsevier. https://doi.org/10.1016/j.bbagrm.2014.02.015

Georgakopoulos-Soares, I., Parada, G. E., Wong, H. Y., Medhi, R., Furlan, G., Munita, R., Miska, E. A., Kwok, C. K., & Hemberg, M. (2022). Alternative splicing modulation by G-quadruplexes. *Nature Communications 2022 13:1*, *13*(1), 1–16. https://doi.org/10.1038/s41467-022-30071-7

Gopinath, C., Law, W. D., Rodríguez-Molina, J. F., Prasad, A. B., Song, L., Crawford, G. E., Mullikin, J. C., Svaren, J., & Antonellis, A. (2016). Stringent comparative sequence analysis reveals SOX10 as a putative inhibitor of glial cell differentiation. *BMC Genomics*, *17*(1). https://doi.org/10.1186/s12864-016-3167-3

Goulet, I., Gauvin, G., Boisvenue, S., & Côté, J. (2007). Alternative splicing yields protein arginine methyltransferase 1 isoforms with distinct activity, substrate specificity, and subcellular localization. *Journal of Biological Chemistry*, *282*(45), 33009–33021.

https://doi.org/10.1074/JBC.M704349200/ATTACHMENT/806A5BE5-1020-4F82-82E9-8F157CCCB4C6/MMC1.PDF

Goutebroze, L., Brault, E., Muchardt, C., Camonis, J., & Thomas, G. (2000). Cloning and Characterization of SCHIP-1, a Novel Protein Interacting Specifically with Spliced Isoforms and Naturally Occurring Mutant NF2 Proteins. *Molecular and Cellular Biology*, *20*(5), 1699. https://doi.org/10.1128/MCB.20.5.1699-1712.2000

Han, S., Kim, J. N., Park, C. H., Byun, J. S., Kim, D. Y., & Ko, H. G. (2024). Modulation of synaptic transmission through O-GlcNAcylation. *Molecular Brain*, *17*(1), 1–5. https://doi.org/10.1186/S13041-023-01072-4/TABLES/1

Hartel, N. G., Chew, B., Qin, J., Xu, J., & Graham, N. A. (2019). Deep Protein Methylation Profiling by Combined Chemical and Immunoaffinity Approaches Reveals Novel PRMT1 Targets. *Molecular & Cellular Proteomics*, *18*(11), 2149–2164. https://doi.org/10.1074/MCP.RA119.001625

Hartley, A. V., & Lu, T. (2020). Modulating the modulators: regulation of protein arginine methyltransferases by post-translational modifications. *Drug Discovery Today*, *25*(9), 1735. https://doi.org/10.1016/J.DRUDIS.2020.06.031

Hayashi, S., Yano, M., Igarashi, M., Okano, H. J., & Okano, H. (2015). Alternative role of HuD splicing variants in neuronal differentiation. *Journal of Neuroscience Research*, *93*(3), 399–409. https://doi.org/10.1002/JNR.23496

Hernandez Cordero, A. I., Gonzales, N. M., Parker, C. C., Sokolof, G., Vandenbergh, D. J., Cheng, R., Abney, M., Sko, A., Douglas, A., Palmer, A. A., Gregory, J. S., & Lionikas, A. (2019). Genome-wide Associations Reveal Human-Mouse Genetic Convergence and

Modifiers of Myogenesis, CPNE1 and STC2. *American Journal of Human Genetics*, *105*(6), 1222. https://doi.org/10.1016/J.AJHG.2019.10.014

Herrmann, F., Pably, P., Eckerich, C., Bedford, M. T., & Fackelmayer, F. O. (2009). Human protein arginine methyltransferases in vivo – distinct properties of eight canonical members of the PRMT family. *Journal of Cell Science*, *122*(5), 667 LP – 677. https://doi.org/10.1242/jcs.039933

Higashimoto, K., Kuhn, P., Desai, D., Cheng, X., & Xu, W. (2007). Phosphorylation-mediated inactivation of coactivator-associated arginine methyltransferase 1 [Article]. *Proceedings of the National Academy of Sciences - PNAS*, *104*(30), 12318–12323. https://doi.org/10.1073/pnas.0610792104

Hiken, J. F., McDonald, J. I., Decker, K. F., Sanchez, C., Hoog, J., Vanderkraats, N. D., Jung, K. L., Akinhanmi, M., Rois, L. E., Ellis, M. J., & Edwards, J. R. (2016a). Epigenetic activation of the prostaglandin receptor EP4 promotes resistance to endocrine therapy for breast cancer. *Oncogene*, *36*(16), 2319. https://doi.org/10.1038/ONC.2016.397

Hiken, J. F., McDonald, J. I., Decker, K. F., Sanchez, C., Hoog, J., Vanderkraats, N. D., Jung, K. L., Akinhanmi, M., Rois, L. E., Ellis, M. J., & Edwards, J. R. (2016b). Epigenetic activation of the prostaglandin receptor EP4 promotes resistance to endocrine therapy for breast cancer. *Oncogene*, *36*(16), 2319. https://doi.org/10.1038/ONC.2016.397

Hirose, T., Ninomiya, K., Nakagawa, S., & Yamazaki, T. (2022a). A guide to membraneless organelles and their various roles in gene regulation. *Nature Reviews Molecular Cell Biology 2022 24:4*, *24*(4), 288–304. https://doi.org/10.1038/s41580-022-00558-8

Hirose, T., Ninomiya, K., Nakagawa, S., & Yamazaki, T. (2022b). A guide to membraneless organelles and their various roles in gene regulation. *Nature Reviews Molecular Cell Biology 2022 24:4*, *24*(4), 288–304. https://doi.org/10.1038/S41580-022-00558-8

Ho, P. J., Lloyd, S. M., & Bao, X. (2019). Unwinding chromatin at the right places: how BAF is targeted to specific genomic locations during development. *Development (Cambridge, England)*, *146*(19). https://doi.org/10.1242/DEV.178780

Hobble, H. V., & Schaner Tooley, C. E. (2024). Intrafamily heterooligomerization as an emerging mechanism of methyltransferase regulation. *Epigenetics and Chromatin*, *17*(1), 1–12. https://doi.org/10.1186/S13072-024-00530-0/TABLES/1

Hofweber, M., & Dormann, D. (2019). Friend or foe—Post-translational modifications as regulators of phase separation and RNP granule dynamics. *Journal of Biological Chemistry*, *294*(18), 7137–7150. https://doi.org/10.1074/JBC.TM118.001189

Hong, E., Lim, Y., Lee, E., Oh, M., & Kwon, D. (2012). Tissue-specific and age-dependent expression of protein arginine methyltransferases (PRMTs) in male rat tissues. *Biogerontology*, *13*(3), 329–336. https://doi.org/10.1007/s10522-012-9379-2

Hsieh-Wilson, L. C., Benfenati, F., Snyder, G. L., Allen, P. B., Nairn, A. C., & Greengard, P. (2003). Phosphorylation of spinophilin modulates its interaction with actin filaments. *Journal of Biological Chemistry*, *278*(2), 1186–1194. https://doi.org/10.1074/JBC.M205754200/ASSET/80422F43-D7D1-4BC2-A5AF-D9786851AC06/MAIN.ASSETS/GR9.JPG

Hu, H., Luo, C., & Zheng, Y. G. (2016). Transient Kinetics Define a Complete Kinetic Model for Protein Arginine Methyltransferase 1. *Journal of Biological Chemistry*, *291*(52), 26722–26738. https://doi.org/10.1074/JBC.M116.757625

Hu, J., Vidovic, M., Chen, M. M., Lu, Q. Y., & Song, Z. M. (2008). Activation of α2A adrenoceptors alters dendritic spine development and the expression of spinophilin in cultured cortical neurones. *Brain Research*, *1199*, 37–45. https://doi.org/10.1016/J.BRAINRES.2007.12.073

Hu, S.-B., Xiang, J.-F., Li, X., Xu, Y., Xue, W., Huang, M., Wong, C. C., Sagum, C. A., Bedford, M. T., Yang, L., Cheng, D., & Chen, L.-L. (2015). Protein arginine methyltransferase CARM1 attenuates the paraspeckle-mediated nuclear retention of mRNAs containing IRAlus. *Genes & Development*, *29*, 630–645. https://doi.org/10.1101/gad.257048

Huber, K., Narasimhan, P., Shtukmaster, S., Pfeifer, D., Evans, S. M., & Sun, Y. (2013). The LIM-Homeodomain transcription factor Islet-1 is required for the development of sympathetic neurons and adrenal chromaffin cells. *Developmental Biology*, *380*(2), 286. https://doi.org/10.1016/J.YDBIO.2013.04.027

Hubers, L., Valderrama-Carvajal, H., Laframboise, J., Timbers, J., Sanchez, G., & Côté, J. (2011). HuD interacts with survival motor neuron protein and can rescue spinal muscular atrophy-like neuronal defects. *Human Molecular Genetics*, *20*(3), 553–579. https://doi.org/10.1093/hmg/ddq500

Hulme, A. J., Maksour, S., St-Clair Glover, M., Miellet, S., & Dottori, M. (2021). Making neurons, made easy: The use of Neurogenin-2 in neuronal differentiation. *Stem Cell Reports*, *17*(1), 14. https://doi.org/10.1016/J.STEMCR.2021.11.015

Hunter, G., Sarvestany, A. A., Roche, S. L., Symes, R. C., & Gillingwater, T. H. (2014). SMN-dependent intrinsic defects in Schwann cells in mouse models of spinal muscular atrophy. *Human Molecular Genetics*, *23*(9), 2235–2250. https://doi.org/10.1093/hmg/ddt612

Hupalowska, A., Jedrusik, A., Zhu, M., Bedford, M. T., Glover, D. M., & Zernicka-Goetz, M. (2018). CARM1 and Paraspeckles Regulate Pre-implantation Mouse Embryo Development. *Cell*, *175*(7), 1902-1916.e13. https://doi.org/10.1016/j.cell.2018.11.027

Huttlin, E. L., Bruckner, R. J., Navarrete-Perea, J., Cannon, J. R., Baltier, K., Gebreab, F., Gygi, M. P., Thornock, A., Zarraga, G., Tam, S., Szpyt, J., Gassaway, B. M., Panov, A., Parzen, H., Fu, S., Golbazi, A., Maenpaa, E., Stricker, K., Guha Thakurta, S., … Gygi, S. P. (2021). Dual proteome-scale networks reveal cell-specific remodeling of the human interactome. *Cell*, *184*(11), 3022-3040.e28. https://doi.org/10.1016/J.CELL.2021.04.011/ASSET/4EA7C308-B3F0-49AD-BEC1-52E645A8B5B4/MAIN.ASSETS/GR7.JPG

Hwang, J. W., Cho, Y., Bae, G. U., Kim, S. N., & Kim, Y. K. (2021). Protein arginine methyltransferases: promising targets for cancer therapy. *Experimental & Molecular Medicine 2021 53:5*, *53*(5), 788–808. https://doi.org/10.1038/s12276-021-00613-y

Iannelli, G., Milite, C., Marechal, N., Cura, V., Bonnefond, L., Troffer-Charlier, N., Feoli, A., Rescigno, D., Wang, Y., Cipriano, A., Viviano, M., Bedford, M. T., Cavarelli, J., Castellano, S., & Sbardella, G. (2022). Turning Nonselective Inhibitors of Type I Protein Arginine Methyltransferases into Potent and Selective Inhibitors of Protein Arginine Methyltransferase 4 through a Deconstruction–Reconstruction and Fragment-Growing Approach. *Journal of Medicinal Chemistry*. https://doi.org/10.1021/acs.jmedchem.2c00252

Ibrahim, A. Y., Khaodeuanepheng, N. P., Amarasekara, D. L., Correia, J. J., Lewis, K. A., Fitzkee, N. C., Hough, L. E., & Whitten, S. T. (2022). Intrinsically disordered regions that drive phase separation form a robustly distinct protein class. *The Journal of Biological Chemistry*, *299*(1), 102801. https://doi.org/10.1016/J.JBC.2022.102801

Ito, D., Walker, J. R., Thompson, C. S., Moroz, I., Lin, W., Veselits, M. L., Hakim, A. M., Fienberg, A. A., & Thinakaran, G. (2004). Characterization of Stanniocalcin 2, a Novel Target of the Mammalian Unfolded Protein Response with Cytoprotective Properties. *Molecular and Cellular Biology*, *24*(21), 9456. https://doi.org/10.1128/MCB.24.21.9456-9469.2004

Itoh, T., Miyake, K., & Iijima, S. (2008). Differentiation-specific expression of chromatin remodeling factor BRM. *Biochemical and Biophysical Research Communications*, *366*(3), 827–833. https://doi.org/10.1016/J.BBRC.2007.12.026

Itonaga, H., Mookhtiar, A. K., Greenblatt, S. M., Liu, F., Martinez, C., Bilbao, D., Rains, M., Hamard, P. J., Sun, J., Umeano, A. C., Duffort, S., Chen, C., Man, N., Mas, G., Tottone, L., Totiger, T., Bradley, T., Taylor, J., Schürer, S., & Nimer, S. D. (2024). Tyrosine phosphorylation of CARM1 promotes its enzymatic activity and alters its target specificity. *Nature Communications 2024 15:1*, *15*(1), 1–19. https://doi.org/10.1038/s41467-024-47689-4

Jakobsson, M. E., Małecki, J., & Falnes, P. (2018). Regulation of eukaryotic elongation factor 1 alpha (eEF1A) by dynamic lysine methylation. *RNA Biology*, *15*(3), 314–319. https://doi.org/10.1080/15476286.2018.1440875/ASSET/FDE6EE1F-6268-402C-8464-673591A41526/ASSETS/IMAGES/KRNB_A_1440875_F0003_OC.JPG

Jayne, S., Rothgiesser, K. M., & Hottiger, M. O. (2009). CARM1 but not Its Enzymatic Activity Is Required for Transcriptional Coactivation of NF-κB-Dependent Gene Expression. *Journal of Molecular Biology*, *394*(3), 485–495. https://doi.org/10.1016/J.JMB.2009.09.032

Jelinic, P., Mueller, J. J., Olvera, N., Dao, F., Scott, S. N., Shah, R., Gao, J., Schultz, N., Gonen, M., Soslow, R. A., Berger, M. F., & Levine, D. A. (2014). Recurrent SMARCA4 mutations

in small cell carcinoma of the ovary. *Nature Genetics*, *46*(5), 424. https://doi.org/10.1038/NG.2922

Jeon, Y., Shin, J. E., Kwon, M., Cho, E., Cavalli, V., & Cho, Y. (2021). In Vivo Gene Delivery of STC2 Promotes Axon Regeneration in Sciatic Nerves. *Molecular Neurobiology*, *58*(2), 750–760. https://doi.org/10.1007/S12035-020-02155-2/FIGURES/5

Jin, J., Xie, X., Chen, C., Gyoon Park, J., Stark, C., Andrew James, D., Olhovsky, M., Linding, R., Mao, Y., & Pawson, T. (2009). Eukaryotic Protein Domains as Functional Units of Cellular Evolution. *Science Signaling*, *3*(98). www.SCIENCESIGNALING.org

Johns, A. E., & Maragakis, N. J. (2022). Exploring Motor Neuron Diseases Using iPSC Platforms. *Stem Cells*, *40*(1), 2. https://doi.org/10.1093/STMCLS/SXAB006

Joseph, B., Orlian, M., & Furneaux, H. (1998a). p21(waf1) mRNA contains a conserved element in its 3'-untranslated region that is bound by the Elav-like mRNA-stabilizing proteins. *Journal of Biological Chemistry*, *273*(32), 20511–20516. https://doi.org/10.1074/jbc.273.32.20511

Joseph, B., Orlian, M., & Furneaux, H. (1998b). p21(waf1) mRNA contains a conserved element in its 3'-untranslated region that is bound by the Elav-like mRNA-stabilizing proteins. *Journal of Biological Chemistry*, *273*(32), 20511–20516. https://doi.org/10.1074/jbc.273.32.20511

Jung, M., & Lee, E. K. (2021). RNA-Binding Protein HuD as a Versatile Factor in Neuronal and Non-Neuronal Systems. *Biology*, *10*(5). https://doi.org/10.3390/BIOLOGY10050361

Kamura, T., Katsuda, Y., Kitamura, Y., & Ihara, T. (2020). G-quadruplexes in mRNA: A key structure for biological function. *Biochemical and Biophysical Research Communications*, *526*(1), 261–266. https://doi.org/10.1016/J.BBRC.2020.02.168

Kang, M. J., Abdelmohsen, K., Hutchison, E. R., Mitchell, S. J., Grammatikakis, I., Guo, R., Noh, J. H., Martindale, J. L., Yang, X., Lee, E. K., Faghihi, M. A., Wahlestedt, C., Troncoso, J. C., Pletnikova, O., Perrone-Bizzozero, N., Resnick, S. M., deCabo, R., Mattson, M. P., & Gorospe, M. (2014). HuD regulates coding and noncoding RNA to induce APP → Aβ processing. *Cell Reports*, *7*(5), 1401. https://doi.org/10.1016/J.CELREP.2014.04.050

Kasashima, K., Terashima, K., Yamamoto, K., Sakashita, E., & Sakamoto, H. (1999). Cytoplasmic localization is required for the mammalian ELAV-like protein HuD to induce neuronal differentiation. *Genes to Cells*, *4*(11), 667–683. https://doi.org/10.1046/J.1365-2443.1999.00292.X

Katsuyama, M., Nishigaki, N., Sugimoto, Y., Morimoto, K., Negishi, M., Narumiya, S., & Ichikawa, A. (1995). The mouse prostaglandin E receptor EP2 subtype: cloning, expression, and Northern blot analysis. *FEBS Letters*, *372*(2–3), 151–156. https://doi.org/10.1016/0014-5793(95)00966-D

Kawabe, Y. I., Wang, Y. X., McKinnell, I. W., Bedford, M. T., & Rudnicki, M. A. (2012). Carm1 Regulates Pax7 Transcriptional Activity through MLL1/2 Recruitment during Asymmetric Satellite Stem Cell Divisions. *Cell Stem Cell*, *11*(3), 333–345. https://doi.org/10.1016/J.STEM.2012.07.001

Kim, D., Lee, J., Cheng, D., Li, J., Carter, C., Richie, E., & Bedford, M. T. (2010a). Enzymatic activity is required for the in Vivo functions of CARM1. *Journal of Biological Chemistry*, *285*(2), 1147–1152. https://doi.org/10.1074/jbc.M109.035865

Kim, D., Lee, J., Cheng, D., Li, J., Carter, C., Richie, E., & Bedford, M. T. (2010b). Enzymatic activity is required for the in Vivo functions of CARM1. *Journal of Biological Chemistry*, *285*(2), 1147–1152. https://doi.org/10.1074/jbc.M109.035865

Kim, E. J., Liu, P., Zhang, S., Donahue, K., Wang, Y., Schehr, J. L., Wolfe, S. K., Dickerson, A., Lu, L., Rui, L., Zhong, X., Wisinski, K. B., Yu, M., Suzuki, A., Lang, J. M., Ong, I. M., & Xu, W. (2021). BAF155 methylation drives metastasis by hijacking super-enhancers and subverting anti-tumor immunity. *Nucleic Acids Research*, *49*(21), 12211–12233. https://doi.org/10.1093/NAR/GKAB1122

Kim, H. H., Lee, S. J., Gardiner, A. S., Perrone-Bizzozero, N. I., & Yoo, S. (2015). Different motif requirements for the localization zipcode element of β-actin mRNA binding by HuD and ZBP1. *Nucleic Acids Research*, *43*(15), 7432. https://doi.org/10.1093/NAR/GKV699

Kim, H., Tan, T. K., Lee, D. Z. Y., Huang, X. Z., Ong, J. Z. L., Kelliher, M. A., Yeoh, A. E. J., Sanda, T., & Tan, S. H. (2024). Oncogenic dependency on SWI/SNF chromatin remodeling factors in T-cell acute lymphoblastic leukemia. *Leukemia 2024 38:9*, *38*(9), 1906–1917. https://doi.org/10.1038/s41375-024-02331-6

Klingler, E., Martin, P. M., Garcia, M., Moreau-Fauvarque, C., Falk, J., Chareyre, F., Giovannini, M., Chédotal, A., Girault, J. A., & Goutebroze, L. (2015). The cytoskeleton-associated protein SCHIP1 is involved in axon guidance, and is required for piriform cortex and anterior commissure development. *Development*, *142*(11), 2026–2036. https://doi.org/10.1242/DEV.119248

Kölbel, K., Ihling, C., Bellmann-Sickert, K., Neundorf, I., Beck-Sickinger, A. G., Sinz, A., Kühn, U., & Wahle, E. (2009). Type I Arginine Methyltransferases PRMT1 and PRMT-3

Act Distributively. *The Journal of Biological Chemistry*, *284*(13), 8274. https://doi.org/10.1074/JBC.M809547200

Komada, M., & Soriano, P. (2002). βIV-spectrin regulates sodium channel clustering through ankyrin-G at axon initial segments and nodes of Ranvier. *The Journal of Cell Biology*, *156*(2), 337. https://doi.org/10.1083/JCB.200110003

Koschinski, A., & Zaccolo, M. (2017). Activation of PKA in cell requires higher concentration of cAMP than in vitro: implications for compartmentalization of cAMP signalling. *Scientific Reports 2017 7:1*, *7*(1), 1–12. https://doi.org/10.1038/s41598-017-13021-y

Kostadinov, R., Malhotra, N., Viotti, M., Shine, R., D'Antonio, L., & Bagga, P. (2005). GRSDB: a database of quadruplex forming G-rich sequences in alternatively processed mammalian pre-mRNA sequences. *Nucleic Acids Research*, *34*(Database issue), D119. https://doi.org/10.1093/NAR/GKJ073

Kouzarides, T. (2007). Chromatin Modifications and Their Function. In *Cell* (Vol. 128, Issue 4, pp. 693–705). https://doi.org/10.1016/j.cell.2007.02.005

Krainer, G., Hartmann, A., Bogatyr, V., Nielsen, J., Schlierf, M., & Otzen, D. E. (2020). SDS-induced multi-stage unfolding of a small globular protein through different denatured states revealed by single-molecule fluorescence. *Chemical Science*, *11*(34), 9141–9153. https://doi.org/10.1039/d0sc02100h

Krause, C. D., Yang, Z. H., Kim, Y. S., Lee, J. H., Cook, J. R., & Pestka, S. (2007). Protein arginine methyltransferases: Evolution and assessment of their pharmacological and therapeutic potential. *Pharmacology and Therapeutics*, *113*(1), 50–87. https://doi.org/10.1016/j.pharmthera.2006.06.007

Kullmann, M., Göpfert, U., Siewe, B., & Hengst, L. (2002). ELAV/Hu proteins inhibit p27 translation via an IRES element in the p27 5′UTR. *Genes & Development*, *16*(23), 3087. https://doi.org/10.1101/GAD.248902

Kurien, B. T., & Scofield, R. H. (2012). Common artifacts and mistakes made in electrophoresis. *Methods in Molecular Biology (Clifton, N.J.)*, *869*, 633. https://doi.org/10.1007/978-1-61779-821-4_58

Kwaśnicka-Crawford, D. A., Carson, A. R., & Scherer, S. W. (2006a). IQCJ–SCHIP1, a novel fusion transcript encoding a calmodulin-binding IQ motif protein. *Biochemical and Biophysical Research Communications*, *350*(4), 890–899. https://doi.org/10.1016/J.BBRC.2006.09.136

Kwaśnicka-Crawford, D. A., Carson, A. R., & Scherer, S. W. (2006b). IQCJ–SCHIP1, a novel fusion transcript encoding a calmodulin-binding IQ motif protein. *Biochemical and Biophysical Research Communications*, *350*(4), 890–899. https://doi.org/10.1016/J.BBRC.2006.09.136

Laemmli, U. K. (1970). Cleavage of Structural Proteins during the Assembly of the Head of Bacteriophage T4. *Nature 1970 227:5259*, *227*(5259), 680–685. https://doi.org/10.1038/227680a0

Laporte, M. H., Chatellard, C., Vauchez, V., Hemming, F. J., Deloulme, J. C., Vossier, F., Blot, B., Fraboulet, S., & Sadoul, R. (2017). Alix is required during development for normal growth of the mouse brain. *Scientific Reports 2017 7:1*, *7*(1), 1–16. https://doi.org/10.1038/srep44767

Laporte, M. H., Chi, K. Il, Caudal, L. C., Zhao, N., Schwarz, Y., Rolland, M., Martinez-Hernandez, J., Martineau, M., Chatellard, C., Denarier, E., Mercier, V., Lemaître, F., Blot,

B., Moutaux, E., Cazorla, M., Perrais, D., Lanté, F., Bruns, D., Fraboulet, S., … Sadoul, R. (2022). Alix is required for activity-dependent bulk endocytosis at brain synapses. *PLoS Biology*, *20*(6), e3001659. https://doi.org/10.1371/JOURNAL.PBIO.3001659

Larios, J., Mercier, V., Roux, A., & Gruenberg, J. (2020). ALIX- And ESCRT-III-dependent sorting of tetraspanins to exosomes. *Journal of Cell Biology*, *219*(3). https://doi.org/10.1083/JCB.201904113/133723/ALIX-AND-ESCRT-III-DEPENDENT-SORTING-OF

Lauria, F., Bernabò, P., Tebaldi, T., Groen, E. J. N., Perenthaler, E., Maniscalco, F., Rossi, A., Donzel, D., Clamer, M., Marchioretto, M., Omersa, N., Orri, J., Dalla Serra, M., Anderluh, G., Quattrone, A., Inga, A., Gillingwater, T. H., & Viero, G. (2020). SMN-primed ribosomes modulate the translation of transcripts related to spinal muscular atrophy. *Nature Cell Biology*, *22*(10), 1239–1251. https://doi.org/10.1038/s41556-020-00577-7

Lawrence, P., Conderino, J. S., & Rieder, E. (2014). Redistribution of demethylated RNA helicase A during foot-and-mouth disease virus infection: Role of Jumonji C-domain containing protein 6 in RHA demethylation. *Virology*, *452–453*, 1–11. https://doi.org/10.1016/J.VIROL.2013.12.040

le, T. H., Duy, P. Q., An, M., Talbot, J., Iyer, C. C., Wolman, M., & Beattie, C. E. (2017). HuD and the Survival Motor Neuron Protein Interact in Motoneurons and Are Essential for Motoneuron Development, Function, and mRNA Regulation. *Journal of Neuroscience*, *37*(48), 11559–11571. https://doi.org/10.1523/JNEUROSCI.1528-17.2017

Le, T. T., Pham, L. T., Butchbach, M. E. R., Zhang, H. L., Monani, U. R., Coovert, D. D., Gavrilina, T. O., Xing, L., Bassell, G. J., & Burghes, A. H. M. (2005). SMNΔ7, the major product of the centromeric survival motor neuron (SMN2) gene, extends survival in mice

with spinal muscular atrophy and associates with full-length SMN. *Human Molecular Genetics*, *14*(6), 845–857. https://doi.org/10.1093/hmg/ddi078

Lee, B. E., Suh, P. G., & Kim, J. I. (2021). O-GlcNAcylation in health and neurodegenerative diseases. *Experimental & Molecular Medicine 2021 53:11*, *53*(11), 1674–1682. https://doi.org/10.1038/s12276-021-00709-5

Lee, C. J., & Irizarry, K. (2003). Alternative splicing in the nervous system: an emerging source of diversity and regulation. *Biological Psychiatry*, *54*(8), 771–776. https://doi.org/10.1016/S0006-3223(03)00375-5

Lee, J. S., Smith, E., & Shilatifard, A. (2010). The Language of Histone Crosstalk. In *Cell* (Vol. 142, Issue 5, pp. 682–685). Elsevier B.V. https://doi.org/10.1016/j.cell.2010.08.011

Lee, J., Sayegh, J., Daniel, J., Clarke, S., & Bedford, M. T. (2005). PRMT8, a New Membrane-bound Tissue-specific Member of the Protein Arginine Methyltransferase Family. *Journal of Biological Chemistry*, *280*(38), 32890–32896. https://doi.org/10.1074/JBC.M506944200

Lee, S. K., Lee, B., Ruiz, E. C., & Pfaff, S. L. (2005). Olig2 and Ngn2 function in opposition to modulate gene expression in motor neuron progenitor cells. *Genes & Development*, *19*(2), 282. https://doi.org/10.1101/GAD.1257105

Lee, Y. H., Coonrod, S. A., Kraus, W. L., Jelinek, M. A., & Stallcup, M. R. (2005). Regulation of coactivator complex assembly and function by protein arginine methylation and demethylimination. *Proceedings of the National Academy of Sciences of the United States of America*, *102*(10), 3611–3616. https://doi.org/10.1073/PNAS.0407159102/SUPPL_FILE/07159FIG9.JPG

Lee, Y.-H., Koh, S. S., Zhang, X., Cheng, X., & Stallcup, M. R. (2002). Synergy among Nuclear Receptor Coactivators: Selective Requirement for Protein Methyltransferase and

Acetyltransferase Activities. *Molecular and Cellular Biology*, *22*(11). https://doi.org/10.1128/mcb.22.11.3621-3632.2002

Leis, O., Eguiara, A., Lopez-Arribillaga, E., Alberdi, M. J., Hernandez-Garcia, S., Elorriaga, K., Pandiella, A., Rezola, R., & Martin, A. G. (2012). Sox2 expression in breast tumours and activation in breast cancer stem cells. *Oncogene*, *31*(11), 1354–1365. https://doi.org/10.1038/ONC.2011.338

Lengerke, C., Fehm, T., Kurth, R., Neubauer, H., Scheble, V., Müller, F., Schneider, F., Petersen, K., Wallwiener, D., Kanz, L., Fend, F., Perner, S., Bareiss, P. M., & Staebler, A. (2011). Expression of the embryonic stem cell marker SOX2 in early-stage breast carcinoma. *BMC Cancer*, *11*, 42. https://doi.org/10.1186/1471-2407-11-42

Lessard, J., Wu, J. I., Ranish, J. A., Wan, M., Winslow, M. M., Staahl, B. T., Wu, H., Aebersold, R., Graef, I. A., & Crabtree, G. R. (2007). An Essential Switch in Subunit Composition of a Chromatin Remodeling Complex during Neural Development. *Neuron*, *55*(2), 201. https://doi.org/10.1016/J.NEURON.2007.06.019

Li, H., Park, S., Kilburn, B., Jelinek, M. A., Henschen-Edman, A., Aswad, D. W., Stallcup, M. R., & Laird-Offringa, I. A. (2002). Lipopolysaccharide-induced methylation of HuR, an mRNA-stabilizing protein, by CARM1. *Journal of Biological Chemistry*, *277*(47), 44623–44630. https://doi.org/10.1074/JBC.M206187200/ASSET/AD2388E4-8A6D-42CF-9453-F57BE9ADCA37/MAIN.ASSETS/FX1.JPG

Li, H., Zhang, Z., Li, H., Pan, X., & Wang, Y. (2023). New Insights into the Roles of p53 in Central Nervous System Diseases. *International Journal of Neuropsychopharmacology*, *26*(7), 465–473. https://doi.org/10.1093/IJNP/PYAD030

Li, K., Wang, B., & Hu, H. (2024). Research progress of SWI/SNF complex in breast cancer. *Epigenetics and Chromatin*, *17*(1), 1–10. https://doi.org/10.1186/S13072-024-00531-Z/FIGURES/3

Li, X., Lai, Y., Li, J., Zou, M., & Zou, C. (2017). Oxidative stress destabilizes protein arginine methyltransferase 4 via glycogen synthase kinase 3β to impede lung epithelial cell migration. *American Journal of Physiology - Cell Physiology*, *313*(3), C285–C294. https://doi.org/10.1152/AJPCELL.00073.2017/ASSET/IMAGES/LARGE/ZH00081781630008.JPEG

Lim, C. S., & Alkon, D. L. (2012a). Protein kinase C stimulates HuD-mediated mRNA stability and protein expression of neurotrophic factors and enhances dendritic maturation of hippocampal neurons in culture. *Hippocampus*, *22*(12), 2303–2319. https://doi.org/10.1002/HIPO.22048

Lim, C. S., & Alkon, D. L. (2012b). Protein kinase C stimulates HuD-mediated mRNA stability and protein expression of neurotrophic factors and enhances dendritic maturation of hippocampal neurons in culture. *Hippocampus*, *22*(12), 2303–2319. https://doi.org/10.1002/HIPO.22048

Lim, C. S., & Alkon, D. L. (2017). Inhibition of coactivator-associated arginine methyltransferase 1 modulates dendritic arborization and spine maturation of cultured hippocampal neurons. *The Journal of Biological Chemistry*, *292*(15), 6402. https://doi.org/10.1074/JBC.M117.775619

Lin, L., Yuan, Q., Gu, J., Bai, G., Cong, X., Hu, Q., Hou, J., Jin, X., Liu, X., Huang, B., Zhang, Y., & Lu, J. (2024). CARM1-mediated OGT arginine methylation promotes non-small cell

lung cancer glycolysis by stabilizing OGT. *Cell Death & Disease 2024 15:12*, *15*(12), 1–12. https://doi.org/10.1038/s41419-024-07313-1

Lionikas, A., Hernandez Cordero, A. I., Kilikevicius, A., Carroll, A. M., Bewick, G. S., Bunger, L., Ratkevicius, A., Heisler, L. K., Harboe, M., & Oxvig, C. (2023). Stanniocalcin-2 inhibits skeletal muscle growth and is upregulated in functional overload-induced hypertrophy. *Physiological Reports*, *11*(15), e15793. https://doi.org/10.14814/PHY2.15793

Litovchick, L. (2018). Preparing Whole-Cell Lysates for Immunoblotting [Article]. *Cold Spring Harbor Protocols*, *2018*(7), pdb.prot098400. https://doi.org/10.1101/pdb.prot098400

Litt, M., Qiu, Y., & Huang, S. (2009). Histone arginine methylations: their roles in chromatin dynamics and transcriptional regulation. *Bioscience Reports*, *29*(2), 131. https://doi.org/10.1042/BSR20080176

Liu, H., Galka, M., Mori, E., Liu, X., Lin, Y. fen, Wei, R., Pittock, P., Voss, C., Dhami, G., Li, X., Miyaji, M., Lajoie, G., Chen, B., & Li, S. S. C. (2013). A method for systematic mapping of protein lysine methylation identifies functions for HP1β in DNA damage response. *Molecular Cell*, *50*(5), 723–735. https://doi.org/10.1016/j.molcel.2013.04.025

Liu, K., Ma, J., Ao, J., Mu, L., Wang, Y., Qian, Y., Xue, J., & Zhang, W. (2021). The Oncogenic Role and Immune Infiltration for CARM1 Identified by Pancancer Analysis. *Journal of Oncology*, *2021*, 2986444. https://doi.org/10.1155/2021/2986444

Liu, R., Zhao, E., Yu, H., Yuan, C., Abbas, M. N., & Cui, H. (2023a). Methylation across the central dogma in health and diseases: new therapeutic strategies. In *Signal Transduction and Targeted Therapy* (Vol. 8, Issue 1). Springer Nature. https://doi.org/10.1038/s41392-023-01528-y

Liu, R., Zhao, E., Yu, H., Yuan, C., Abbas, M. N., & Cui, H. (2023b). Methylation across the central dogma in health and diseases: new therapeutic strategies. *Signal Transduction and Targeted Therapy 2023 8:1*, *8*(1), 1–46. https://doi.org/10.1038/s41392-023-01528-y

Liu, Y., Li, J., Shang, Y., Guo, Y., & Li, Z. (2019). CARM1 contributes to skeletal muscle wasting by mediating FoxO3 activity and promoting myofiber autophagy. *Experimental Cell Research*, *374*(1), 198–209. https://doi.org/10.1016/J.YEXCR.2018.11.024

Liu, Y., Wang, T., Ji, Y. J., Johnson, K., Liu, H., Johnson, K., Bailey, S., Suk, Y., Lu, Y. N., Liu, M., & Wang, J. (2018a). A C9orf72–CARM1 axis regulates lipid metabolism under glucose starvation-induced nutrient stress. *Genes and Development*, *32*(21–22), 1380–1397. https://doi.org/10.1101/GAD.315564.118/-/DC1

Liu, Y., Wang, T., Ji, Y. J., Johnson, K., Liu, H., Johnson, K., Bailey, S., Suk, Y., Lu, Y. N., Liu, M., & Wang, J. (2018b). A C9orf72–CARM1 axis regulates lipid metabolism under glucose starvation-induced nutrient stress. *Genes and Development*, *32*(21–22), 1380–1397. https://doi.org/10.1101/GAD.315564.118/-/DC1

Lu, J., Wu, H., Zhan, P., Lu, Y., Fang, Q., Luo, C., Wang, F., Wen, J., Xie, C., & Yin, Z. (2025). PSMD14-mediated deubiquitination of CARM1 facilitates the proliferation and metastasis of hepatocellular carcinoma by inducing the transcriptional activation of FERMT1. *Cell Death & Disease 2025 16:1*, *16*(1), 1–16. https://doi.org/10.1038/s41419-025-07416-3

Ma, H., Baumann, C. T., Li, H., Strahl, B. D., Rice, R., Jelinek, M. A., Aswad, D. W., Allis, C. D., Hager, G. L., & Stallcup, M. R. (2001). Hormone-dependent, CARM1-directed, arginine-specific methylation of histone H3 on a steroid-regulated promoter. *Current Biology*, *11*(24), 1981–1985. https://doi.org/10.1016/S0960-9822(01)00600-5

Ma, W. J., Cheng, S., Campbell, C., Wright, A., & Furneaux, H. (1996). Cloning and characterization of HuR, a ubiquitously expressed Elav-like protein. *Journal of Biological Chemistry*, *271*(14), 8144–8151. https://doi.org/10.1074/jbc.271.14.8144

Ma, Y. C., Song, M. R., Park, J. P., Henry Ho, H. Y., Hu, L., Kurtev, M. V., Zieg, J., Ma, Q., Pfaff, S. L., & Greenberg, M. E. (2008). Regulation of Motor Neuron Specification by Phosphorylation of Neurogenin 2. *Neuron*, *58*(1), 65–77. https://doi.org/10.1016/J.NEURON.2008.01.037

Ma, Z., Lyu, X., Qin, N., Liu, H., Zhang, M., Lai, Y., Dong, B., & Lu, P. (2023). Coactivator-associated arginine methyltransferase 1: A versatile player in cell differentiation and development [Article]. *Genes & Diseases*, *10*(6), 2383–2392. https://doi.org/10.1016/j.gendis.2022.05.021

Machida, Y., Murai, K., Miyake, K., & Lijima, S. (2001). Expression of Chromatin Remodeling Factors during Neural Differentiation [Article]. *Journal of Biochemistry (Tokyo)*, *129*(1), 43–49. https://doi.org/10.1093/oxfordjournals.jbchem.a002834

Maher, J., Stagg, N., Cain, G., Andaya, R., Katavolos, P., Gallardo-Chang, F., Pham, A., Ye, X., Januario, T., Alcantar, T., Caothien, R., Roose-Girma, M., Zhang, D., Li, R., Chen, S., & Yauch, R. L. (2023). Smarca2 genetic ablation is phenotypically benign in a safety assessment of tamoxifen-inducible conditional knockout rats. *Toxicology and Applied Pharmacology*, *475*, 116627. https://doi.org/10.1016/J.TAAP.2023.116627

Mahul-Mellier, A. L., Hemming, F. J., Blot, B., Fraboulet, S., & Sadoul, R. (2006). Alix, Making a Link between Apoptosis-Linked Gene-2, the Endosomal Sorting Complexes Required for Transport, and Neuronal Death In Vivo. *The Journal of Neuroscience*, *26*(2), 542. https://doi.org/10.1523/JNEUROSCI.3069-05.2006

Małecki, J. M., Davydova, E., & Falnes, P. (2022). Protein methylation in mitochondria. In *Journal of Biological Chemistry* (Vol. 298, Issue 4). American Society for Biochemistry and Molecular Biology Inc. https://doi.org/10.1016/j.jbc.2022.101791

Mammarella, N., Fairfield, B., Di Domenico, A., D'Onofrio, L., Stuppia, L., & Gatta, V. (2016). The modulating role of ADRA2B in emotional working memory: Attending the negative but remembering the positive. *Neurobiology of Learning and Memory*, *130*, 129–134. https://doi.org/10.1016/J.NLM.2016.02.009

Maniaci, M., Boffo, F. L., Massignani, E., & Bonaldi, T. (2021). Systematic Analysis of the Impact of R-Methylation on RBPs-RNA Interactions: A Proteomic Approach. *Frontiers in Molecular Biosciences*, *8*, 688973. https://doi.org/10.3389/FMOLB.2021.688973/FULL

Mansfield, K. D., & Keene, J. D. (2011). Neuron-specific ELAV/Hu proteins suppress HuR mRNA during neuronal differentiation by alternative polyadenylation. *Nucleic Acids Research*, *40*(6), 2734. https://doi.org/10.1093/NAR/GKR1114

Maor-Nof, M., Shipony, Z., Lopez-Gonzalez, R., Nakayama, L., Zhang, Y. J., Couthouis, J., Blum, J. A., Castruita, P. A., Linares, G. R., Ruan, K., Ramaswami, G., Simon, D. J., Nof, A., Santana, M., Han, K., Sinnott-Armstrong, N., Bassik, M. C., Geschwind, D. H., Tessier-Lavigne, M., … Gitler, A. D. (2021). p53 is a central regulator driving neurodegeneration caused by C9orf72 poly(PR). *Cell*, *184*(3), 689-708.e20. https://doi.org/10.1016/J.CELL.2020.12.025

Maron, M. I., Lehman, S. M., Gayatri, S., DeAngelo, J. D., Hegde, S., Lorton, B. M., Sun, Y., Bai, D. L., Sidoli, S., Gupta, V., Marunde, M. R., Bone, J. R., Sun, Z. W., Bedford, M. T., Shabanowitz, J., Chen, H., Hunt, D. F., & Shechter, D. (2021). Independent transcriptomic

and proteomic regulation by type I and II protein arginine methyltransferases. *IScience*, *24*(9), 102971. https://doi.org/10.1016/J.ISCI.2021.102971

Martens, J. A., & Winston, F. (2003). Recent advances in understanding chromatin remodeling by Swi/Snf complexes. *Current Opinion in Genetics & Development*, *13*(2), 136–142. https://doi.org/10.1016/S0959-437X(03)00022-4

Martin, E. W., & Holehouse, A. S. (2020). Intrinsically disordered protein regions and phase separation: sequence determinants of assembly or lack thereof [Article]. *Emerging Topics in Life Sciences*, *4*(3), 307–329. https://doi.org/10.1042/etls20190164

Martin, P. M., Carnaud, M., Del Caño, G. G., Irondelle, M., Irinopoulou, T., Girault, J. A., Dargent, B., & Goutebroze, L. (2008a). Schwannomin-Interacting Protein-1 Isoform IQCJ-SCHIP-1 Is a Late Component of Nodes of Ranvier and Axon Initial Segments. *The Journal of Neuroscience*, *28*(24), 6111. https://doi.org/10.1523/JNEUROSCI.1044-08.2008

Martin, P. M., Carnaud, M., Del Caño, G. G., Irondelle, M., Irinopoulou, T., Girault, J. A., Dargent, B., & Goutebroze, L. (2008b). Schwannomin-Interacting Protein-1 Isoform IQCJ-SCHIP-1 Is a Late Component of Nodes of Ranvier and Axon Initial Segments. *The Journal of Neuroscience*, *28*(24), 6111. https://doi.org/10.1523/JNEUROSCI.1044-08.2008

Martin, P. M., Cifuentes-Diaz, C., Devaux, J., Garcia, M., Bureau, J., Thomasseau, S., Klingler, E., Girault, J. A., & Goutebroze, L. (2016a). Schwannomin-interacting Protein 1 Isoform IQCJ-SCHIP1 Is a Multipartner Ankyrin- and Spectrin-binding Protein Involved in the Organization of Nodes of Ranvier. *The Journal of Biological Chemistry*, *292*(6), 2441. https://doi.org/10.1074/JBC.M116.758029

Martin, P. M., Cifuentes-Diaz, C., Devaux, J., Garcia, M., Bureau, J., Thomasseau, S., Klingler, E., Girault, J. A., & Goutebroze, L. (2016b). Schwannomin-interacting Protein 1 Isoform

IQCJ-SCHIP1 Is a Multipartner Ankyrin- and Spectrin-binding Protein Involved in the Organization of Nodes of Ranvier. *The Journal of Biological Chemistry*, *292*(6), 2441. https://doi.org/10.1074/JBC.M116.758029

Martin, P. M., Cifuentes-Diaz, C., Devaux, J., Garcia, M., Bureau, J., Thomasseau, S., Klingler, E., Girault, J. A., & Goutebroze, L. (2016c). Schwannomin-interacting Protein 1 Isoform IQCJ-SCHIP1 Is a Multipartner Ankyrin- and Spectrin-binding Protein Involved in the Organization of Nodes of Ranvier. *The Journal of Biological Chemistry*, *292*(6), 2441. https://doi.org/10.1074/JBC.M116.758029

Martin, P. M., Cifuentes-Diaz, C., Devaux, J., Garcia, M., Bureau, J., Thomasseau, S., Klingler, E., Girault, J. A., & Goutebroze, L. (2017). Schwannomin-interacting protein 1 isoform IQCJ-SCHIP1 is a multipartner ankyrin- and spectrin-binding protein involved in the organization of nodes of Ranvier. *Journal of Biological Chemistry*, *292*(6), 2441–2456. https://doi.org/10.1074/jbc.M116.758029

McLeod, V. M., Chiam, M. D. F., Lau, C. L., Rupasinghe, T. W., Boon, W. C., & Turner, B. J. (2020). Dysregulation of Steroid Hormone Receptors in Motor Neurons and Glia Associates with Disease Progression in ALS Mice. *Endocrinology*, *161*(9). https://doi.org/10.1210/ENDOCR/BQAA113

Mentch, S. J., & Locasale, J. W. (2016). One-carbon metabolism and epigenetics: understanding the specificity [Article]. *Annals of the New York Academy of Sciences*, *1363*(1), 91–98. https://doi.org/10.1111/nyas.12956

Mi, R., Chen, W., & Höke, A. (2007). Pleiotrophin is a neurotrophic factor for spinal motor neurons. *Proceedings of the National Academy of Sciences of the United States of America*, *104*(11). https://doi.org/10.1073/pnas.0603243104

Miao, B., Ge, L., He, C., Wang, X., Wu, J., Li, X., Chen, K., Wan, J., Xing, S., Ren, L., Shi, Z., Liu, S., Hu, Y., Chen, J., Yu, Y., Feng, L., Flores, N. M., Liang, Z., Xu, X., … Lan, F. (2024). SMYD5 is a ribosomal methyltransferase that catalyzes RPL40 lysine methylation to enhance translation output and promote hepatocellular carcinoma. *Cell Research 2024*, 1–13. https://doi.org/10.1038/s41422-024-01013-3

Miller, J. L., & Grant, P. A. (2013). The role of DNA methylation and histone modifications in transcriptional regulation in humans. *Subcellular Biochemistry*, *61*, 289–317. https://doi.org/10.1007/978-94-007-4525-4_13

Missotten, M., Nichols, A., Rieger, K., & Sadoul, R. (1999). Alix, a novel mouse protein undergoing calcium-dependent interaction with the apoptosis-linked-gene 2 (ALG-2) protein. *Cell Death & Differentiation 1999 6:2*, *6*(2), 124–129. https://doi.org/10.1038/sj.cdd.4400456

Mitsuzawa, S., Suzuki, N., Akiyama, T., Ishikawa, M., Sone, T., Kawada, J., Funayama, R., Shirota, M., Mitsuhashi, H., Morimoto, S., Ikeda, K., Shijo, T., Ohno, A., Nakamura, N., Ono, H., Ono, R., Osana, S., Nakagawa, T., Nishiyama, A., … Aoki, M. (2021). Reduced PHOX2B stability causes axonal growth impairment in motor neurons with TARDBP mutations. *Stem Cell Reports*, *16*(6), 1527. https://doi.org/10.1016/J.STEMCR.2021.04.021

Mobarak, C. D., Anderson, K. D., Morin, M., Beckel-Mitchener, A., Rogers, S. L., Furneaux, H., King, P., & Perrone-Bizzozero, N. I. (2000). The RNA-binding Protein HuD Is Required for GAP-43 mRNA Stability, GAP-43 Gene Expression, and PKC-dependent Neurite Outgrowth in PC12 Cells. *Molecular Biology of the Cell*, *11*(9), 3191. https://doi.org/10.1091/MBC.11.9.3191

Molliex, A., Temirov, J., Lee, J., Kim, H. J., Mittag, T., Paul, J., & Correspondence, T. (2015). Phase Separation by Low Complexity Domains Promotes Stress Granule Assembly and Drives Pathological Fibrillization. *Cell*, *163*, 123–133. https://doi.org/10.1016/j.cell.2015.09.015

Morettin, A., Bourassa, J., Mahadevan, K., Trinkle-Mulcahy, L., & Cote, J. (2019). Using affinity purification coupled with stable isotope labeling by amino acids in cell culture quantitative mass spectrometry to identify novel interactors/substrates of protein arginine methyltransferases. *Methods*. https://doi.org/10.1016/j.ymeth.2019.11.015

Muhammad, K., Reddy-Alla, S., Driller, J. H., Schreiner, D., Rey, U., Böhme, M. A., Hollmann, C., Ramesh, N., Depner, H., Lützkendorf, J., Matkovic, T., Götz, T., Bergeron, D. D., Schmoranzer, J., Goettfert, F., Holt, M., Wahl, M. C., Hell, S. W., Scheiffele, P., … Sigrist, S. J. (2015). Presynaptic spinophilin tunes neurexin signalling to control active zone architecture and function. *Nature Communications 2015 6:1*, *6*(1), 1–15. https://doi.org/10.1038/ncomms9362

Murn, J., & Shi, Y. (2017a). The winding path of protein methylation research: milestones and new frontiers [Article]. *Nature Reviews. Molecular Cell Biology*, *18*(8), 517–527. https://doi.org/10.1038/nrm.2017.35

Murn, J., & Shi, Y. (2017b). The winding path of protein methylation research: Milestones and new frontiers. In *Nature Reviews Molecular Cell Biology* (Vol. 18, Issue 8, pp. 517–527). Nature Publishing Group. https://doi.org/10.1038/nrm.2017.35

Murray, L. M., Beauvais, A., Bhanot, K., & Kothary, R. (2013). Defects in neuromuscular junction remodelling in the Smn2B/- mouse model of spinal muscular atrophy. *Neurobiology of Disease*, *49*(1), 57–67. https://doi.org/10.1016/j.nbd.2012.08.019

Najbauers, J., Johnson, B. A., Young, A. L., & Aswadg, D. W. (1993). *THE JOURNAL OF BIOLOGICAL CHEMISTRY Peptides with Sequences Similar to Glycine, Arginine-rich Motifs in Proteins Interacting with RNA Are Efficiently Recognized by Methyltransferase(s) Modifying Arginine in Numerous Proteins*. 268*(14), 10501–10509. https://doi.org/10.1016/S0021-9258(18)82227-X

Nakao, A., Yoshihama, M., & Kenmochi, N. (2004). RPG: the Ribosomal Protein Gene database. *Nucleic Acids Research*, *32*(suppl_1), D168–D170. https://doi.org/10.1093/NAR/GKH004

Nakayama, K., Szewczyk, M. M., Sena, C. dela, Wu, H., Dong, A., Zeng, H., Li, F., de Freitas, R. F., Eram, M. S., Schapira, M., Baba, Y., Kunitomo, M., Cary, D. R., Tawada, M., Ohashi, A., Imaeda, Y., Saikatendu, K. S., Grimshaw, C. E., Vedadi, M., … Brown, P. J. (2018). TP-064, a potent and selective small molecule inhibitor of PRMT4 for multiple myeloma. *Oncotarget*, *9*(26), 18480–18493. https://doi.org/10.18632/oncotarget.24883

Narayanan, R., Pirouz, M., Stoykova, A., & Staiger, J. F. (2015). Loss of BAF (mSWI/SNF) Complexes Causes Global Transcriptional and Chromatin State Changes in Forebrain Development. *Cell Reports*, *13*. https://doi.org/10.1016/j.celrep.2015.10.046

Nelson, A. D., & Jenkins, P. M. (2017). Axonal Membranes and Their Domains: Assembly and Function of the Axon Initial Segment and Node of Ranvier. *Frontiers in Cellular Neuroscience*, *11*. https://doi.org/10.3389/FNCEL.2017.00136

Ng, Y. K., Tajoddin, N. N., Scrosati, P. M., & Konermann, L. (2021). Mechanism of Thermal Protein Aggregation: Experiments and Molecular Dynamics Simulations on the High-Temperature Behavior of Myoglobin. *Journal of Physical Chemistry B*, *125*(48), 13099–13110. https://doi.org/10.1021/acs.jpcb.1c07210

Nguyen, L., He, Q., & Meiri, K. F. (2009). Regulation of GAP-43 at serine 41 acts as a switch to modulate both intrinsic and extrinsic behaviors of growing neurons, via altered membrane distribution. *Molecular and Cellular Neuroscience*, *41*(1), 62–73. https://doi.org/10.1016/J.MCN.2009.01.011

Nicholson, T. B., Chen, T., & Richard, S. (2009). The physiological and pathophysiological role of PRMT1-mediated protein arginine methylation [Article]. *Pharmacological Research*, *60*(6), 466–474. https://doi.org/10.1016/j.phrs.2009.07.006

Niu, L., Lu, F., Pei, Y., Liu, C., & Cao, X. (2007). Regulation of flowering time by the protein arginine methyltransferase AtPRMT10. *EMBO Reports*, *8*(12), 1190–1195. https://doi.org/10.1038/sj.embor.7401111

Nott, T. J., Petsalaki, E., Farber, P., Jervis, D., Fussner, E., Plochowietz, A., Craggs, T. D., Bazett-Jones, D. P., Pawson, T., Forman-Kay, J. D., & Baldwin, A. J. (2015). Phase Transition of a Disordered Nuage Protein Generates Environmentally Responsive Membraneless Organelles. *Molecular Cell*, *57*(5), 936. https://doi.org/10.1016/J.MOLCEL.2015.01.013

O'Brien, K. B., Alberich-Jordà, M., Yadav, N., Kocher, O., DiRuscio, A., Ebralidze, A., Levantini, E., Sng, N. J. L., Bhasin, M., Caron, T., Kim, D., Steidl, U., Huang, G., Halmos, B., Rodig, S. J., Bedford, M. T., Tenen, D. G., & Kobayashi, S. (2010). CARM1 is required for proper control of proliferation and differentiation of pulmonary epithelial cells. *Development*, *137*(13), 2147–2156. https://doi.org/10.1242/dev.037150

Odorizzi, G. (2006). The multiple personalities of Alix. *Journal of Cell Science*, *119*(Pt 15), 3025–3032. https://doi.org/10.1242/JCS.03072

Okano, H. J., & Darnell, R. B. (1997). A Hierarchy of Hu RNA Binding Proteins in Developing and Adult Neurons. *The Journal of Neuroscience*, *17*(9), 3024. https://doi.org/10.1523/JNEUROSCI.17-09-03024.1997

Orti, F., Navarro, A. M., Rabinovich, A., Wodak, S. J., & Marino-Buslje, C. (2021). Insight into membraneless organelles and their associated proteins: Drivers, Clients and Regulators. *Computational and Structural Biotechnology Journal*, *19*, 3964. https://doi.org/10.1016/J.CSBJ.2021.06.042

Ou, C. Y., LaBonte, M. J., Manegold, P. C., So, A. Y. L., Ianculescu, I., Gerke, D. S., Yamamoto, K. R., Ladner, R. D., Kahn, M., Kim, J. H., & Stallcup, M. R. (2011a). A coactivator role of CARM1 in the dysregulation of β-catenin activity in colorectal cancer cell growth and gene expression. *Molecular Cancer Research*, *9*(5), 660–670. https://doi.org/10.1158/1541-7786.MCR-10-0223/79366/AM/A-COACTIVATOR-ROLE-OF-CARM1-IN-THE-DYSREGULATION

Ou, C. Y., LaBonte, M. J., Manegold, P. C., So, A. Y. L., Ianculescu, I., Gerke, D. S., Yamamoto, K. R., Ladner, R. D., Kahn, M., Kim, J. H., & Stallcup, M. R. (2011b). A coactivator role of CARM1 in the dysregulation of β-catenin activity in colorectal cancer cell growth and gene expression. *Molecular Cancer Research : MCR*, *9*(5), 660. https://doi.org/10.1158/1541-7786.MCR-10-0223

Ouyang, Y., Wu, Q., Li, J., Sun, S., & Sun, S. (2020). S-adenosylmethionine: A metabolite critical to the regulation of autophagy. In *Cell Proliferation* (Vol. 53, Issue 11). Blackwell Publishing Ltd. https://doi.org/10.1111/cpr.12891

Paik, W. K., Paik, D. C., & Kim, S. (2007). Historical review: the field of protein methylation. In *Trends in Biochemical Sciences* (Vol. 32, Issue 3, pp. 146–152). https://doi.org/10.1016/j.tibs.2007.01.006

Palikhe, N. S., Sin, H. J., Kim, S. H., Sin, H. J., Hwang, E. K., Ye, Y. M., & Park, H. S. (2012). Genetic variability of prostaglandin E2 receptor subtype EP4 gene in aspirin-intolerant chronic urticaria. *Journal of Human Genetics 2012 57:8*, *57*(8), 494–499. https://doi.org/10.1038/jhg.2012.55

Panamarova, M., Cox, A., Wicher, K. B., Butler, R., Bulgakova, N., Jeon, S., Rosen, B., Seong, R. H., Skarnes, W., Crabtree, G., & Zernicka-Goetz, M. (2016). The BAF chromatin remodelling complex is an epigenetic regulator of lineage specification in the early mouse embryo. *Development (Cambridge)*, *143*(8), 1271–1283. https://doi.org/10.1242/DEV.131961/-/DC1

Pang, L., Tian, H., Chang, N., Yi, J., Xue, L., Jiang, B., Gorospe, M., Zhang, X., & Wang, W. (2013). Loss of CARM1 is linked to reduced HuR function in replicative senescence. *BMC Molecular Biology*, *14*, 1–11. https://doi.org/10.1186/1471-2199-14-15

Papageorgiou, L., Christou, E., Louka, E., Papakonstantinou, E., Diakou, I., Pierouli, K., Dragoumani, K., Bacopoulou, F., Chrousos, G. P., Eliopoulos, E., & Vlachakis, D. (2022). ADRA2B and HTR1A: An updated study of the biogenic amine receptors reveals novel conserved motifs which play key role in Mental Disorders. *BioRxiv*, 2022.09.16.508280. https://doi.org/10.1101/2022.09.16.508280

Papsdorf, K., & Brunet, A. (2019). Linking Lipid Metabolism to Chromatin Regulation in Aging. In *Trends in Cell Biology* (Vol. 29, Issue 2, pp. 97–116). Elsevier Ltd. https://doi.org/10.1016/j.tcb.2018.09.004

Park, S., Myszka, D. G., Yu, M., Littler, S. J., & Laird-Offringa, I. A. (2000). HuD RNA Recognition Motifs Play Distinct Roles in the Formation of a Stable Complex with AU-Rich RNA. *Molecular and Cellular Biology*, *20*(13), 4765. https://doi.org/10.1128/MCB.20.13.4765-4772.2000

Park-Lee, S., Kim, S., & Laird-Offringa, I. A. (2003). Characterization of the interaction between neuronal RNA-binding protein HuD and AU-rich RNA. *Journal of Biological Chemistry*, *278*(41), 39801–39808. https://doi.org/10.1074/JBC.M307105200/ASSET/003AC0B2-1284-4706-A399-711414628B8A/MAIN.ASSETS/GR8.JPG

Pattyn, A., Hirsch, M. R., Goridis, C., & Brunet, J. F. (2000). Control of hindbrain motor neuron differentiation by the homeobox gene Phox2b. *Development*, *127*(7), 1349–1358. https://doi.org/10.1242/DEV.127.7.1349

Pawlak, M. R., Scherer, C. A., Chen, J., Roshon, M. J., & Ruley, H. E. (2000a). Arginine N-Methyltransferase 1 Is Required for Early Postimplantation Mouse Development, but Cells Deficient in the Enzyme Are Viable. *Molecular and Cellular Biology*, *20*(13), 4859. https://doi.org/10.1128/MCB.20.13.4859-4869.2000

Pawlak, M. R., Scherer, C. A., Chen, J., Roshon, M. J., & Ruley, H. E. (2000b). Arginine N-Methyltransferase 1 Is Required for Early Postimplantation Mouse Development, but Cells Deficient in the Enzyme Are Viable. *Molecular and Cellular Biology*, *20*(13), 4859. https://doi.org/10.1128/MCB.20.13.4859-4869.2000

Peng, B. L., Ran, T., Chen, X., Ding, J. C., Wang, Z. R., Li, W. J., & Liu, W. (2024). A CARM1 Inhibitor Potently Suppresses Breast Cancer Both In Vitro and In Vivo. *Journal of Medicinal Chemistry*, *67*(10), 7921–7934. https://doi.org/10.1021/acs.jmedchem.3c02315

Perrone-Bizzozero, N., & Bird, C. W. (2013). Role of HuD in nervous system function and pathology. *Frontiers in Bioscience - Scholar*, *5 S*(2), 554–563. https://doi.org/10.2741/S389/PDF

Peuget, S., Zhou, X., & Selivanova, G. (2024). Translating p53-based therapies for cancer into the clinic. *Nature Reviews Cancer 2024 24:3*, *24*(3), 192–215. https://doi.org/10.1038/s41568-023-00658-3

Pfaff, S. L., Mendelsohn, M., Stewart, C. L., Edlund, T., & Jessell, T. M. (1996). Requirement for LIM homeobox gene Isl1 in motor neuron generation reveals a motor neuron-dependent step in interneuron differentiation. *Cell*, *84*(2), 309–320. https://doi.org/10.1016/S0092-8674(00)80985-X

Poulard, C., Rambaud, J., Hussein, N., Corbo, L., & Le Romancer, M. (2014). JMJD6 Regulates ERα Methylation on Arginine. *PLoS ONE*, *9*(2), 87982. https://doi.org/10.1371/JOURNAL.PONE.0087982

Prakash, K., & Fournier, D. (2017). Histone Code and Higher-Order Chromatin Folding: A Hypothesis. *Genomics and Computational Biology*, *3*(2), 41. https://doi.org/10.18547/gcb.2017.vol3.iss2.e41

Pretegiani, E., Mari, F., Renieri, A., Penco, S., & Dotti, M. T. (2016). Nicolaides–Baraitser syndrome: defining a phenotype. *Journal of Neurology*, *263*(8), 1659–1660. https://doi.org/10.1007/S00415-016-8194-0/METRICS

Pringle, J. R. (1975). Methods for avoiding proteolytic artefacts in studies of enzymes and other proteins from yeasts [Article]. *Methods in Cell Biology*, *12*, 149–184.

Pukala, T. L. (2023). Mass spectrometric insights into protein aggregation. *Essays in Biochemistry*, *67*(2), 243. https://doi.org/10.1042/EBC20220103

Qamar, S., Wang, G. Z., Randle, S. J., Ruggeri, F. S., Varela, J. A., Lin, J. Q., Phillips, E. C., Miyashita, A., Williams, D., Ströhl, F., Meadows, W., Ferry, R., Dardov, V. J., Tartaglia, G. G., Farrer, L. A., Kaminski Schierle, G. S., Kaminski, C. F., Holt, C. E., Fraser, P. E., … St George-Hyslop, P. (2018). FUS Phase Separation Is Modulated by a Molecular Chaperone and Methylation of Arginine Cation-π Interactions. *Cell*, *173*(3), 720. https://doi.org/10.1016/J.CELL.2018.03.056

Qie, S., & Sang, N. (2022). Stanniocalcin 2 (STC2): a universal tumour biomarker and a potential therapeutical target. *Journal of Experimental & Clinical Cancer Research 2022 41:1*, *41*(1), 1–19. https://doi.org/10.1186/S13046-022-02370-W

Qie, S., Xiong, H., Liu, Y., Yan, C., Wang, Y., Tian, L., Wang, C., & Sang, N. (2024). Stanniocalcin 2 governs cancer cell adaptation to nutrient insufficiency through alleviation of oxidative stress. *Cell Death & Disease 2024 15:8*, *15*(8), 1–15. https://doi.org/10.1038/s41419-024-06961-7

Qiu, Y., Wang, H., Liao, P., Xu, B., Hu, R., Yang, Y., & Li, Y. (2022). Systematic pan-cancer landscape identifies CARM1 as a potential prognostic and immunological biomarker. *BMC Genomic Data*, *23*(1). https://doi.org/10.1186/s12863-021-01022-w

Qu, L., Yin, T., Zhao, Y., Lv, W., Liu, Z., Chen, C., Liu, K., Shan, S., Zhou, R., Li, X., & Dong, H. (2023). Histone demethylases in the regulation of immunity and inflammation. *Cell Death Discovery 2023 9:1*, *9*(1), 1–15. https://doi.org/10.1038/s41420-023-01489-9

Quoc, H., Pham, H., Tao, X., & Yang, Y. (2023). Protein arginine methylation in transcription and epigenetic regulation. *Frontiers in Epigenetics and Epigenomics*, *1*, 1245832. https://doi.org/10.3389/FREAE.2023.1245832

Ramazi, S., & Zahiri, J. (2021). Post-translational modifications in proteins: Resources, tools and prediction methods. In *Database* (Vol. 2021). Oxford University Press. https://doi.org/10.1093/database/baab012

Rasch, B., Spalek, K., Buholzer, S., Luechinger, R., Boesiger, P., Papassotiropoulos, A., & De Quervain, D. J. F. (2009). A genetic variation of the noradrenergic system is related to differential amygdala activation during encoding of emotional memories. *Proceedings of the National Academy of Sciences of the United States of America*, *106*(45), 19191–19196. https://doi.org/10.1073/PNAS.0907425106/SUPPL_FILE/0907425106SI.PDF

Ratti, A., Fallini, C., Colombrita, C., Pascale, A., Laforenza, U., Quattrone, A., & Silani, V. (2008). Post-transcriptional regulation of neuro-oncological ventral antigen 1 by the neuronal RNA-binding proteins ELAV. *Journal of Biological Chemistry*, *283*(12), 7531–7541. https://doi.org/10.1074/JBC.M706082200/ATTACHMENT/ED459CD8-DB6A-4DB5-BB46-D1D47CEFA0B4/MMC1.PDF

Raudvere, U., Kolberg, L., Kuzmin, I., Arak, T., Adler, P., Peterson, H., & Vilo, J. (2019). g:Profiler: a web server for functional enrichment analysis and conversions of gene lists (2019 update). *Nucleic Acids Research*, *47*(W1), W191–W198. https://doi.org/10.1093/NAR/GKZ369

Ravel-Chapuis, A., Haghandish, A., Daneshvar, N., Jasmin, B. J., & Côte, J. (2022). A novel CARM1-HuR axis involved in muscle differentiation and plasticity misregulated in spinal muscular atrophy. *Human Molecular Genetics*, *31*(9), 1453–1470. https://doi.org/10.1093/hmg/ddab333

Rho, J., Choi, S., Seong, Y. R., Cho, W. K., Kim, S. H., & Im, D. S. (2001). PRMT5, Which Forms Distinct Homo-oligomers, Is a Member of the Protein-arginine Methyltransferase

Family. *Journal of Biological Chemistry*, *276*(14), 11393–11401. https://doi.org/10.1074/JBC.M008660200

Rudolph, L. M., & Sengelaub, D. R. (2012). CRITICAL PERIOD FOR ESTROGEN-DEPENDENT MOTONEURON DENDRITE GROWTH IS COINCIDENT WITH ERα EXPRESSION IN TARGET MUSCULATURE. *Developmental Neurobiology*, *73*(1), 72. https://doi.org/10.1002/DNEU.22040

Ryu, S., Jung, M., Kim, C., Kang, H., Han, S., Cha, S., Jeong, S. M., & Lee, E. K. (2022a). Loss of RNA binding protein HuD facilitates the production of the senescence-associated secretory phenotype. *Cell Death & Disease 2022 13:4*, *13*(4), 1–10. https://doi.org/10.1038/s41419-022-04792-y

Ryu, S., Jung, M., Kim, C., Kang, H., Han, S., Cha, S., Jeong, S. M., & Lee, E. K. (2022b). Loss of RNA binding protein HuD facilitates the production of the senescence-associated secretory phenotype. *Cell Death & Disease 2022 13:4*, *13*(4), 1–10. https://doi.org/10.1038/s41419-022-04792-y

Saber, J., & Rudnicki, M. A. (2022a). Carm1 and the Epigenetic Control of Stem Cell Function. *Stem Cells Translational Medicine*, *11*(11), 1143–1150. https://doi.org/10.1093/stcltm/szac068

Saber, J., & Rudnicki, M. A. (2022b). Carm1 and the Epigenetic Control of Stem Cell Function. *Stem Cells Translational Medicine*, *11*(11), 1143. https://doi.org/10.1093/STCLTM/SZAC068

Sabra, M., Texier, P., El Maalouf, J., & Lomonte, P. (2013). The Tudor protein survival motor neuron (SMN) is a chromatin-binding protein that interacts with methylated lysine 79 of histone H3. *Journal of Cell Science*, *126*(16), 3664–3677.

https://doi.org/10.1242/JCS.126003/263468/AM/THE-TUDOR-PROTEIN-SURVIVAL-MOTOR-NEURON-SMN-IS-A

Sagne, C., Isambert, M.-F., Henry, J.-P., & Gasnier, B. (1996). SDS-resistant aggregation of membrane proteins : application to the purification of the vesicular monoamine transporter. In *Biochem. J* (Vol. 316).

Sahoo, P. K., Smith, D. S., Perrone-Bizzozero, N., & Twiss, J. L. (2018). Axonal mRNA transport and translation at a glance. *Journal of Cell Science*, *131*(8), jcs196808. https://doi.org/10.1242/JCS.196808

Saito, K., Fujiwara, T., Katahira, J., Inoue, K., & Sakamoto, H. (2004). TAP/NXF1, the primary mRNA export receptor, specifically interacts with a neuronal RNA-binding protein HuD. *Biochemical and Biophysical Research Communications*, *321*(2), 291–297. https://doi.org/10.1016/J.BBRC.2004.06.140

Sakabe, K., & Hart, G. W. (2010). O-GlcNAc Transferase Regulates Mitotic Chromatin Dynamics. *The Journal of Biological Chemistry*, *285*(45), 34460. https://doi.org/10.1074/JBC.M110.158170

Salazar-Grueso, E. F., Kim, S., & Kim, H. (1991). Embryonic mouse spinal cord motor neuron hybrid cells. In *NeuroReport* (Vol. 2, pp. 505–508).

Sanchez, G., Bondy-Chorney, E., Laframboise, J., Paris, G., Didillon, A., Jasmin, B. J., & Côté, J. (2015). A novel role for CARM1 in promoting nonsense-mediated mRNA decay: Potential implications for spinal muscular atrophy. *Nucleic Acids Research*, *44*(6), 2661–2676. https://doi.org/10.1093/nar/gkv1334

Sanchez, G., Dury, A. Y., Murray, L. M., Biondi, O., Tadesse, H., El fatimy, R., Kothary, R., Charbonnier, F., Khandjian, E. W., & Côté, J. (2013). A novel function for the survival

motoneuron protein as a translational regulator. *Human Molecular Genetics*, *22*(4), 668–684. https://doi.org/10.1093/hmg/dds474

Santos, M., Hwang, J. W., & Bedford, M. T. (2023). CARM1 arginine methyltransferase as a therapeutic target for cancer. *The Journal of Biological Chemistry*, *299*(9), 105124. https://doi.org/10.1016/J.JBC.2023.105124

Scardigli, R., Bäumer, N., Gruss, P., Guillemot, F., & Le Roux, I. (2003). Direct and concentration-dependent regulation of the proneural gene Neurogenin2 by Pax6. *Development*, *130*(14), 3269–3281. https://doi.org/10.1242/DEV.00539

Schaefer, T., & Lengerke, C. (2019). SOX2 protein biochemistry in stemness, reprogramming, and cancer: the PI3K/AKT/SOX2 axis and beyond. *Oncogene 2019 39:2*, *39*(2), 278–292. https://doi.org/10.1038/s41388-019-0997-x

Schindelin, J., Arganda-Carreras, I., Frise, E., Kaynig, V., Longair, M., Pietzsch, T., Preibisch, S., Rueden, C., Saalfeld, S., Schmid, B., Tinevez, J. Y., White, D. J., Hartenstein, V., Eliceiri, K., Tomancak, P., & Cardona, A. (2012). Fiji: an open-source platform for biological-image analysis. *Nature Methods 2012 9:7*, *9*(7), 676–682. https://doi.org/10.1038/nmeth.2019

Sena, R. M., Twiss, J. L., Gardiner, A. S., Dell'orco, M., Linsenbardt, D. N., & Perrone-Bizzozero, N. I. (2021). The RNA-binding protein HuD regulates alternative splicing and alternative polyadenylation in the mouse neocortex. *Molecules*, *26*(10). https://doi.org/10.3390/molecules26102836

Shafey, D., MacKenzie, A. E., & Kothary, R. (2008). Neurodevelopmental abnormalities in neurosphere-derived neural stem cells from SMN-depleted mice. *Journal of Neuroscience Research*, *86*(13). https://doi.org/10.1002/jnr.21743

Sharma, G., Paganin, M., Lauria, F., Perenthaler, E., & Viero, G. (2024). The SMN-ribosome interplay: a new opportunity for Spinal Muscular Atrophy therapies. *Biochemical Society Transactions*, *52*(1), 465. https://doi.org/10.1042/BST20231116

Shen, H., Zhao, X., Chen, J., Qu, W., Huang, X., Wang, M., Shao, Z., Shu, Q., & Li, X. (2021). O-GlcNAc transferase Ogt regulates embryonic neuronal development through modulating Wnt/β-catenin signaling. *Human Molecular Genetics*, *31*(1), 57–68. https://doi.org/10.1093/HMG/DDAB223

Shishkova, E., Zeng, H., Liu, F., Kwiecien, N. W., Hebert, A. S., Coon, J. J., & Xu, W. (2017). Global mapping of CARM1 substrates defines enzyme specificity and substrate recognition. *Nature Communications*, *8*. https://doi.org/10.1038/ncomms15571

Siarheyeva, A., Senisterra, G., Allali-Hassani, A., Dong, A., Dobrovetsky, E., Wasney, G. A., Chau, I., Marcellus, R., Hajian, T., Liu, F., Korboukh, I., Smil, D., Bolshan, Y., Min, J., Wu, H., Zeng, H., Loppnau, P., Poda, G., Griffin, C., … Vedadi, M. (2012). An Allosteric Inhibitor of Protein Arginine Methyltransferase 3. *Structure*, *20*(8), 1425–1435. https://doi.org/10.1016/J.STR.2012.06.001

Sikorsky, T., Hobor, F., Krizanova, E., Pasulka, J., Kubicek, K., & Stefl, R. (2012). Recognition of asymmetrically dimethylated arginine by TDRD3. *Nucleic Acids Research*, *40*(22), 11748. https://doi.org/10.1093/NAR/GKS929

Simon, C. M., Dai, Y., Van Alstyne, M., Koutsioumpa, C., Pagiazitis, J. G., Chalif, J. I., Wang, X., Rabinowitz, J. E., Henderson, C. E., Pellizzoni, L., & Mentis, G. Z. (2017). Converging mechanisms of p53 activation drive motor neuron degeneration in spinal muscular atrophy. *Cell Reports*, *21*(13), 3767. https://doi.org/10.1016/J.CELREP.2017.12.003

Smith, C. L., Afroz, R., Bassell, G. J., Furneaux, H. M., Perrone-Bizzozero, N. I., & Burry, R. W. (2004). GAP-43 mRNA in growth cones is associated with HuD and ribosomes [Article]. *Journal of Neurobiology*, *61*(2), 222–235. https://doi.org/10.1002/neu.20038

Sokpor, G., Kerimoglu, C., Nguyen, H., Pham, L., Rosenbusch, J., Wagener, R., Nguyen, H. P., Fischer, A., Staiger, J. F., & Tuoc, T. (2021). Loss of BAF Complex in Developing Cortex Perturbs Radial Neuronal Migration in a WNT Signaling-Dependent Manner. *Frontiers in Molecular Neuroscience*, *14*, 687581. https://doi.org/10.3389/FNMOL.2021.687581/BIBTEX

Soleymani, F., Paquet, E., Viktor, H., Michalowski, W., & Spinello, D. (2022). Protein–protein interaction prediction with deep learning: A comprehensive review. In *Computational and Structural Biotechnology Journal* (Vol. 20, pp. 5316–5341). Elsevier B.V. https://doi.org/10.1016/j.csbj.2022.08.070

Solomon, E., Davis-Anderson, K., Hovde, B., Micheva-Viteva, S., Harris, J. F., Twary, S., & Iyer, R. (2021). Global transcriptome profile of the developmental principles of in vitro iPSC-to-motor neuron differentiation. *BMC Molecular and Cell Biology*, *22*(1), 1–21. https://doi.org/10.1186/S12860-021-00343-Z/TABLES/7

Sprung, R., Chen, Y., Zhang, K., Cheng, D., Zhang, T., Peng, J., & Zhao, Y. (2008). Identification and validation of eukaryotic aspartate and glutamate methylation in proteins. *Journal of Proteome Research*, *7*(3), 1001–1006. https://doi.org/10.1021/pr0705338

Staahl, B. T., Tang, J., Wu, W., Sun, A., Gitler, A. D., Yoo, A. S., & Crabtree, G. R. (2013). Kinetic Analysis of npBAF to nBAF Switching Reveals Exchange of SS18 with CREST and Integration with Neural Developmental Pathways. *The Journal of Neuroscience*, *33*(25), 10348. https://doi.org/10.1523/JNEUROSCI.1258-13.2013

Stark, G. R., Wang, Y., & Lu, T. (2011). Lysine methylation of promoter-bound transcription factors and relevance to cancer. *Cell Research*, *21*(3), 375. https://doi.org/10.1038/CR.2010.174

Stetler, A., Winograd, C., Sayegh, J., Cheever, A., Patton, E., Zhang, X., Clarke, S., & Ceman, S. (2006). Identification and characterization of the methyl arginines in the fragile X mental retardation protein Fmrp. *Human Molecular Genetics*, *15*(1), 87–96. https://doi.org/10.1093/HMG/DDI429

Stewart, E. J., Åslund, F., & Beckwith, J. (1998). Disulfide bond formation in the Escherichia coli cytoplasm: an in vivo role reversal for the thioredoxins. *The EMBO Journal*, *17*(19), 5543–5550. https://doi.org/10.1093/EMBOJ/17.19.5543

Stouth, D. W., vanLieshout, T. L., Ng, S. Y., Webb, E. K., Manta, A., Moll, Z., & Ljubicic, V. (2020). CARM1 Regulates AMPK Signaling in Skeletal Muscle. *IScience*, *23*(11), 101755. https://doi.org/10.1016/J.ISCI.2020.101755

Strappazzon, F., Torch, S., Chatellard-Causse, C., Petiot, A., Thibert, C., Blot, B., Verna, J. M., & Sadoul, R. (2010). Alix is involved in caspase 9 activation during calcium-induced apoptosis. *Biochemical and Biophysical Research Communications*, *397*(1), 64–69. https://doi.org/10.1016/J.BBRC.2010.05.062

Su, C., & Schwarz, T. L. (2017). O-GlcNAc Transferase Is Essential for Sensory Neuron Survival and Maintenance. *The Journal of Neuroscience*, *37*(8), 2125. https://doi.org/10.1523/JNEUROSCI.3384-16.2017

Sugimoto, Y., & Narumiya, S. (2007). Prostaglandin E Receptors. *Journal of Biological Chemistry*, *282*(16), 11613–11617. https://doi.org/10.1074/JBC.R600038200

Suresh, S. (2021). *Analysis of the Protein Arginine Methyltransferases 1 (PRMT1) and 4 (PRMT4) in Triple-Negative Breast Cancer* [Université Paris-Saclay]. https://theses.hal.science/tel-03917555v1

Tadesse, H., Deschênes-Furry, J., Boisvenue, S., & Côté, J. (2008). KH-type splicing regulatory protein interacts with survival motor neuron protein and is misregulated in spinal muscular atrophy. *Human Molecular Genetics*, *17*(4), 506–524. https://doi.org/10.1093/hmg/ddm327

Taga, A., Peyton, M. A., Goretzki, B., Gallagher, T. Q., Ritter, A., Harper, A., Crawford, T. O., Hellmich, U. A., Sumner, C. J., & McCray, B. A. (2022). TRPV4 mutations causing mixed neuropathy and skeletal phenotypes result in severe gain of function. *Annals of Clinical and Translational Neurology*, *9*(3). https://doi.org/10.1002/acn3.51523

Takakuwa, H., Yamazaki, T., Souquere, S., Adachi, S., Yoshino, H., Fujiwara, N., Yamamoto, T., Natsume, T., Nakagawa, S., Pierron, G., & Hirose, T. (2023). Shell protein composition specified by the lncRNA NEAT1 domains dictates the formation of paraspeckles as distinct membraneless organelles [Article]. *Nature Cell Biology*, *25*(11), 1664–1675. https://doi.org/10.1038/s41556-023-01254-1

Tang, J., Frankel, A., Cook, R. J., Kim, S., Paik, W. K., Williams, K. R., Clarke, S., & Herschman, H. R. (2000). PRMT1 is the predominant type I protein arginine methyltransferase in mammalian cells. *Journal of Biological Chemistry*, *275*(11), 7723–7730. https://doi.org/10.1074/jbc.275.11.7723

Tanner, D. C., Qiu, S., Bolognani, F., Partridge, L. D., Weeber, E. J., & Perrone-Bizzozero, N. I. (2008). Alterations in mossy fiber physiology and GAP-43 expression and function in transgenic mice overexpressing HuD. *Hippocampus*, *18*(8), 814–823. https://doi.org/10.1002/HIPO.20442

Tebaldi, T., Zuccotti, P., Peroni, D., Köhn, M., Gasperini, L., Potrich, V., Bonazza, V., Dudnakova, T., Rossi, A., Sanguinetti, G., Conti, L., Macchi, P., D'Agostino, V., Viero, G., Tollervey, D., Hüttelmaier, S., & Quattrone, A. (2018). HuD Is a Neural Translation Enhancer Acting on mTORC1-Responsive Genes and Counteracted by the Y3 Small Non-coding RNA. *Molecular Cell*, *71*(2), 256-270.e10. https://doi.org/10.1016/J.MOLCEL.2018.06.032/ATTACHMENT/24024B9A-9CC9-4404-BC0B-E20809B0A55A/MMC4.PDF

Tedeschi, A., Nguyen, T., Puttagunta, R., Gaub, P., & Di Giovanni, S. (2008). A p53-CBP/p300 transcription module is required for GAP-43 expression, axon outgrowth, and regeneration. *Cell Death & Differentiation 2009 16:4*, *16*(4), 543–554. https://doi.org/10.1038/cdd.2008.175

Tee, W. W., Pardo, M., Theunissen, T. W., Yu, L., Choudhary, J. S., Hajkova, P., & Surani, M. A. (2010a). Prmt5 is essential for early mouse development and acts in the cytoplasm to maintain ES cell pluripotency. *Genes & Development*, *24*(24), 2772–2777. https://doi.org/10.1101/GAD.606110

Tee, W. W., Pardo, M., Theunissen, T. W., Yu, L., Choudhary, J. S., Hajkova, P., & Surani, M. A. (2010b). Prmt5 is essential for early mouse development and acts in the cytoplasm to maintain ES cell pluripotency. *Genes & Development*, *24*(24), 2772. https://doi.org/10.1101/GAD.606110

Teo, S., & Salinas, P. C. (2021). Wnt-Frizzled Signaling Regulates Activity-Mediated Synapse Formation. *Frontiers in Molecular Neuroscience*, *14*, 683035. https://doi.org/10.3389/FNMOL.2021.683035/BIBTEX

Teperino, R., Schoonjans, K., & Auwerx, J. (2010). Histone Methyl Transferases and Demethylases; Can They Link Metabolism and Transcription? [Article]. *Cell Metabolism*, *12*(4), 321–327. https://doi.org/10.1016/j.cmet.2010.09.004

Tewary, S. K., Zheng, Y. G., & Ho, M.-C. (2019). Protein arginine methyltransferases: insights into the enzyme structure and mechanism at the atomic level. *Cellular and Molecular Life Sciences*, *0123456789*, 1–16. https://doi.org/10.1007/s00018-019-03145-x

Teyssier, C., Chen, D., & Stallcup, M. R. (2002). Requirement for Multiple Domains of the Protein Arginine Methyltransferase CARM1 in Its Transcriptional Coactivator Function. *Journal of Biological Chemistry*, *277*(48), 46066–46072. https://doi.org/10.1074/JBC.M207623200

Teyssier, C., Ma, H., Emter, R., Kralli, A., & Stallcup, M. R. (2005). Activation of nuclear receptor coactivator PGC-1α by arginine methylation. *Genes & Development*, *19*(12), 1466. https://doi.org/10.1101/GAD.1295005

Thandapani, P., O'Connor, T. R., Bailey, T. L., & Richard, S. (2013). Defining the RGG/RG Motif. *Molecular Cell*, *50*(5), 613–623. https://doi.org/10.1016/J.MOLCEL.2013.05.021/ATTACHMENT/22582BE2-4310-4DC0-B908-27BA3259A435/MMC6.XLSX

Thandapani, P., Song, J., Gandin, V., Cai, Y., Rouleau, S. G., Garant, J. M., Boisvert, F. M., Yu, Z., Perreault, J. P., Topisirovic, I., & Richard, S. (2015). Aven recognition of RNA G-quadruplexes regulates translation of the mixed lineage leukemia protooncogenes. *ELife*, *4*(AUGUST2015), e06234. https://doi.org/10.7554/ELIFE.06234

Thiebaut, C., Eve, L., Poulard, C., & Le Romancer, M. (2021). Structure, Activity, and Function of PRMT1. *Life*, *11*(11), 1147. https://doi.org/10.3390/LIFE11111147

Thiry, L., Hamel, R., Pluchino, S., Durcan, T., & Stifani, S. (2020). Characterization of Human iPSC-derived Spinal Motor Neurons by Single-cell RNA Sequencing. *Neuroscience*, *450*, 57–70. https://doi.org/10.1016/J.NEUROSCIENCE.2020.04.041

Tradewell, M. L., Yu, Z., Tibshirani, M., Boulanger, M. C., Durham, H. D., & Richard, S. (2012). Arginine methylation by PRMT1 regulates nuclear-cytoplasmic localization and toxicity of FUS/TLS harbouring ALS-linked mutations. *Human Molecular Genetics*, *21*(1), 136–149. https://doi.org/10.1093/HMG/DDR448

Trinkle-Mulcahy, L. (2012). Resolving protein interactions and complexes by affinity purification followed by label-based quantitative mass spectrometry. *Proteomics*, *12*(10), 1623–1638. https://doi.org/10.1002/PMIC.201100438

Trinkle-Mulcahy, L. (2019). Recent advances in proximity-based labeling methods for interactome mapping. *F1000Research 2019 8:135*, *8*, 135. https://doi.org/10.12688/f1000research.16903.1

Trinkle-Mulcahy, L., Boulon, S., Lam, Y. W., Urcia, R., Boisvert, F. M., Vandermoere, F., Morrice, N. A., Swift, S., Rothbauer, U., Leonhardt, H., & Lamond, A. (2008). Identifying specific protein interaction partners using quantitative mass spectrometry and bead proteomes. *The Journal of Cell Biology*, *183*(2), 223. https://doi.org/10.1083/JCB.200805092

Tripsianes, K., Madl, T., Machyna, M., Fessas, D., Englbrecht, C., Fischer, U., Neugebauer, K. M., & Sattler, M. (2011). Structural basis for dimethylarginine recognition by the Tudor domains of human SMN and SPF30 proteins [Article]. *Nature Structural & Molecular Biology*, *18*(12), 1414–1420. https://doi.org/10.1038/nsmb.2185

Troffer-Charlier, N., Cura, V., Hassenboehler, P., Moras, D., & Cavarelli, J. (2007). Functional insights from structures of coactivator-associated arginine methyltransferase 1 domains. *EMBO Journal*, *26*(20), 4391–4401. https://doi.org/10.1038/sj.emboj.7601855

Tyanova, S., Temu, T., Sinitcyn, P., Carlson, A., Hein, M. Y., Geiger, T., Mann, M., & Cox, J. (2016). The Perseus computational platform for comprehensive analysis of (prote)omics data. *Nature Methods 2016 13:9*, *13*(9), 731–740. https://doi.org/10.1038/nmeth.3901

Valkov, N., & Das, S. (2020). Y RNAs: Biogenesis, Function and Implications for the Cardiovascular System. *Adv Exp Med Biol*, *1229*, 327–342. https://doi.org/10.1007/978-981-15-1671-9

Van Haren, M. J., Marechal, N., Troffer-Charlier, N., Cianciulli, A., Sbardella, G., Cavarelli, J., & Martin, N. I. (2017). Transition state mimics are valuable mechanistic probes for structural studies with the arginine methyltransferase CARM1. *Proceedings of the National Academy of Sciences of the United States of America*, *114*(14), 3625–3630. https://doi.org/10.1073/pnas.1618401114

Van Houdt, J. K. J., Nowakowska, B. A., Sousa, S. B., Van Schaik, B. D. C., Seuntjens, E., Avonce, N., Sifrim, A., Abdul-Rahman, O. A., Van Den Boogaard, M. J. H., Bottani, A., Castori, M., Cormier-Daire, V., Deardorff, M. A., Filges, I., Fryer, A., Fryns, J. P., Gana, S., Garavelli, L., Gillessen-Kaesbach, G., … Vermeesch, J. R. (2012). Heterozygous missense mutations in SMARCA2 cause Nicolaides-Baraitser syndrome. *Nature Genetics*, *44*(4), 445–451. https://doi.org/10.1038/NG.1105

Vanevski, F., & Xu, B. (2015). HuD Interacts with Bdnf mRNA and Is Essential for Activity-Induced BDNF Synthesis in Dendrites. *PLoS ONE*, *10*(2), e0117264. https://doi.org/10.1371/JOURNAL.PONE.0117264

vanLieshout, T. L., Stouth, D. W., Hartel, N. G., Vasam, G., Ng, S. Y., Webb, E. K., Rebalka, I. A., Mikhail, A. I., Graham, N. A., Menzies, K. J., Hawke, T. J., & Ljubicic, V. (2022). The CARM1 transcriptome and arginine methylproteome mediate skeletal muscle integrative biology. *Molecular Metabolism*, *64*, 101555. https://doi.org/10.1016/J.MOLMET.2022.101555

Varderidou-Minasian, S., Verheijen, B. M., Harschnitz, O., Kling, S., Karst, H., van der Pol, W. L., Pasterkamp, R. J., & Altelaar, M. (2021). Spinal Muscular Atrophy Patient iPSC-Derived Motor Neurons Display Altered Proteomes at Early Stages of Differentiation. *ACS Omega*, *6*(51), 35375–35388. https://doi.org/10.1021/acsomega.1c04688

Vaughan, R. M., Kupai, A., Foley, C. A., Sagum, C. A., Tibben, B. M., Eden, H. E., Tiedemann, R. L., Berryhill, C. A., Patel, V., Shaw, K. M., Krajewski, K., Strahl, B. D., Bedford, M. T., Frye, S. V., Dickson, B. M., & Rothbart, S. B. (2020). The histone and non-histone methyllysine reader activities of the UHRF1 tandem Tudor domain are dispensable for the propagation of aberrant DNA methylation patterning in cancer cells. *Epigenetics and Chromatin*, *13*(1), 1–15. https://doi.org/10.1186/S13072-020-00366-4/FIGURES/6

Vedula, P., & Kashina, A. (2018). The makings of the “actin code”: Regulation of actin’s biological function at the amino acid and nucleotide level. *Journal of Cell Science*, *131*(9). https://doi.org/10.1242/JCS.215509/57120

Vhuiyan, M., Thomas, D., Hossen, F., & Frankel, A. (2013). Targeting protein arginine N-methyltransferases with peptide-based inhibitors: Opportunities and challenges. *Future Medicinal Chemistry*, *5*(18), 2199–2206. https://doi.org/10.4155/fmc.13.184

Vijayakumar, A., Majumder, M., Yin, S., Brobbey, C., Karam, J., Howley, B., Howe, P. H., Berto, S., Madan, L. K., Gan, W., & Palanisamy, V. (2024). PRMT5-mediated arginine

methylation of FXR1 is essential for RNA binding in cancer cells. *Nucleic Acids Research*, *52*(12), 7225–7244. https://doi.org/10.1093/NAR/GKAE319

Vorreiter, C., Robaa, D., & Sippl, W. (2024). Exploring Aromatic Cage Flexibility Using Cosolvent Molecular Dynamics Simulations─An In-Silico Case Study of Tudor Domains. *Journal of Chemical Information and Modeling*, *64*(11), 4553–4569. https://doi.org/10.1021/ACS.JCIM.4C00298/SUPPL_FILE/CI4C00298_SI_002.ZIP

Walport, L. J., Hopkinson, R. J., Chowdhury, R., Schiller, R., Ge, W., Kawamura, A., & Schofield, C. J. (2016a). Arginine demethylation is catalysed by a subset of JmjC histone lysine demethylases. *Nature Communications 2016 7:1*, *7*(1), 1–12. https://doi.org/10.1038/ncomms11974

Walport, L. J., Hopkinson, R. J., Chowdhury, R., Schiller, R., Ge, W., Kawamura, A., & Schofield, C. J. (2016b). *Arginine demethylation is catalysed by a subset of JmjC histone lysine demethylases*. https://doi.org/10.1038/ncomms11974

Wang, B., Zhang, L., Dai, T., Qin, Z., Lu, H., Zhang, L., & Zhou, F. (2021). Liquid–liquid phase separation in human health and diseases. *Signal Transduction and Targeted Therapy 2021 6:1*, *6*(1), 1–16. https://doi.org/10.1038/s41392-021-00678-1

Wang, F., Zhang, J., Tang, H., Pang, Y., Ke, X., Peng, W., Chen, S., Abbas, M. nadeem, Dong, Z., Cui, Z., & Cui, H. (2021). Nup54-induced CARM1 nuclear importation promotes gastric cancer cell proliferation and tumorigenesis through transcriptional activation and methylation of Notch2. *Oncogene 2021 41:2*, *41*(2), 246–259. https://doi.org/10.1038/s41388-021-02078-9

Wang, L., Charoensuksai, P., Watson, N. J., Wang, X., Zhao, Z., Coriano, C. G., Kerr, L. R., & Xu, W. (2013). CARM1 automethylation is controlled at the level of alternative splicing. *Nucleic Acids Research*, *41*(14), 6870–6880. https://doi.org/10.1093/nar/gkt415

Wang, L., & Li, P. (2024). Arginine methylation-enabled FUS phase separation with SMN contributes to neuronal granule formation. *Cell Reports*, *43*(8). https://doi.org/10.1016/j.celrep.2024.114537

Wang, L., & Tang, J. (2023). SWI/SNF complexes and cancers [Article]. *Gene*, *870*, 147420–147420. https://doi.org/10.1016/j.gene.2023.147420

Wang, L., Zhao, Z., Meyer, M. B., Saha, S., Yu, M., Guo, A., Wisinski, K. B., Huang, W., Cai, W., Pike, J. W., Yuan, M., Ahlquist, P., & Xu, W. (2014a). CARM1 Methylates Chromatin Remodeling Factor BAF155 to Enhance Tumor Progression and Metastasis. *Cancer Cell*, *25*(1), 21. https://doi.org/10.1016/J.CCR.2013.12.007

Wang, L., Zhao, Z., Meyer, M. B., Saha, S., Yu, M., Guo, A., Wisinski, K. B., Huang, W., Cai, W., Pike, J. W., Yuan, M., Ahlquist, P., & Xu, W. (2014b). CARM1 Methylates Chromatin Remodeling Factor BAF155 to Enhance Tumor Progression and Metastasis. *Cancer Cell*, *25*(1), 21. https://doi.org/10.1016/J.CCR.2013.12.007

Wang, Q., Li, Z., Zhang, S., Li, Y., Wang, Y., Fang, Z., Ma, Y., Liu, Z., Zhang, W., Li, D., Liu, C., & Ye, M. (2022). Global profiling of arginine dimethylation in regulating protein phase separation by a steric effect–based chemical-enrichment method. *Proceedings of the National Academy of Sciences of the United States of America*, *119*(43), e2205255119. https://doi.org/10.1073/PNAS.2205255119/SUPPL_FILE/PNAS.2205255119.SAPP.PDF

Wang, X., Haswell, J. R., & Roberts, C. W. M. (2014). Molecular Pathways: SWI/SNF (BAF) complexes are frequently mutated in cancer—mechanisms and potential therapeutic

insights. *Clinical Cancer Research : An Official Journal of the American Association for Cancer Research*, *20*(1), 21. https://doi.org/10.1158/1078-0432.CCR-13-0280

Wang, X., & Roberts, C. W. M. (2014). CARMA: CARM1 methylation of SWI/SNF in breast cancer. *Cancer Cell*, *25*(1), 3. https://doi.org/10.1016/J.CCR.2013.12.017

Wang, X., & Tanaka Hall, T. M. (2001). Structural basis for recognition of AU-rich element RNA by the HuD protein [Article]. *Nature Structural Biology*, *8*(2), 141–145. https://doi.org/10.1038/84131

Wang, Y., & Bedford, M. T. (2023). Effectors and effects of arginine methylation. *Biochemical Society Transactions*, *51*(2), 725. https://doi.org/10.1042/BST20221147

Wang, Y. C., & Li, C. (2012). Evolutionarily conserved protein arginine methyltransferases in non-mammalian animal systems. In *FEBS Journal* (Vol. 279, Issue 6, pp. 932–945). https://doi.org/10.1111/j.1742-4658.2012.08490.x

Wang, Y., Wysocka, J., Sayegh, J., Lee, Y. H., Pertin, J. R., Leonelli, L., Sonbuchner, L. S., McDonald, C. H., Cook, R. G., Dou, Y., Roeder, R. G., Clarke, S., Stallcup, M. R., Allis, C. D., & Coonrod, S. A. (2004). Human PAD4 regulates histone arginine methylation levels via demethylimination. *Science*, *306*(5694), 279–283. https://doi.org/10.1126/SCIENCE.1101400/SUPPL_FILE/WANG.SOM.PDF

Wang, Y., Zhou, J., He, W., Fu, R., Shi, L., Dang, N. K., Liu, B., Xu, H., Cheng, X., & Bedford, M. T. (2024). SART3 reads methylarginine-marked glycine- and arginine-rich motifs. *Cell Reports*, *43*(7), 114459. https://doi.org/10.1016/J.CELREP.2024.114459

Wang, Z., Hou, J., Lu, L., Qi, Z., Sun, J., Gao, W., Meng, J., Wang, Y., Sun, H., Gu, H., Xin, Y., Guo, X., & Yang, G. (2013). Small Ribosomal Protein Subunit S7 Suppresses Ovarian

Tumorigenesis through Regulation of the PI3K/AKT and MAPK Pathways. *PLoS ONE*, *8*(11), e79117. https://doi.org/10.1371/JOURNAL.PONE.0079117

Wang, Z., & Liu, H. (2024). *Roles of Lysine Methylation in Glucose and Lipid Metabolism: Functions, Regulatory Mechanisms, and Therapeutic Implications*. https://doi.org/10.3390/biom14070862

Webb, E. K., Ng, S. Y., Mikhail, A. I., Stouth, D. W., vanLieshout, T. L., Syroid, A. L., & Ljubicic, V. (2023). Impact of short-term, pharmacological CARM1 inhibition on skeletal muscle mass, function, and atrophy in mice. *American Journal of Physiology - Endocrinology and Metabolism*, *325*(3), E252. https://doi.org/10.1152/AJPENDO.00047.2023

Wei, H. H., Fan, X. J., Hu, Y., Tian, X. X., Guo, M., Mao, M. W., Fang, Z. Y., Wu, P., Gao, S. X., Peng, C., Yang, Y., & Wang, Z. (2021). A systematic survey of PRMT interactomes reveals the key roles of arginine methylation in the global control of RNA splicing and translation. *Science Bulletin*, *66*(13), 1342–1357. https://doi.org/10.1016/j.scib.2021.01.004

Wein, G., Rössler, M., Klug, R., & Herget, T. (2003). The 3′-UTR of the mRNA coding for the major protein kinase C substrate MARCKS contains a novel CU-rich element interacting with the mRNA stabilizing factors HuD and HuR. *European Journal of Biochemistry*, *270*(2), 350–365. https://doi.org/10.1046/J.1432-1033.2003.03396.X

Wen, Y., An, Z., Qiao, B., Zhang, C., & Zhang, Z. (2019). RPS7 promotes cell migration through targeting epithelial-mesenchymal transition in prostate cancer. *Urologic Oncology: Seminars and Original Investigations*, *37*(5), 297.e1-297.e7. https://doi.org/10.1016/J.UROLONC.2019.01.011

Wiedemann, C., Kumar, A., Lang, A., & Ohlenschläger, O. (2020). Cysteines and Disulfide Bonds as Structure-Forming Units: Insights From Different Domains of Life and the Potential for Characterization by NMR. *Frontiers in Chemistry*, *8*, 280. https://doi.org/10.3389/FCHEM.2020.00280/FULL

Wood, H. (2018). Benefits of nusinersen extend to later-onset SMA. *Nature Reviews Neurology*, *14*(4), 196. https://doi.org/10.1038/NRNEUROL.2018.24

Wu, J., & Xu, W. (2012). Histone H3R17me2a mark recruits human RNA Polymerase-Associated Factor 1 Complex to activate transcription. *Proceedings of the National Academy of Sciences of the United States of America*, *109*(15), 5675–5680. https://doi.org/10.1073/PNAS.1114905109/SUPPL_FILE/PNAS.201114905SI.PDF

Wu, L., Kou, F., Ji, Z., Li, B., Zhang, B., Guo, Y., & Yang, L. (2021). SMYD2 promotes tumorigenesis and metastasis of lung adenocarcinoma through RPS7. *Cell Death & Disease*, *12*(5), 439. https://doi.org/10.1038/S41419-021-03720-W

Wu, Q., Bruce, A. W., Jedrusik, A., Ellis, P. D., Andrews, R. M., Langford, C. F., Glover, D. M., & Zernicka-Goetz, M. (2009). CARM1 is Required in Embryonic Stem Cells to Maintain Pluripotency and Resist Differentiation. *Stem Cells (Dayton, Ohio)*, *27*(11), 2637. https://doi.org/10.1002/STEM.131

Wu, Q., Schapira, M., Arrowsmith, C. H., & Barsyte-Lovejoy, D. (2021). Protein arginine methylation: from enigmatic functions to therapeutic targeting [Article]. *Nature Reviews. Drug Discovery*, *20*(7), 509–530. https://doi.org/10.1038/s41573-021-00159-8

Xie, H., Bacabac, M. S., Ma, M., Kim, E.-J., Wang, Y., Wu, W., Li, L., Xu, W., & Tang, W. (2023). Development of Potent and Selective Coactivator-Associated Arginine

Methyltransferase 1 (CARM1) Degraders. *Journal of Medicinal Chemistry*. https://doi.org/10.1021/acs.jmedchem.3c00982

Xie, W., Cappiello, M., Meng, M., Rosenthal, R., & Zhang, W. (2018). ADRA2B deletion variant and enhanced cognitive processing of emotional information: A meta-analytical review. *Neuroscience & Biobehavioral Reviews*, *92*, 402–416. https://doi.org/10.1016/J.NEUBIOREV.2018.05.010

Xie, Z., Tian, Y., Guo, X., & Xie, N. (2024). The emerging role of CARM1 in cancer. *Cellular Oncology*. https://doi.org/10.1007/s13402-024-00943-9

Xu, W., Cho, H., Kadam, S., Banayo, E. M., Anderson, S., Yates, J. R., Emerson, B. M., & Evans, R. M. (2004). A methylation-mediator complex in hormone signaling. *Genes & Development*, *18*(2), 144. https://doi.org/10.1101/GAD.1141704

Yadav, N., Lee, J., Kim, J., Shen, J., C-T Hu, M., Marcelo Aldaz, C., & Bedford, M. T. (2003). *Specific protein methylation defects and gene expression perturbations in coactivator-associated arginine methyltransferase 1-deficient mice*. www.pnas.orgcgidoi10.1073pnas.1232272100

Yan, W., Liang, Y., Zhang, Q., Wang, D., Lei, M., Qu, J., He, X., Lei, Q., & Wang, Y. (2018). Arginine methylation of SIRT 7 couples glucose sensing with mitochondria biogenesis . *EMBO Reports*, *19*(12). https://doi.org/10.15252/EMBR.201846377/SUPPL_FILE/EMBR201846377-SUP-0002-TABLEEV1.XLSX

Yang, G., Zhou, C., Wang, R., Huang, S., Wei, Y., Yang, X., Liu, Y., Li, J., Lu, Z., Ying, W., Li, X., Jing, N., Huang, X., Yang, H., & Qiao, Y. (2019). Base-Editing-Mediated R17H Substitution in Histone H3 Reveals Methylation-Dependent Regulation of Yap Signaling

and Early Mouse Embryo Development. *Cell Reports*, *26*(2), 302-312.e4. https://doi.org/10.1016/j.celrep.2018.12.046

Yang, Y., & Bedford, M. T. (2013). Protein arginine methyltransferases and cancer [Article]. *Nature Reviews. Cancer*, *13*(1), 37–50. https://doi.org/10.1038/nrc3409

Yang, Y., Hadjikyriacou, A., Xia, Z., Gayatri, S., Kim, D., Zurita-Lopez, C., Kelly, R., Guo, A., Li, W., Clarke, S. G., & Bedford, M. T. (2015). PRMT9 is a Type II methyltransferase that methylates the splicing factor SAP145. *Nature Communications 2015 6:1*, *6*(1), 1–12. https://doi.org/10.1038/ncomms7428

Yang, Y., Lu, Y., Espejo, A., Wu, J., Xu, W., Liang, S., & Bedford, M. T. (2010). TDRD3 Is an Effector Molecule for Arginine-Methylated Histone Marks. *Molecular Cell*, *40*(6), 1016–1023. https://doi.org/10.1016/j.molcel.2010.11.024

Yokoyama, U., Iwatsubo, K., Umemura, M., Fujita, T., & Ishikawa, Y. (2013). The Prostanoid EP4 Receptor and Its Signaling Pathway. *Pharmacological Reviews*, *65*, 1010–1052. https://doi.org/10.1124/pr.112.007195

Yoo, S., Kim, H. H., Kim, P., Donnelly, C. J., Kalinski, A. L., Vuppalanchi, D., Park, M., Lee, S. J., Merianda, T. T., Perrone-Bizzozero, N. I., & Twiss, J. L. (2013). A HuD-ZBP1 ribonucleoprotein complex localizes GAP-43 mRNA into axons through its 3′ untranslated region AU-rich regulatory element. *Journal of Neurochemistry*, *126*(6), 792. https://doi.org/10.1111/JNC.12266

Zeiger, W., Ito, D., Swetlik, C., Oh-hora, M., Villereal, M. L., & Thinakaran, G. (2011). Stanniocalcin 2 Is a Negative Modulator of Store-Operated Calcium Entry. *Molecular and Cellular Biology*, *31*(18), 3710. https://doi.org/10.1128/MCB.05140-11

Zhang, X., Chen, H., Song, Y., Chen, Z., Liu, X., Rong, P., & Ma, R. (2022). Ten-year follow-up of Nicolaides–Baraitser syndrome with a de novo mutation and analysis of 58 gene loci of SMARCA2-associated NCBRS. *Molecular Genetics & Genomic Medicine*, *10*(9), e2009. https://doi.org/10.1002/MGG3.2009

Zhang, X., & Cheng, X. (2003a). Structure of the predominant protein arginine methyltransferase PRMT1 and analysis of its binding to substrate peptides. *Structure*, *11*(5), 509–520. https://doi.org/10.1016/S0969-2126(03)00071-6

Zhang, X., & Cheng, X. (2003b). Structure of the Predominant Protein Arginine Methyltransferase PRMT1 and Analysis of Its Binding to Substrate Peptides. *Structure (London, England : 1993)*, *11*(5), 509. https://doi.org/10.1016/S0969-2126(03)00071-6

Zhao, H. yong, Zhang, Y. jun, Dai, H., Zhang, Y., & Shen, Y. fei. (2011). CARM1 Mediates Modulation of Sox2. *PLoS ONE*, *6*(10), e27026. https://doi.org/10.1371/JOURNAL.PONE.0027026

Zhao, M., Yao, X., Wei, P., Zhao, C., Cheng, M., Zhang, D., Xue, W., He, W., Xue, W., Zuo, X., Jiang, L., Luo, Z., Song, J., Shu, W., Yuan, H., Liang, Y., Sun, H., Zhou, Y., Zhou, Y., … Du, H. (2021). O-GlcNAcylation of TDP-43 suppresses proteinopathies and promotes TDP-43's mRNA splicing activity. *EMBO Reports*, *22*(6). https://doi.org/10.15252/EMBR.202051649/SUPPL_FILE/EMBR202051649-SUP-0015-TABLEEV1.DOCX

Zhao, X., Jankovic, V., Gural, A., Huang, G., Pardanani, A., Menendez, S., Zhang, J., Dunne, R., Xiao, A., Erdjument-Bromage, H., David Allis, C., Tempst, P., & Nimer, S. D. (2008). *Methylation of RUNX1 by PRMT1 abrogates SIN3A binding and potentiates its transcriptional activity*. https://doi.org/10.1101/gad.1632608

Zhou, H. L., Hinman, M. N., Barron, V. A., Geng, C., Zhou, G., Luo, G., Siegel, R. E., & Lou, H. (2011). Hu proteins regulate alternative splicing by inducing localized histone hyperacetylation in an RNA-dependent manner. *Proceedings of the National Academy of Sciences of the United States of America*, *108*(36), E627. https://doi.org/10.1073/PNAS.1103344108/-/DCSUPPLEMENTAL

Zhou, H.-X., & Pang, X. (2018). Electrostatic Interactions in Protein Structure, Folding, Binding, and Condensation Graphical Abstract HHS Public Access. *Chem Rev*, *118*(4), 1691–1741. https://doi.org/10.1021/acs.chemrev.7b00305

Zhou, Y. J., Yang, M. L., He, X., Gu, H. Y., Ren, J. H., Cheng, S. T., Fu, Z., Zhang, Z. Z., & Chen, J. (2024). RNA-binding protein RPS7 promotes hepatocellular carcinoma progression via LOXL2-dependent activation of ITGB1/FAK/SRC signaling. *Journal of Experimental & Clinical Cancer Research : CR*, *43*(1), 45. https://doi.org/10.1186/S13046-023-02929-1

Zhu, H., Hasman, R. A., Barron, V. A., Luo, G., & Lou, H. (2006). A Nuclear Function of Hu Proteins as Neuron-specific Alternative RNA Processing Regulators. *Molecular Biology of the Cell*, *17*(12), 5105. https://doi.org/10.1091/MBC.E06-02-0099

Zhu, H., Hinman, M. N., Hasman, R. A., Mehta, P., & Lou, H. (2007). Regulation of Neuron-Specific Alternative Splicing of Neurofibromatosis Type 1 Pre-mRNA. *Molecular and Cellular Biology*, *28*(4), 1240. https://doi.org/10.1128/MCB.01509-07

Zhu, Q., Wang, D., Liang, F., Tong, X., Liang, Z., Wang, X., Chen, Y., & Mo, D. (2022). Protein arginine methyltransferase PRMT1 promotes adipogenesis by modulating transcription factors C/EBPβ and PPARγ. *Journal of Biological Chemistry*, *298*(9), 102309. https://doi.org/10.1016/j.jbc.2022.102309

Zhu, Y., Poyurovsky, M. V., Li, Y., Biderman, L., Stahl, J., Jacq, X., & Prives, C. (2009). Ribosomal Protein S7 is both a Regulator and Substrate of MDM2. *Molecular Cell*, *35*(3), 316. https://doi.org/10.1016/J.MOLCEL.2009.07.014

Zuccotti, P., 1#, T. T., Peroni, D., Köhn, M., Gasperini, L., Potrich, V., Dudnakova, T., Sanguinetti, G., Conti, L., Macchi, P., Tollervey, D., Hüttelmaier, S., & Quattrone, A. (2017). HuD is a neural enhancer of global translation acting on mTORC1-responsive genes and sponged by the Y3 small non-coding RNA. *BioRxiv*, 205658. https://doi.org/10.1101/205658

Additional Results

Throughout this project, many research avenues were considered. Something that was not expanded upon in this work is CARM1's ability to methylate HuR. The interaction was found to be particularly relevant to skeletal muscle biology. Akin to HuD, CARM1's methylation of HuR mediated its interaction with SMN and altered its localization in the myogenic process. (Ravel-Chapuis et al., 2022). Given the similarities between the two RBPs at a functional and structural level, our group proposed that CARM1's influence on MNs and muscle may have mirroring influences and contributing to neuromuscular biology as a whole.

It was previously found that CARM1 be overexpressed about 18 fold in the gastrocnemius muscle of the $SMN^{2B/-}$ SMA mice model at PND22 as assessed by WB (Ravel-Chapuis et al., 2022). With this striking change in expression, this model was considered to evaluate CARM1's contributions to muscle and SMA pathology.

Surprisingly, replicating this experiment gave very different results. In my hands, the gastrocnemius of $SMN^{2B/-}$ SMA mice at PND22 expressed about a third of CARM1 compared to age matched control (Figure 27). Needless to say, when comparing to the previously reported 18 fold overexpression, this finding was very puzzling. This discrepancy could be explained two ways, first being the strain used between each experiment.

In the original investigation, the SMA mice were in a C57BL/6 (BL6) X CD1 background (Ravel-Chapuis et al., 2022), while the ones used here were bred in a BL6 background. It was previously shown that the background could have drastic changes to the phenotype of the $SMN^{2B/-}$ SMA mice (Eshraghi et al., 2016). For that reason, despite expressing the same transgene, the two strains could display different levels of CARM1 expression.

Secondly, it must be considered that as described in Chapter 3, CARM1 has outstanding biochemical properties that are detrimental to its quantification by WB. In Figure 7, the distinct requirements of CARM1 for accurate quantification were considered to ensure that aggregates did not influence results. Still, it cannot be confirmed that CARM1 aggregations were involved in the 18 fold change in CARM1 expression observed in the C57BL/6 (BL6) X CD1 $SMN^{2B/-}$ SMA mice. Since the C57BL/6 (BL6) X CD1 strain is no longer available, a direct comparison is not possible. Regardless, both findings highlight CARM1 as being deregulated in the gastrocnemius muscle of the $SMN^{2B/-}$ SMA mice model. This argues for a contributing role of CARM1 in muscular biology and the pathologies associated to the neurodegenerative disease of SMA.

Lastly, the protein levels of CARM1 were assessed in SMA patient fibroblasts using the appropriate WB conditions defined in Chapter 3. Our group had previously found that Type 1 SMA patient fibroblasts (GM00232) overexpressed CARM1 when compared to those of a healthy patient (GM08333) (Sanchez et al., 2013). In my hands, the same result was not replicated. The fibroblasts showed to have a lot of variability between replicates. The same variability was also seen through SMN levels, suggesting that other factors are involved. Since both CARM1 and SMN did not reach significance between patients this was not further explored.

These findings highlight how CARM1 in SMA needs to be better understood. The results presented in this section are still an incomplete overlook but should be considered in future studies.

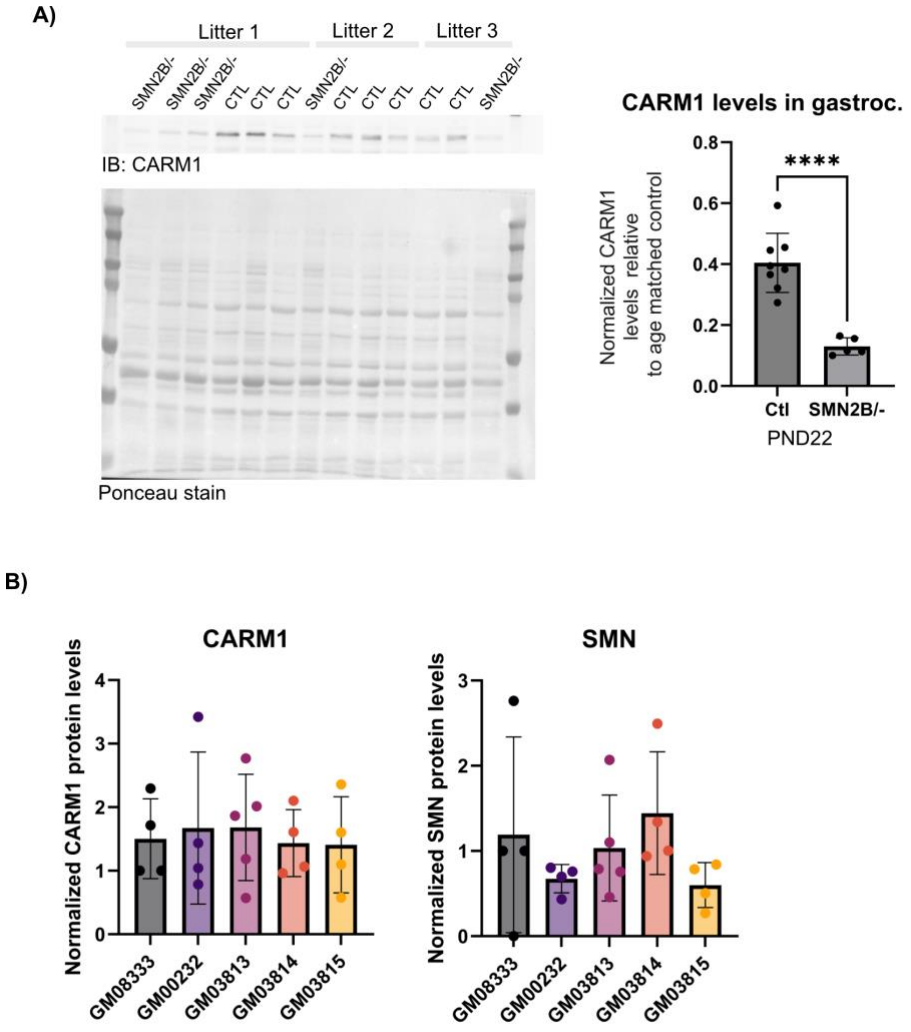

Figure 27: **CARM1 protein levels in the gastrocnemius muscle of SMA mice and SMA patient fibroblasts.**

(A) The gastrocnemius muscles of $SMN^{2B/-}$ mice and control littermates were collected at PND22 and lysed prior to SDS-PAGE and WB analysis. CARM1 was quantified through densitometry analysis and normalized to Ponceau Stain. Statistical analysis; Unpaired T-test. $P<0.05$, Error bars represent SD. N=5-8. (B) Patient primary fibroblasts of healthy (GM08333), Type 1 (GM00232) or Type 2 SMA patients (GM03813), and SMA carriers (GM03814, GM03815) were used to quantify CARM1 and SMN protein levels as analysed by WB analysis.

CARM1 and SMN were normalized to Tubulin. Statistical analysis; One-way ANOVA with Tukey's multiple comparisons test. $P<0.05$, Error bars represent SD. N=4-5. All CARM1 samples were prepared using conditions that prevent its aggregation. SMN samples were prepared using standard sample preparation conditions. IB; Immunoblot.

Supplementary Data

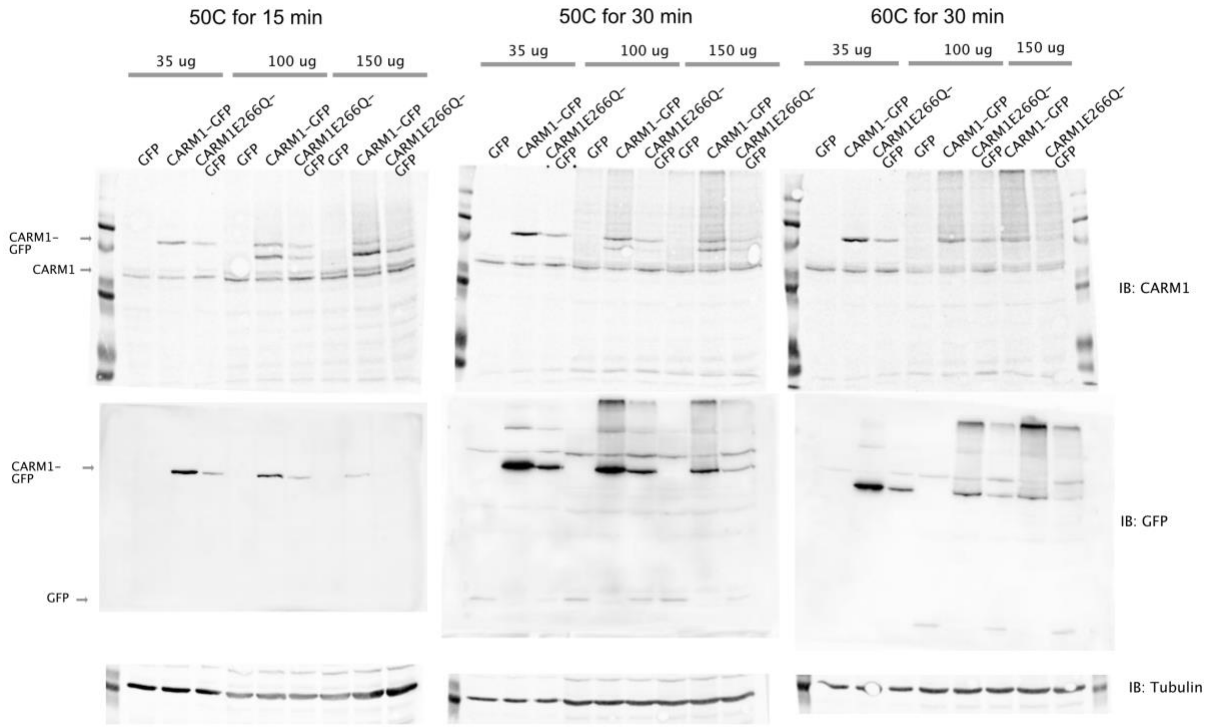

Figure S1: MN-1 cell protein lysate sample preparation using intermediate heat denaturation temperatures.

Samples were denatured using intermediate temperatures prior to SDS-PAGE and WB. All samples contained 35 μg of protein in a final volume of 30 μL and were heat denatured as indicated (50˚C for 15 min, 30 min, or 60˚C for 30 min). IB; immunoblot.

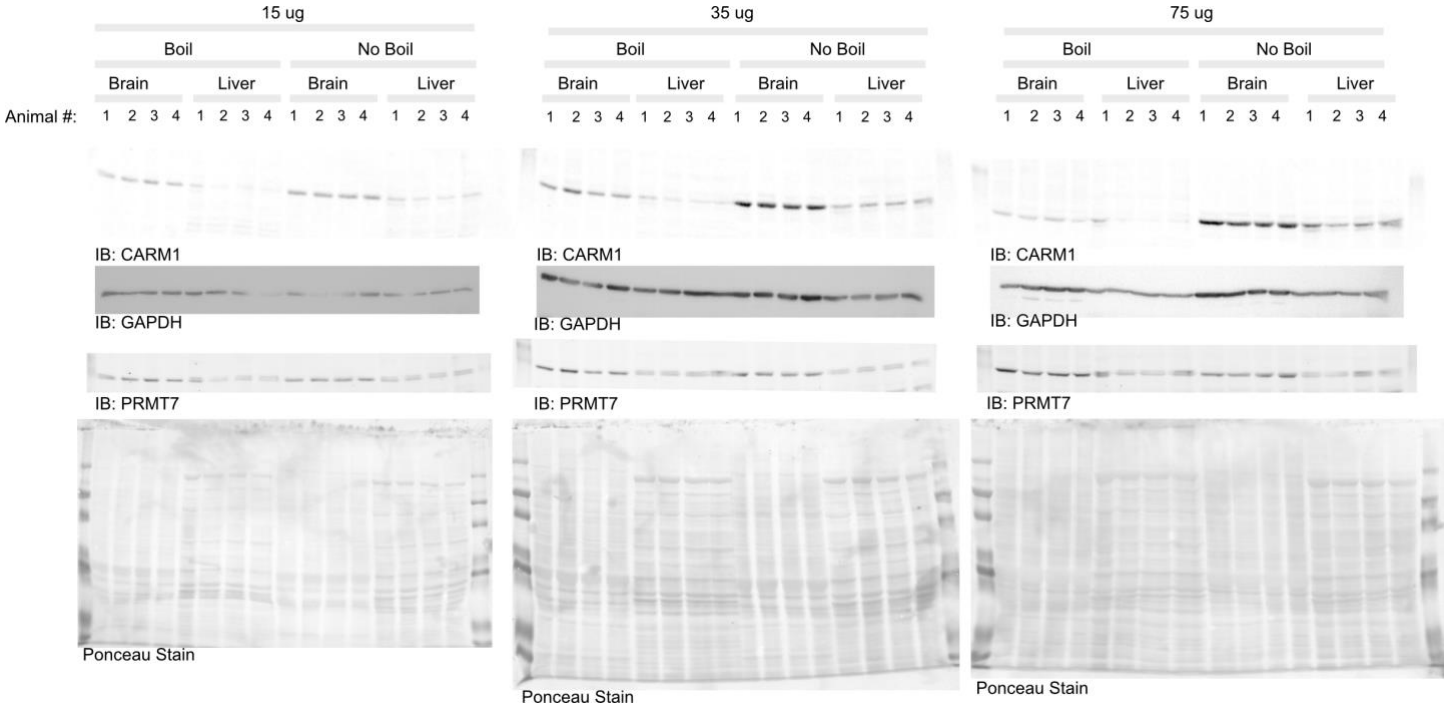

Figure S2: CARM1 aggregation in mouse tissues.

Brain and liver mouse tissue samples were prepared to contain different protein amounts in equal volume using standard protocol and incubated at room temperature or heat denatured at 95˚C for 8 min. IB; immunoblot.

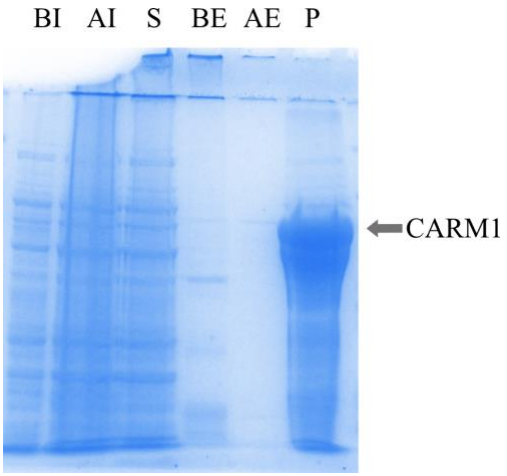

Figure S3: Recombinant CARM1 protein accumulates in insoluble pellets.

The BL21 competent cells (BI; Before Induction) were induced to express recombinant CARM1-GST (AI; After Induction). After lysis, the supernatant (S) was incubated with GST beads which were isolated (BE; Before Elution) and eluted (AE; After Elution). The insoluble pellet (P) was resuspended in urea. All samples were mixed with lammli buffer, run on SDS-PAGE and Coomassie stained.

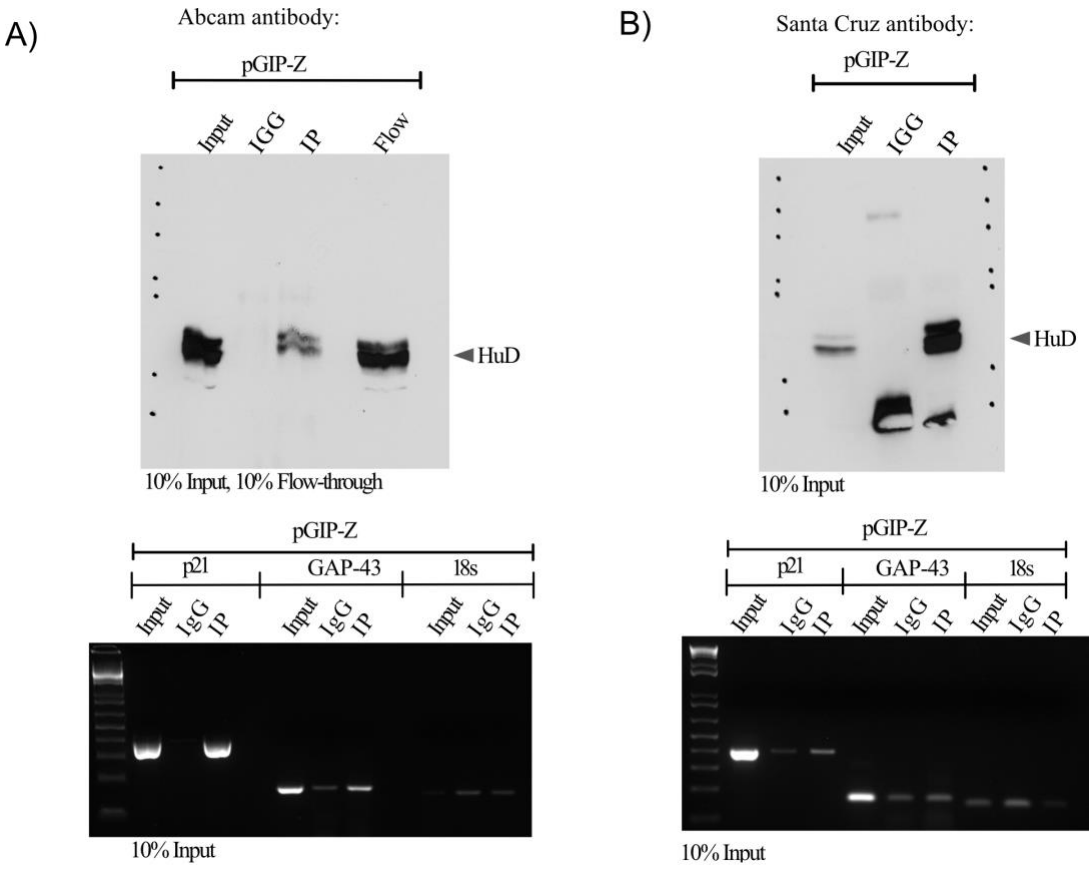

Figure S4: Comparison of HuD IP and RIP yields with two different antibodies.

In MN-1 pGIP-Z cells, the efficiency of HuD's IP and RIP was tested using two different antibodies. HuD was immunoprecipitated using an Abcam (Ab96474) (A) or a Santa Cruz antibody (sc-28299) (B) and compared by WB (top panels). In parallel, the coimmunoprecipitated RNA was extracted, and HuD mRNA targets p21 and Gap-43 were amplified via RT-PCR(bottom panels).

Supplementary Table 1: Genes enriched with HuD in pGIP-Z cells

The genes identified in a HuD RIP performed in MN-1 pGIP-Z and shCARM1 cells were analyzed for differential enrichment using GFOLD. An arbitrary threshold of a GFOLD value of -2 and below was set to highlight the genes enriched with HuD in pGIP-Z cells. The genes of interest in this study were highlighted in grey.

Gene symbol	Gene name	GFOLD	RPKM pGIP-Z	RPKM shCARM1	log_2RPKM pGIPZ
ENSMUSG00000027777.15	Schip1	-8.56791	10.8211	0.00995752	3.43577526
ENSMUSG00000102422.1	Iqschfp	-8.44373	21.3844	0.021445	4.41848682
ENSMUSG00000024921.17	Smarca2	-4.73732	0.740888	0.0183954	-0.4326726
ENSMUSG00000005124.10	Ccn4	-4.73632	0.271901	0	-1.8788466
ENSMUSG00000031442.21	Mcf2l	-4.70682	0.114207	0	-3.130277
ENSMUSG00000055737.12	Ghr	-4.50452	0.142627	0	-2.809681
ENSMUSG00000046027.17	Stard5	-4.05777	0.352879	0.00620308	-1.5027545
ENSMUSG00000042686.5	Jph1	-3.97053	0.363296	0.00677648	-1.4607826
ENSMUSG00000110523.1	C230057M02Rik	-3.83269	0.229778	0	-2.1216874
ENSMUSG00000086496.1	Gm14204	-3.71742	0.264421	0.00686438	-1.9190913
ENSMUSG00000040280.10	Ndufa4l2	-3.68474	2.95716	0.131454	1.5642123
ENSMUSG00000026220.6	Slc16a14	-3.6618	0.439373	0.0101041	-1.1864819
ENSMUSG00000087141.1	Plcxd2	-3.58914	0.196382	0.00474353	-2.3482654
ENSMUSG00000048015.4	Neurod4	-3.53999	2.12305	0.131628	1.08613835
ENSMUSG00000056073.16	Grik2	-3.49456	0.140126	0.00447459	-2.8352034
ENSMUSG00000059588.13	Calcrl	-3.43997	0.727327	0.0416249	-0.459324
ENSMUSG00000105102.1	Gm35507	-3.32106	0.288633	0.00613344	-1.7926918
ENSMUSG00000108151.1	Gm33201	-3.11935	0.814081	0.0198063	-0.2967557
ENSMUSG00000043310.4	Olfr571	-3.09363	1.51372	0.13625	0.59809837
ENSMUSG00000033740.17	St18	-3.05896	1.63236	0.157188	0.70695926
ENSMUSG00000042351.9	Grap2	-2.98696	0.171276	0.00678136	-2.5456051
ENSMUSG00000000416.16	Cttnbp2	-2.97891	0.13482	0.00575413	-2.8908936
ENSMUSG00000022272.17	Myo10	-2.97683	0.18138	0.0125477	-2.4629127
ENSMUSG00000116720.1	Gm31641	-2.93491	0.225234	0.00619854	-2.1505035
ENSMUSG00000031284.16	Pak3	-2.93115	0.410809	0.0372302	-1.2834603
ENSMUSG00000109186.1	Gm34821	-2.92586	0.174538	0	-2.5183869
ENSMUSG00000029092.9	D5Ertd615e	-2.86688	0.357024	0.0265986	-1.485907
ENSMUSG00000030228.18	Pik3c2g	-2.85602	0.0335001	0	-4.8996908
ENSMUSG00000050587.14	Lrrc4c	-2.83835	0.183172	0.00732141	-2.4487291
ENSMUSG00000055639.16	Dach1	-2.82707	0.19301	0.011572	-2.3732525
ENSMUSG00000093839.2	Olfr462	-2.76493	0.144159	0.00605017	-2.7942672
ENSMUSG00000020303.2	Stc2	-2.72565	12.7561	1.79161	3.67311541
ENSMUSG00000034457.10	Eda2r	-2.71899	0.542819	0.0560552	-0.8814569
ENSMUSG00000044864.16	Ankrd50	-2.6654	0.0605964	0.00199463	-4.0446241
ENSMUSG00000041642.18	Kif21b	-2.62741	0.327861	0.038222	-1.6088438
ENSMUSG00000031497.9	Tnfsf13b	-2.59727	0.437694	0.049314	-1.1920055
ENSMUSG00000032517.16	Mobp	-2.58105	0.0515496	0	-4.277895
ENSMUSG00000025328.9	Padi3	-2.51817	0.462381	0.0466716	-1.112846
ENSMUSG00000032185.15	Carm1	-2.4728	5.45333	0.879529	2.44713746

ENSMUSG00000110018.2	5430437J10Rik	-2.41166	0.408341	0.0253889	-1.2921537
ENSMUSG00000111360.1	Gm38642	-2.38114	0.990309	0.127883	-0.0140493
ENSMUSG00000109503.1	Gm44786	-2.37078	0.420314	0.0168	-1.2504606
ENSMUSG00000045667.14	Smtnl2	-2.34683	0.0793252	0.00221945	-3.6560769
ENSMUSG00000110115.1	Gm32486	-2.34683	0.0793044	0.00221887	-3.6564553
ENSMUSG00000018698.15	Lhx1	-2.34647	1.5929	0.249525	0.6716557
ENSMUSG00000022996.15	Wnt10b	-2.32298	4.1584	0.717011	2.05602854
ENSMUSG00000032182.15	Yipf2	-2.23397	5.03448	0.907479	2.33184277
ENSMUSG00000042826.13	Fgfl1	-2.21181	0.838418	0.125172	-0.2542584
ENSMUSG00000001739.14	Cldn15	-2.19125	0.455933	0.0478373	-1.1331063
ENSMUSG00000033227.7	Wnt6	-2.16902	0.487809	0.0579417	-1.0356117
ENSMUSG00000039741.15	Bahcc1	-2.16735	0.373814	0.0632109	-1.4196075
ENSMUSG00000108634.1	Gm38534	-2.14829	2.83761	0.505637	1.50467632
ENSMUSG00000058620.5	Adra2b	-2.14521	10.6304	2.22333	3.41012398
ENSMUSG00000041261.9	Car8	-2.1373	0.295845	0.0373586	-1.7570866
ENSMUSG00000063376.6	Ifna13	-2.13481	1.90912	0.2688	0.93290779
ENSMUSG00000097416.3	Gm26670	-2.11502	0.353841	0.046087	-1.4988269
ENSMUSG00000030465.19	Psd3	-2.11328	1.3828	0.288131	0.46759251
ENSMUSG00000024846.6	Cst6	-2.10456	0.261437	0.0331236	-1.9354648
ENSMUSG00000087211.7	Lhx1os	-2.06741	0.361301	0.0121307	-1.4687268
ENSMUSG00000110008.5	Olfr560	-2.05777	1.36605	0.254806	0.45001029
ENSMUSG00000040380.14	Cbln3	-2.0538	0.402174	0.0643828	-1.3141083
ENSMUSG00000085298.2	F730035M05Rik	-2.04956	0.93403	0.130667	-0.0984592
ENSMUSG00000110682.1	A530010L16Rik	-2.03396	0.32693	0.028886	-1.6129463
ENSMUSG00000102945.1	Gm37884	-2.02823	3.89689	0.703876	1.96232321
ENSMUSG00000054763.9	Defb42	-2.02667	2.27957	0.446929	1.18876171
ENSMUSG00000026167.14	Wnt10a	-2.02202	1.02592	0.178401	0.03691824
ENSMUSG00000035420.7	Fam170a	-2.00443	0.170854	0	-2.5491641
ENSMUSG00000089512.3	Gm26287	-2.00236	355.803	81.0134	8.47493486

Supplementary Table 2: **Genes enriched with HuD in shCARM1 cells**

The genes identified in a HuD RIP performed in MN-1 pGIP-Z and shCARM1 cells were analyzed for differential enrichment using GFOLD. An arbitrary threshold of a GFOLD value of 2 and above was set to highlight the genes enriched with HuD in shCARM1 cells. The genes of interest in this study were highlighted in grey.

Gene symbol	Gene name	GFOLD	RPKM pGIP-Z	RPKM shCARM1	log_2RPKM pGIPZ
ENSMUSG00000072694.8	1500011B03Rik	5.63987	0	1.24823	-
ENSMUSG00000027220.2	Syt13	5.54559	0	0.83749	-
ENSMUSG00000087598.9	Zfp111	5.4527	0.0367361	2.35015	-4.7666577
ENSMUSG00000034764.15	1700006J14Rik	4.85851	0.0524481	2.74414	-4.2529657
ENSMUSG00000001555.10	Fkbp10	4.5999	0	0.559672	-
ENSMUSG00000031845.15	Bco1	3.99006	0.00793356	0.586012	-6.9778159
ENSMUSG00000021318.15	Gli3	3.76902	0.0767952	1.38103	-3.7028401
ENSMUSG00000039304.11	Tnfsf10	3.65469	0.00383119	0.225106	-8.0279917
ENSMUSG00000042396.10	Rbm7	3.46951	0.0122496	0.39757	-6.3511215
ENSMUSG00000021732.14	Fgf10	3.39459	0.188552	2.56537	-2.4069656
ENSMUSG00000015579.5	Nkx2-5	3.38886	0.211257	3.27556	-2.2429289
ENSMUSG00000022836.11	Mylk	3.21674	0.0277647	0.393929	-5.1706044
ENSMUSG00000091594.2	Gm17067	3.20636	0.0192248	0.493325	-5.7008876
ENSMUSG00000030075.10	Cntn3	3.08444	0	0.0868109	-
ENSMUSG00000035395.11	Dcaf8l	3.0409	0	0.135621	-
ENSMUSG00000103133.1	Gm37303	2.90181	0	0.331302	-
ENSMUSG00000044674.6	Fzd1	2.8757	0.0961403	1.0289	-3.3787149
ENSMUSG00000024269.11	Tpgs2	2.83848	0.280209	2.39409	-1.8354248
ENSMUSG00000074227.12	Spint2	2.80556	0.385257	3.24304	-1.3761069
ENSMUSG00000097156.7	Gm3764	2.79198	0.0260301	0.330648	-5.2636753
ENSMUSG00000113890.1	Gm48368	2.77469	0	0.26284	-
ENSMUSG00000049556.5	Lingo1	2.7123	0.00427891	0.132889	-7.868541
ENSMUSG00000008734.9	Gprc5b	2.69269	0.00217873	0.0969248	-8.8422969
ENSMUSG00000048142.9	Nat8l	2.64719	0.012099	0.203111	-6.3689684
ENSMUSG00000060985.15	Tdrd5	2.54443	0.145416	1.08388	-2.7817421
ENSMUSG00000049252.17	Lrp1b	2.51865	0.00084862	0.02315	-10.202597
ENSMUSG00000038535.17	Zfp280d	2.48575	0.0434967	0.31924	-4.5229502
ENSMUSG00000068617.5	Efcab1	2.44109	0.0455316	0.420399	-4.456988
ENSMUSG00000048988.8	Elfn1	2.42936	0.432806	2.80684	-1.2082076
ENSMUSG00000032035.16	Ets1	2.40119	0.218984	1.38956	-2.1911026
ENSMUSG00000022456.18	Septin3	2.39993	0.0982197	0.680919	-3.3478438
ENSMUSG00000100552.1	Gm29019	2.37994	0	0.64555	-
ENSMUSG00000031661.12	Nkd1	2.3446	0.00221315	0.0780217	-8.819683
ENSMUSG00000007682.6	Dio2	2.3446	0	0.0611561	-
ENSMUSG00000045034.12	Ankrd34b	2.3446	0	0.0748995	-
ENSMUSG00000060480.5	Olfr171	2.3446	0	0.252932	-

ENSMUSG00000026589.14	Sec16b	2.31689	0.0857719	0.611955	-3.5433511
ENSMUSG00000046159.16	Chrm3	2.28091	0.0225852	0.208532	-5.4684785
ENSMUSG00000079584.2	Gm364	2.27959	0.0140364	0.270982	-6.1546832
ENSMUSG00000009687.14	Fxyd5	2.2619	0.0601594	0.466585	-4.055066
ENSMUSG00000026768.10	Itga8	2.24014	0.0177983	0.165483	-5.8121167
ENSMUSG00000044646.15	Zbtb7c	2.22735	0.0213177	0.236194	-5.5518044
ENSMUSG00000012520.10	Phox2b	2.18657	6.29329	30.2659	2.65381443
ENSMUSG00000050315.14	Synpo2	2.17914	0.0924825	0.525926	-3.4346758
ENSMUSG00000039942.15	Ptger4	2.14983	1.16231	5.66009	0.2169949
ENSMUSG00000106350.2	Gm4869	2.14359	0.0443783	0.386827	-4.4940018
ENSMUSG00000074457.10	S100a16	2.13949	0.0499074	0.596946	-4.3246024
ENSMUSG00000057182.15	Scn3a	2.13164	0.38551	1.89692	-1.3751598
ENSMUSG00000105322.1	Gm43751	2.09883	0.0558411	0.427358	-4.1625288
ENSMUSG00000044229.9	Nxpe4	2.08182	0.0187722	0.174759	-5.7352585
ENSMUSG00000043903.4	Zfp469	2.05016	0.151585	0.75348	-2.7218011
ENSMUSG00000027500.10	Stmn2	2.02747	0.0648252	0.397514	-3.9473014
ENSMUSG00000079350.2	Magea8	2.02571	0	0.1749	-
ENSMUSG00000028438.16	Kif24	2.01854	0.0679718	0.385642	-3.8789199
ENSMUSG00000074892.9	B3galt5	2.00337	0.0376706	0.250208	-4.7304172

Confirmation of CARM1-GFP enzymatic activity

The CARM1-GFP construct has already been demonstrated in the past to be enzymatically active (Herrmann et al., 2009). In the same line of thought, the CARM1 E266Q mutant has also been used for its lack of catalytic activity (Cheng et al., 2007). Mechanistically, the mutation of the glutamic acid to a glutamine residue described locates to the double-E loop motif within the PRMT catalytic core and abrogates any methyl transfer. As such, the constructs are a reliable means of investigation towards the impact of catalytic activity of CARM1 on protein interaction. Nevertheless, the activity, or lack thereof, was investigated in the cellular context relevant to this study to ensure the biological relevance of the findings outlined in this work.

Before discussing the results, it is important to note that the experiment presented in Figure S5, was processed according to standard WB practices. When this experiment was carried through, the factors contributing to CARM1 aggregation discussed in Chapter 3 were not defined. However, despite the evident aggregation of CARM1, it was detectable at its expected molecular weight. Since the premise of this specific experiment is not reliant on CARM1 quantification, the interpretation of the data remains unchanged.

WT MN-1 cells transiently expressing the GFP, CARM1-GFP and CARM1 E266Q-GFP constructs were used to express the exogenous proteins. Accordingly, the cell lysate shows a strong expression of the constructs, with the anticipated CARM1-GFP and GFP bands (Figure S5A). A GFP-AP was performed for each transfection and the purified product (Figure S5B) was incubated with purified core histones *in vitro* in a buffer conducive to protein methylation. After incubation, the methylation product was analyzed by WB and blotted for dimethyl H3R17; a CARM1 substrate and known methylation site (Figure S5C). The resulting blot shows the presence of the dimethylated product in the CARM1-GFP lane, consistent with the anticipated

activity from the construct. This suggests that the exogenous protein be conformationally consistent with the endogenous protein. There was a detectable, albeit fainter band within the mutant lane. The considerable difference in signal between the CARM1 constructs is consistent with the expected methylation activity. While the faint band in the mutant lane could argue for potential residual activity, it is likely that endogenous CARM1 be responsible for its presence. CARM1 homodimers are prominent *in vivo* and it is expected that exogenous and catalytically active endogenous CARM1 be contained within the AP product used as an enzyme source for the methylation assay. A band at endogenous CARM1's molecular weight in the AP product within the CARM1 construct expressing lanes further supports this (Figure S5B). Therefore, these blots confirm the drastically different abilities of each CARM1 construct, supporting their use for downstream experiments.

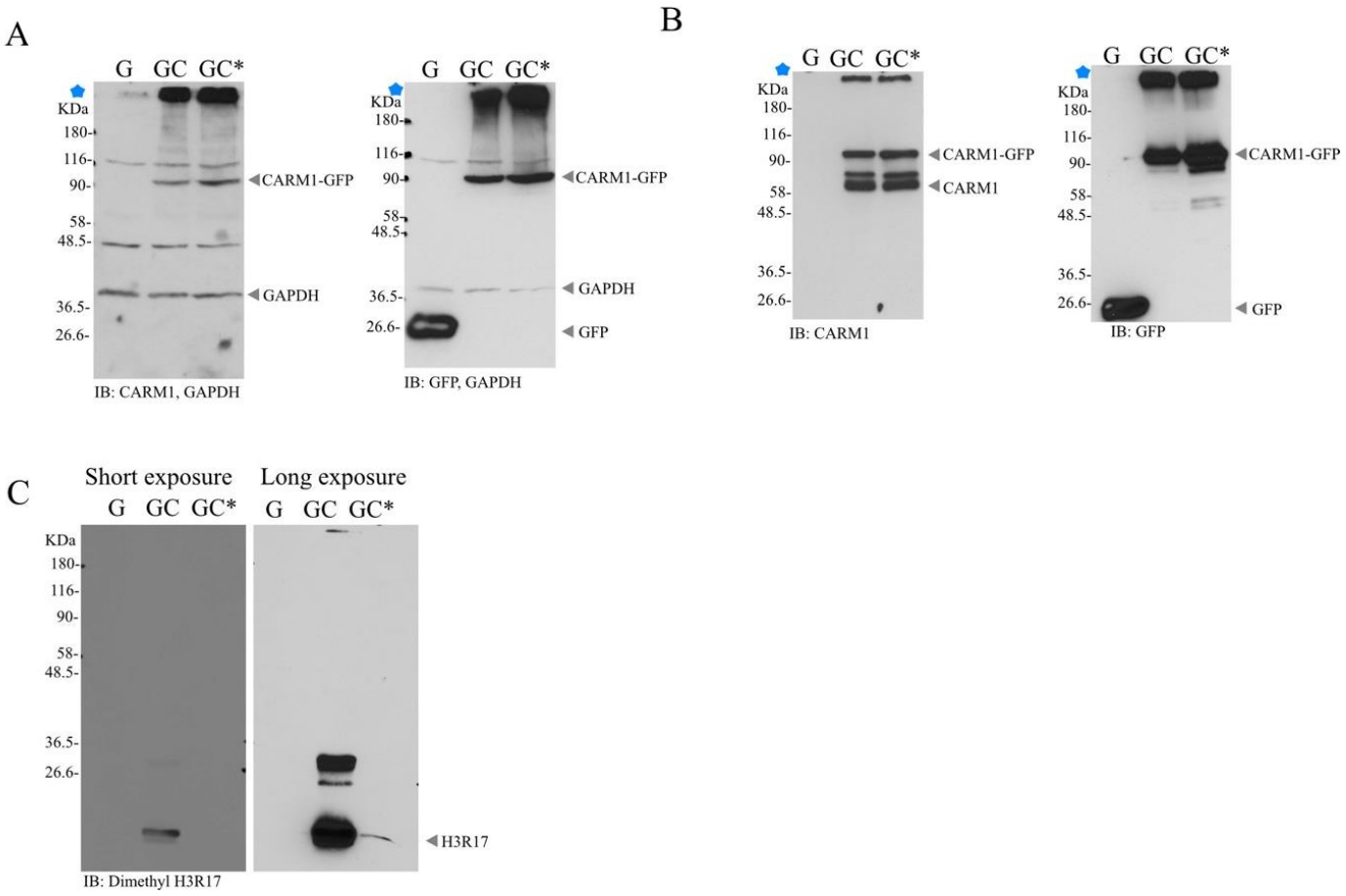

Figure S5: In vitro methylation assay of purified histones using CARM1-GFP or CARM1-GFP E266Q. The lysates of WT MN-1 cells transfected with GFP (G), CARM1-GFP (CG) and CARM1-GFP E266Q (CG*) (A), were used in a GFP affinity purification (B) as an enzyme source for an *in vitro* methylation assay (C). The methylation of CARM1 susbtrate H3R17 was used as readout of methylation activity as measured by a dimethyl specific H3R17 antibody.

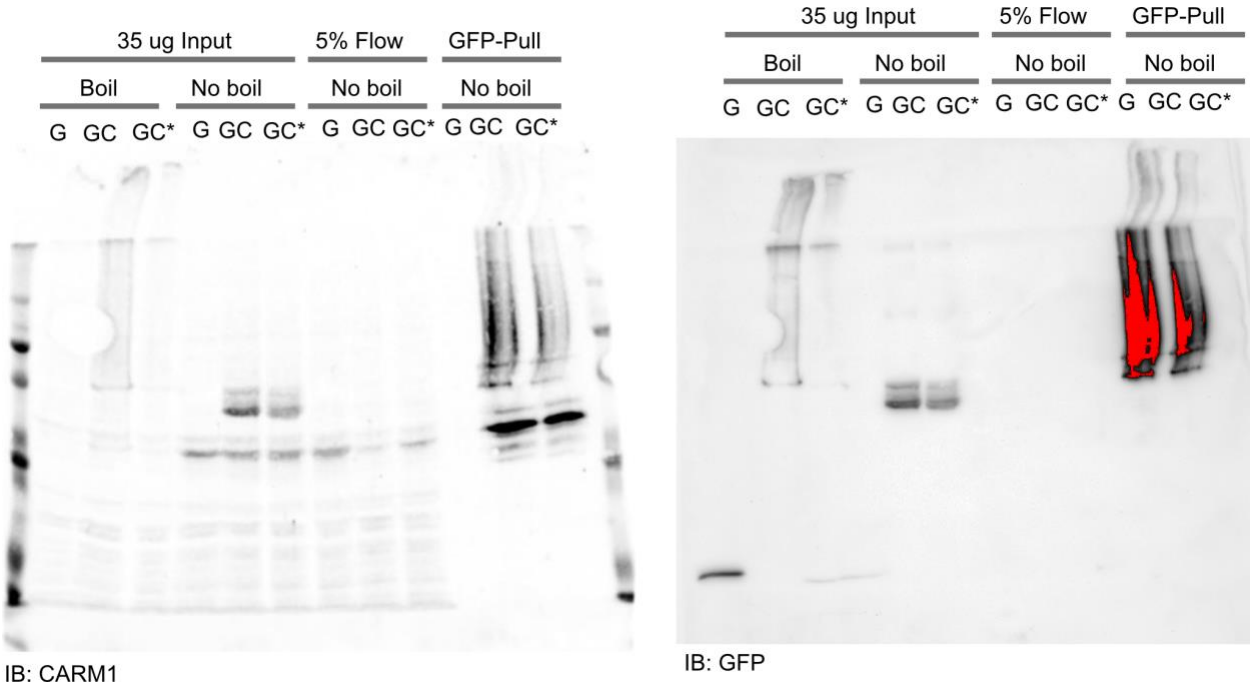

Figure S6: CARM1-GFP aggregation following a GFP affinity purification.

A total of 2mg of protein originating from the lysates of MN-1 cells stably expressing GFP (G), CARM1-GFP (CG) and CARM1-GFP E266Q (CG*) were used in a GFP-AP. The AP product was incubated at room temperature (termed no boil) or heat denatured at 95˚C for 8 min (termed boil) in Laemmlli buffer.

Supplementary Table 3: Primer sequences

The primers listed were used in RT-PCRs or mutagenesis experiments carried in this work.

	Forward sequence (5' to 3')	Reverse sequence (5' to 3')
Ptger4	CTCATCTGCTCCATTCCGCT	GGATGGGGTTCACAGAAGCA
Stc2	TTCGATGCCCAGGGAAAGTC	TCTCCACAATCACACCGACG
Schip1/Iqschfp	AAGAGAGCCATCCACCAGAGAA	ATAGCACCGTCATTTACAGTTCCTC
Phox2B	GCCTCAACGAGAAACGCAAG	GCGAAGACCCTCTCCAACTC
Adra2B	CCCTCATCTACAAGGGCGAC	GGCTGCGTTTGGCAATTACA
p21	CAGCGATATCCAGACATTCAGA	CTCAGACACCAGAGTGCAAGAC
GAP-43	TTTGTTTCTTGGTGTTGTTATGGC	GAACGGAACATTGCACACACA
18s	GTAACCCGTTGAACCCCATT	CCATCCAATCGGTAGTAGCG
CARM1 E266Q Mutagenesis	CTACATGCTCTTCAACCAGCGCATG CTGGAGAG	CTCTCCAGCATGCGCTGGTTGAAGA GCATGTAG
Oligo-dT	TTTTTTTTTTTTTTTTT	N/A